Assessing adenoviral delivery of prolylcarboxypeptidase and extracellular vesicle-mediated delivery of angiotensin converting enzyme 2 as therapies in hypertensive heart disease

Ahmad Mohammed A Alhajoj

BSc, MSc

Submitted in fulfilment of the requirements for the degree of Doctor of Philosophy to the School of Cardiovascular and Metabolic Health, University of Glasgow.

Research conducted at the British Heart Foundation Glasgow Cardiovascular Research Centre, Institute of Cardiovascular and Metabolic Health, College of Medical, Veterinary and Life Sciences, University of Glasgow, U.K.

2023

Author's Declaration

I declare that this thesis was written entirely by myself and is a record of the work performed by me with some exceptions as detailed below. The femoral vein injections were carried out by Dr Delyth Graham.

This thesis has not been submitted previously for a higher degree. The work included in this thesis was completed at the BHF Glasgow Cardiovascular Research Centre, Institute of Cardiovascular and Medical Sciences, College of Medical, Veterinary and Life Sciences, University of Glasgow, UK, under the supervision of Professor Stuart A. Nicklin and Professor Christopher M. Loughrey.

Acknowledgements

I would like to express my sincere gratitude to my two supervisors, Professor Stuart Nicklin and Professor Christopher Loughrey for their guidance, insights, and support during my PhD journey. Thank you Stu, for inspiring me and for the endless support and encouragement particularly at difficult times during and after the lockdown. Your contagious positive and optimistic attitude has kept me going and provided me with hope despite challenges.

I would also like to thank Dr. Lisa McArthur for her help and advice with cloning work, Dr. Laura Downie, the EV Queen, for helping with EVs work, Dr. Delyth Graham for helping with in vivo project, and Lluis Matas for his help with basic in vitro work when I started the lab. I would like to thank all other Nicklin group lab members: Sami, Eleni, Antoniya, and Julian.

I would also thank all people in level 4 lab for their help and guidance particularly Ryszard, Sheon, Nic, and Dylan.

A huge thanks must go to my dad and mum for being always supportive and for their sincere prayers and good wishes for me.

Finally, and most importantly, my lovely family who were with me during this long journey. My loving wife, Wadiah, thank you so much, this work wouldn't have been done without your outstanding support and help. My beloved kids; Yousef, Jaber, and the little one Taha, many thanks for all the joy you brought during that time, and sorry for not being always available for you!

List of Figures

List of Table

List of Abbreviation

AAV	Adeno-associated virus
AAV9	Adeno-associated virus 9
ACE	Angiotensin converting enzyme
ACE2	Angiotensin converting enzyme 2
ACE-AS	ACE antisense
ACEi	Angiotensin converting enzyme inhibitors
Ac-SDKP	N-acetyl-seryl-aspartyl-lysyl-proline
Ad5	Adenovirus serotype 5
ADA	Adenosine deaminase
ALIX	Apoptosis-linked gene 2-interacting protein X
AMI	Acute myocardial infarction
AMPK	AMP-activated protein kinase
ANF	Atrial natriuretic factor
Ang I	Angiotensin I
Ang II	Angiotensin II
Ang-(1-7)	Angiotensin-(1-7)
Ang-(1-9)	Angiotensin-(1-9)
ANOVA	Analysis of variance
ANP	Atrial natriuretic peptide
AP-1	Activator protein 1
ARB	Angiotensin II type 1 receptor blocker
ARB	Angiotensin II type 1 receptor blocke
ARCFs	Adult rat cardiac fibroblasts
AT_1R	Angiotensin II type 1 receptor
AT1R-AS	AT1R antisense
AT_2R	Angiotensin II type 2 receptor
ATP	Adenosine triphosphate
B2	Bradykinin B2 Receptor

BCA	Bicinchoninic acid
BHF	British heart foundation
BMI	Body mass index
BNP	Brain natriuretic peptide
BP	Blood pressure
BSA	Bovine serum albumin
CAD	Coronary artery disease
CAR	Coxsackie and adenovirus receptor
CCL2	C-C motif ligand 2
CCL3	C-C motif ligand 3
CCL4	C-C motif ligand 4
CHO	Chinese hamster ovary
CNS	Central nervous system
COPD	Chronic obstructive pulmonary disease
CVD	Cardiovascular disease
CxA	Carboxypeptidase A
CXCL1	C-X-C motif ligand 1
CXCL2	C-X-C motif ligand 2
CXCL9	C-X-C motif ligand 9
CXCL10	C-X-C motif ligand 10
DAPI	4′,6-diamidino-2-phenylindole
DMSO	Dimethyl sulfoxide DNA Deoxyribonucleic acid
dsDNA	Double stranded DNA
ECG	Electrocardiogram
ECM	Extracellular matrix
EDHF	Endothelium-derived hyperpolarizing factor
EF	Ejection fraction
EGFR	Epidermal growth factor receptor
eNOS	Endothelial NO synthase
ERK	Extracellular signal-regulated kinases
ESC	European Society of Cardiology
ET-1	Endothelin-1

EVs	Extracellular vesicles
gACE	Germinal ACE
GPCR	G protein-coupled receptors
hAdV-5	Human adenovirus serotype 5
HAoEC	Human aortic endothelial cells
HEK	Human embryonic kidney
HF	Heart failure
HFmrEF	Heart failure with mid-range ejection fraction
HFpEF	Heart failure with preserved ejection fraction
HFrEF	Heart failure with reduced ejection fraction
hHO-1	Human heme oxygenase-1
HIV	human immunodeficiency virus
HK	High molecular weight kininogen
HSPG	Heparan sulphate proteoglycans
HUVEC	human umbilical endothelial cells
IHD	Ischemic heart disease
IP3	Inositol 1,4,5-trisphosphate
ITR	Inverted terminal repeat
KO	Knockout
LDL	Low-density lipoprotein
Lenti-ACE2	Lentiviral vector containing ACE2
LNP	Lipid-nanoparticle
LTR	Long terminal repeat
LVEDD	Left ventricular end diastolic diameter
LVEDV	Left ventricular end diastolic volume
LVEF	Left ventricular ejection fraction
LVEF	Left ventricular ejection fraction
LVESD	Left ventricular end systolic diameter
LVESV	Left ventricular end systolic volume
LVM	Left ventricular mass
LVPWT	Left ventricular posterior wall thickness
LVW	Left ventricular wall thickness

MAPK	Mitogen-activated protein kinase
MasR	Mas receptor
MHC	Major histocompatibility complex
MI	Myocardial infarction
MI	Myocardial infarction
MMLV	Molony murine leukemia virus
MMPs	Matrix metalloproteinases
mRNA	Messenger ribonucleic acid
MYH7	Myosin heavy chain 7
NEP	Neprilysin
NO	Nitric oxide
NPs	Natriuretic peptides WHO
NRCM	Neonatal rat cardiomyocytes
ODNs	Oligodeoxynucleotides
PAH	Pulmonary atrial hypertension
PDGF	Platelet-derived growth factor
PEG	Polyethylene glycol
PK	Prekallikrein
PKC	Protein kinase C
POP	Prolyloligopeptidase
PRCP	Prolyl carboxypeptidase
rAAV	Recombinant AAV
RAS	Renin Angiotensin System
RCR	Replication-competent retrovirus
RNAi	RNA interference
ROS	Reactive oxygen species
sACE	Somatic ACE
SARS-CoV	Severe acute respiratory syndrome
SHR	Spontaneously hypertensive rat
SHRSP	Stroke-prone spontaneously hypertensive rat
SMA	Spinal muscular atrophy
SMN	Survival motor neuron

TGFB-1	Transforming growth factor-beta 1
UK	United Kingdom
WT	Wild type
WHO	World health organization

Summary

Cardiovascular diseases (CVD) are group of disorders that involve the heart and blood vessels and are considered the main cause of death globally. Chronic activation of the classical renin angiotensin system (RAS) via angiotensin converting enzyme (ACE)/Angiotensin II (Ang II) type 1 receptor (AT_1R) is associated with CVD including cardiac hypertrophy, and inhibition of this signalling pathway via ACE inhibitors or AT_1R blockers (ARBs) can reduce or inhibit cardiac remodelling. Another mechanism to protect the heart from Ang II-dependent remodelling is via stimulation of the counter-regulatory axis of the RAS, mainly angiotensin converting enzyme 2 (ACE2)/angiotensin-(1-7) Ang-(1-7)/Mas receptor signalling pathway. Prolylcarboxypeptidase (PRCP) is an alternative enzyme contributing to the counter-regulatory axis of the RAS via converting Ang II into the protective peptide Ang-(1-7). However, less attention has been given to PRCP's role in CVD.

The aims of this thesis were to generate an adenoviral (Ad) gene transfer vector expressing rat PRCP (Ad-PRCP), and to load EVs-with ACE2 (ACE2 EV) and study their therapeutic effects on angiotensin peptides metabolism and cardiac hypertrophy *in vitro* and *in vivo*.

Successful generation of Ad-PRCP was confirmed by sequencing and PRCP gene expression *in vitro*. Next, Ang II was added to HeLa cells and levels measured at specific time points following transduction with Ad-PRCP or control Ad-GFP. Reduced Ang II levels were observed in Ad-PRCP transduced HeLa cells after 24hr of Ang II stimulation. In H9c2 cardiomyocytes, Ang II levels were significantly higher in Ang II only treated and in Ad-GFP+Ang II groups compared to control. Ad-PRCP+Ang II did not significantly change at 24h from either control or other Ang II stimulated groups. Furthermore, 48hr Ang II stimulation significantly increased Ang-(1-7) levels in Ad-PRCP+Ang II, but not Ad-GFP+Ang II transduced cardiomyocytes, compared to control untreated cells. Assessment of cardiomyocyte hypertrophy following Ang II stimulation revealed that cell surface area was significantly increased in comparison to control, an effect also observed following Ad-GFP+Ang II, but not in Ad-PRCP+Ang II treated groups. These data suggested that overexpression of PRCP might diminish Ang II-

mediated cardiomyocyte hypertrophy *in vitro*. Next, the protective effect of Ad-PRCP following 3 weeks of Ang II infusion in Wistar Kyoto rats (WKY) was investigated. Ad-PRCP showed no effect on Ang-II-dependent hypertension or cardiac remodelling. Analysis of cardiac function showed no significant changes in ejection fraction (EF%) and fractional shortening (FS%) within a group over time. However, after 3 weeks EF% and FS% were significantly reduced in Ang II group compared to Ad-PRCP+Ang II group. No other significant changes in cardiac function were observed between groups at 3 week time point.

The potential to load EVs with ACE2 and their therapeutic effects on Ang II-dependent H9c2 cardiomyocyte hypertrophy was assessed. EVs were isolated from media of H9c2 cardiomyocytes transduced with Ad-ACE2 (ACE2 EV), Ad-GFP (GFP EV) or untransduced (control EV). The concentration of ACE2 EV was significantly greater than control EV and GFP EV. The average mean size for all EV groups was less than 200 nm. EV-associated markers, CD63 and TSG101, were detected in ACE2 EV and GFP EV via western blot, while ACE2 was observed only in ACE2 EV. Furthermore, ACE2 protein expression was detected in the cell lysate of H9c2 cardiomyocytes treated with ACE2 EV, but not in control or GFP EV treated groups. This observation suggested ACE2 could be loaded into EVs and is detectable via western immunoblotting. Next, ACE2 activity in each EV group was assessed revealing significantly higher ACE2 enzyme activity only in ACE2 EV group. Ang II and Ang-(1-7) levels were measured in control untreated cells or cells stimulated with Ang II alone or Ang II with either ACE2 EV or GFP EV. No statistically significant changes in Ang II or Ang-(1-7) were observed. The protective effects of ACE2 EV against Ang II-mediated cardiomyocyte hypertrophy were investigated. ACE2 EV diminished Ang II-induced H9c2 cardiomyocyte hypertrophy. These data suggested ACE2 EVs might be protective against Ang II-dependent H9c2 cardiomyocyte hypertrophy.

In conclusion, the delivery of both enzymes, PRCP via adenoviral gene transfer vector and ACE2 via extracellular vesicles, exhibited potential therapeutic effects against Ang II-induced cardiac remodelling. Further studies are required to fully investigate each therapeutic approach in CVDs.

Chapter 1 General introduction

1.1 Cardiovascular disease

1.1.1 Overview

Cardiovascular diseases (CVD) are group of disorders that involve the heart and blood vessels and represent the primary cause of death globally. According to the World Health Organization (WHO), approximately 17.9 million deaths were attributed to cardiovascular disease in 2019, which represents thirty two percent of total world deaths. Most CVD deaths were reported in low- and middle-income countries (WHO). However, in the United Kingdom (UK), CVD markedly contributed to the mortality and morbidity rate. It was reported that more than 7.6 million people are suffering from CVD in the UK with an estimated mortality rate of one death every three minutes, and morbidity rate of one patient every five minutes being admitted into the hospital (BHF 2022 report). Furthermore, it was estimated that more than half of people living in the UK will develop a heart or circulatory disease sometime during their life (BHF 2022 report). Heart and circulatory disease cost the UK economy around £19 billion every year.

Hypertension is one of the most common indicators of increasing risk of CVD. Patients with high blood pressure may suffer from vasoconstriction in small and large vessels, decreased nutrient blood flow and myocardial ischemia (Glasser, Selwyn, & Ganz, 1996). There are other common behavioural risk factors for CVD including: sedentary lifestyle, tobacco smoke, unhealthy food, high level of alcohol consumption, being overweight and obesity. Avoiding those risk factors has been shown to be effective in minimizing the CVD risk (WHO). Furthermore, exposure to environmental pollutants, where people usually have limited control, could also contribute to the development and/or the severity of CVD. The heart and blood vessels could be highly affected by a variety of environmental contaminants including solvents, pesticides, arsenic, and other air or metal pollutants, as well as exposure to high levels of temperature and noise (Cosselman, Navas-Acien, & Kaufman, 2015). Understanding the environmental risk factors and their effects on cardiovascular system are crucial in preventing and treating cardiovascular disease (Cosselman et al., 2015).

1.1.2 Hypertension

Hypertension has been recognized as one of the most crucial risk factors for CVD. If untreated, hypertension can lead to cardiac hypertrophy, heart attack, heart failure, stroke, vascular dementia and kidney disease (Raizada &

Sarkissian, 2006; I. M. Robbins, Christman, Newman, Matlock, & Loyd, 1998). The normal range of blood pressure (BP) is <120 to 139 mmHg for systolic blood pressure, and <80 to 89 mmHg for diastolic BP. Hypertension is defined as systolic BP of 140 mmHg or higher and diastolic BP of 90 mmHg or more (Staessen, Wang, Bianchi, & Birkenhäger, 2003). More details about hypertension categories are summarized in Table 1 (Carretero & Oparil, 2000). According to the BHF, approximately 15 million adults (28%) are diagnosed with high BP in the UK and at least half of them (6-8 million) are not receiving proper treatment. Furthermore, around 50% of heart attacks and strokes are associated with high BP in the UK (BHF 2022 report).

Table 1. Classification and category of blood pressure levels (Carretero & Oparil, 2000).

Category	Systolic BP, mm Hg	Diastolic BP, mmHg
Optimal	<120	<80
Normal	<130	<85
High normal	130-139	85-89
Hypertension		
Stage 1 (mild)	140-159	90-99
Stage 2 (moderate)	160-179	100-109
Stage 3 (severe)	≥180	≥110

Obesity, particularly abdominal obesity, is a main risk factor for the development of hypertension and insulin resistance (Carretero & Oparil, 2000). It has been reported that people with body mass index (BMI) of 26 to 28 are at increased incidence of high BP by 180% and insulin resistance by more than 1000% compared to subjects with BMI of less than 23 (Carretero & Oparil, 2000). Aging is another critical factor in the development of hypertension. Diastolic BP increases until the age of 50 years and then remains constant or may start to decline gradually. In contrast, systolic BP continue to raise with the age until eighth decade of life. Patients less than 50 years old are most likely to have high diastolic blood pressure (Staessen et al., 2003).

1.1.3 Coronary artery disease

Coronary artery disease (CAD), also called ischemic heart disease (IHD), is the most common type of heart disease and represents the leading cause of heart attacks. It is a clinical syndrome that refers to abnormality of the major blood vessels that supply the heart (coronary arteries), causing insufficient supply of blood, oxygen and nutrients to the heart muscle. This abnormality is usually caused by atheroma deposition or build up in the coronary arteries leading to arterial luminal stenosis or occlusion and wall thickening (Conte, Baumgartner, Dorman, & Owens, 2007). Cholesterol storage and inflammation as well as interaction between the arterial cell wall (endothelial cell) and blood and molecular signals (proinflammatory cytokines or adhesion molecules) are all involved in promoting CAD. Patients with CAD may remain asymptomatic for several years as symptoms develop over time and occur when the heart does not get enough oxygen-rich blood. The Patients may suffer from angina-like symptoms such as chest pain and shortness of breath as well as other symptoms including nausea, feeling faint, and pain that spreads throughout the body, while complete blockage of the arteries can cause myocardial infarction or stroke (Libby & Theroux, 2005).

1.1.4 Atherosclerosis

Atherosclerosis is the main underlying cause for CAD and can lead to changes in the heart vasculature causing myocardial infarction, and cerebral infarction or stroke in the brain, as well as loss of peripheral vascular function (Ross, 1995).

Atherosclerosis is a chronic inflammatory vascular disease that affects the inner wall (intima) of large and medium size arteries and is characterized by forming fibroinflammatory lipid plaques and atheroma. Most acute and fatal myocardial infarction episodes are caused by a physical disruption of the atheromatous plaques (Libby, Ridker, & Maseri, 2002). Studies have reported that patients with plaque morphology containing high amount of lipid cores and thin fibrous caps are at high risk of cardiovascular events (Loftus, 2014). Atherosclerosis could be trigged by variety of risk factors such as smoking, high fat diet, obesity, cholesterol deposits, high blood pressure, hyperglycaemia, and insulin resistance. Those factors can promote the expression of adhesion molecules by endothelial cells which in turn facilitate the attachment of leukocytes to the arterial wall (Libby, 2006). The endothelial injury initiated by one or more of risk factors causing accumulation of low-density lipoprotein (LDL) inside the intima layer of the blood vessels. LDL is converted to oxidized LDL which in turn leads to release of inflammatory cytokines such as (interleukin-6, IL-6; interleukin-1, IL-1; TNF- α, monocyte chemoattractant protein-1, MCP-1), and monocyte migration into the affected area(Libby & Theroux, 2005; Santos-Gallego, Picatoste, & Badimón, 2014). Inside the intima, monocytes become macrophages that work to provide antigens for lymphocytes, an action that trigger the immune response(Ross, 1993). Macrophages use oxidized LDL to produce macrophage-derived foam cells, which increase the release of growth factors and cytokines leading to proliferation and migration of smooth muscle cells from media to intima(Ross, 1993). Extra lipid uptake by smooth muscle cells causes foam cell formation which leads to accumulation of pale-yellow lipid plaques on the intima surface alongside collagen fibril proliferation that ultimately lead to coronary atherosclerosis and angina(Ross, 1995). These plaques can be stable or disrupted and transformed to unstable form via proteolytic enzymes such as matrix metalloproteases (enzymes that digest the collagen and produce a thinner plaque cap), inflammatory proteins such as tissue factor(making the lesion more thrombogenic), and immune cells such as T-cells (Gerhardt, Haghikia, Stapmanns, & Leistner, 2022) . Disrupted plaques cause platelet aggregation and thrombosis in coronary arteries that might result in acute myocardial ischemia and necrosis (Rafieian-Kopaei, Setorki, Doudi, Baradaran, & Nasri, 2014; Santos-Gallego et al., 2014; Zmysłowski & Szterk, 2017).

1.1.5 Myocardial infarction

Myocardial infarction (MI) is a major cause of morbidity in the UK with an estimated rate of hospital admission of one patient every 5 minutes attributed to heart attack (BHF 2022), and patients may still face 40% risk of mortality within the first 30-days of cardiogenic shock (a state of low or ineffective cardiac output that lead to severe end-organ hypoperfusion and hypoxia, and mainly caused by acute myocardial infarction)(M. Saleh & Ambrose, 2018; Van Diepen et al., 2017). Acute myocardial infarction (AMI) is described as heart muscle necrosis resulting from decreased or a blockage of blood flow to a portion of the heart. This is mainly caused by a blood clot in the epicardial artery that provides blood to that part of the heart. Unstable coronary atherosclerosis (characterized by ruptured plaque surface that stimulate thrombotic process in vascular lumen via allowing haemorrhage into the plaque) with active inflammation in the blood vessel wall is considered the main driver of thrombosis and stenosis that may lead to development of MI, unstable angina, or ischemic sudden death (Falk, 1985; Thygesen, Alpert, White, & Infarction, 2007). However, the INTERHEART global control study that includes participants from 52 countries with a total number of 27 098 participants, determined nine risk factors for MI in both men and women (Anand et al., 2008). Among those risk factors; hypertension, diabetes, physical activity, and alcohol consumption are more strongly associated with MI in women than in men. The other risk factors: abdominal obesity, current smoking, abnormal lipid, high risk diet, and psychological stress showed similar contribution to MI development in both men and women. The study also reported that men are more likely to develop AMI nine years earlier than women and that might be explained by exposing to more risk factors at earlier ages in men (Anand et al., 2008). Taking advance action to reduce these risk factors may prevent the event of heart attack. Identifying and detecting the symptoms of MI in a proper time might also be effective in preventing the heart attack or reducing its severity. Symptoms of MI include chest pain that usually travels to the left arm or the left side of the neck, dyspnea, cardiac arrythmia, nausea and vomiting, sweeting, fatigue, anxiety (L. Lu, Liu, Sun, Zheng, & Zhang, 2015). However, approximately 64 % of people who have MI are asymptomatic (silent MI) and showed only minor and atypical symptoms that could be detected only during the routine electrocardiogram (ECG) check showing the existence of the abnormal Q waves. Asymptomatic MI is

most common in diabetic patients who are at high risk of CAD (Valensi, Lorgis, & Cottin, 2011).

1.1.6 Cardiac remodelling

1.1.6.1 Cardiac hypertrophy

The heart must pump continuously to supply peripheral body organs with oxygenated blood and nutrients during both normal and stress conditions (Nakamura & Sadoshima, 2018). To maintain this role, the heart and cardiac cells (particularly cardiomyocytes) undergo multiple biological and physiological changes that allow adaptation to alteration in the increase of the afterload (the systolic load on the left ventricle after contraction has started) or preload (the workload imposed on the heart before contraction begins or at the end of diastole) which result in cardiac hypertrophy (Nakamura & Sadoshima, 2018). Cardiomyocyte growth, angiogenesis, and metabolic plasticity are involved in regulating cardiac homeostasis(Shimizu & Minamino, 2016). Cardiac hypertrophy can be classified into two types: physiological and pathological which are regulated by distinct cellular signalling pathways. Physiological hypertrophy occurs in healthy individuals in response to normal growth of new-born children or during pregnancy as well as during exercise in athletes (Barry, Davidson, & Townsend, 2008). Human cardiomyocyte diameter increased approximately 3-fold from infants to adults (Shimizu & Minamino, 2016). Normal physiological enlargement of the heart (except for postnatal hypertrophy), is characterized by a mild increase in the heart mass accompanied with enlargement in the cardiomyocyte width and length (Figure1.1) (Nakamura & Sadoshima, 2018). Contractile function is increased or preserved in the physiological cardiac hypertrophy individual without initiating cardiac fibrosis or cell death, and it's completely reversible and is not considered a risk factor for heart failure (Shimizu & Minamino, 2016). Furthermore, there is either no changes or decrease in the expression of the fetal genes that often used as biomarkers for pathological hypertrophy (Nakamura & Sadoshima, 2018). These genes are expressed in the myocardium in response to a variety of conditions such as ventricular wall stress, hypertrophy and fluid overload (Wright & Thomas, 2018) and include: atrial natriuretic peptide (ANP), brain natriuretic peptide (BNP), skeletal muscle α-actin, and cardiac muscle ß-isoform (MYHCß) also known as myosin 7 or (MYH7) (Nakamura & Sadoshima, 2018).

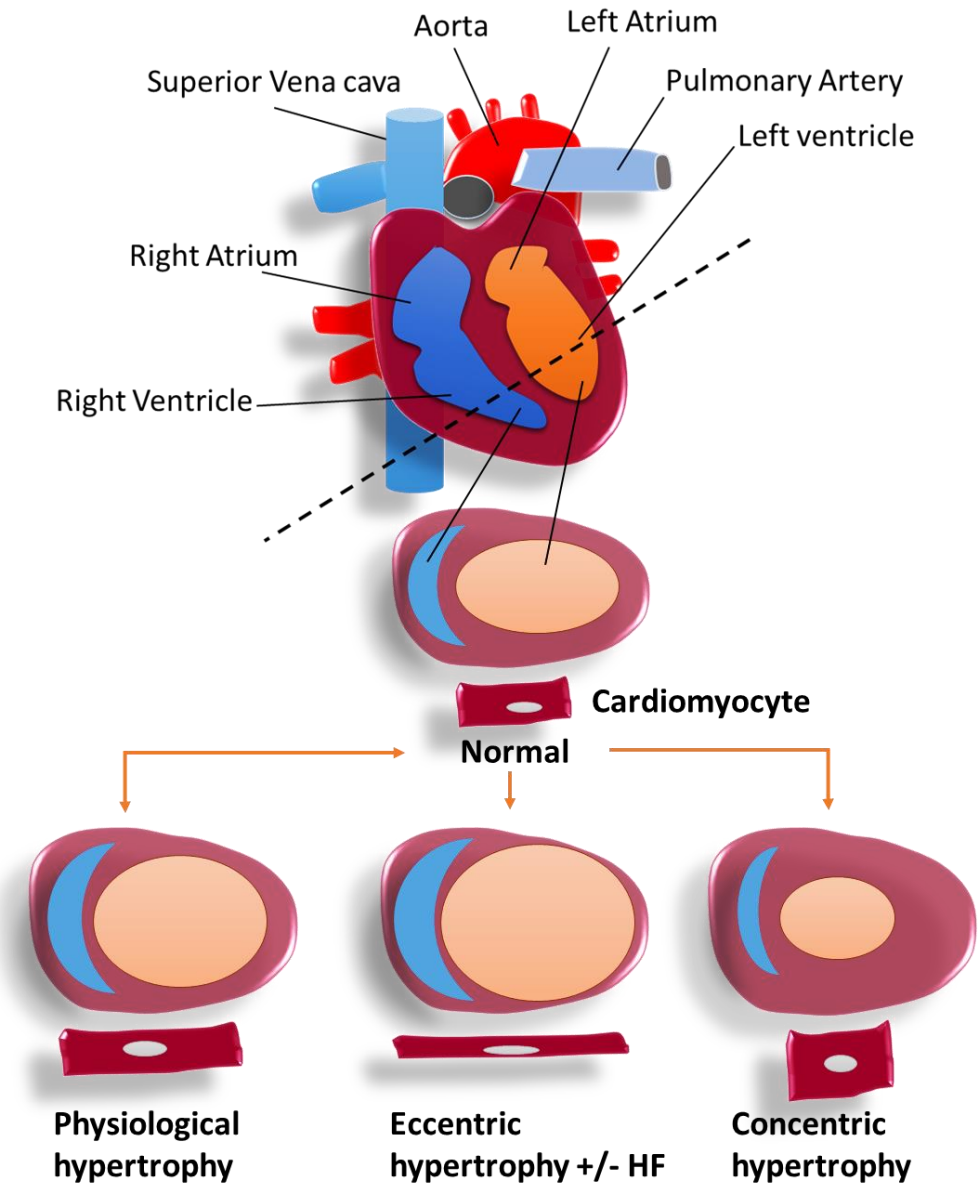

Figure 1.1 The heart and different types of cardiac hypertrophy

Physiological hypertrophy showed uniform growth of the myocardium and increases in chamber size and cardiomyocytes width and length. Eccentric hypertrophy (physiological): preserved, mild increased in cardiac function e.g.; during pregnancy cardiac output increased to meet placental blood flow resulting in a condition of continuous volume overload which leads to reversible modest eccentric hypertrophy (Dorn, 2007). Concentric hypertrophy is characterized by increased wall thickening and cardiomyocytes width compared to length and reduction in chamber size. Under pathological condition such as MI, eccentric hypertrophy showed excessive cardiomyocytes length and

decreased width leading to greater chamber enlargement and loss of wall and septal thickness (Van Berlo, Maillet, & Molkentin, 2013).

Conversely, in pathological cardiac hypertrophy cardiomyocyte growth to exceed the capacity of the capillaries to maintain supply enough oxygenated blood leading to cardiac structural changes and hypoxia in mice (Shimizu et al., 2010). This type of hypertrophy progresses to expand the ventricular chamber with wall thinning via increase in the length of cardiomyocytes, and also causes contractile dysfunction, and heart failure (Schiattarella & Hill, 2015). Heart failure with preserved ejection fraction (HFpEF) might occur without systolic contractile dysfunction, however, it is usually associated with diastolic dysfunction as well as microvascular rarefaction and myocardial fibrosis (Mohammed et al., 2015). Perivascular fibrosis and death of cardiac cells as well as elevation in the type I collagen and change in the expression of hypertrophy markers genes is usually associated with pathological cardiac hypertrophy (Shimizu & Minamino, 2016). Other maladaptive decompensation mechanisms resulting from pathological cardiac hypertrophy include dysregulation of Ca^{2+}-handling proteins, dysfunction of mitochondria, change in sarcomere structure, and inadequate angiogenesis. Pathological hypertrophy caused is by a variety of pathological conditions such as: high blood pressure, myocardial hypoxia (resulting from MI, diabetes mellitus, anaemia, obesity, or chronic obstructive pulmonary disease (COPD)), volume overload initiated by mitral or aortic regurgitation and chronic renal disease, storage diseases such as lipid storage disorder, and inherited disease such as hypertrophic cardiomyopathy (Nakamura & Sadoshima, 2018).

Based on left ventricular geometries, cardiac hypertrophy can also be classified into eccentric and concentric, (Figure 1.1) (Shimizu & Minamino, 2016). Eccentric hypertrophy is usually linked to non-pathological hypertrophy and characterized with ventricular volume overload, in response to significant valvular regurgitation or high cardiac load, with coordinated increase in wall and septal thickness, coupled with growth in cardiomyocyte width and length (Shimizu & Minamino, 2016). This kind of hypertrophy can be seen in elite athletes and shows normal blood pressure and peripheral resistance (Marwick, 2015). Echocardiography data for patients with eccentric hypertrophy revealed

high cavity size of the left ventricle, normal left ventricular wall thickness and elevated left ventricular mass (LVM) (Marwick, 2015). In patients with heart disease such as MI and dilated cardiomyopathy, eccentric cardiac hypertrophy can be also developed causing ventricular dilatation and increase in cardiomyocyte length (Shimizu & Minamino, 2016). Conversely, concentric hypertrophy is pathological and associated with cardiac disorders such as MI, hypertension, valvular disease and metabolic disorder (Nakamura & Sadoshima, 2018). Concentric hypertrophy showed reduction in left ventricular chamber dimension along with increase in wall and septal thickness. Cardiomyocytes tend to grow in thickness more than length (addition of sarcomere in parallel) in concentric hypertrophy leading to increase in cardiomyocyte cross sectional area(Marwick et al., 2015) .

1.1.6.2 Cardiac fibrosis

Cardiac fibrosis is “a state in which extracellular deposition of collagen fibers and extracellular matrix (ECM) occurs in the heart” (Kurose, 2021). Heart contains multiple types of cells that mainly include cardiomyocytes, fibroblasts, endothelial cells, lymphocytes, macrophages, and mast cells (Kurose, 2021). Among these cell types, cardiac fibroblasts count for approximately 20% to 60% in rats and human (C. Hall, Gehmlich, Denning, & Pavlovic, 2021). The number of fibroblasts increase in some cases such as during development, disease, and aging (C. Hall et al., 2021). Fibroblasts play a crucial role in normal heart function, and in cell-cell interaction and synthesis and degradation of ECM during remodelling process (Howard & Baudino, 2014). Heart injury caused by disease such as hypertrophy or myocardial infarction triggers the differentiation of fibroblasts into stress-fiber expressing myofibroblasts which produce ECM (Kurose, 2021). These pathological conditions cause increased matrix stiffness and abnormalities in cardiac function (Hinderer & Schenke-Layland, 2019). In healthy heart the ECM make up around 6%, while in disease states it can increased more than 5-fold (Graham-Brown et al., 2017). Several mechanisms can participate in the activation of cardiac fibroblasts which include: local cardiac injury resulting in damage or dying cardiomyocyte, increased biochemical stress such as infectious agents or cardiotoxic drugs, neurohormonal pathways such as the renin angiotensin system, inflammatory signalling cascade that triggered by cytokines and chemokines..etc.(Ravassa et al., 2023)

There are 3 types of myocardium fibrosis include reactive interstitial fibrosis, infiltrative interstitial fibrosis, and replacement fibrosis (Hinderer & Schenke-Layland, 2019). Reactive interstitial fibrosis does not cause loss of cardiomyocytes but is characterized by excess ECM deposition that leads to a pressure overload and cardiomyopathy. Infiltrative interstitial fibrosis is known by glycolipid build up in multiple cardiac cells. The replacement fibrosis comes as a consequence of cardiac injury like myocardial infarction where the heart cells are damaged (Hinderer & Schenke-Layland, 2019).

The collagens occurs in the myocardium are collagen type I which represents approximately 85% of total collagen protein and makes up thick fibers that are important for strength, and type III collagen that builds thin and flexible fibers that are important for elasticity (Ravassa et al., 2023).

Transforming growth factor ß (TGF-ß) is a fibrogenic cytokine that is markedly upregulated in infarcted and remodelling heart and plays an important role in the development of myocardial fibrosis (Bujak & Frangogiannis, 2007). TGF-ß is involved in the transformation of fibroblast to myofibroblast, increased production of ECM proteins, prevents ECM proteins degradation via inhibition of Matrix metalloproteinases (MMPs), an enzyme responsible for catalysis of the ECM by fibrillar collagen denaturation and degradation (Segura, Frazier, & Buja, 2014). Angiotensin II induces the expression of TGF-ß via acting on angiotensin II type I receptor on myocytes and fibroblasts (Segura et al., 2014). Other heart disorders that promote myocardial fibrosis include hypertensive heart disease, idiopathic dilated cardiomyopathy and diabetic hypertrophic cardiomyopathy (Hinderer & Schenke-Layland, 2019).

1.1.7 Heart failure

Heart failure (HF) describes as a condition where the heart is unable to maintain regular cardiac output required to meet metabolic needs and accommodate venous return (Kemp & Conte, 2012). According to European Society of Cardiology (ESC), heart failure is “a clinical syndrome characterised by typical symptoms (e.g., difficult breathing, ankle swelling, and fatigue) that may be accompanied by signs (e.g., elevated jugular venous pressure, pulmonary crackles, peripheral oedema) caused by a structural and/or functional cardiac abnormality, leading to a reduced cardiac output and/or elevated intracardiac pressures at rest or during stress” (UK et al., 2016) . Left ventricular ejection

fraction (LVEF), normal values between 55% and 70%, is the proportion of blood ejected from the heart for each heartbeat and is an important measurement for the diagnosis of heart failure (Wright & Thomas, 2018). Based on LVEF heart failure can be classified into HF with reduced ejection fraction (HFrEF) when EF is less than 40%, HF with preserved ejection fraction (HFpEF) with EF of more than 50% (Wright & Thomas, 2018). Patients with ejection fraction range of 40–49% share a grey area and defined as heart failure with mid-range ejection fraction(HFmrEF) (UK et al., 2016). Cardiac output is low in patients with HFrEF as a result of reduced stroke volume, and patients suffer mainly from systolic dysfunction (inability of the left ventricle to contract efficiently) (Wright & Thomas, 2018). HFrEF is characterised by cardiomyocytes loss or damage causing LV structural change (e.g. fibrosis) and eccentric remodelling with LV dilatation but normal wall thickness (Simmonds, Cuijpers, Heymans, & Jones, 2020). In contrast, HFpEF is associated with diastolic dysfunction and stiffness and slow LV relaxation as well as development of concentric cardiomyocytes hypertrophy with greater LV wall thickness (Redfield, 2016). Patients with chronic CVD such as hypertension, renal insufficiency, obesity and type 2 diabetes mellitus are more likely to develop HFpEF (Simmonds et al., 2020). Elevated plasma levels of natriuretic peptides(NPs) can be used in the initial diagnosis of HF, and patients with normal NPs values are unlikely to have HF (UK et al., 2016).

1.2 Renin Angiotensin system

1.2.1 Background and history

The renin angiotensin system (RAS) is a physiological system that controls cardiovascular physiology through its effects in regulating blood pressure and fluid hemostasis. Renin is a proteolytic enzyme that is mainly synthesized, secreted and stored by Juxtaglomerular or (granular) epithelioid cells in the kidney and has an important role in regulating blood pressure and electrolyte balance (Persson, 2003). The first link between renin and blood pressure was reported in 1898, when Robert Tigerstedt and his assistant Per Bergman conducted a study on the effect of renal cortex extract on the arterial pressure(Tigerstedt & Bergman, 1898). The authors observed that blood pressure was consistently increased in rabbits received an intravenous injection of renal extract that contained a pressor agent which they named “renin”. They further demonstrated that the connection between renal disease and cardiac

hypertrophy was related to kidney secretion of a vasoactive compound that promote a contraction of the blood vessels(Tigerstedt & Bergman, 1898). However, the study did not determine whether renin works directly on the blood vessels or not, and they concluded if renin accumulated (produced in high amount with low excretion in rat) that will lead to cardiac hypertrophy via increasing vascular resistance (M. Ian Phillips & Schmidt-Ott, 1999; Tigerstedt & Bergman, 1898). The finding of this study encouraged many researchers to develop an experimental model of blood pressure via manipulating kidney function for the following years. However, none of these attempts were reliable, possibly due to unsuitable techniques and/or insufficient methods used to assess blood pressure(Basso & Terragno, 2001). Approximately thirty-six years later, Harry Goldblatt was able to successfully induce increased systolic blood pressure in a dog model via constriction of the main renal arteries(Goldblatt, Lynch, Hanzal, & Summerville, 1934). The study showed that when both renal arteries are partially constricted, elevation of systolic blood pressure was observed without signs of reduced renal function, while complete constriction of the main renal arteries resulted in higher blood pressure accompanied by marked disturbance in kidney function and uremia(Goldblatt et al., 1934). Following this finding, two groups independently attempted to understand the underlying mechanism of hypertension produced by acute renal ischemia using the same procedure of Goldblatt (J. M. Muñoz, Braun-Menéndez, Fasciolo,& Leloir,1939; Page & Helmer, 1940) . Both groups' investigations led to discovery of another pressor substance that was extracted from the venous blood of kidney with acute ischemia and mainly characterized by its shorter duration of action. This compound was named hypertensin or angiotonin, which was called later angiotensin I (Ang I) (Braun-Menendez & Page, 1958). The investigation revealed that renin is an enzyme that produce a pressor effect via formation of hypertensin (Ang I) in the blood and the substrate for renin was reported and named angiotensinogen, and the enzymes that catalyze the peptides were named angiotensinases(J. M. MuÑOz, Braun-MenÉNdez, Fasciolo, & Leloir, 1939). The discovery of the renin angiotensin system cascade continued when further studies found that hypertensin I (angiotensin I) is actually inactive and is converted to another vasoactive compound hypertinsin II (angiotensin II) by a chloride-activated enzyme present in the plasma (Bumpus, Schwarz, & Page, 1957; Skeggs Jr, Kahn, & Shumway, 1956). Angiotensin II (Ang II) was then

recognized as the main vasoactive octapeptide of the renin angiotensin system cascade and responsible for most of the cardiovascular effects produced by the classical RAS and the system was first described as renin hypertensin system (Skeggs Jr et al., 1956). Secretion of renin is mainly triggered by the autonomic nervous system when sympathetic stimulus such as adrenalin and/or noradrenalin act on ß1 adrenergic receptors on the Juxtaglomerular cells causing release of renin into the circulation and then, the activation of the renin angiotensin system (RAS) (Kurtz, 2011; Torretti, 1982). Renin secretion could be also controlled by feedback mechanisms where a drop in blood pressure or blood volume, sodium depletion and dehydration trigger Juxtaglomerular cells to release renin in order to restore normal blood pressure and blood volume as well as maintaining electrolyte homeostasis(Schweda & Kurtz, 2011). Conversely, elevation in blood pressure and volume as well as angiotensin II (AngII) exert inhibitory effects on sympathetic parameters and consequently inhibits the release of renin (Torretti, 1982). Some other factors/substances that influence the release of renin include; prostaglandins, nitric oxide, cyclic AMP, cyclic GMP, calcium, atrial natriuretic peptide (ANP), and the electrophysiology of Juxtaglomerular cells(Schweda & Kurtz, 2011).

The classical RAS cascade activation begins when renin converts angiotensinogen into the inactive decapeptide angiotensin I (Ang I) (Figure 1.2). Angiotensinogen (the unique substrate of renin) is a twelve amino acid glycoprotein polypeptide that is mainly generated from the liver hepatocyte and acts as a precursor protein for Ang I and Ang II production. In adult rat, but not in fetus, the liver represents the primary source of angiotensinogen, and the mRNA expression of the polypeptide has also been reported in the brown adipose tissues, brain and kidney (Gomez et al., 1988). Plasma concentration of angiotensinogen is affected by different pathological and physiological states as it has been reported to be higher during inflammation (Soden, Klett, Hasmann, & Hackenthal, 1994), pregnancy (Kotchen, Kotchen, Guthrie Jr, & Cottrill, 1979) and in patients using oral contraceptive (Skinner, Lumbers, & Symonds, 1969). Low levels of angiotensinogen was observed in subjects with adrenal insufficiency and in response to angiotensin converting enzyme inhibitors, captopril (Clauser, Gaillard, Wei, & Corvol, 1989). Angiotensinogen plays a crucial role in maintaining regular blood pressure and body weight and its global

reduction via genetic manipulation (e.g. in hepatocyte-angiotensinogen deficient mice) leads to chronic hypotension and marked decrease in plasma Ang II concentration and blood pressure in both lean and obese male mice (Yiannikouris et al., 2015). Angiotensinogen-deficient mice has also showed complete loss of angiotensin I accompanied with significantly lower blood pressure, lower neonatal survival rate, and impaired growth and body weight compared to wildtype mice (H. S. Kim et al., 1995; Tanimoto et al., 1994). In contrast, overexpression of angiotensinogen via adeno-associated viral vector (AAV) into hepatocyte-specific angiotensinogenase-deficient (hepAGT-/-) mouse showed restored plasma angiotensinogen level, systolic blood pressure, atherosclerosis and body weight gain (Congqing Wu et al., 2015). Antisense oligonucleotides could degrade or inhibit angiotensinogen via targeting its mRNA in liver, kidney and adipose tissues leading to reductions in renal function, blood pressure, atherosclerosis, and obesity in LDL receptor knockout mice (a model of atherosclerosis) (H. Lu et al., 2016).

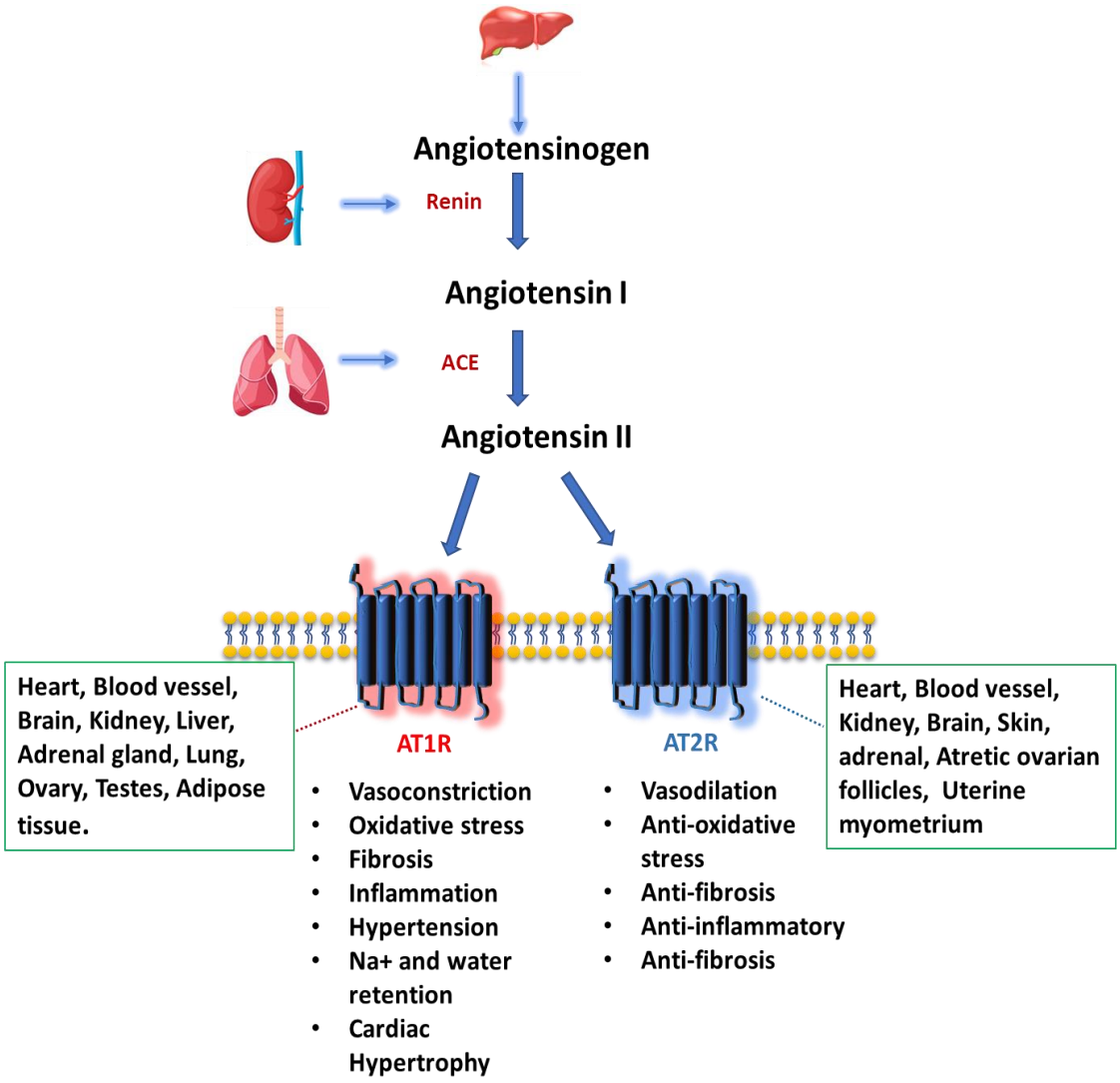

Figure 1.2 The classical RAS cascade and its effect on cardiovascular system.

Angiotensinogen produced from the liver is converted to Ang I by renin that is released from Juxtaglomerular cells in the kidney. Ang I is catalyzed by ACE (mainly in the pulmonary vessels) into the vasoactive pressor Ang II which binds to either AT_1R causing vasoconstriction and promote cell growth fibrosis and hypertension or to AT_2R to oppose the action of AT_1R (M. Paul, Poyan Mehr, & Kreutz, 2006).

1.2.2 Angiotensin converting enzyme

Angiotensin converting enzyme (ACE), also named as peptidyl-dipeptidase or kininase II, is a transmembrane ectopeptidase of vascular endothelial cells and represents the main enzyme that catalyzes the conversion of Ang I into the vasoactive octapeptide Ang II via cleaving 2 amino acids from the C-terminus, particularly cleaving Phe^{8}–His^{9}-bond (Michael J Peach,1977). However, ACE is not specific to Ang I and can catalyze a wide range of substrates including; bradykinin, neurotensin, substance P, enkephalins, N-formyl-Met-Leu-Phe, GnRH, acetyl Ser-Asp-Lys-Pro (Ac-SDKP), cholecystokinin-8 and angiotensin-(1-7) (Ang-(1-7))(Bernstein et al., 2013). There are two forms of ACE present in human; somatic ACE (sACE) and the testis or sperm specific germinal ACE (gACE).

Somatic ACE is longer (with 1306 amino acid residues) than gACE (732 amino acid residues) and contains two active sites; the transmembrane domain and two similar extracellular domains (amino or N domain, and the carboxy or C domain, while gACE possess only one catalytic site (Bernstein et al., 2013). Somatic human ACE is abundant in the endothelial cells of the lung and is also expressed in various tissues including endothelial cells of blood vessels, retina, kidney, heart, adrenal gland, small intestine, liver, epididymis etc(Riordan, 2003). Germinal ACE is expressed in both developing and mature sperm cells and plays an essential role in male fertility (Hagaman et al., 1998). Mice lacking testis ACE revealed impaired male fertility despite their ability to produce normal sperm number, morphology, and motility (Esther, Marino, & Bernstein, 1997). While the link between ACE inhibitor and male infertility has not been reported, the mechanism by which testis ACE promotes male fertility is still ambiguous. Originally it was thought that plasma is the site of catalyzing Ang I (Skeggs Jr et al., 1956), however, it was reported later that pulmonary vessels are where the majority of Ang I to Ang II conversion occurs in dogs, rats and rabbits (K. K. F. Ng & Vane, 1968) (Peach, 1977). As it plays a major role in Ang II production, ACE is crucial in blood pressure regulation. ACE knockout mice showed reduction in systolic blood pressure to 73 mmHg compared to wild type with 110 mmHg(Cole, Ertoy, & Bernstein, 2000). Furthermore, mice lacking ACE showed abnormal growth of the renal medulla and papilla as well as thickening of the vascular wall of the kidney accompanied with inability to concentrate urine (Cole et al., 2000).

Another major function for ACE is to degrade bradykinin into inactive metabolite; BK-(1-7) and further to BK-(1-5)(Dorer, Kahn, Lentz, Levine, & Skeggs, 1974). Bradykinin is a vasoactive nonapeptide that is released from the plasma kininogens and binds to bradykinin 2 (B2) receptors causing the release of nitric oxide (NO), prostacyclin, endothelium-derived hyperpolarizing factor (EDHF) and tissue plasminogen activator, which provokes protective effects on the cardiovascular system including vasodilation, regulation of coagulation, fibrinolysis, and electrolyte homeostasis (Ancion, Tridetti, Nguyen Trung, Oury, & Lancellotti, 2019). Bradykinin 1 (B1) receptors are normally expressed at very low levels, however, once activated, they could also play a significant role in inflammation via enhancing NO production (J. M. Hall, 1992).

Angiotensin converting enzyme inhibitors (ACE I) have been widely used clinically to treat high blood pressure in hypertensive patients. The initial goal in hypertensive patients is to manage blood pressure levels that might be achieved via using a combination of blood pressure lowering drugs such as diuretics, ACE I, calcium channel blockers, beta blocker and angiotensin receptor blockers (ARBs) (Lopez-Sendon et al., 2004) . ACE I's exert antihypertensive effects via reducing Ang II production and increasing the vasodilator bradykinin. ACE I's are also considered the first-line therapy for the treatment of heart failure with reduced left ventricular systolic function (left ventricular EF <40–45%) (Lopez-Sendon et al., 2004). ACE I's are beneficial in managing other cardiovascular disease including AMI, diastolic heart failure, asymptomatic left ventricular systolic dysfunction, prevention of sudden cardiac death, and reduction in the primary stroke (Lopez-Sendon et al., 2004). ARBs are also considered in the treatment of hypertension if ACE Is are not tolerated and they are very effective in the treatment of other CVD such as LV hypertrophy and stroke (Poulter, 2010)

However, it was reported that although ACE I's are effective in reducing Ang II levels and minimizing its harmful effects in patients with cardiovascular disease, they do not completely inhibit the Ang II formation, which indicates the possibility of ACE-independent pathway for Ang I to Ang II conversion (M. Li et al., 2004). Chymase, a human mast cell protease, has been identified as another enzyme that participate in catalyzing Ang I into Ang II particularly in the interstitial compartment of the heart and blood vessels (M. Li et al., 2004). Indeed, the chymase inhibitor, SUNC8257 (Chy I), significantly reduced cardiac

Ang II levels and decreased left ventricular end-diastolic pressure and prevents cardiac fibrosis in dogs with heart failure (Matsumoto et al., 2003). Other enzymes that might be also involved in generating Ang II including cathepsin G, tissue plasminogen activator, elastase, and tonin (Schmidt, Drexler, & Schieffer, 2004). However, ACE is still the predominant enzyme for Ang II production.

1.2.3 Angiotensin II

Ang II (also named Ang-(1-8)) is an octapeptide (Asp-Arg-Val-Tyr-Ile-His-Pro-Phe) that represents the main member in the RAS and has a major role in regulating hemodynamic function and renal hemostasis. Ang II has a wide variety of effects on various body organs including vital organs such as the kidney, heart, lung and the brain. In Male Sprague-Dawley rats the tissue levels of Ang II are much higher than plasma (Campbell, Kladis, & Duncan, 1993) and the Ang II levels were also significantly higher in pig's heart than in plasma (Danser et al., 1994). Under normal physiological condition, Ang II levels in human are also present in higher amount in tissues than in plasma (Schalekamp & Danser, 2006). In case of sodium restrictions or diuretic ingestion the plasma concentration of Ang II (normal plasma levels for healthy individual is ~97pg/mL) might increase up to 10-fold and further to more than 100-fold under pathological condition (Bellomo et al., 2020; Schalekamp & Danser, 2006). The main actions of Ang II are mediated via angiotensin II type 1 receptors (AT_1R) and angiotensin II type 2 receptors (AT_2R), which are seven-transmembrane domain with only 34% similarity in their nucleic acid sequence (Y. Y. Li, Li, & Yuan, 2012). Acute stimulation of Ang II elicits effects mediated via AT_1R such as generalized vasoconstriction, regulation of sodium and water homeostasis and manipulating blood pressure, while chronic activation promotes cardiac hypertrophy and remodeling, hypertension, hyperplasia, in-stent restenosis, reduced fibrinolysis, renal fibrosis and other cardiovascular disorders (Mehta & Griendling, 2007). Ang II has been studied for decades in order to explore its biological function and deleterious effects on various body organs and Ang II chronic stimulation/ infusion are often used in experimental cell culture and animal models to promote essential hypertension and cardiac functional and structural change (Malpas, Groom, & Head, 1997; Mezzano, Ruiz-Ortega, & Egido, 2001). Ang II is forty times as potent as noradrenaline in increasing blood pressure via acting directly on AT_1R causing increased peripheral vascular resistance and electrolyte and water retention

(Rang, Ritter, Flower, & Henderson, 2020). Ang II could also elevate blood pressure indirectly via triggering aldosterone and vasopressin secretion (Sandmann & Unger, 2002). It has been reported that Ang II elicits inotropic effects directly on human myocardium as well as on hamster cardiac muscle via activating AT_1R (Moravec et al., 1990). Exposure to excessive endogenous or exogenous Ang II promotes harmful effects on myocardium via alteration of sarcolemmal permeability and myocytolysis with subsequent fibroblast proliferation or via alteration or damaging of coronary microvascular endothelial cells (I. Gavras & Gavras, 2002; L.-B. Tan, Jalil, Pick, Janicki, & Weber, 1991). Intravenous infusion of large doses of Ang II for three days caused myocardial infarction and acute renal failure with uremia accompanied with a drop in urine/serum-urea ratio in rabbit (H. Gavras, Lever, Brown, Macadam, & Robertson, 1971). Angiotensin II induced left ventricular hypertrophy via increasing vascular resistance and rising blood pressure, and stimulating protein synthesis and cell proliferation as well as triggering smooth muscle cells and blood cells to release other growth factors such as the platelet-derived growth factor (PDGF) (I. Gavras & Gavras, 2002). Another mechanism of Ang II-induced myocardial injury is via enhancing the activity of the NADH and NADPH oxidases, with subsequent formation of high amounts of reactive oxygen species leading to damage to various cellular structures including membrane and proteins (I. Gavras & Gavras, 2002). It has been reported that endogenous endothelin-1 (another potent vasoconstrictor) mediated the hypertrophic response of both Ang II and phenylephrine in neonatal rat cardiomyocytes (Xia & Karmazyn, 2004). Ang II-induced cardiac fibrosis was enhanced via chronic blockade of nitric oxide synthase activity which led to 60-fold increase in fibronectin mRNA expression as well as type III and Type I collagen production in male Wistar rats (Hou, Kato, Cohen, Chobanian, & Brecher, 1995). Angiotensin II might produce direct chronotropic effect or cardiac arrythmia via alteration of the conduction system of the heart (cardiac vagus ganglia, sinus node, and atrioventricular node) (I. Gavras & Gavras, 2002). Angiotensin II is involved in pro-inflammatory process in vascular smooth muscle cells via increasing the expression of cytokines (such as interleukin-6) and enhancing the activity of the transcription factor nuclear factor (NF)-κB, as well as the expression of P-selectin (cell adhesion protein that plays significant role in vascular leukocyte recruitment during inflammation), (I. Gavras & Gavras, 2002; Piqueras et al., 2000).

1.2.4 Angiotensin II type I receptors AT_1R

AT_1R is a G protein-coupled receptors (GPCR), with 359 amino acid residues, that mediates the majority of known classical physiological RAS functions in the cardiovascular and renal system. Upon activation by Ang II, AT_1R promotes constriction of blood vessels, thirst, release of noradrenaline from sympathetic nerve terminals, aldosterone production, and secretion from the adrenal cortex, which consequently lead to increases in peripheral vascular resistance, stimulation of proximal tubular reabsorption for salt and water, increased blood volume, and systemic blood pressure (Martini, 2004). There are two main subtypes of AT_1R in rodents; AT_1a and AT_1b (located in chromosomes 17 and 2 respectively), and they share more than 95% identity in protein structure and both have almost the same ligand binding and transduction characteristics, thus, it is not known if both receptors exert different functions in natural cells (Z. Zhu et al., 1998). However, they are different in their distribution and tissue expression. AT_1a receptors are the most abundant and expressed in many body organs including heart, brain, kidney, liver, adrenal gland, lung ovary, testes, and adipose tissue, of 6-10 week old mice, while AT_1b receptor expression is detected only in the brain, adrenal gland, and testicular tissues (Burson, Aguilera, Gross, & Sigmund, 1994). AT_1b receptor expression has not been reported in human tissues (Z. Zhu et al., 1998). There are various pathophysiological conditions that affect the expression of the AT_1 receptors e.g. upregulation of AT_1 receptors was observed in renovascular hypertension(W. Cai, Zhang, Huang, Sun, & Qiu, 2018), myocardial infarction (Busche et al., 2000), ventricular hypertrophy(Y. C. Zhu et al., 2003), hypercholesteremia (Kaschina, Steckelings, & Unger, 2018), while down regulation was reported in sepsis as the reduced AT_1R may contributes to septic shock (Kaschina et al., 2018).

Upon binding to Ang II, AT_1 receptors act via a variety of intracellular signaling pathways starting with G-protein (mainly $\mathbf{G_{\alpha q}}$) and phospholipase C activation, followed by an enhancement in intracellular inositol 1,4,5-trisphosphate (IP3) and diacylglycerol which in turn causes the release of calcium (Berry, Touyz, Dominiczak, Webb, & Johns, 2001). The production of IP_3 is markedly accelerated within a few seconds and peaks at 15 seconds, and then gradually returns to the normal levels. Next, protein kinase C (PKC) and tyrosine kinase

cascades are amplified which affect the pathway of extracellular regulated kinase 1/2 (ERK1/2)/ MAP kinase cascade and p38 as well as JAK-STAT (Janus kinase–signal transducers and activators of transcription). Some transcription factors such as activator protein 1 (AP-1), STATs, and NF-κB are also activated and promote the expression of growth related genes (Bader, 2010). Moreover, AT_1R increases ROS production via activation of NADPH oxidase which further activates other receptors such as epidermal growth factor receptor (EGFR) in the plasma membrane and mineralocorticoid receptor leading to constriction of vascular smooth muscle and increased systemic BP as well as vascular remodeling and endothelial dysfunction (Bader, 2010; Welch, 2008). AT_1R mediated Ang II-induced cardiac hypertrophy in neonatal rat cardiomyocytes occurs via induction of the immediate/early genes such as; Egr-1, c-fos, c-jun, jun B, and c-myc, and other hypertrophy markers that are expressed later, within 6 hours, such as atrial natriuretic factor (ANF) and skeletal alpha-actin(Sadoshima & Izumo, 1993). Ang II increased the gene expression of angiotensinogen and TGFB-1 (transforming growth factor-beta 1) in NRCM which was inhibited by selective AT_1R blocker (losartan)(Sadoshima & Izumo, 1993). Moreover, losartan inhibited both early (immediate-early gene induction) and late (fetal-type gene induction) hypertrophy markers in response to stretch-induced cardiac hypertrophy in NRCM (Sadoshima, Xu, Slayter, & Izumo, 1993). However, while some studies reported that AT_1R induced cardiac hypertrophy directly via activation of heterotrimeric G proteins particularly Gαq/Gαi in the heart (Molkentin & Dorn, 2001), other studies suggested that AT_1R initiates hypertrophy through $G_\alpha q$- or $G_\alpha i$-independent mechanisms (Zhai et al., 2005). Overexpression of an AT_1R mutant lacking heterotrimeric G proteins via adenoviral vector showed severe cardiac hypertrophy and bradycardia accompanied with impaired cardiac function, but less apoptosis and fibrosis than overexpression of wild-type AT_1R, an effect that was further enhanced upon Ang II infusion in mice (Zhai et al., 2005). ß-arrestin is a signaling protein that functions to desensitize GPCRs response (Iaccarino & Sorriento, 2018) . Recent studies suggested that mechanical stress directly and specifically activates ß-arrestin–biased signaling of AT_1Rs via allosterically stabilizing a unique ß-arrestin–biased AT_1R conformation (Jialu Wang, Gareri, & Rockman, 2018). However, it has been reported that internalization of most of the GPCRs is mediated via ß-arrestin and dynamin-dependent mechanisms via clathrin-

coated vesicles (Gáborik et al., 2001). Induction of chronic pressure overload via TAC (transverse aortic constriction: a common experimental model used to induce pressure overload, cardiac remodeling and heart failure (Kuang et al., 2013)) in AT_1R knockout and WT mice showed similar cardiac hypertrophy and remodeling for both groups, but significantly reduced cardiac arrythmia and left ventricular tachycardia in AT_1R knockout group which suggested a direct role of AT_1R in arrhythmogenicity in hypertrophied hearts (Yasuno et al., 2013). Whether or not AT_1 receptors have a direct role in inducing cardiac hypertrophy has been recently investigated in a mouse line with cell-specific deletion of AT_1a receptors from the heart and vascular smooth muscle. The study suggested that AT_1a receptors promotes cardiac hypertrophy primarily indirectly via increasing peripheral blood pressure while its direct activation has minimal influence in cardiac myocyte hypertrophy (Sparks et al., 2021). However, other reports indicated that AT_1R induced direct cardiac hypertrophy, fibrosis and dysfunction in the absence of systemic blood pressure changes in mice (Ainscough et al., 2009). AT_1 receptor blockers have been used clinically in the treatment of hypertension and other cardiovascular diseases and they have advantage over ACE inhibitor as they completely inhibit the effect of Ang II with less side effect (Johnston, 2000). Dry cough is a very common side effect associated with ACE inhibitors (E. C. Li, Heran, & Wright, 2014). Furthermore, the inhibition of ACE can affect other substances such as bradykinin, beside the fact that ACE inhibitors are not able to block Ang II production mediated by other enzymes, while some ARBs (such as candesartan) are selectively and noncompetitively binding to AT_1R providing more blockade of the negative cardiovascular effects of Ang II (Johnston, 2000).

1.2.5 Angiotensin II type II receptors AT_2R

The AT_2R is also a seven transmembrane GPCR that is located on chromosome X in human with 363 amino acids and 41 kDa molecular weight, and is 34% identical in amino acid sequence to AT1R (Mukoyama et al., 1993). Fetal tissues widely express AT_2R particularly in the heart and aorta while other organs such as brain, liver, kidney and lung express AT_2R at average levels which indicate a role for this receptor in fetal development(Shanmugam & Sandberg, 1996). In the fetal kidney AT_2R expression was mainly detected in mesenchymal tissues, while in adult kidney AT_2R was expressed in adventitia of the arcuate and

interlobular arteries and the renal capsule (Kaschina, Namsolleck, & Unger, 2017). Some reports indicated that AT_2R could be detected in glomerular as well (Kaschina et al., 2017). In the rat fetus, the expression of AT_2R was detected as early as 14 days of gestation and the maximum expression was observed between 19 and 21 days of gestation which was followed by a dramatic decrease (within 12 hours) after birth (Shanmugam & Sandberg, 1996). In adult rat the expression of AT_2R is limited to some organs including heart, kidney, brain, skin, adrenal, atretic ovarian follicles, and uterine myometrium (Riet, Esch, Roks, van den Meiracker, & Danser, 2015). However, the gene expression of AT_2R can be markedly increased in pathological setting such as myocardial infarction (Y.-C. Zhu, Zhu, Gohlke, Stauss, & Unger, 1997). AT_2R belongs to the protective arm of the RAS as it counteracts many actions of AT_1R in cardiovascular system. AT_2R exerts antihypertrophic effects, antiproliferative effects, promotes apoptosis, and maintains blood pressure via controlling vascular tone through vasodilation (Dasgupta & Zhang, 2011). In rat mesenteric artery segments stimulated with Ang II , AT_2R mediated vasodilation via local production of bradykinin in a flow-dependent manner (Katada & Majima, 2002). Moreover, overexpression of AT_2R in C57BL/6 (AT_2-TG) mice inhibited AT_1R-mediated pressor effects in response to chronic Ang II infusion, an action that was abolished by a B2 receptor inhibitor (icatibant), and by NO synthase inhibitor (l-NAME) suggesting that AT_2R promotes vasodilation through increase bradykinin production which stimulates the NO/cGMP system (Tsutsumi et al., 1999). AT_2-TG mice infused with Ang II showed significantly decreased blood pressure response compared to WT mice, an effect that was blocked by an AT_2R antagonist, PD123319 (Masaki et al., 1998). This reduction in blood pressure in AT_2-TG mice caused by strong negative chronotropic effect mediated via AT_2R. In hearts isolated from AT_2-TG mice and perfused using a Langendorff apparatus, AT_2R promoted negative chronotropic effects and inhibition of Ang II–induced activity of mitogen-activated protein kinase (MAPK) as well as attenuating the sensitivity of pacemaker cells to Ang II (Masaki et al., 1998). The AT_2R plays an important role in controlling sympathetic tone through promoting inhibitory effects. Overexpression of AT_2R via adenoviral vector in the rostral ventrolateral medulla of male Sprague-Dawley rats significantly decreased the nocturnal arterial blood pressure and noradrenalin excretion and induced diuresis, actions that might be mediated via sympathoinhibition (Gao et al., 2008). It has been reported that AT_2R exerts a

protective effect in vascular injury via inhibition of neointima formation, cell proliferation and inflammation (Dasgupta & Zhang, 2011). In AT_2R-null (-/-) mice, the survival rate after AMI, induced by coronary artery ligation, was significantly lower than WT (43% versus 67%) respectively, and significantly higher levels of brain natriuretic peptide BNP mRNA expression were observed in AT_2R-/- mice (Adachi et al., 2003). In addition to Ang II, AT_2R can be activated by Ang III (Carey, 2017), Ang-(1-7), Ang-(1-9) (McKINNEY, Fattah, Loughrey, Milligan, & Nicklin, 2014) and potentially Ang A (Jankowski et al., 2007).

Despite being classified as a GPCR and maintaining key amino acid residues found in most GPCR, AT_2R signaling pathway is clearly different from AT_1R. In COS-7 cells, AT_2R did not increase IP3 production neither intracellular calcium, and there was no significant changes observed in cAMP and cGMP levels and phosphatase activity (Mukoyama et al., 1993). However, AT_2R can activate protein phosphatases leading to protein dephosphorylation and increase phospholipase A2 and release of arachidonic acid (Lemarié & Schiffrin, 2010).

1.2.6 The Counter-Regulatory axis of the Renin Angiotensin System

The historic treatment of cardiovascular disease has been focused on the inhibition/blocking of the classical RAS signalling pathway through ACE/AT_1R, however, the discovery of the counter-regulatory axis of RAS signalling via ACE2/Mas receptor has given a new insight in targeting the RAS (McFall, Nicklin, & Work, 2020). Classically, renin cleaves angiotensinogen to produce Ang I which will be converted to Ang II by ACE. Ang II binds to either AT_1R or AT2R with the same affinity to exert the known physiological function of RAS. However, The counter-regulatory or (non-canonical) axis of RAS consist of Ang-(1-7), angiotensin-(1-9) (Ang-(1-9)), angiotensin converting enzyme 2 (ACE2), AT_2R, and Mas receptor (Paz Ocaranza et al., 2020). In 2000, the identification of ACE2 was one of the most interesting findings in the field of cardiovascular disease pharmacology (Donoghue et al., 2000). The main action of ACE2 is to catalyze the conversion of Ang II to Ang-(1-7) which is a protective enzyme that binds to Mas receptor causing reduced blood pressure and noradrenalin release (Paz Ocaranza et al., 2020). It has been reported that ACE2 can also degrade Ang I into Ang-(1-9) which is another peptide that signals through AT_2R to stimulate natriuresis and NO production causing vasodilation (Paz Ocaranza et al., 2020). ACE2 is the primary enzyme that degrades Ang II to produce Ang-(1-7) and that

the counter-regulatory axis of RAS mainly refers to ACE2/Ang-(1-7)/Mas1 receptor axis. Prolylcarboxypeptidase (PRCP) is another enzyme that is implicated in catalyzing the conversion of Ang II to Ang-(1-7). The optimal enzyme activity of PRCP occurs at acidic pH. However, there is little information available about PRCP role in cardiovascular pathophysiology despite being identified much earlier than ACE2 (H. Y. T. Yang, ErdÖS, & Chiang, 1968). Cathepsin G can also degrade Ang II into inactive fragments which may participate in reducing the unwanted effect of Ang II (Ramaha & Patston, 2002) .

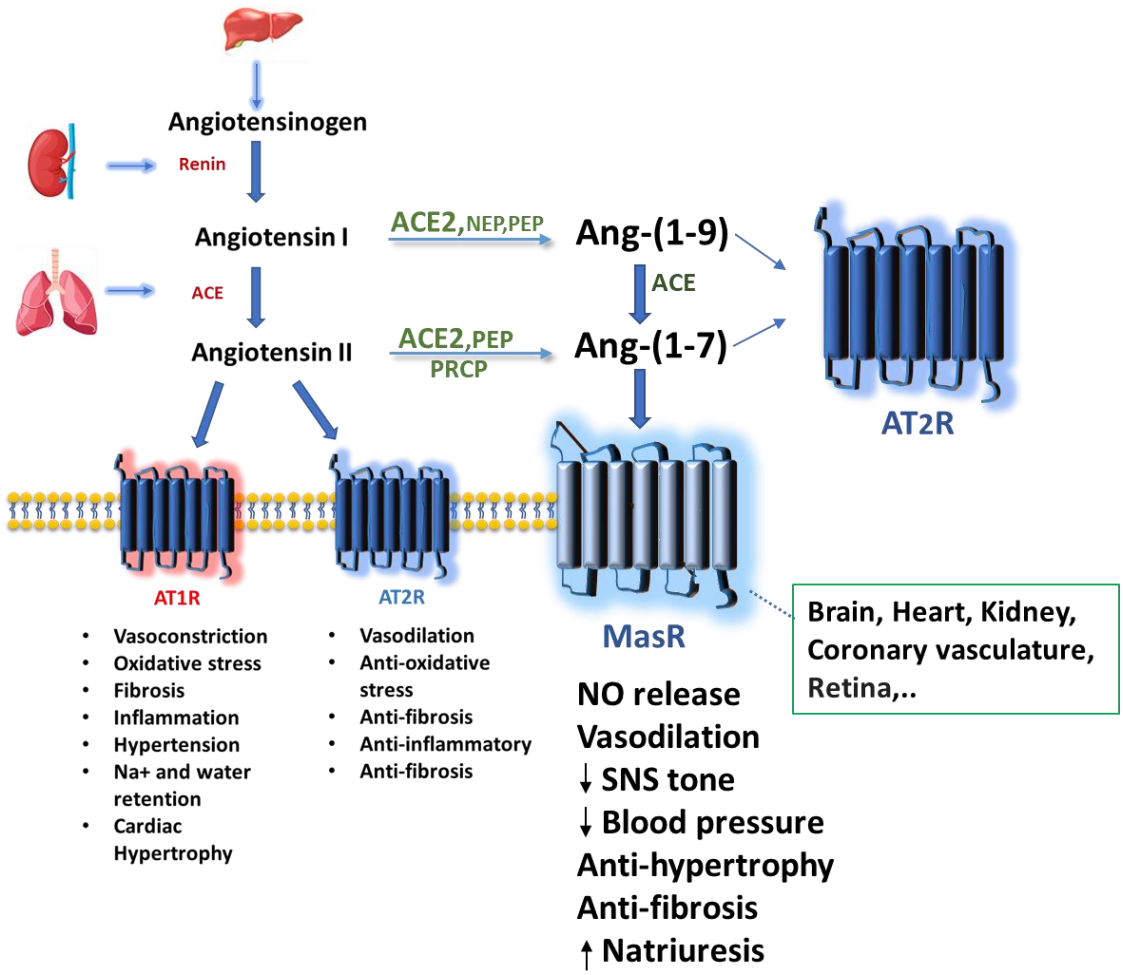

Figure 1.3 The counterregulatory axis of RAS

The counter regulatory axis of RAS involved conversion of Ang I to Ang-(1-9), and Ang II to Ang-(1-7). Ang I is metabolized to Ang-(1-9) mainly by ACE2. Ang-(1-9) can bind to AT_2R to provoke vasodilation and antihypertrophic effects or it is converted by ACE into Ang-(1-7) which binds to Mas1R to enhance NO release leading to vasodilation, antihypertrophic and anti-hypertensive effects. Ang I is also cleaved by neutral endopeptidase (NEP) and prolyl endopeptidase (PEP) to yield Ang-(1–9). Ang II is metabolized mainly by ACE2 into Ang-(1-7) that works on MasR to exert effects that oppose AT_1R actions. Prolylcarboxypeptidase (PRCP) and PEP also can degrade Ang II into Ang-(1-7) but with lower catalytic efficiency than ACE2 (Brosnihan et al., 2004).

1.2.6.1 Angiotensin Converting Enzyme2 (ACE2)

1.2.6.1.1 ACE2 structure and distribution

ACE2, also named ACEH, is a human zinc metalloprotease that was first cloned from a human heart failure tissue and lymphoma cDNA libraries in 2000 by two independent groups, and named due to high similarity to ACE gene structure with 40% or 42% identity to the N- and C-terminal domains of mammalian ACE (Donoghue et al., 2000; Tipnis et al., 2000). Genomic assessment for ACE2 sequence showed that it has 18 exons that were located in chromosome Xp22, the HEXXH motif (zinc binding site) is located in exon 9 and the full length of human ACE2 protein is 805 amino acid which is similar to mice and rat ACE2 length (Burrell, Johnston, Tikellis, & Cooper, 2004). Like ACE, ACE2 is a type I transmembrane glycoprotein where the N-terminus is the extracellular/luminal part of the protein with 17 amino acid signal sequence, and the C-terminus comprises the cytosolic region of the membrane protein (Tipnis et al., 2000). While ACE contains two active catalytic sites, ACE2 functions as a mono-carboxypeptidase with one active domain, as it can cleave exclusively the C-terminal residues from both Ang I and Ang II forming Ang-(1-9) and Ang-(1-7) respectively. ACE2 has 7 potential N linked glycosylation sites and is therefore likely to be glycosylated and the molecular mass of glycosylated ACE2 is ~120 KDa while the deglycosylated form migrates at approximately 85 KDa (Tipnis et al., 2000). In vitro investigation revealed that the catalytic efficiency of ACE2 for Ang II is 400-fold higher than for Ang I, and ACE2 activity could be completely inhibited by 10mM of EDTA (Ethylenediaminetetraacetic acid), but not by classical ACE inhibitors (Huang et al., 2003; Tipnis et al., 2000).

Early analysis of ACE2 distribution showed it has more specific tissue-expression compared to ACE, as ACE2 was expressed only in 3 human organs (heart, kidney and testes) out of 23 examined, while ACE mRNA was detected in 16 human tissues (Donoghue et al., 2000). Tipnis et al. 2000 was able to detect ACE2 mRNA expression at moderate levels in colon, small intestine, and ovary. Later investigators reported more tissue expression of ACE2 mRNA including: bronchus, lung parenchyma, and the gastrointestinal system tissues including ileum, duodenum, jejunum, caecum, and colon. Interestingly, the expression of ACE2 is greater in gastrointestinal tissues, particularly in ileum and duodenum, compared to cardiovascular system, while there was limited expression of ACE2

in the central nervous system and lymphoid tissues (Harmer, Gilbert, Borman, & Clark, 2002). More recent reports revealed that ACE2 is expressed nearly in all human organs in different levels (Ni et al., 2020).

1.2.6.1.2 ACE2 physiological function

ACE2 has multiple functions that relate to its expression and activation state in various body organs. The first reported function for ACE2 was the catalyzing of Ang I to Ang-(1-9) via removing the single C-terminal Leu residue which could be further converted to Ang-(1-7) by ACE(Donoghue et al., 2000). Ang-(1-9) was first identified in rat and human plasma and it can competitively inhibit ACE (Donoghue et al., 2000). However, ACE2 has higher affinity to Ang II than Ang I and it is more potent in catalyzing Ang II to produce the cardioprotective peptide Ang-(1-7) which is the principle function of ACE2(Ferrario, Italia, & Varagic, 2020). Despite high structural similarity to ACE, ACE2 counteracts the ACE function via negatively regulating Ang II levels and hence, provides a protective effect in cardiovascular system. ACE2 null mice exhibited high Ang II levels, impaired cardiac contractility, and upregulation of hypoxia-induced genes (BNIP3, PAI-1) in the heart compared to control (Crackower et al., 2002). This observation was associated with significant decline in fractional shortening percentage and higher left ventricular hypertrophy in those animals, an effect mediated by Ang II (Crackower et al., 2002). In 2003, another major function for ACE2 was identified which was acting as the main functional receptors for coronaviruses, including the coronavirus that causes severe acute respiratory syndrome (SARS-CoV) infection, and the most recent COVID-19 infection, and is involved in mediating virus entry and cell fusion (Wenhui Li et al., 2003). Other substrates for ACE2 includes des-Arg9 -bradykinin (B1 receptor agonist), apelin-13 (a vascular tone controller), and other peptides such as kinetensin (a neurotensin-like peptide), dynorphin A (an agonist kappa receptor) and neurotensin (Danilczyk & Penninger, 2006). Studies have shown ACE2 is protective in different tissues, for example overexpression of ACE2 via adenoviral gene therapy exerts protective effect in diabetic (*db*/*db*) mice via prevention of ß-cell dysfunction and apoptosis developed in type 2 diabetes, an effect inhibited by Ang-(1-7) receptor blocker (d-Ala^{7}–Ang-(1-7)) (Bindom, Hans, Xia, Boulares, & Lazartigues, 2010).

In the lung, Ang II exerts harmful effect including vasoconstriction, inflammation and proliferation which participate in the development of pulmonary atrial hypertension (PAH) (Shenoy, Qi, Katovich, & Raizada, 2011). Overexpression of ACE2 in the lung via lentiviral vector decreased monocrotaline (MCT)-induced increase in right ventricular systolic pressure and attenuates right ventricular hypertrophy in animal model of PAH and lung fibrosis (Shenoy et al., 2011).

In the small intestine, ACE2 also showed high expression where it plays a pivotal role in regulating amino acid transport and link diet to the composition of the gut microbiome (Perlot & Penninger, 2013).

1.2.6.1.3 ACE2 as a therapeutic target for CVD

Accumulating reports indicated that ACE2 plays an important role in cardiovascular homeostasis, and loss of ACE2 or altered expression is associated with impaired cardiac and vascular function, especially in the case of pathological conditions. For instance, four-week old ACE2 deficient mice displayed increased heart weight, coronary artery thickening, perivascular fibrosis, cardiac expression of collagen and TIMP as well as greater TGF-ß mRNA expression which suggests a crucial role for ACE2 in the development of the postnatal heart (Moritani et al., 2013). Another investigation was consistent with aforementioned Crackower study, showed that Ang II infusion at 1000 ng/kg per min, into ACE2 knockout (KO) mice for 4 weeks led to significant reduction in ejection fraction and fractional shortening percentage accompanied with hypertrophic cardiomyopathy shown by increased in heart/body weight ratio, increased left-ventricular wall thickness, as well as enhanced cardiac fibrosis and oxidative stress in the myocardium and aorta in comparison to WT(Alghamri et al., 2013). However, ACE2KO mice and wild type mice both showed high blood pressure in response to long term Ang II infusion despite the significant cardiac functional and structural change between groups and that might be related, partially, to the fact that ACE2 was not detected in the plasma of WT mice and the fact that Ang II could be catalyzed by ACE2 independent pathway (Alghamri et al., 2013; Elased, Cunha, Gurley, Coffman, & Morris, 2006). Conversely, overexpression of ACE2 via lentiviral gene transfer (Lenti-ACE2) in the spontaneously hypertensive rat (SHR) significantly attenuated blood pressure, left ventricular wall thickness and perivascular fibrosis compared to SHR received control virus (Díez-Freire et al., 2006). Furthermore, recombinant

human ACE2 (rhACE2) markedly attenuated Ang II-mediated myocardial hypertrophy, superoxide production, fibrosis and diastolic dysfunction (J. Zhong et al., 2010). Inhibiting the production of Ang II by ACEi (Enalapril) or its actions by Ang II receptor blocker (Losartan) has been shown to increase ACE2 transcription and translation in MI-induced cardiac hypertrophy in adult Sprague Dawley rats (M. a. P. Ocaranza et al., 2006; Jingwei Wang, Guo, & Dhalla, 2004).

However, prolonged (11 week) and efficient overexpression of ACE2 via adeno-associated viruses 6 (AAV6) mediated gene transfer into myocardium of SHRSP led to sever cardiac fibrosis and dysfunction showing by reduced ejection fraction and fractional shortening (Masson et al., 2009). These detrimental effects in cardiac function and structure occurred despite attenuated high blood pressure in SHRSP received ACE2. This low BP in SHRSP might be due to the beneficial effect of ACE2 in converting Ang II to Ang-(1-7) in the peripheral circulation and the consequent vasodilation, or it could be caused by severe cardiac dysfunction and fibrosis following sustained ACE2 overexpression (Masson et al., 2009). Collectively, these data highlighted the crucial role of ACE2 in cardiovascular pathophysiology.

1.2.6.1.4 ACE2 as the main entry receptor for COVID-19 infection

ACE2 has gained more attention recently due its role in coronaviruses infections particularly SARS-CoV-2(O. Paul & Chatterjee, 2021). By the end of 2019, SARS-CoV-2 has become a global pandemic and ACE2 acts as the main entry receptors for SARS-CoV-2 into the human body which is a fundamental step in the process of the virus infection (Ni et al., 2020). It has been reported that SARS-CoV-2 can invade only ACE2 expression cells/tissues with binding affinity between SARS-CoV-2 to ACE2 more than 10-20-fold change compared to SARS-CoV to ACE2. The mechanism of viral entry into the host cell involved binding of the spike glycoprotein on the virus to the tip of subdomain I of ACE2 to activate the membrane fusion of the virus and the host cell. Then, infection is promoted via releasing viral RNA into the cytoplasm. However, the active catalytic domain of ACE2 is not affected by spike glycoprotein (Ni et al., 2020). Another study suggested more steps in SARS-CoV-2 entry to host cells including of the spike protein into ACE2 receptor and then the host cell cleaves the spike protein at two sites by a cell protease; furin that cleaves at a polybasic site, producing the S1 and S2 subunits, and the second cleaving site located immediately upstream

of the hydrophobic fusion peptide which is mediated by transmembrane serine protease 2 (TMPRSS2) and related proteases (Keller, Böttcher-Friebertshäuser, & Lohoff, 2022).

1.2.6.2 Angiotensin-(1-7)

Ang-(1-7) is a main member in the counter regulatory arm of RAS. Ang-(1-7) is a heptapeptide that can be produced via enzymatic degradation of either Ang I or Ang II. It can be generated directly from Ang I by various endopeptidases including neprilysin (NEP), prolyl-endopeptidase, and thimet oligopeptidase (TOP) (LJ Wang et al., 2005). Ang-(1-7) can be also produced indirectly from Ang I through its metabolism to Ang-(1-9). ACE2 converts Ang I to Ang-(1-9) which can be further degraded into Ang-(1-7). It has been reported that incubation of Ang-(1-9) with neonatal rat cardiomyocytes (NRCM), that produce ACE, generated Ang-(1-7) and Ang-(1-5) as well as Ang-(1-4) by cleavage of C-terminal dipeptides (Donoghue et al., 2000). Ang-(1-7) can be also synthesized from Ang II by the action of three enzymes: ACE2, prolyl carboxypeptidase (PRCP), and prolyloligopeptidase (POP). The conversion of Ang II to Ang-(1-7) by ACE2 is almost 500-fold more efficient than the catalysis of Ang I to Ang-(1-9). Furthermore, it has been indicated that the catalytic efficiency of ACE2 is 600-fold greater than PRCP in converting Ang II to Ang-(1-7), and 10-fold higher than prolyloligopeptidase in catalyzing the same reaction (Brosnihan et al., 2004). However, the role of or the crosstalk between these enzymes in catalyzing Ang II to Ang-(1-7) still needs further investigations. Some reports indicated multiple factors that may affect the efficiency of the enzyme-catalytic reaction such as the surrounding pH and the enzyme tissue distribution (N. Grobe et al., 2013; P. Serfozo et al., 2020), For more details see (section 3.3).

The half-life of Ang-(1–7) in the circulation is approximately 10 seconds and the average normal concentration in healthy human is 20.1 (pg/mL)(Vilas-Boas et al., 2009). Ang-(1-7) acts on Mas receptor to produce cardioprotective effect and oppose Ang II actions in the heart and blood vessels. It is distributed throughout cardiomyocytes in healthy heart tissue of the Lewis rat strain and its expression increased during ischemic cardiomyopathy (Averill, Ishiyama, Chappell, & Ferrario, 2003). Intravenous infusion of Ang-(1-7) by osmotic minipumps for 8 weeks in the development of heart failure in rats resulting from MI showed preserved cardiac function, attenuated myocyte hypertrophy, preservation of

coronary flow, and aortic endothelial function in comparison to saline infusion group (Loot et al., 2002). Furthermore, Ang-(1-7) attenuated Ang II-induced cardiac hypertrophy via activation of the ANG-(1–7)/Sirt3 signaling pathway in rats model (Guo et al., 2017). It has been also reported that Ang-(1-7) protects against neointima formation after stent implantation in rats (Langeveld, Van Gilst, Tio, Zijlstra, & Roks, 2005). It has been also reported that circulating Ang-(1-7) increased during pregnancy (Brosnihan et al., 2004) and that may explain "partially" the lower sensitivity to high dose of Ang II infusion (1000 ng/kg/min) in pregnant SHRP rats (Morgan et al., 2018). These effects suggested the importance of Ang-(1-7) in cardiovascular protection.

Alamandine is one of the recent recognized peptide that belong to the counter regulatory arm of RAS and is synthesized via decarboxylation of the *N*-terminal aspartic acid of Ang-(1-7) to alanine (Villela, Passos-Silva, & Santos, 2014).

1.2.6.3 Mas receptor

Mas was described as the most complex GPCR, with seven hydrophobic transmembrane domains, that is expressed predominantly in the brain(particularly piriform cortex, hippocampus, forebrain, and olfactory bulb) and testis as it might be involved in the development of these organs (Alenina, Böhme, Bader, & Walther, 2015; Metzger et al., 1995). Mas protooncogene was also expressed in the cardiac fibroblasts (Iwata et al., 2005), cardiomyocyte(R. A. Santos et al., 2006), and the coronary vasculature(Sampaio et al., 2007), and was detectable in the kidney as well (Metzger et al., 1995). Mouse Mas gene is mapped to chromosome 17 (Metzger et al., 1995), while human and rat Mas genes are located in chromosomes 6 and 1 respectively (Alenina et al., 2015). The discovery of a selective antagonist of Mas receptors (A-779) or [Asp^1-Arg^2-Val^3-Tyr^4-Ile^5-His^6-D-Ala^7], provided a significant proof for the presence of the Ang-(1-7) Mas receptors (MasR) and that they are distinct from other angiotensin receptors (Ambühl, Felix, & Khosla, 1994; R. A. Santos et al., 1994). A radioligand-binding study in a kidney section of Mas-knockout mice showed that the binding of ^{125}I-Ang (1–7) was absent, while Mas WT group revealed low-level of ^{125}I-Ang (1–7) binding which was consistent with previous reports of low Mas mRNA expression in murine kidney (R. A. Santos et al., 2003). Moreover, high binding affinity of ^{125}I-Ang-(1–7) was observed in Chinese hamster ovary (CHO)

cell line transfected with Mas receptor. This binding affinity was abolished by MasR blocker A-779 (R. A. Santos et al., 2003).

Upon stimulation with Ang-(1-7), HEK 293T cells transfected with Mas1R showed increases in Akt and ERK 1/2 activation, and the internalization of Mas receptor occurs by either clathrin-coated pits (CCP) and/or caveolar pathways in a dynamin-dependant pathway (Cerniello et al., 2017). Co-transfection of HEK 293T cells with the dominant negative for dynamin or the dominant negative for Eps15Δ95/295 (Eps15)(a protein that involved in the Mas1R endocytosis via CCP) inhibited Ang-(1-7)-induced Akt phosphorylation (Cerniello et al., 2017). The inhibition of B-arrestin2 by shRNA attenuated ERK 1/2 activity resulting from Ang-(1-7) stimulation which indicated that this activity was mediated by B-arrestin2. After 30 minutes inside the cells, Mas1R was recycled back into the plasma membrane via binding to Rab 11 (a slow recycling vesicle), but not Rab 4 (fast recycling vesicles) (Cerniello et al., 2017). Another study on Mas-transfected CHO cells and stimulated with Ang-(1-7) demonstrated that Ang-(1-7) caused increased arachidonic acid release in a dose-dependent manner, an action that was inhibited by MasR antagonist A-779 (R. A. Santos et al., 2003).

Cultured endothelial cells of both human and animal (bovine and porcine) are capable of generating Ang-(1-7) from its precursor Ang I via an ACE-independent pathway (R. Santos, Brosnihan, Jacobsen, DiCorleto, & Ferrario, 1992). Ang-(1-7)-induced endothelial NO synthase (eNOS) phosphorylation and NO release in endothelial cells causing vasodilation (Sampaio et al., 2007). This action was mediated via Mas receptor (as verified by using MasR antagonist, A-779) and involved the activation of Akt pathways (Sampaio et al., 2007).

In the heart, chronic (4 week) infusion of Ang II in Sprague-Dawley rats caused significant increase in blood pressure, myocardium fibrosis and myocyte hypertrophy, all except blood pressure, was attenuated by co-infusion of Ang-(1-7) via acting on Mas receptors (Justin L. Grobe et al., 2007). Higher levels of collagen types I and III and fibronectin were observed in the hearts of both adult and neonate Mas-knockout ($Mas^{-/-}$) mice compared to WT (Gava et al., 2012). This was accompanied with higher expression of protein kinases such as p38 and ERK1/2 MAP kinase in neonatal and adult $Mas^{-/-}$ mice hearts which suggested that Ang-(1-7)/Mas axis could be involved in the regulation of extracellular

matrix proteins via acting on the regulation of MAP kinase activity (Gava et al., 2012). Another report suggested that Ang-(1-7) attenuated Ang-II induced cardiac hypertrophy and fibrosis in Sprague-Dawley rats via inhibiting the phosphorylation of both MAPK kinase proteins (ERK1 and ERK2) (McCollum, Gallagher, & Tallant, 2012). The dephosphorylation of MAPK kinase proteins by Ang-(1-7) was possibly due to upregulation of DUSP-1 dual-specificity phosphatase-1 (McCollum et al., 2012). Moreover, Ang-(1-7) inhibited Ang II-induced endothelin-1 (ET-1) and leukemia inhibitory factor (LIF) mRNA expression in adult rat cardiac fibroblasts (ARCFs) (Iwata et al., 2005). It has been previously reported that cardiac remodelling in heart failure is associated with elevated levels of transforming growth factor beta-1 (TGF-β1) (Peterson, 2005). Ang-(1-7) diminished TGF-β1 mRNA expression levels induced by Ang II in ARCFs (Iwata et al., 2005), and co-infusion of Ang-(1-7) reduced circulating TGF-β1 expression in adult Sprague-Dawley rats by approximately 40% (Justin L. Grobe et al., 2007).

1.2.6.4 Angiotensin-(1-9)

Angiotensin-(1-9) (Ang-(1-9)) is a nonapeptide with 9 amino acids that results from hydrolysis of Ang I by ACE2(Keidar, Kaplan, & Gamliel-Lazarovich, 2007). Other enzymes contribute to Ang-(1-9) production from Ang I include carboxypeptidase A (CxA) and cathepsin A (Jackman et al., 2002; M. P. Ocaranza et al., 2014). Reports indicated that Ang-(1-9) levels decreased in the circulation in the case of hypertension and heart failure and increased in the plasma under ACE inhibition and AT_1R blocker conditions (M. P. Ocaranza et al., 2014). Studies indicated that Ang-(1-9) plays a role in regulating cardiac hypertrophy both in vitro and in vivo. Rats undergo coronary artery ligation (MI) and infused with Ang-(1-9) for 14 days showed significant decrease in left ventricular wall thickness (LVW), LVW/body weight ratio, and LV posterior wall thickness in comparison to untreated MI group. Ang-(1-9) also prevent the effect of MI on other hypertrophy parameters such as left ventricular end systolic diameter (LVESD), left ventricular end diastolic diameter (LVEDD), left ventricular posterior wall thickness (LVPWT), left ventricular end diastolic volume (LVEDV) and left ventricular end systolic volume (LVESV) suggesting antihypertrophic effect. However, Ang-(1-9) did not improve cardiac function parameters (left ventricular ejection fraction, LVEF, and left ventricular fractional shortening,

LVFS) and the infarct size in comparison to untreated group. Furthermore, the study also indicated that Ang-(1-9) prevented cardiomyocyte hypertrophy in vitro resulting from two stimuli: norepinephrine and IGF-1(M. P. Ocaranza et al., 2010). The cardioprotective and antihypertrophic effects of Ang-(1-9) are mediated mainly via AT_2R (Flores-Muñoz, Smith, Haggerty, Milligan, & Nicklin, 2011). Infusion of Ang-(1-9) for 4 week attenuated cardiac fibrosis by 50% in stroke-prone spontaneously hypertensive rat (SHRSP), an action that was reversed by AT_2R blocker, PD123 319 (Flores-Munoz et al., 2012). Some studies have also suggested that Ang-(1-9) can be a competitive endogenous inhibitor for ACE in rabbit lung (Snyder & Wintroub, 1986).

1.2.6.5 Prolylcarboxypeptidase (PRCP) origin and structure

The role of prolylcarboxypeptidase (PRCP) in regulating blood pressure was first reported by Yang et al in 1968 as it was reported that angiotensinase C minimized the pressor effect of Ang II by cleaving the Pro^7 -Phe^8 bond in the hydrophobic C-terminal domain. The enzyme was extracted from swine kidney lysosomal fractions and was also detected in human urine and given the name angiotensinase C or (EC 3.4.16.2) (H. Y. T. Yang et al., 1968). Human PRCP enzyme showed high homology to rat and mouse PRCP. It has been reported that PRCP is a lysosomal enzyme belonging to the single chain serine peptidase S28 family and has 496 amino acid residues with six potential N-glycosylation sites, indicating that it undergoes post-translational modifications (J. Mallela, Yang, & Shariat-Madar, 2009). The putative catalytic domain of PRCP sequence is 30-67% identical to both the serine carboxypeptidases (e.g. deamidase or lysosomal protective protein) and to the prolylendopeptidase families suggesting that PRCP may provide a potential link or relationship between those two families (F. Tan, Morris, Skidgel, & Erdös, 1993). PRCP consists of an α/ß hydrolase domain encompassing the catalytic Asp333-His411-Ser134 triad and a novel helical structural domain (SKS domain) that covers the active site. The molecular mass of PRCP is 55.8 kDa, however, initially it was reported that the enzyme has 115 KDa molecular weight in gel electrophoresis. Then during heating in the presence of urea, SDS, and 2-mercaptoethanol, PRCP dissociated into two unequal subunits based on the finding of two bands;45 KDa and 66 kDa (Odya, Marinkovic, Hammon, Stewart, & Erdös, 1978).

Further PRCP gene analysis revealed it mapped to chromosome 11q14 and contains 9 exons, the signal peptide and the pro-peptide together are 46 amino acids and encoded in the 5′ end of the 1st exon, while exon 4-9 represents the catalytic part of the gene and encode the putative active-site residues (S//D//H). The role of exons 2-4 is still unknown. Single nucleotide polymorphisms (SNPs) analysis for the PRCP gene revealed that the rs7104980 G allele was a susceptible factor for essential hypertension (EH) and can be used as a marker for EH (Y. Wu, Yang, Yang, Yang, & Xiao, 2013) .Two forms/variants of PRCP gene have been identified in humans, PRCP1 (NCBI: NM-005040) and PRCP2 (NCBI: NM_199418). PRCP2 isoform has longer transcript with extra 21 amino acid in comparison to PRCP1, however, the biological function of PRCP2 has not been identified (J. Mallela et al., 2009; Jingjing Wang, 2014).

1.2.6.5.1 PRCP distribution

Even though PRCP was first purified from lysosomes, it could also be expressed extracellularly and on the surface of the cell membrane(Jeong & Diano, 2013). PRCP protein concentration was detected in high amount in spleen, kidney cortex and to the tubular apical membrane, and lung (alveolar macrophages) followed by the esophagus, while PRCP activity was lower in aorta and left ventricle of heart (Grobe, Leiva, Morris, & Elased, 2015; Maier, Schadock, Haber, Wysocki, Ye, Kanwar, Flask, Yu, Hoit, & Adams, 2017). In the heart, PRCP is colocalized with lysosomal-associated membrane protein 1 in lysosomes (Nguyen et al., 2023). PRCP is expressed in many other organs including hypothalamus, liver, placenta, adipose tissues, and brain (Jeong & Diano, 2013). Furthermore, it has been reported that PRCP was purified from human neutrophils (a type of white blood cells) which indicated that these cells express PRCP at high levels (Kehoe et al., 2018). Plasma PRCP levels have been reported to be higher in pathological condition such as cardiovascular dysfunction, obesity, and diabetes (Kehoe et al., 2018). This wide range of PRCP distribution suggests possible multiple tissue-specific functions, with different substrates.

1.2.6.5.2 Physiological function of PRCP

PRCP cleaves the C-terminal amino acid portion of the target peptides if they contain a free carboxyl group linked to a proline as a penultimate amino acid. Moreover, PRCP prefer catalysing peptides with sequences like Xxx-Pro-Phe-OH and Xxx-Pro-Val-OH, where Xxx refers to any amino acid. It was also reported

that PRCP has an optimum acid pH, however, between 20-90% of the activity is still maintained at regular or natural pH (Kumamoto, Stewart, Johnson, & Erdös, 1981). PRCP mediates various biological functions as summarized in (Figure 1.4).

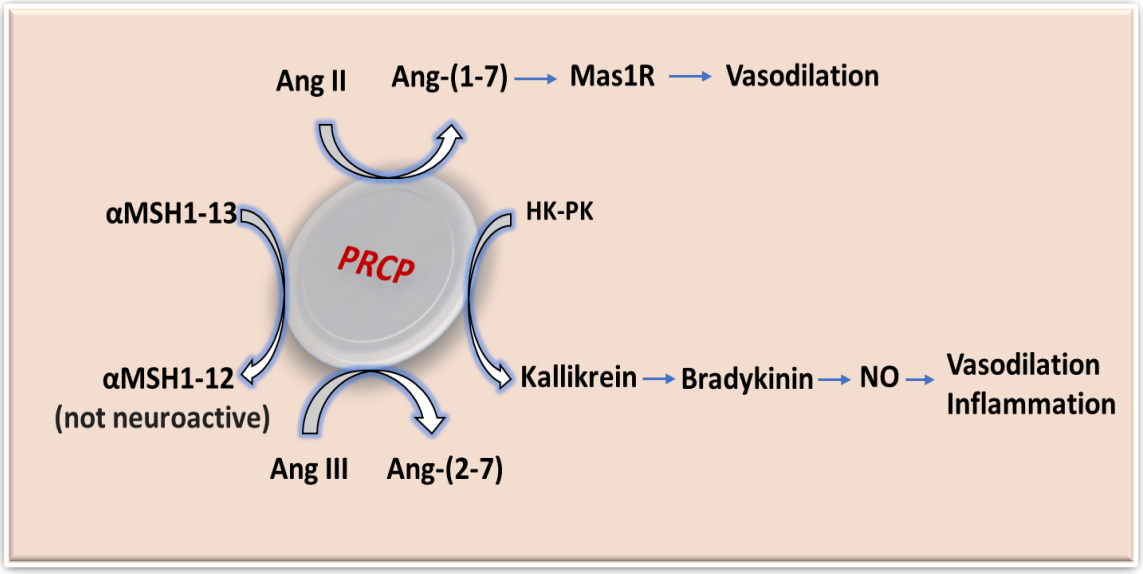

Figure 1.4 Summary of the physiological functions of PRCP.

PRCP degrades Ang II into Ang-(1-7) causing vasodilation, converts prekallikrein (PK) to active kallikrein causing release of bradykinin and release of NO leading to vasodilation and inflammation, metabolizes (α-MSH_{1-13}) into inactive form, and converts Ang III to Ang-(2-7).

Like ACE2, PRCP cleaves the C-terminal Pro^{7} -Phe^{8} bond in angiotensin II to form the cardioprotective peptide Ang-(1-7). Inactivation of Ang II results in two protective effects that PRCP exerts to the cardiovascular system. Like ACE2, first it leads to negative regulation of the classical RAS via downregulation of vasopressor Ang II levels. Second, PRCP causes endothelial relaxation via increased production of Ang-(1-7) that binds to Mas1 receptor to promote nitric oxide and prostaglandin generation leading to vasodilation. PRCP can also catalyse the conversion of Angiotensin III (des-Aspl-angiotensin II) to angiotensin-(2-7) via cleaving the C-terminal Pro^{7} -Phe^{8} bond as well, however, PRCP metabolizes Angiotensin III more readily than Ang II (Kumamoto et al., 1981).

While angiotensin-(2-7) has no known function, Angiotensin III can bind and activate both AT_1R and AT_2R (Ames, Atkins, & Pitt, 2019). Furthermore, studies reported that Angiotensin III directly promotes the secretion of aldosterone leading to increased sodium reabsorption by kidney tubules, salivary glands, and gastrointestinal mucosa(Aloul, LI, Benditt, & Tholakanahalli, 2006). However, Angiotensin III can also provide protective effect against ischemic injury via AT_2 receptor and ATP-sensitive K^+ (K_{ATP}) channels (Park, Gao, Cha, Park, & Kim, 2013).

High level production of aldosterone in Conn's syndrome (hyperaldosteronism) leads to arterial hypertension, hypokalemia, and metabolic alkalosis. In such case, inactivation of Angiotensin III by PRCP could be protective via inhibiting aldosterone secretion and decreasing blood pressure (Aloul et al., 2006). Moreover, high molecular weight kininogen (HK) serves as a receptor for prekallikrein (PK) in the cell membrane. When PK binds to HK in endothelium membrane, PRCP converts PK to the active kallikrein that liberates bradykinin which acts on B2 and B1 receptor leading to NO and PGI2 formation and consequently causing vasodilatation (J. Wang et al., 2014). Overexpression of human PRCP on Chinese hamster ovary (CHO) cells via plasmid transfection significantly increased endogenous PK activation on the cell membrane by almost 100% (Z. Shariat-Madar, Rahimy, Mahdi, & Schmaier, 2005). Bradykinin can also increase the secretion of tissue plasminogen activator which in turn metabolizes plasminogen to plasmin, that then inhibits platelet aggregation, thrombus formation and induces fibrinolysis (Pawluczyk, Patel, & Harris, 2006).

It has been reported that hypothalamic Proopiomelanocortin (POMC)-expressing neurons have been shown to possess a critical role in metabolic and energy regulation(Ibrahim et al., 2003). PRCP is expressed in different parts of the central nervous system (CNS) including hypothalamus, hippocampus and cerebral cortex. In lateral hypothalamus, PRCP is expressed in melanin-concentrating neurons (MCH) and hypocretin/orexin (Hcrt) neurons, the areas where the anorexigenic alpha-melanocyte-stimulating hormone (α-MSH_{1-13}) is released from axon terminals (Wallingford, Perroud, Gao, Coppola, Gyengesi, Liu, Gao, Diament, Haus, et al., 2009). α-MSH is a neuropeptide with thirteen amino acid residues in which the proline located in position 12 before the last valine which is in position 13, and has an important role in regulating food intake. PRCP

converts α-MSH (by removing the valine residue) to an inactive form (α-MSH_{1-12}) that has no effective role in inhibiting food intake(Wallingford, Perroud, Gao, Coppola, Gyengesi, Liu, Gao, Diament, Haus, et al., 2009). Food consumption and body weight were markedly decreased in PRCP knockout (KO) mice compared to control group (Wallingford, Perroud, Gao, Coppola, Gyengesi, Liu, Gao, Diament, Haus, et al., 2009). This data suggesting that PRCP inhibitors might be a potential therapeutic target for the treatment of metabolic disorders such as obesity and type 2 diabetes (Jeong & Diano, 2013). Furthermore, It has been reported that plasma PRCP concentration increased in human patients with obesity and diabetes mellitus as well as cardiovascular abnormalities (Xu, Lind, Zhao, Lindahl, & Venge, 2012).

PRCP activity has been detected in joints of patients with rheumatoid arthritis and in inflammatory exudates (Kumamoto et al., 1981), and upregulation of PRCP led to promotion of inflammation in the endothelium suggesting a role of PRCP in inflammation pathophysiology (J. Mallela et al., 2009). The exact mechanism of how PRCP promotes an inflammatory response has not been fully understood. However, it has been shown that α-MSH is a putative anti-inflammatory mediator via MCRs in the CNS, immune cells, and resident cells of peripheral tissues(Jeong & Diano, 2013). Therefore, due to its role in degrading α-MSH, PRCP might be a potential target for therapeutic treatment for inflammatory disease, including obesity and leptin resistance (Jeong & Diano, 2013).

Apelin receptor is a GPCR member and shares 40–50% of the hydrophobic transmembrane regions with AT_1R (Cheng, Luo, Huang, & Chen, 2019). Apelin is widely expressed in various body tissues including heart, lung, liver, kidney, and especially highly expressed in endothelial cells, and thus it might be involved in multiple physiological and pathophysiological situations. It has been reported that intravenous administration of apelin-12, apelin-13, and apelin-36 significantly reduced mean arterial BP in Wistar rats with higher potency of apelin-12 (Tatemoto et al., 2001). This effect was abolished in animal group injected with nitric oxide synthase inhibitor, N^G-nitro-l-arginine methyl ester (l-NAME) (Tatemoto et al., 2001). Furthermore, Apelin plays a role in promoting human umbilical endothelial cells (HUVEC) proliferation via activating the ERK/PI3K-p70S6K pathways(Masri, Morin, Cornu, Knibiehler, & Audigier, 2004)

and myocardial microvascular endothelial cells (MMVECs) proliferation via phosphorylation of AMP-activated protein kinase (AMPK) and endothelial nitric oxide synthase (eNOS) (J. Cheng et al., 2019). Recently, it has been shown that PRCP present on the cell membrane and in lysosomes of HUVEC can cleave (pyr)-apelin-13 at C-terminal in both HUVEC and human aortic endothelial cells (HAoEC) , while ACE2 can catalyse (pyr)-apelin-13 only in HAoEC (De Hert, Bracke, Pintelon, et al., 2021). These data reflect the potential role of PRCP in respiratory and vascular pathophysiological function via inactivation of apelin/APJ system particularly apelin-13.

1.2.6.5.3 PRCP as a therapeutic target for CVD

PRCP's role in cardiovascular pathophysiology has not been well studied even though it was identified several decades ago. Carlos et al 2013, described PRCP as a forgotten kidney angiotensinase that should be considered as an alternative pathway to regulate endogenous Ang II metabolism in the kidney. However, a growing number of studies have reported a protective role of PRCP in the vasculature. PRCP depleted mice exhibit higher reactive oxygen species (ROS) and uncoupled endothelial nitric oxide synthase (eNOS) in aortic and renal tissue as well as elevated blood pressure and a higher tendency for thrombosis formation (Adams et al., 2011). It has been shown that PRCP also contributes to reducing blood pressure via converting Ang II to Ang-(1-7) in mice (N. Grobe et al., 2013). PRCP is more efficient in catalyzing Ang II to Ang (1-7) under acidic pH, in contrast to ACE2 that is more efficient under normal or basic pH for degrading AngII in mice (N. Grobe et al., 2013). Arguably, one of the recent and more interesting studies on the role of PRCP on cardiac function has been conducted by (Maier, Schadock, Haber, Wysocki, Ye, Kanwar, Flask, Yu, Hoit, et al., 2017). The study first demonstrated that PRCP is efficient in metabolizing Ang II to Ang-(1-7) in vitro only at acidic pH. The study also reported that PRCP did not degrade Ang II in the plasma which might be explained by lack of the PRCP activity in neutral pH plasma environment. Second, cardiac function and hypertrophy were assessed by echocardiography and revealed increased left ventricular hypertrophy as early as 13 weeks in two lines of PRCP-deficient mice compared to control. Third, mean arterial blood pressure was also elevated in mice lacking PRCP which might be related, in part, to aggregation of Ang II in

the nephron leading to increased sodium reabsorption (Maier, Schadock, Haber, Wysocki, Ye, Kanwar, Flask, Yu, Hoit, et al., 2017).

Furthermore, blood samples were collected from 110 patients with ST-segment–elevated AMI and analysis revealed elevation of plasma level and activity of PRCP as well as of Ang-(1–7) and BK-(1–9) levels in comparison to healthy volunteers. PRCP exhibited a protective effect against myocardial Ischemia/Reperfusion Injury in rats by paradoxical regulation of cardiomyocyte mitophagy during the ischemia and reperfusion phases (Hao et al., 2020). These reports suggested that PRCP is a potential new therapeutic target for CVD and a gene therapy approach could be one strategy to overexpress PRCP for investigation and treatment purposes.

1.3 Gene therapy

1.3.1 Definition and background

Gene therapy is a promising and novel approach to develop new treatments for many disorders including heart disease. The concept of gene therapy is based on identifying the target gene (mutated or potential target candidate gene for overexpression or knockdown) and deliver the correct or the healthy copy of the gene using specific vectors (Wolfram & Donahue, 2013). Those vectors are either viral e.g. adenoviruses (Ad) or adeno-associated virus (AAV), or non-viral such as plasmid DNA, liposomes, and cationic lipid (Nayerossadat, Maedeh, & Ali, 2012; Wolfram & Donahue, 2013).

The American Food and Drug Administration FDA describes gene therapy as "a technique that modifies a person's genes to treat or cure disease" that works by either replacing or inactivating the disease-causing gene and introducing a new or modified gene into the patient to help treat the disease. Initially, the notion of gene therapy started in 1960 when a cell line that could be used to test the uptake and expression of a foreign DNA fragment stably and functionally was developed (Friedmann, 1992). The original concept of DNA-mediated genetic transformation derived from Avery, McLeod and McCarty studies nearly 20 years earlier as they were able to transfer genetic materials derived from a specific type of Pneumococcus (Friedmann, 1992). In 1972 Theodore Friedmann and Richard Roblin suggesting a potential role for gene therapy in treating people with genetic disease in the future. However, they were not supporting attempts in applying gene therapy to human patients at that time due to reasons including lacking adequate information about the basic mechanism of gene regulation and genetic recombination in human cells, insufficient information about acute or chronic side effects of gene therapy, and the relation between the molecular defect and the disease state was not well perceived (Neufeld & Sweeley, 1972). Later in 1990, the development of safety and availability of efficient techniques allowed for the first clinical trial of gene therapy to be conducted using retroviral-mediated transfer of the adenosine deaminase (ADA) gene into the T cells of two female patients with 4 and 9 years old diagnosed with severe combined immunodeficiency(ADA-SCID)(Blaese et al., 1995). Both patients responded positively to the gene therapy and showed significant improvement in peripheral blood T cell numbers and general body weight. After 4 years of

starting the treatment, this experiment concluded that gene transfer can be an effective and safe technique for patients with Severe combined immunodeficiency disease (Blaese et al., 1995). On October 2003, China State Food and Drug Administration awarded approval for product recombinant adenovirus (Ad-p53) injection developed by Gendicine to be the first country to approve a gene therapy based molecule for clinical use (Wirth, Parker, & Ylä-Herttuala, 2013). However, in August 2018 the US FDA has announced the first approval for a gene therapy product (Kymriah) for the treatment of leukemia in some adults and juvenile patients. Recently, more than 2000 clinical trials of gene therapy have been approved throughout the world (Crenshaw, Jones, Bell, Kumar, & Matthews, 2019).

1.3.2 Non-viral vectors

The delivery method/system represents the most important challenge in the process of gene therapy and the kind of vector used is the core for an efficient and safe strategy. It might not be plausible to find a delivery system that suits all conditions of gene therapy as the gene expression is needed in different tissues with various expression times and levels. The vector used for gene transfer must be able to overcome both extracellular barriers such as preventing particle clearance and avoiding nucleic acid degradation, and cellular barriers such as cellular uptake and lysosomal escape. Minimal or lack of the host immune response is necessary for the delivery vehicle and it would allow for repeated administration if needed. Furthermore, the safety, transduction efficiency, specificity and the duration of infection/expression should be considered for an ideal delivery vector (Gascón, del Pozo-Rodríguez, & Solinís, 2013).

Non-viral vectors are less commonly used in clinical trials due to their significantly lower transfection efficiency compared to recombinant viral vectors. However, non-viral vectors have several advantages over viral vectors including having lower immunogenicity reaction, the ability to deliver large genetic DNA fragments, more reproducible and repeated administration (due to lack of a memory immune response), cost effective and easy to produce. Small RNA delivery such as short interfering RNAs (siRNA), microRNA (miRNA) and RNA interference (RNAi) faced some challenges due to high cost and difficulty to scale up because they turn over rapidly.

Non-viral system exists mainly in two categories; physical approach such as naked DNA, electroporation, gene gun, ultrasound, and magnetoception, and chemical approach such as cationic polymers, cationic lipids, and lipid polymers (Nayerossadat et al., 2012).

Naked DNA plasmid is capable to carry genes with size range between 2-19Kb when injected directly via needle into some tissues such as skin and heart muscle, however, multiple injections are required for more efficient gene delivery. Purified plasmid DNA of B-galactosidase was cloned into the Rous sarcoma virus (RSV) long terminal repeat (LTR) promoter (*p*RSV*β*gal) and injected directly into the left ventricle wall of adult Sprague-Dawley rats(H. Lin, Parmacek, Morle, Bolling, & Leiden, 1990). The expression of B-galactosidase was observed at day 3 and lasted for at least 4 weeks post injection although it was expressed at low levels and restricted to the site of injection (H. Lin et al., 1990). Gene gun delivery or ballistic DNA transfer can be an alternative method to injection of naked DNA where gold or tungsten spherical particles encapsulating plasmid DNA and then particles are accelerated to sufficient velocity by highly pressurized inert gas to generate force to deliver genetic material into the target tissue(N. Yang, 1991). Antisense oligonucleotides are short single strands of DNA with 12-20 bases, and have been used to inhibit mRNA translation of the target protein and hence, inhibits its expression (M Ian Phillips & Kimura, 2005). Synthetic antisense oligodeoxynucleotides (ODNs) of angiotensinogen mRNA and AT1R mRNA have been injected intracerebroventricularly (I.C.V) into spontaneously hypertensive rats (SHR) showed reduction of mRNA expression of both genes in the brain as well as attenuation in blood pressure in both group of animal (Gyurko, Wielbo, & Phillips, 1993).

Chemical based vectors are the most utilized non-viral vectors for gene delivery. Cationic lipid and liposome-mediated gene transfer or lipofection are extensively studied and perhaps the most used chemical based vehicle due to possessing some advantages such as the capability to incorporate hydrophilic and hydrophobic agents, high safety, avoid triggering the immune system, and targeted delivery of genetic cargo to the site of action (Nayerossadat et al., 2012). However, the quick degradation of liposomes and the inability to maintain sustained gene delivery for long term or permanent expression are

limitations for this transfer system. These drawbacks could be improved via manipulating the liposome surface with hydrophilic polymers e.g. polyethylene glycol (PEG)(Nayerossadat et al., 2012).

Cationic lipid gained more interest recently as its being used in some of COVID-19 vaccines manufacture. Pfizer and bioNTech (Pfizer-BioNTech) as well as Moderna vaccines were developed using a lipid-nanoparticle (LNP) vector to transfer mRNA that express the RBD (trimeric form) of spike protein into the target tissue(Batty, Heise, Bachelder, & Ainslie, 2021). The vaccines have shown 94-95% efficacy in clinical trials and the vectors showed relatively high levels of safety as millions of people already received such kind of vaccines throughout the world between 2021 and 2022(Moreira Jr et al., 2022; Olliaro, 2021). LNP contains PEG lipid, ionizable lipid cholesterol and other neutral/helper lipid. At acidic pH, Ionizable lipid are cationic but they have neutral charge at normal pH. This characteristic could enable encapsulating mRNA at acidic pH and to lower toxicity at neutral pH in the physiological environment (Uddin & Roni, 2021).

Extracellular vesicles (EVs) (see section 1.4) could be considered another non-viral vector for gene therapy. Accumulating number of evidence showed that EVs can curry genetic materials efficiently to the target tissues and produce subsequent effects. EVs are characterized by having low or no immunogenicity compared to viral vectors such as adenoviral or AAV vectors (A. F. Saleh et al., 2019). Therapeutic DNA can be loaded into EVs using electroporation or/and isolated from cell culture media or biological fluids (e.g. plasma, saliva, and urine) using one of the EVs isolation method such as ultracentrifugation (Lamichhane, Raiker, & Jay, 2015).

1.3.3 Viral vectors

Viruses have traditionally been considered as a pathogen that must be controlled or eliminated. However, later, viruses have been identified as valuable agents that can be used as a vehicle in gene therapy and vaccines. Earlier in 2022, some Arabic news agencies announced that a crowdfunding campaign in Egypt has successfully secured $2.1 million to purchase a single dose of the most expensive product in the world (Zolgensma) to treat a child before turning two years old. The child was diagnosed with a serious genetic neuromuscular disorder called spinal muscular atrophy (SMA) that makes the muscles weaker and causes

problems with movement due to a mutation in survival motor neuron (SMN) gene. According to NHS, most children affected with type 1 SMA might die within the first few years, while type 2 SMA patients could survive into adulthood and may live longer. Type 3 and type 4 SMA cases are less severe and not usually affecting life expectancy. Zolgensma is a viral vector-based gene therapy, using adeno-associated virus 9 (AAV9), that transfer the missing SMN gene to the target area. Zolgensma is manufactured by Novartis Gene Therapies, Inc., and approved by American FDA in 2019 and UK NHS in 2021 to treat paediatric patients less than 2 years of age with SMA (Keeler & Flotte, 2019).

Viral vectors are the most commonly used vehicles for gene therapy as they represent more than 70% of clinical gene therapy trials worldwide due to their high efficiency gene transfer property associated with high gene expression. Viral vectors are genetically modified viruses containing genes of a virus that are partially or totally eliminated to make the vector replication deficient (such as pathogenic or replicative gene in adenovirus) and replaced by the gene of interest, while the competency of cell transduction, gene delivery and expression is retained (Walther & Stein, 2000). The first and critical step of virus infection is the attachment of viral particles to the host cells and then the virus relies on the recipient cells machinery for replicating and expressing their cargo material. The binding process required elements on the surface of both the virus (e.g capsid proteins or envelope glycoproteins) and the host cells (e.g, a glycoprotein or carbohydrate moiety). The cell surface elements (viral receptors) on the host cell-surface play an important role in defining the tissue specificity (tropism) of a virus, which in turn determine the virus pathogenic potential and/or the nature of the effect it exerts. The type of viral receptors also affect the type of organism or the host species that a virus can invade (Claude & Fauquet, 2004). Although the binding affinity between the virus particles and the host cell receptors might be low, the virus contains many binding sites that contribute to enhancing the binding affinity via multiple virus/receptor interactions. This, however, makes the viral-cells interaction highly nonselective and nonspecific which may result in high transgene expression in multiple tissues. Therefore, research has been conducted to develop suitable retargeting system for production of more selective viral vectors e.g. tropism-modified adenoviral vectors (Douglas et al., 1996).

However, even though viral vectors showed some crucial advantages, they also have some drawbacks such as high immunogenicity reaction, small or limited packaging capacity, difficulties in vector production, oncogenesis, and broad tropism. Therefore, choosing a proper viral vector for a given application rely on various factors including the target cells or tissues, tropism, in vivo or in vitro gene delivery, the capability to deliver gene of the required (or large) size, length of transgene expression, potential for genome integration, and the level of immunogenicity (Shirley, de Jong, Terhorst, & Herzog, 2020).

1.3.4 Example for viral vectors applied for gene therapy

1.3.5 Retrovirus, Lentivirus, Herps simplex virus

1.3.5.1Retrovirus

The first clinical trial for human gene therapy was conducted using retroviral-mediated gene transfer (Nabel, Plautz, & Nabel, 1990). Retroviral vector is a group of RNA viruses that replicate through a DNA intermediate and was originally derived from Molony murine leukemia virus (MMLV) and can provide site-specific gene expression that could be further refined by using tissue specific enhancer elements in the vector (Nabel et al., 1990). Retrovirus contains reverse transcriptase enzyme that produces cDNA from the RNA template for functional gene production. Retroviral vectors transduce the target cells via a specific interaction between the viral envelope protein and a cell surface receptor on the target cell. Then the virion is uncoated and introduced to the cytoplasm of host cell and the single stranded RNA reverse-transcribed into pro-viral double-stranded DNA (dsDNA) by viral reverse transcriptase inside the capsid. The dsDNA then enters the nucleus and integrates into the host genome. Mitosis, and thus the nucleus membrane disruption, is required for many types of retroviruses (except lentivirus) to enable transport into the host cell nucleus (Nisole & Saïb, 2004). Inside the nucleus, the viral integrase can randomly integrate the proviral DNA genome into the host genome where the host transcription and translation machinery increased the expression of the viral genome (Stone, David, Bolognani, Lowenstein, & Castro, 2000). The MMLV genome encodes for three polyproteins, *gag*, *pol*, and *env*, which are responsible *in trans* for viral replication and packaging. The retroviral vectors are generated by removing the *gag, pol* and *env* genes and replacing by heterologous or therapeutic genes. The MMLV genome also possesses a packaging signal (Ψ) and

cis-acting sequences, named long terminal repeats (LTRs) at each end, which play a role in regulating transcription and integration. Almost all retroviral genes are deleted from recombinant retroviral vectors and replaced with genes of interest (up to 8 kb) except LTRs and Ψ sequences which remain in the vector. For propagation purpose, it is necessary to create a cell line that expresses the removed genes *gag, pol* and *env* in *trans* in a stable manner (P. D. Robbins & Ghivizzani, 1998; Stone et al., 2000). Some limitations of retroviral vectors include: produced in low titer (10^5 – 10^7) colony forming unit/mL, could only transduce actively dividing-cells, uncontrolled insertion into the host genome which might cause oncogene activation or tumour suppressor gene inhibition, and the possibility of shut off transgene expression over time (Stone et al., 2000). Retroviral-mediated gene transfer of AT_1R antisense (AT_1R-AS) reduced BP in 5-day-old spontaneously hypertensive rat (SHR), an action that was maintained throughout development and exist until 3 months of the initial treatment (Iyer, Lu, Katovich, & Raizada, 1996). Intracardiac delivery of ACE antisense (ACE-AS) via lentiviral vector provides significant long-term decrease in elevated BP in SHR associated with prevention of ventricular hypertrophy and renovascular pathophysiology (H. Wang et al., 2000).

1.3.5.2 Lentivirus

Lentiviruses are members of the retrovirus family with a single stranded RNA genome. They have all the advantages of MMLV alongside the capability to transduce and express their genes with high efficiency in both dividing and postmitotic cells (e.g. neurons) as well as stem cells, hepatocytes, cardiomyocytes and other cardiac cells(Naldini, Blömer, Gage, Trono, & Verma, 1996). They are characterized by having 2 virion proteins (Matrix and Vpr) that can carry the pre-integration complex throughout the nuclear membrane from the cytoplasm to the nucleus via interaction with nuclear import machinery in the absence of mitosis (Naldini et al., 1996). Lentiviral vectors provide stable integration into the host cell genome and are capable to produce long term gene expression which allows for stable cell line generation (Blömer et al., 1997). It has been reported that lentivirus vector was able to infect quiescent cells (the striatum and hippocampus) of adult rats efficiently and stably with transgene expression for more than six months (Blömer et al., 1997). Furthermore, they do not generate immunogenic responses and they possess broad tissue tropism.

Lentivirus vectors have large packaging capacity as they could carry transgene fragments as large as 8 kb. The most common lentivirus is the human immunodeficiency virus (HIV), from where the replication-defective lentiviral vector is derived. Lentiviral vectors are widely used in pre-clinical research for the cardiovascular system, however, their use in clinical trials is yet to be started due to outstanding biosafety questions regarding replication-competent retrovirus (RCR) formation, off target gene expression, and potential insertional mutagenesis that still need further investigation (Di Pasquale, Latronico, Jotti, & Condorelli, 2012; Sahoo, Kariya, & Ishikawa, 2021). It has been shown that lentiviral system efficiently mediated transfer of prodynorphin in mouse stem cells which led to significant enhancement of the expression of 2 cardiac promoting genes *GATA-4* and *Nkx2.5*, and therefore caused remarkable increase in spontaneous beating activity (Maioli et al., 2007). Furthermore, a lentiviral vector containing SERCA2 gene was infused into rats with myocardial infarction to assess the long term (six months) effect on cardiac function and remodelling (Niwano et al., 2008). The study revealed that although the transduction efficiency was approximately 40%, the SERCA2 gene was successfully integrated into the rat heart, and showed significant protection against left ventricular hypertrophy, and improved systolic and diastolic function for post-MI heart failure (Niwano et al., 2008). Myotrophin causes activation of NF-kappaB which was associated with cardiac hypertrophy. Lentiviral-mediated gene delivery of small hairpin RNA (shRNA) to silence and downregulate myotrophin expression has been effective in attenuating cardiac hypertrophy in NRCM and in myotrophin transgenic mice (Gupta, Maitra, Young, Gupta, & Sen, 2009). Lentiviral vector was also efficient in delivering RAS genes and producing therapeutic effect to the heart in hypertensive animal models (Metcalfe et al., 2004). Overexpression of AT_2R via lentiviral gene transfer (lenti-AT_2R) into the left ventricle of spontaneously hypertensive rats (SHR) attenuated cardiac hypertrophy, but not the elevated blood pressure (Metcalfe et al., 2004). Overexpression of ACE2 via lentivirus vector exerts protective effect on rat heart following myocardial infarction, preserving cardiac function, and attenuating left ventricular hypertrophy (Der Sarkissian et al., 2008).

1.3.5.3 Adeno-associated virus

Adeno-associated virus (AAV) is a non-enveloped linear single-stranded DNA (ssDNA) genome of approximately 4.7 kb. AAV was first observed in 1965 under electron microscopy when a stock preparation of simian adenovirus type 15 (SV15) was found contaminated with small particles (approximately 22-25nm diameter of virion shell) that differed antigenically from the adenovirus (R. W. Atchison, Casto, & Hammon, 1965). The particles were then purified and classified as a member of parvovirus family and they were named defective AAV viruses as they needed helper viruses (mainly adenoviruses) in order to replicate and hence produce and amplify (R. Atchison, Casto, & Hammon, 1966). AAV is not pathogenic and could establish a latent infection in the host cell by either persisting in the episomal forms or by integration into the host cell DNA genome. Multiple infections of latently infected cells with a helper virus (adenovirus or herpesvirus) may result in re-activating the AAV replication (Laughlin, Cardellichio, & Coon, 1986). AAV contains mainly three genes: replication (Rep), capsid (Cap), and assembly activating (aap). These coding sequences are flanked by inverted terminal repeats (ITRs) that are the only *cis*-acting elements required for genome replication and packaging signalling. The *Rep* gene is located in the left open reading frame (ORF) and encodes proteins that are responsible for viral replication and packaging which include: Rep78, Rep68, Rep52, and Rep40 (Naso, Tomkowicz, Perry, & Strohl, 2017). AAV cap gene expression leads to enhance the three structural viral capsid proteins VP1, VP2, and VP3 which encoded in the right ORF and play an important role in cell binding and internalization as well as protecting the viral genome from degradation (Naso et al., 2017). Even though there are more than 100 AAV variants identified so far, only AAV serotypes 1 through 5 and AAV7 through 9 can be classified as true serotypes. The serology of AAV6 is closely related to AAV1, while AAV10 and AAV11 could provide a broader choice of pseudotyped AAV vectors and their serological profiles have not been well characterized (Z. Wu, Asokan, & Samulski, 2006). AAV2 was one of the earliest AAV serotypes identified and characterized and one of the most widely used in gene therapy clinical trials (Z. Wu et al., 2006). However, among those identified serotypes, only AAV 1, 6, 8, and 9 have shown cardiac tropism (Hammoudi, Ishikawa, & Hajjar, 2015; Naso et al., 2017). Targeting vascular endothelium is important in the treatment of cardiovascular disease, and it has been reported that AAV

vector serotypes including: AAV-2, AAV-3 through 6, AAV-7 and AAV-8, transduce vascular endothelial cells inefficiently compared to other cells (Denby, Nicklin, & Baker, 2005). Therefore, there have been multiple attempts to genetically manipulate AAV tropism in order to enhance the transduction efficiency to endothelial cells(Stuart A Nicklin et al., 2001).

For generation of recombinant AAV (rAAV), the *cap* and *rep* genes are removed and replaced by gene of interest (e.g., therapeutic gene) and internal promoter/s for controlling gene expression. However, rAAV vector has limited packaging capacity for foreign DNA fragments ranging from 4.1 to 4.9 kb compared to adenovirus vector (7-8 kb), but produce lower immunogenicity and longer transgene expression in both dividing and nondividing cells (Walther & Stein, 2000). Due to low immunogenicity and the capability to evoke long transgene expression, AAV has been utilized to deliver therapeutic proteins to the heart in animal models. AAV-mediated transfer of human heme oxygenase-1 (hHO-1) gene, which has been reported to exert a cytoprotective and antioxidant effect, was injected directly into the myocardium of the rat heart for 8 weeks before acute coronary artery ligation(Melo et al., 2002). The study showed remarkable reduction (>75%) in left ventricular myocardium infarct size accompanied with decrease proinflammatory interleukin-1ß protein, myocardial lipid peroxidation and in proapoptotic Bax, which suggested that AAV mediated gene transfer can provide cardioprotective effects by attenuating oxidative stress, inflammation and apoptotic cell death (Melo et al., 2002). AAV containing Ang-(1-9) was injected into mice model with myocardial infarction via single tail vein and cardiac function was assessed over 8 weeks (Fattah et al., 2016). The study showed that Ang-(1-9) gene therapy preserved LV systolic function and significantly decreased cardiac fibrosis post MI (Fattah et al., 2016).

The first human gene therapy trial used AAV-1 vector to transfer a therapeutic gene, the sarcoplasmic reticulum calcium ATPase gene (AAV1/SERCA2a), into patients with advanced heart failure conducted in 2013 (Zsebo et al., 2014). Long term effect (3 years) of intracoronary infusion of AAV1/SERCA2a into thirty-nine patients with severe heart failure was analysed. The results showed that the number of cardiovascular events, including mortality rate, was the lowest in high dose gene therapy treated patients, while the highest mortality rate

observed in placebo group (Zsebo et al., 2014). The death rate was high but delayed in patients received low and mild dose. The data for this study showed positive safety and efficacy signals over long term treatment with AAV1/SERCA2a in patient with heart failure (Zsebo et al., 2014).

1.3.5.4 Adenovirus

Adenovirus was found by chance during an *in vitro* study on the growth of human adenoid tissues isolated from young children. The investigators noticed a cytopathogenic agent that produce spontaneous degeneration of adenoid tissues which could be transmissible to fresh adenoid culture or to other cell line culture such as HeLa cells (Rowe, Huebner, Gilmore, Parrott, & Ward, 1953). It has been found that the activity of the agent is stable at storage condition of 3°C for a week or post 3 cycles of quick-freezing and thawing, while exposing the agent to 62 °C for 30 minutes could inhibit or destroy the activity. This agent was then named "adenoid degeneration agent" or (A.D. agent) (Rowe et al., 1953). Adenovirus belongs to Adenoviridae family which have more than 130 different types that infect several different species. Human adenoviruses belong to the genus Mastadenovirus that comprises seven species (A-G), classified based on phylogenetics and serological characteristics including neutralisation and hemagglutination, which are mostly pathogenic and infectious. They cause mild infection/symptom to the gastrointestinal tract, upper and lower respiratory system, and conjunctiva, which are usually self-limiting as it could be counteracted efficiently by the host individual immune system (Hidalgo & González, 2022). However, adenovirus infection could also lead to serious pneumonia, hepatitis, encephalitis and haemorrhagic cystitis, in vulnerable people such as in impaired immunity patients and in infants (Hidalgo & González, 2022).

Recombinant adenoviral vectors are well characterised and have broad tropism that could be genetically altered to increase selectivity and efficiency. They have various characteristics that make then among the most utilized vectors in gene therapy both *in vitro* and *in vivo* which include: the capability to transduce multiple cell types (including dividing and non-dividing cells), produce high level transgene expression, relative ease to manipulate and generate replication deficient vectors and the possibility to produce stable high-viral-titer stocks for repeated use (SM Wold & Toth, 2013). The most extensively used adenoviral

vectors in gene therapy are genetically derived from the species C human adenovirus serotype 5 (hAdV-5) (Lee et al., 2017). Since Ad5 is the vector of choice for the studies in this thesis the remaining sections on adenoviral vector are focusing on Ad5 . Adenoviruses are nonenveloped icosahedral-shaped capsids consist of ~36 kb double-stranded linear DNA flanked with inverted terminal repeat (ITR) sequences at each end (Chaurasiya & Hitt, 2016). They have a virion diameter range of 70–90 nm and capsid consisting of three main exposed structural proteins: the fiber, penton base and hexon (Figure 5).

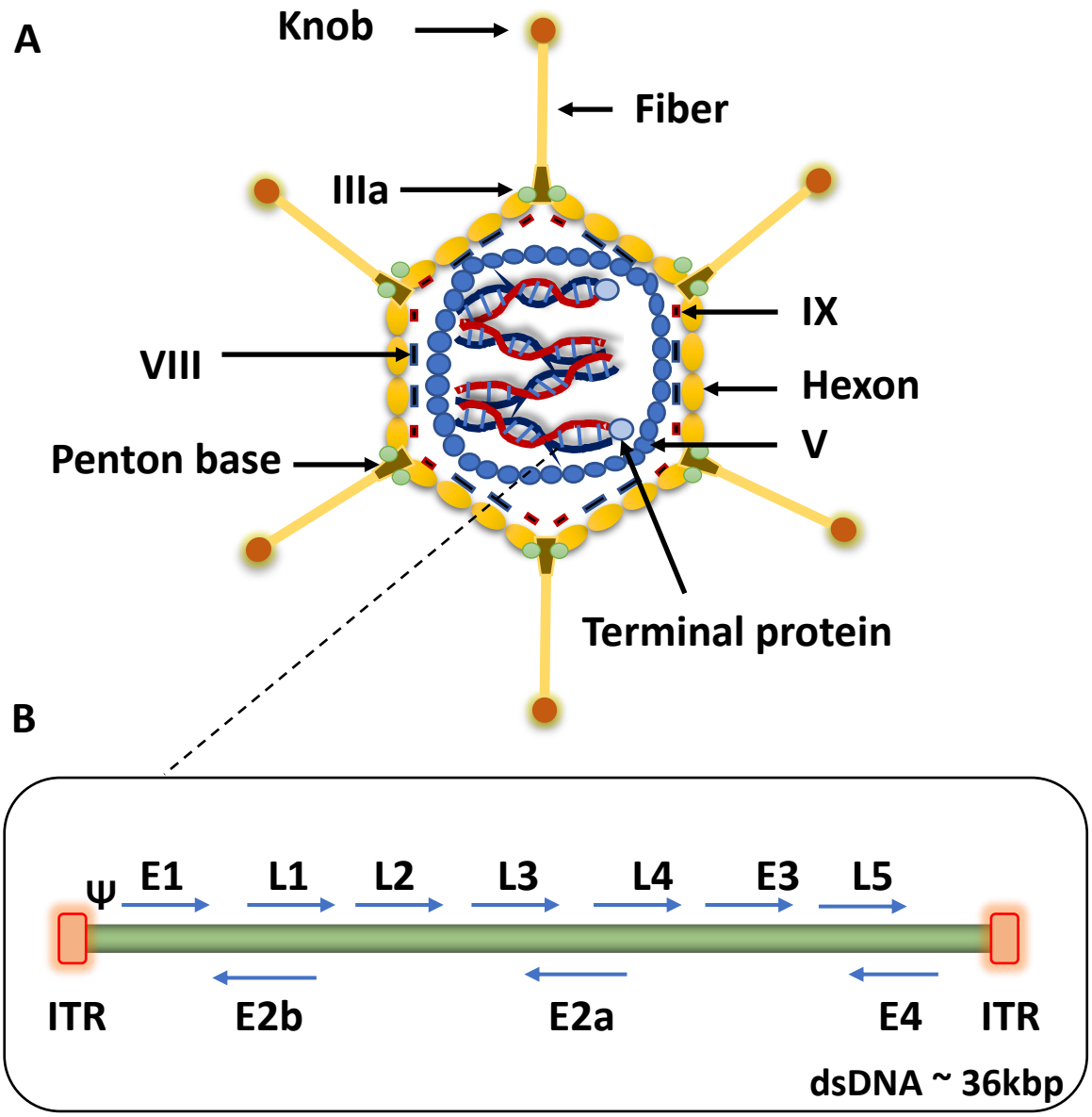

Figure 1.5 Structure of human adenovirus 5 (hAdV-5).

(A) Schematic representation of Ad5 major proteins (hexon, penton base, and fiber), some minor proteins (IX, VIII, and IIIa) and some of the core proteins (terminal protein, and V). (**B**) Diagram of the adenovirus genome virions and transcription units showing the position of the inverted terminal repeat (ITR) sequences at the end left and right, the packaging sequence Ψ, the four early regions (E1, E2, E3, and E4), and the 5 late regions (L1-L5). The capsid consists of ~36 kb linear dsDNA. Arrows showed the direction of transcription (McConnell & Imperiale, 2004).

The hexon forms the majority of capsid structure with 240 trimeric hexon capsomeres, alongside 12 pentameric penton bases and 12 trimeric fibre proteins (S. A. Nicklin, Wu, Nemerow, & Baker, 2005). The fibre protein of the adenovirus vector is distinguished from other icosahedral viruses by being thin and long and it acts to promote the attachment of the viral capsid to the cell surface via its interaction with a cellular receptor (S. A. Nicklin et al., 2005). The fibre proteins of all human adenoviruses share marked structural similarity and consist mainly of two domains: the N-terminal tail and C-terminal globular knob domain. The N-terminal tail has a central shaft, made of repeating sequences, which connect the N-terminal tail with the globular knob structure that is responsible for interaction with the target cell receptor. However, the length of the fiber shaft domain and fiber knob-primary receptor interaction could influence the infectivity of the adenoviral vector (S. A. Nicklin et al., 2005; Shayakhmetov & Lieber, 2000). It has been shown that hAdV-5 capsid-based vectors with long-shafted fibers derived from hAdV-5, and adenovirus serotype 9(Ad9) (with coxsackie and adenovirus receptor, CAR, binding affinity) attached and internalized more efficiently into the host cells more than short-shafted counterpart (Shayakhmetov & Lieber, 2000).

1.3.5.4.1 Mechanism of Adenovirus cell entry

The mechanism of adenovirus cell attachment and internalization involves the binding to one of various types of cell surface receptors that mediate endocytosis including the coxsackie and adenovirus receptor (CAR), the main receptor for species C adenoviruses including HAd-V5, major histocompatibility complex (MHC)-I, heparan sulphate proteoglycans (HSPG), vascular cell adhesion molecule (VCAM)-1, and integrins (JT, Wam, Ac, & Sa, 2022). The first step involves the binding of the fiber knob domain to the CAR (Figure 1.6). Next, RGD motif, within the penton base, is engaged to activate virus internalization and to induce membrane penetration via integrins (S. A. Nicklin et al., 2005). RGD peptide acts as a recognition site for many cellular integrins. The engagement of integrins (mainly αvβ3, αvβ5) by the penton base promotes activation of PI3 kinase, Rho GTPases, and $p130^{CAS}$ which facilitate rearrangements in the actin cytoskeleton and hence viral internalization (Chaurasiya & Hitt, 2016; Yuanming Zhang & Bergelson, 2005). Some of the identified integrins that recognize RGD ligands and are involved in the internalization process include: the vitronectin

receptors αvβ3, αvβ5, αvβ1, α3β1, and α5β1 (Yuanming Zhang & Bergelson, 2005). The virus enters the cell via a clathrin-coated vesicle and is transported into the endosome. Next, the acidic environment of the endosome causes disassembly of the virus capsid which results in a further pH drop and lysis of the endosomal membrane allowing the virus particles to traffick into the nuclear pore complex via microtubules and interactions with dynein. Inside the nucleus, the virus utilizes other receptors (the nuclear pore complex receptor CAN/ Nup214 and histone H1) to release viral genome and start to replicate (S. A. Nicklin et al., 2005). After approximately 6-8 h, viral DNA replication begins, and it takes 24-36 h for the virus to complete its life cycle (Chaurasiya & Hitt, 2016). For generation of human adenoviral vectors for gene therapy, the early region 1 (E1), including E1A and E1B, that is responsible for viral replication is deleted resulting in generating replication-deficient viral vectors and creating a space inside the capsid to insert an expression cassette encoding the therapeutic gene (SM Wold & Toth, 2013). E1 deleted adenoviral vectors propagation requires specific helper cells, the HEK 293 cell line, which has the adenoviral E1 region integrated into its chromosomes enabling the vector to replicate and therefore be amplified and produced only in these cells (Chaurasiya & Hitt, 2016). HEK 293 cells contain the left end of hAd5 viral genome, including E1 (Graham, Smiley, Russell, & Nairn, 1977), and are easy to infect and can produce high pfu (plaque-forming units) titer e.g. 10^{10}, which is an advantage over other vectors such as retroviral vectors. Additional cloning capacity for larger transgenes in adenoviral vectors can be achieved via deletion of the early region 3 (E3). E3 (encodes at least 7 proteins) is not essential for virus production as it functions to inhibit the immune response to viral infection(Chaurasiya & Hitt, 2016). The deletion of both E1 and E3 creates space for up to 8.2 kb of foreign transgene DNA, but still not the maximum insertion capacity (Chaurasiya & Hitt, 2016). After transport into the target cell, the therapeutic gene is released into the nucleus, remains extrachromosomal, and exerts therapeutic gene expression (Meier & Greber, 2004).

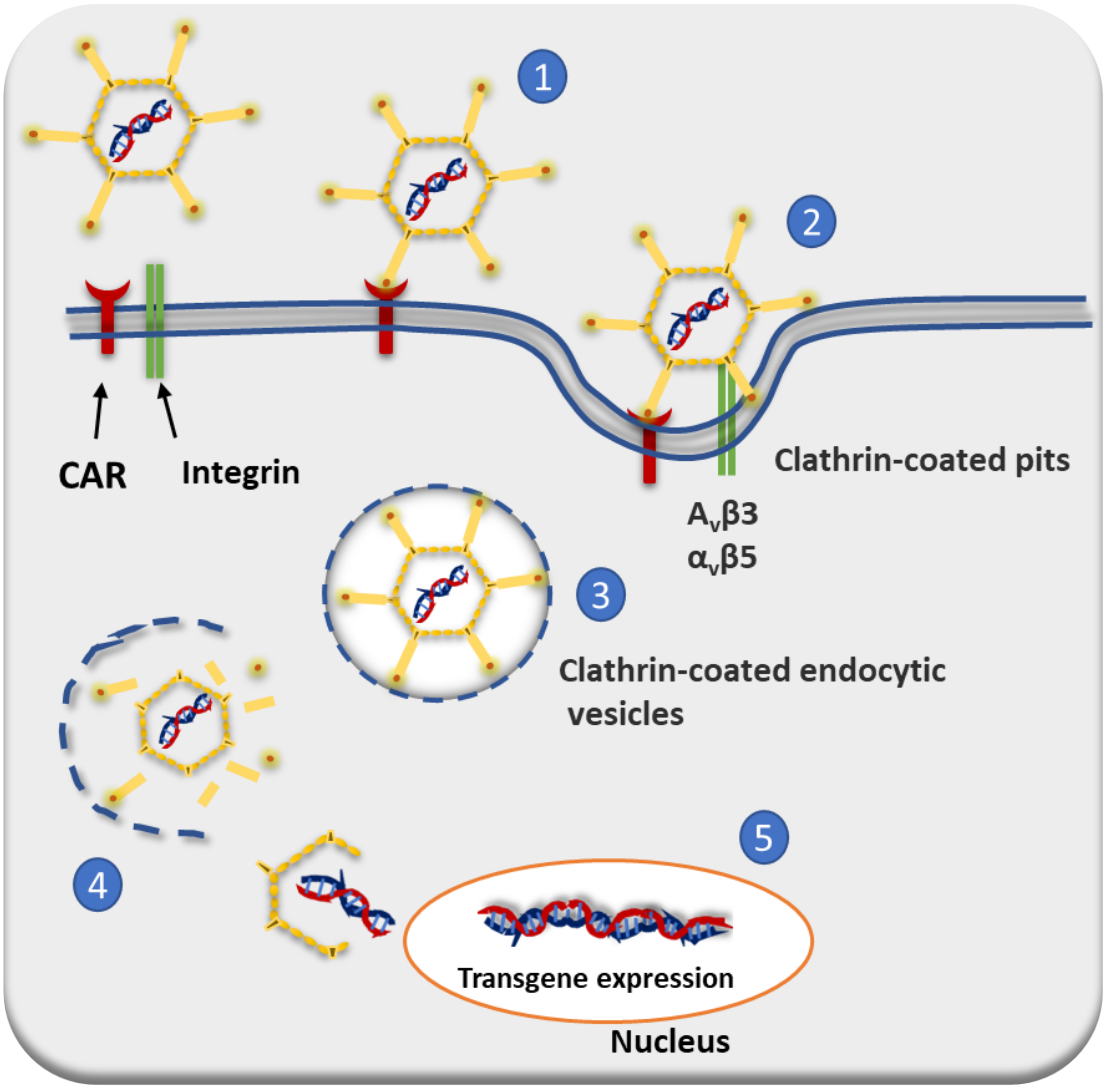

Figure 1.6 Mechanism of adenovirus cell entry.

(1) The virus binds to CAR in the cell surface. **(2)** Engagement of integrins (mainly αvβ3 and αvβ5) by penton base to promote internalization. **(3)** The virus inters the cell via a clathrin-coated vesicle and enter the endosome. **(4)** The low pH environment of the endosome causes disassembly of the virus capsid. **(5)** Virus particles traffick into the nuclear pore complex.

1.3.5.4.2 Development of adenovirus serotype 5 as a gene transfer vector

One of the most common drawbacks for adenoviral vector is that it could trigger strong innate immune response in vivo. Mice begin to produce neutralizing antibodies and memory T-cells against capsid proteins immediately after intravenous injection of Ad vector in a dose dependent manner, with maximum immune response observed within 6 hours (SM Wold & Toth, 2013). Most important antigens are the major capsid proteins (the hexon, penton base, and fiber) with the majority of antibodies released against the hexon (most abundant protein in the capsid) (Muruve, 2004). The route of administration as well as the dose of adenoviral vector, and the species are crucial in producing the required effect (Weaver, 2019). Injection of Ad-*β*gal (adenoviral vector containing Escherichia coli ß-galactosidase gene) via iliac vein showed 80% transduction efficiency of the liver of Wistar rats at dose of $5x10^{11}$ vp/kg as indicated by X-gal staining (Marquez–Aguirre et al., 2009) . Recombinant adenovirus 5 (rAd5) vaccine doses of 10^7 to 10^{10} viral particle (vp)/animal showed higher antibodies response at higher doses following intramuscular injection, whereas intranasal (IN) delivery revealed lower immune response to higher vaccine doses in mice (Weaver, 2019). In rats, however, intramuscular injection of rAd vaccines exerts the same level of immune response at doses between 10^9 to 10^{11}vp/animal (Weaver, 2019). High dose of intravascular (I.V) injection of hAdV-5 can cause the release of pro-inflammatory cytokines such as IL-1, IL-6, TNFα, IFNγ, and IL-12 and chemokines CCL2, CCL3, CCL4, CXCL1, CXCL2, CXCL9, and CXCL10 (Atasheva & Shayakhmetov, 2022). This inflammatory response appears in human serum within 24h post transduction, while some cytokines (IL-1α) can be detected in mice within 10 minutes of virus injection (Atasheva & Shayakhmetov, 2022). However, natural adenovirus infection can also trigger the inflammatory response and cause significant amount of cytokines to be released and detectable at day 7 of infection (Atasheva & Shayakhmetov, 2022).

Another major limitation for hAdV-5 is the accumulation in liver tissues after intravascular administration as it mainly infects the Kupffer cells of the liver via non-CAR-dependent mechanism when administered in vivo (Khare et al., 2011). hAdV-5 hexon protein also binds to blood coagulation factor X in the blood,

which mediates hepatocyte transduction via heparan sulfate proteoglycans (SM Wold & Toth, 2013) .

hAdV-5 vectors consist of overlapping early and late transcriptional regions as follow: one immediate early gene (E1A) and 4 early transcription units (E1B, E2, E3, and E4), 2 intermediate or early delayed transcription units (proteins IX and IVa2), and one major late unit that produces 5 groups of mRNAs (L1 to L5), which encode structural proteins for the capsid and internal core (Douglas, 2007). E1A is the first transcriptional region to be activated and expressed during infection and is therefore essential for viral replication, leading to activation of other early genes (E1B, E2, E3, and E4). In addition, E1A binds to retinoblastoma protein (pRb) causes the release of E2F which in turn force the infected cells to enter S-phase. E1B is involved in blocking mRNA transport in the host cell, while inducing viral mRNA transport and prevent premature death resulting from E1A-induce apoptosis (Chaurasiya & Hitt, 2016). In the first generation of Ad vector E1 (E1A and E1B) gene is deleted and replaced by the therapeutic gene of interest, up to approximately 5kb (Alba, Baker, & Nicklin, 2012), resulting in replication-incompetent vector (Figure1. 7). Many first generation Ad vectors have been also produced with E3 gene partially or totally deleted to increase the size of foreign transgene (Y. Yang et al., 1994). However, first generation Ad vectors still show marked levels of immune response specially after repeated administration despite deletion of some genes which ultimately lead to short duration of gene expression alongside the limited packaging capacity (Y. Yang et al., 1994). Another limitation of the E1±E3 deleted Ad vectors is their transient gene expression that might become undetectable after two weeks of administration (Naim, Yerevanian, & Hajjar, 2013), and that is because they don’t integrate and they trigger the immune response against transduced cells or tissues (Naim et al., 2013).

The second-generation Ad vectors could encode larger transgenes (up to 10 kb) with deletion of E4 gene in addition to E1 and/or E3. E4 has a crucial role in maintaining long transgene expression and is also involved in regulation of various function during infection process including transcription, DNA replication, RNA splicing and processing, synthesis of late proteins and the transition from the early regions to late stages of infection (Weitzman, 2005). Further deletion of E2 (E2A and E2B) could provide larger packaging capacity of

up to 14kb for foreign DNA. E2 transcription units encoding genes that also participate in DNA viral replication. The removal of all these genes (E1, E2, E3 and E4) have been shown to reduce the cytotoxicity and immune response in the host cell (Danthinne & Imperiale, 2000; Luo et al., 2007), however, a significant in vivo liver toxicity and inflammatory immune response has been reported in this generation of Ad vector despite removal of all the aforementioned genes (Lusky et al., 1999). In addition, the 2nd generation Ad vector is difficult to develop as it needs particular cell line for E2 to be expressed to allow replication and production and E2 can be toxic to cells in culture (Heshan Zhou, O'Neal, Morral, & Beaudet, 1996)

In the third generation Ad vector, also called helper-dependent adenoviral vectors, the whole adenoviral genome including L1, L2, VA and TP are deleted allowing for the maximum space for insertion of foreign expression cassettes with size of 36 kb (Kochanek et al., 1996). The helper-dependent vector only keeps the essential *cis* elements (the two inverted terminal repeats (ITRs) and the packaging signal) from the wild-type adenovirus. As it lacks the essential packaging components, the third generation Ads require helper virus or complementary virus to provide the necessary proteins for propagation (Lee et al., 2017). These generation Ads showed remarkable reduction in the host immune responses and exert long-term expression of multiple transgenes in vivo and in vitro (Luo et al., 2007). C57BL/6J mice were injected with 2x 10^{10} particles/animal of either first or third generation Ad vectors and the transgene expression was analysed over 10 months. The first-generation Ad vector showed gene expression levels that peaked (around 2 µg/mL) after 3 days of transduction and reduced to less than 10% over 10 months. In contrast, the third generation Ad vector, using the Cre-loxP helper-dependent system, exerted gene expression that reach the maximum levels of approximately 50 µg/ml within 3 weeks after injection without decline over period of 10 months (Schiedner et al., 1998).

However, an efficient method to completely isolate the contaminating helper virus from the final third Ad vector preparation is also required in order to obtain relatively pure gutless Ad vector and therefore it has been challenging to translate helper dependent Ads to the clinic (Lee et al., 2017).

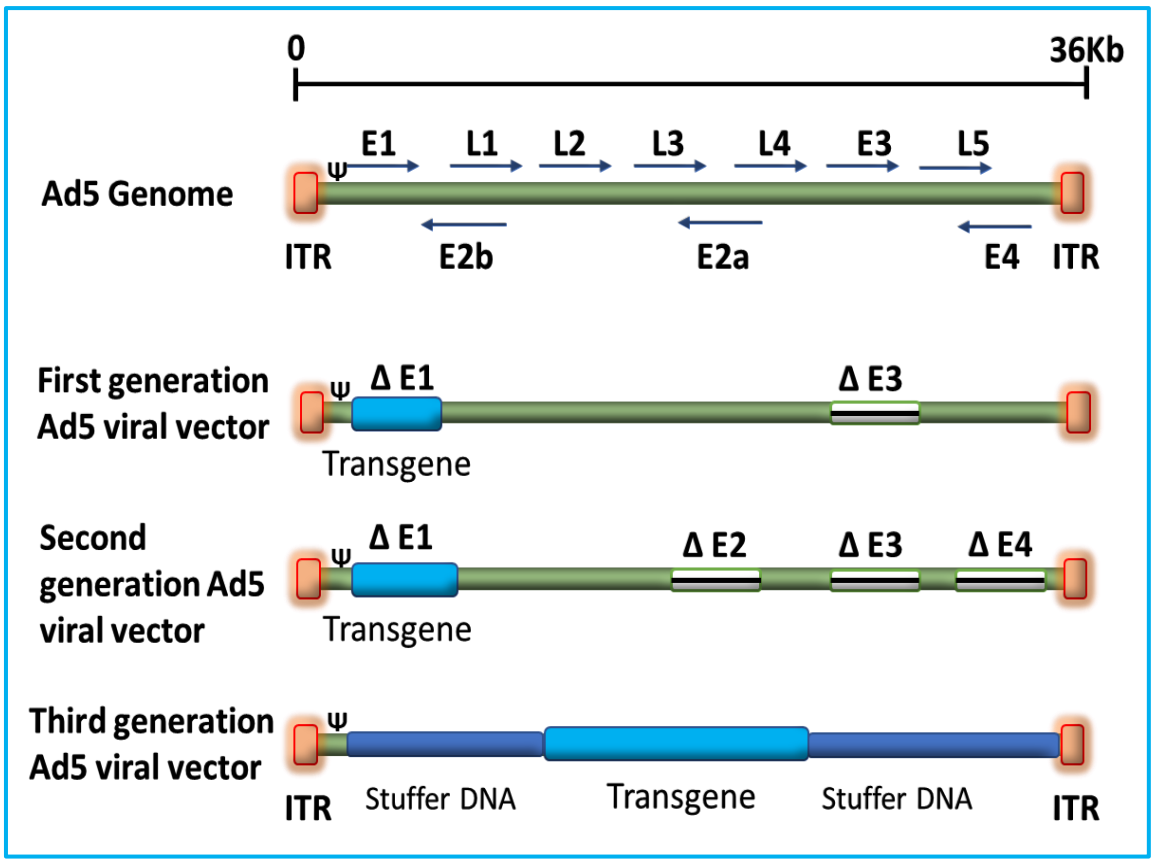

Figure 1.7 Diagram showing the evolution of the three Ad5 vector generations.

Diagram showing the evolution of the three Ad5 vector generations. The first-generation is developed by removing E1 and E3 regions from Ad5 genome creating a space of 8.2 kb for exogenous transgene. The second- generation Ad5 vector is constructed by further deletion of E2 and E4 regions providing capacity of up to 14 kb for transgene cassette. In the third-generation or gutless Ad5 vector, also known as helper-dependant adenovirus (HD-Ad), or high-capacity adenoviral vectors (HC-AdVs) all viral proteins coding genes are removed, leaving only the 5′ and 3′ ITRs and the packaging signal (Ψ) which allow for up to 36 kb insertion space for foreign DNA (Lee et al., 2017).

1.3.5.4.3 Adenoviral gene therapy for cardiovascular disease

Ad vectors, particularly hAdV-5, are the most extensively used vector for cardiovascular gene therapy with a total of 54 trials by 2012 according to (Tilemann, Ishikawa, Weber, & Hajjar, 2012). For cancer gene therapy, the Ad vectors have been widely used in clinical trials and the American FDA has already approved "Adstiladrin" (Ad vector-mediated transfer of interferon alfa-2b) to treat adult patients with high-risk, Bacillus Calmette-Guérin (BCG)-unresponsive non-muscle invasive bladder cancer (NMIBC)(Narang). In a vaccine clinical trial against Ebola virus, Ad26 vector-based vaccine was safe and well tolerated after two doses (Pollard et al., 2021). However, the use of Ad vector in vaccines clinical trial has been dramatically increased in response to SARS-CoV-2 and COVID-19 pandemic (Jacob-Dolan & Barouch, 2022). Some of these Ad vector-based vaccines include; chimpanzee Ad (ChAdOx1 nCoV-19) from AstraZeneca, Ad26.COV2.S from Janssen/Johnson & Johnson (JnJ), and Ad5-nCoV vaccine from CanSino (Jacob-Dolan & Barouch, 2022).

In the vascular system, hAdV-5 has been used in clinical trial to deliver fibroblast growth factor-4 (Ad5FGF-4) into patients with critical limb ischemia via intramuscular injection. The Ad5 doses of $2.87x10^{8}$ to $2.87x10^{10}$ VP were shown to be safe and well tolerated over 12-week period. However, the transduction efficiency at this concentration was limited (Matyas et al., 2005).

Current clinical trial used limited number (33) of patients with refractory angina (RA) to investigate the epicardial delivery of XC001 (hAdV-5 contains multiple isoforms of vascular endothelial growth factor (VEGF)) (Povsic et al., 2021). The primary concern in this study is for assessing the safety via administering of multiple doses range of $1x10^{9}$_ $1x10^{11}$VP for six months(Povsic et al., 2021)

In preclinical trials, Ad vector has been shown to be effective in transfer of therapeutic genes in cardiovascular disease. In rat model of myocardial infarction (MI), Ad vector mediated overexpression of ACE2 for 4 weeks showed high levels of ACE2 expression and activity in the myocardium in comparison with the Ad-EGFP and model groups (Y. X. Zhao et al., 2010). Furthermore, the expression of ACE2 exhibited therapeutic effect as it reduced left ventricular (LV) volume, extent of myocardial fibrosis, and expression levels of ACE, Ang II, and collagen I, as well as increased the endogenous Ang-(1-7) levels in the myocardium. The cardiac systolic function was also improved as shown by

increased left ventricular ejection fraction after ACE2 gene transfer. These results suggested that Ad vector mediated efficient transfer of ACE2 to the target area and provide therapeutic effect in animal model with MI(Y. X. Zhao et al., 2010). Adenoviral mediated transfer of human beta2-adrenergic receptor (Adeno-B_2AR) into the myocardium of a rabbit model of heart failure produced 5-10-fold B_2AR overexpression at 7 and 21 days after transduction compared to rabbits receiving control Ad vector. Enhanced cardiac contractility was observed in Adeno-B_2AR group at 21 days of injection despite the decline in B_2AR expression by that time (Maurice et al., 1999). Ad vectors have been reported as an efficient transfer vehicle to target atherosclerosis in vivo. Human paraoxonase 3 (PON3), has been reported to provoke antiatherogenic properties in vitro. Therefore, Ad vector was utilised to mediate transfer of PON3 into 26-week-old apolipoprotein E-deficient (apoE$^{-/-}$) mice with a dose of 3×10^{11} VP injected intravenously for three weeks. The study showed high levels of PON3 increases the anti-inflammatory properties of high density lipoproteins (HDL), inhibits the progression of atheromatous lesion formation, and increases the cholesterol efflux potential of serum, which suggested a protective role of Ad-mediated transfer of PON3 against atherosclerosis in vivo (C. J. Ng et al., 2007). Moreover, human paraoxonase (PON) 2 has also exhibited protective effects against the development of atherosclerosis when overexpressed via Ad-vector in (apoE$^{-/-}$) mice (C. J. Ng, Hama, Bourquard, Navab, & Reddy, 2006). Ad vector has also been efficient in delivering therapeutic proteins into larger animals with ischemic heart disease. In Yorkshire swine model of cardiomyopathy (with left ventricular dysfunction induced by using rapid ventricular pacing system), Ad mediated transfer of a 121-amino-acid isoform of vascular endothelial growth factor Ad(CU)VEGF121.1 or AdNull were injected into animals and cardiac function and structure were monitored over 21 days. Rapid recovery of cardiac function and structure was observed in Ad(CU)VEGF121.1 treated animals compared to AdNull group (Leotta et al., 2002).

It has also been reported that Ad5 vector mediated delivery of protective peptides, Ang-(1-7) and Ang-(1-9), to cardiomyocytes in vitro which inhibits Ang II-induced cardiomyocyte hypertrophy (Flores-Muñoz et al., 2012). Nonetheless,

Ad vector has also been used to deliver proteins that enhance cardiac hypertrophy in vitro such as AT_1R (Thomas et al., 2002).

1.4 Extracellular Vesicles (EVs)

1.4.1 Types and biogenesis of extracellular vesicles

Cell to cell communication is a fundamental process in both prokaryotic and eukaryotic cells, including humans, to maintain body haemostasis. Cells secrete and release various molecules into the extracellular space for intercellular communication. It has been known that these cell signals are mediated via several substances including hormones, neurotransmitters, chemokines, growth factors, neurotransmitters, and bioactive lipids (Gho & Lee, 2017) . Recently, it has been reported that almost all cells, including healthy and pathogenic cells, can produce extracellular vesicles (EVs) that also play an important role in intercellular signalling as well as conveying messages to distant cells and tissues within the body. In 1983, Bin-Tao Pan and Rose M. Johnston were investigating the fate of the transferrin receptor during in vitro maturation of sheep reticulocytes and reported loss of transferrin receptor by release of small vesicles (Pan & Johnstone, 1983). The vesicles isolated from cell culture media by ultracentrifugation at 100,000xg for 90 min were shown to possess some activities and characteristics of the parent reticulocytes plasma membrane that disappeared during maturation. The vesicles were described as lipoprotein structures with a phospholipid composition and given the name exosomes (Johnstone, Adam, Hammond, Orr, & Turbide, 1987). This, arguably, could be considered the beginning of the new EVs research era although the term “exosome” has been used earlier. However, the exact role of EVs remain ambiguous as it was first linked to membrane debris with no important biological function until Raposo and colleagues reported that those nanoparticles can transfer proteins from one cell to another (Raposo et al., 1996). In 2007, it has been shown that EVs derived from mouse and human mast cell lines can transfer functional mRNA and microRNA to other recipient cells, a function that was thought to be restricted to viral vectors at that time (Valadi et al., 2007), but highlighting that EVs could also be therapeutic delivery vectors. Another similarity to viral vectors is the specificity for the target tissues. However, in terms of cargo and contents, viral vectors might be more specific as it can be engineered to be replication deficient and carry only the gene of interest with

other parts of the viral genome with known function, while EVs may contain a variety of biologically functional cargo. While viral vector genes could be removed totally or partially during production/generation, it's not plausible to control the exact cargo of EVs as they inherit most of the contents from the parent cells or tissues with wide range of proteins and RNAs (Nolte-'t Hoen, Cremer, Gallo, & Margolis, 2016). EVs are formed by late endosomes via inward budding and invaginating of the plasma membrane incorporating various and heterogenous nanoparticle molecules that are close to the cell surface (McNamara & Dittmer, 2020). Therefore, viruses or some of viral genetic materials could be also encapsulated inside the EVs and transported into the cells via receptor-independent mechanism (McNamara & Dittmer, 2020). EVs and viruses have complex relationship as they share physical, biochemical and functional properties such as size, marker distribution and the ability to migrate and transform signals between different tissues and cells (Metzner & Zaruba, 2021). For more details about the crosstalk between viruses and EVs see (chapter 4).

The capability of EVs to carry soluble proteins, lipid, and different types of ribonucleic acids (mRNA, microRNA, tRNA, rRNA, and small nucleolar RNA), alongside the advantages of having negligible toxicity levels and immune response make them an attractive novel vehicle for targeting drug delivery and therapeutics (E. L. Muñoz, Fuentes, Felmer, Yeste, & Arias, 2022). Encapsulating the therapeutic entity into the EVs protects them from degradation by several degrading enzymes and maintains their integrity, composition and activity in the circulation as well as facilitating delivery to target cells. Furthermore, it has been reported that EVs, particularly exosomes, can cross blood brain barrier which suggested a potential role for exosome as a therapeutic vehicles for the treatment of the central nervous system disease (C. C. Chen et al., 2016).

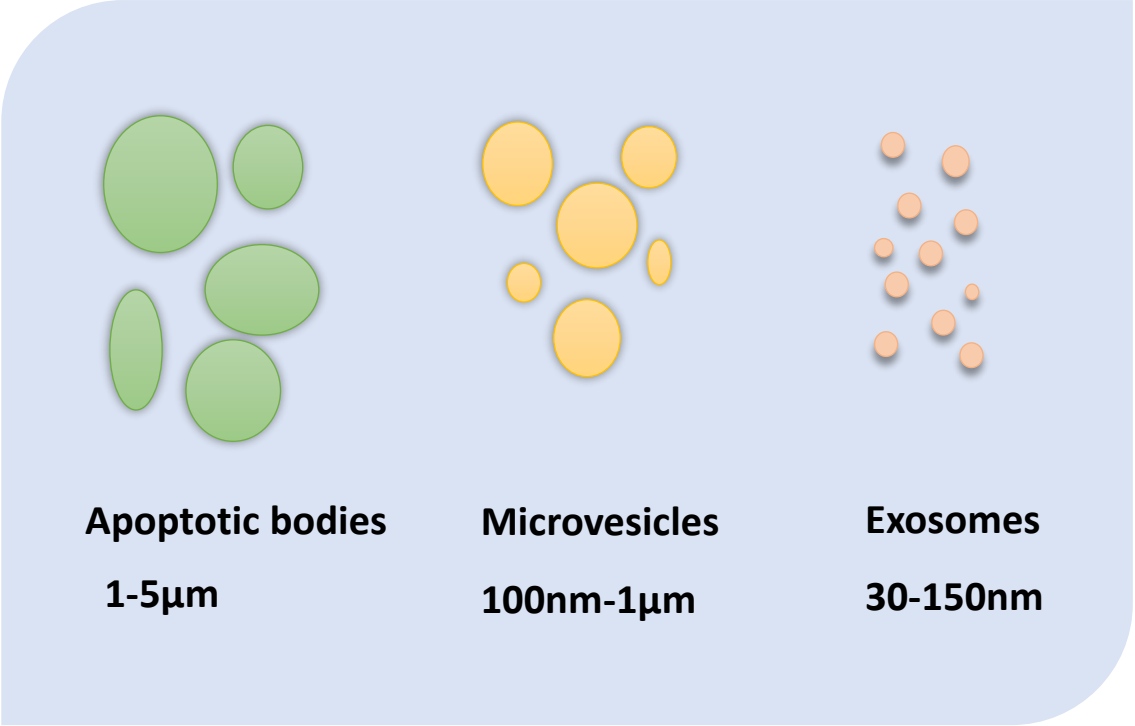

Figure 1.8 The main types of extracellular vesicles classified according to their size.

Apoptotic bodies range in size between 1-5µm. Microvesicles with diameter of 100nm-1µm. Exosomes are the smallest EVs with size range of 30-150nm.

EVs were described by the International Society of the Extracellular Vesicles (ISEV) as particles that are normally released by cells and delimited by a lipid bilayer and cannot replicate as they do not contain functional nuclei (Théry et al., 2018). EVs, range in size between 30-5000 nm diameter, can be mainly classified into three populations: exosomes, microvesicles, and apoptotic bodies, according to their size, biogenesis pathway and proteins biomarkers. According to ISEV classification by size, small extracellular vesicles (sEVs) are those with diameter smaller than 200nm, while medium and large EVs "medium/large EVs" (m/lEVs) are those with dimeter larger than 200nm (Théry et al., 2018).However, the heterogeneity between EV subtype as well as the particle size overlap and the lack of unique and specific marker protein/s for each subtype hindered their characterisation and the ability to clearly distinguish between EVs subtypes (de Castilla et al., 2021). EVs have been detected in many body fluids including blood, plasma, serum, saliva, urine, breast milk, cerebrospinal fluid, bronchoalveolar lavage and bile (Konoshenko, Lekchnov, Vlassov, & Laktionov, 2018). EVs could be also harvested from cell culture conditioned media which represents the major sources of EVs studied by researchers according to ISEV 2018 report (Théry et al., 2018).

1.4.2 Exosome

Exosomes are the smallest EVs subtype with diameter range of 30-150nm and they are derived from endosomal compartment(Alzhrani et al., 2021). Exosomes are formed via inward budding of the limited multivesicular body (MVB) membrane. The intraluminal vesicles (ILVs) form within the MVB as a result of invagination of the late endosomal membrane. During exosome formation, specific proteins incorporate into the invaginating membrane, while the cytosolic contents are engulfed and enclosed within the ILVs (Figure 1.9) (Yuan Zhang, Liu, Liu, & Tang, 2019). The majority of ILVs fuse back with the plasma membrane and release into the extracellular environment as exosomes (Yuan Zhang et al., 2019). The sorting of the exosome protein contents during the inward budding of the membrane is a crucial step in the process of exosome synthesis. There are some factors that might affect the cargo of the exosomes such as the ESCRT (the endosomal sorting complex required for transport) function, tetraspanins and lipid-dependent mechanisms (Villarroya-Beltri, Baixauli, Gutiérrez-Vázquez, Sánchez-Madrid, & Mittelbrunn, 2014). In general,

the small protein particles are marked with a single subunit that facilitates recognition by ESCRT and consequently allows for suitable sorting into budding ILVs. Budding efficacy could be enhanced by increasing the ubiquitin subunits as ILVs formation required ubiquitination and the sequential action of different components of the ESCRT (Ghossoub et al., 2014). ESCRT is composed of five separate proteins: ESCRT-0, ESCRT-I, ESCRT-II, ESCRT-III, and the Vps4 (Vacuolar protein sorting 4) that play a crucial role in the biogenesis of the MVB and cargo selection as well as recycling of ESCRT components (Umbaugh & Jaeschke, 2021). The process of ESCRT is started by recognition and sequestration of the cargo to particular domains of the endosomal membrane ubiquitin-binding subunits of ESCRT-0 (Henne, Buchkovich, & Emr, 2011). ESCRT-0 recruits ESCRT-I machinery via the interaction of Hrs PSAP domains with TSG101(tumour susceptibility gene 101) (Henne et al., 2011). Then, ESCRT I and II complexes induce bud formation. The entire complexes are then combined with ESCRT-III which is involved in promoting the budding process and vesicle release, while the Vps4 protein is responsible for dissociating ESCRT-III protein back into its monomeric soluble forms (Henne et al., 2011; Umbaugh & Jaeschke, 2021). Furthermore, Alix is an exosome protein associated with various ESCRT proteins such as TSG101 and CHMP4 (Villarroya-Beltri et al., 2014). It has been reported that Alix is also involved in the endosomal budding of MVB and the selection of the exosome protein contents via interaction with syndecan (Villarroya-Beltri et al., 2014).

Tetraspanins (CD81, CD63, CD9 and CD10) are integral membrane proteins that are highly abundant in exosomes. Tetraspanins also play a role in exosome cargo composition via interaction with other transmembrane proteins, cytosolic proteins and lipids (Escola et al., 1998). Tetraspanin-enriched microdomains (TEMs) along with CD81 participate in exosome composition via the physical organization of membranes in microdomains, and the interactome of its cytoplasmic domain. CD63 tetraspanin regulates the loading of EBV protein LMP1 into exosomes as well as the loading of PMEL into ILVs during melanogenesis (Villarroya-Beltri et al., 2014). It has been shown that redirecting the exosomal CD63 to the plasma membrane increased its vesicular secretion by up to 6-fold, which indicates that the budding of exosome cargo is more efficient from the

plasma membrane than from the endosome membrane (Fordjour, Guo, Ai, Daaboul, & Gould, 2022).

Other proteins that are repeatedly found in exosomes include: tetraspanins (CD82, CD37, CD53), which play a role in exosome formation and cell internalization, heat shock proteins (HSP70, HSP90, HSP27, HSP60) which involved in stress response. Other proteins include: ESCRT molecules (Alix, TSG101 and Vps) that promote MVB formation and causing exosome release, annexins and Rab proteins that are involved in membrane transport and fusion (Yuan Zhang et al., 2019). Additional proteins include Lysosomal-associated membrane protein 1 / 2, GTPase HRas, and Ras-related protein. However, proteins that commonly used as exosome biomarkers are TSG101, CD63, HSP70, and CD81 (Yuan Zhang et al., 2019).

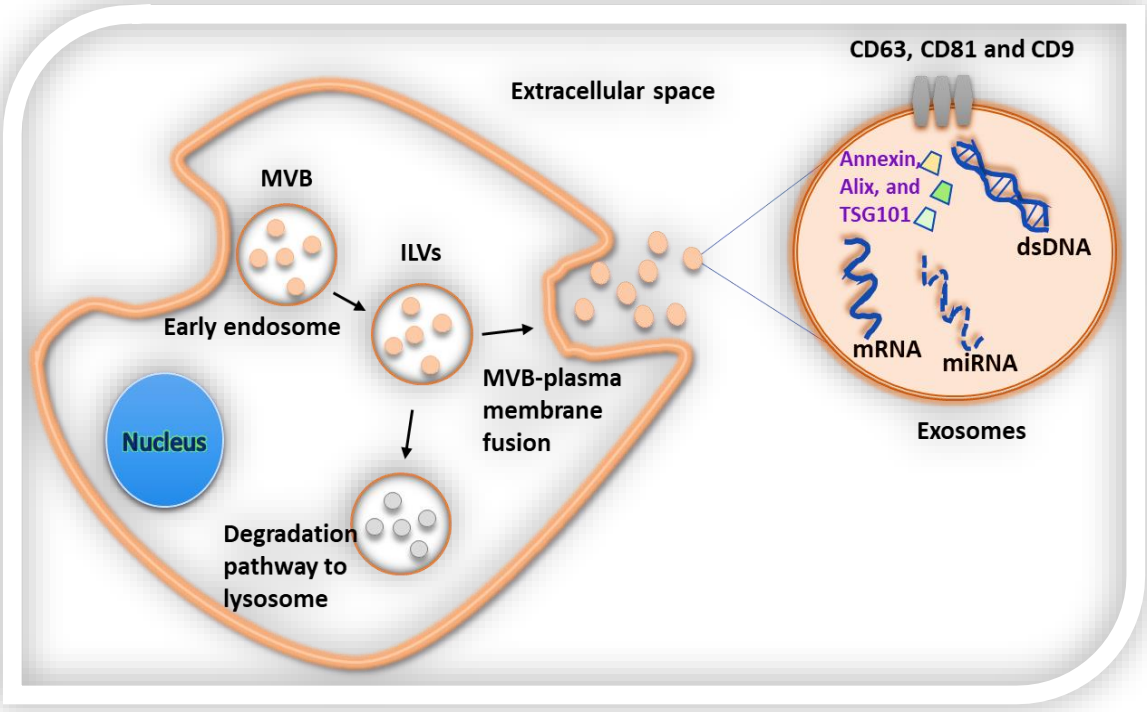

Figure 1.9 Mechanism of exosome biogenesis.

The formation of exosomes occurs via inward budding of a multivesicular body (MVB) membrane forming an endosome. Then the protein, mRNA, and miRNA invaginate the endosomal membrane forming exosomes.

Lipids are essential components of EVs and they have been shown to play a role in exosome formation as well. More than 107 lipid species have been detected in EVs isolated from urine samples. Among those lipids, cholesterol was the most abundant with 63%, and represents an essential part of the membrane as it supports membrane lipid order, prevents ion leakage and affects membrane fusion(Skotland, Sagini, Sandvig, & Llorente, 2020). Phosphatidylserine was found to be the second most abundant lipid in EVs, while other like phosphatidylethanolamine (PE) species were also identified in the EVs (Skotland et al., 2017). It has been reported that enzymes that regulate metabolism of some types of lipid, such as glycerophospholipids or glycerolipids, can be involved in the formation and release of exosomes. For example, in MCF-7 cells (a human breast cancer cell), the enzyme phospholipase D2, the enzyme that is responsible for degrading the head group of phospholipids (mainly phosphatidylcholine, PC) to produce phosphatidic acid (PA), is needed for the inward budding and the formation of ILVs within MVBs containing syntenin (Skotland et al., 2020).

1.4.3 Exosome uptake

Following release into the extracellular space via membrane fusion, exosomes can be efficiently internalized into the recipient cells and release their cargo to produce the subsequent effect. Exosome uptake by target cells is mediated via several mechanisms including endocytosis, direct fusion to the cell membrane, and receptor- ligand interaction(Mulcahy, Pink, & Carter, 2014). The most common mechanism of exosome internalization is endocytosis. This method is an energy-dependent process and is relatively fast as the exosome could be uptaken into the cells within 15 minutes of the initial introduction(Mulcahy et al., 2014). A common example for this entry is clathrin-mediated endocytosis (CME) which acts via progressive and sequential assembly of clathrin-coated vesicles that contain various transmembrane receptors and their ligands 1. Once inside the cell, the vesicles undergo clathrin un-coating and fuse with the endosome to release their contents (Mousavi, Malerød, Berg, & Kjeken, 2004). It has been reported that inhibition of CME decrease EVs internalisation and uptake by ovarian cancer recipient cells (Escrevente, Keller, Altevogt, & Costa, 2011). Caveolin, and lipid raft-mediated endocytosis are other examples of endocytosis-mediated exosome internalisation(Clayton et al., 2004). However, the uptake

mechanism is affected by specificity of the target cells and the exosomes surface proteins (Clayton et al., 2004).

1.4.4 EVs role in cardiovascular disease signaling

The most common methods used for analytical and diagnostic purpose for cardiovascular disease (CVD) include: electrocardiography, echocardiography, cardiac computerized tomography, cardiac catheterization and coronary angiography (Raimondi & Warin-Fresse, 2016). Even though those techniques are effective and provide some levels of reliable diagnostic information, they could only provide data at relatively late stage of the disease because of resolution limitations and the demand for finding new diagnostic tool/biomarkers is crucial for the management and prognosis of CVD (Chong et al., 2019). Therefore, looking for the expression of specific cardiac marker proteins such as troponin, brain natriuretic peptide (BNP), and fibrinogen might provide more accurate diagnostic information for cardiovascular disease even at an earlier stage or before the disease markedly progress (Doran & Voora, 2016).

Because EVs are released from both healthy and diseased cells and are found in many biological fluids, they have great potential role as a diagnostic and prognostic marker. EVs participate in regulating the physiological and pathophysiological processes of the cardiovascular system such as tissue repair and coagulation, atherosclerosis, hypertension, and MI via releasing their cargoes into the target tissues. Therefore, EVs contents (proteins, lipid, and RNA) could be potential tools to provide useful diagnostic information faster, simpler and by non-invasive method to prevent and/or treat cardiovascular disease (Femminò et al., 2020). Analysis of EVs components revealed that they encode a wide range of molecules including around 4400 proteins, 1639 mRNAs, 764 miRNAs, and 194 lipids which suggested complexity and potential multiple functions for EVs (Yuan Zhang et al., 2019). EVs cargo as well as EVs release are influenced by various factors such as inflammatory process, drugs, aging, oxygen content, and disease. For instance, EVs isolated from aged (21- month old) Wistar rats showed reduced CD63 levels and increased acetylcholinesterase activity as well as higher reactive oxygen species levels (parameter of age-related oxidative stress) in the circulating exosomes in comparison to young groups (Bertoldi et al., 2018). Patients with cardiovascular risk factors or those already diagnosed with CVD showed higher levels of circulating EVs than healthy

people (Jansen, Nickenig, & Werner, 2017). Thus, EVs cargo could be utilized as biomarkers for early detection of some CVD. For example, hsa-miRNA-208a has been detected in almost all patients with acute MI as early as 4 h after chest pain suffering, while it was not detectable in healthy subjects (G.-K. Wang et al., 2010). Moreover, circular RNA (cirRNA), that could be carried by EVs, is involved in regulating mitochondrial dynamics and apoptosis in the cardiomyocytes which suggested a potential biomarker for CVD (K. Wang et al., 2017). Analysis of miRNA of plasma exosomes in HF patients showed significant upregulation of miR-21 and downregulation of miR-425 and miR-744 in comparison to healthy people, which suggested a potential role of these miRNA in detection of cardiac fibrosis and heart failure (Lu Wang, Liu, Xu, Liu, & Liu, 2018). Patients with coronary artery disease, particularly diabetic patients, showed a reduction in expression of vascular endothelial miRNA-126-3p and miRNA-26 in circulating endothelial microvesicles (Jansen et al., 2017). Cardiomyocytes, fibroblasts, macrophages, and endothelial cells are the main source of EVs in the heart. When cultured under ischemic or hypoxic conditions, cardiomyocytes release EVs with altered cargo that can act on other cardiac cells. EVs derived from hypoxic/ischemic cardiomyocytes induced inflammatory response and angiogenesis consistently in the recipient cells (Han, Yang, Sun, & Qin, 2021).

1.4.5 EVs as therapeutic delivery vectors in CVD

Much research has investigated the potential therapeutic effect of EVs in CVD both in vitro and in vivo. Most of the time, EVs isolated and/or manipulated for therapeutic application in vitro provide functional protective effect in the recipient cells. For example, it has been reported that miR-21 containing exosomes derived from cardiac progenitor cells inhibited H9C2 cardiomyocyte apoptosis through downregulating PDCD4 (Xiao et al., 2016). Furthermore, it has been shown that microvesicles derived from endothelial progenitor cells (EPCs) protect H9c2 cardiomyocytes from AngII-induced hypertrophy and apoptosis via activating PI3K/Akt/eNOS (Gu et al., 2014). EVs have also been shown to be protective against ischemic heart disease in cell culture. Exosomes of bone-marrow stromal cells (BMSC-exo) induced the proliferation of H9C2 cardiomyocytes and inhibited apoptosis resulting from hypoxia/reoxygenation conditions, via miR-486-5p targeting the PTEN/PI3K/AKT signalling pathway (X.-

H. Sun, Wang, Zhang, & Hui, 2019). Similarly, EVs exhibited therapeutic actions when administered into an animal model with specific type of cardiovascular event. Exosomes isolated from human mesenchymal stem cell (MSC)-conditioned medium (CM) showed cardioprotective response as they reduced the infarct size in a mouse model of myocardial ischemia/reperfusion injury (an injury that induced by restoring blood flow to the ischemic myocardium) (Lai et al., 2010). This observation explained a previous finding that suggested a cardioprotective role of human MSC-CM based on computational analysis of the CM products (Sze et al., 2007). Furthermore, mice exposed to 30 minutes of ischemia by reperfusion, received either human MSC-derived exosomes or saline and cardiac function was monitored for 28 days(Arslan et al., 2013). Exosome treated mice showed a reduction in infarct size by 45% compared to the saline group. Significant improvements in left ventricular geometry and contractile performance was also observed in the exosome treated group over the treatment period. Analysis of the heart tissues revealed elevation in ATP, NADH, phosphorylated-Akt and phosphorylated-GSK-3β, and a reduction in oxidative stress and phosphorylated-c-JNK in exosome treated mice (Arslan et al., 2013).

Cell lines can also be engineered via silencing or overexpression of specific proteins or RNA to reduce or enhance specific EVs cargo production. Overexpression of miRNA-21 in HEK 293T cells via transfection with pMIR-miR21(plasmid that overexpress miRNA-21) led to increased miRNA-21 EVs (miR21-EVs) production (Song et al., 2019). miR21-EVs effectively delivered into H9c2 and neonatal mouse cardiomyocyte as well as HUVECs and exerted antiapoptotic effects (Song et al., 2019). Furthermore, exogenous cargo, e.g., linear DNA, can be loaded into EVs via non-transfection methods such as electroporation and that the EVs can mediate transfer of the DNA into recipient cells (Lamichhane et al., 2015).

Several clinical trials have been already conducted for utilizing EVs in the treatment of cancer disease e.g. colorectal cancer, and indicated that EVs are safe and can provide alternative option in immunotherapy for colorectal cancer (Dai et al., 2008). However, clinical trials for EVs in cardiovascular disease might be still restricted to the diagnostic purpose as biomarkers, as they crucially rely on the development of highly efficient production and isolation techniques, as well as a strategy for efficient and accurate drug loading either before or post

isolation (Sahoo et al., 2021). Available techniques for isolation, characterization and scaling up the EVs still raise a considerable challenge suggesting more studies are needed to determine the most suitable strategy to be used. For EVs as delivery vector for RAS components see (chapter 4).

1.5 Hypothesis and Aims

Both PRCP and ACE2 belong to the counter regulatory axis of the renin angiotensin system and have been targeted as therapeutic agents for cardiovascular disease. However, the molecular therapeutic potential of PRCP in cardiac function needs investigation. The therapeutic potential of ACE2 for cardiovascular disease treatment has been demonstrated by both viral gene therapy approaches and through administration of recombinant ACE2, however other methods for delivering ACE2 to cardiac cells might enhance its therapeutic efficacy.

Here it was first hypothesised that adenoviral gene transfer of PRCP would be an effective therapeutic approach in Ang II induced hypertrophy and Ang II induced hypertension. Second, it was hypothesised that loading EVs with ACE2 would be an alternative method of delivering ACE2 as a therapeutic intervention.

Aims

1- To develop adenoviral vectors which overexpress PRCP to study the effect of PRCP gene transfer against Ang II-induced cardiomyocyte hypertrophy in-vitro.
2- To study whether delivery of PRCP using adenoviral vector-mediated gene therapy is protective against Ang II-induced cardiac hypertrophy and dysfunction in vivo.
3- To generate and characterize EVs as therapeutic vehicles for delivery of ACE2 to the heart.
4- To study the protective effect of ACE2-EVs on cardiomyocyte hypertrophy induced by Ang II.

Chapter 2 Materials and Methods

2.1 Materials

All tissue culture reagents as well as TaqMan™ Gene expression assay reagents were purchased from ThermoFisher Scientific (Paisley, UK). All plastics used in tissue culture including tissue culture flasks (T-150 cm^2 tissue and T-75 cm^2), several size well plates (6, 12, 96 well plates), and centrifuge tubes were purchased from Avantor-VWR (Leicestershire, England). The restriction endonucleases enzymes used in cloning process were purchased from New England BioLabs (NEB) (Ipswich, UK). pShuttle-CMV, Ad-ACE2, and Ad-GFP were provided by Prof. Stuart Nicklin lab.

Solutions

For preparing 10x stock citric saline (in mM): 100 g of KCl, 44 g of sodium citrate dehydrate were added into 100 mL dH_2O. The solution was sterilized by autoclaving. For 1x working solution: dilute 10x stock with sterile phosphate buffer saline.

For 10x Tris-buffer saline (TBS) preparation: 24.2 g Tris-Base, 87.7 g sodium chloride, and 900 mL of dH_2O. Then the pH was adjusted to 7.4 using HCl at room temperature. The solution was topped up to 1 L with dH_2O.

For 10x Tris-EDTA (TE) stock buffer: 12.1 g Tris–HCl, 3.72 g EDTA. The pH was adjusted to 8.0 in 1 L of dH_2O. The solution was then autoclaved.

For TD 10x stock buffer (1 L dH2O): 80 g NaCl (750 mM), 3.8 g KCl (50 mM), 2.5 g Na2HPO4·12H2O (10 mM), 30 g Tris–base (250 mM). The pH was brought to 7.4 with 10 N HCl. The solution was sterilized by autoclave and store at 4°C.

Preparation of Cesium chloride (CsCl) solutions:

1.25 g/mL Density: 36.16 g CsCl plus 100 mL 1× TD buffer.

1.40 g/mL Density: 62.20 g CsCl plus 100 mL 1× TD buffer.

1.34 g/mL Density: 51.20 g CsCl plus 100 mL 1× TD buffer.

Solutions were sterilized by passing through 0.22 mm filter.

Dialysis buffer for virus preparation: 200 mL of 1xTris EDTA (TE) and 1800 mL of sterile H_2O.

10% glycerol Dialysis buffer preparation: 100 mL of autoclaved glycerol was added to 900 mL of dialysis buffer.

Preparation of western immunoblotting buffers:

1x Running buffer for 1L: 50 ML of 20x NuPAGE Blot running buffer (cat. no: NP002, Thermo Fisher Scientific, MA, USA) plus 950 mL deionized water.

1x transfer buffer for 1L: 14.4 g of glycine, 3.03 g of Tris (Base), 200 ML of Methanol, and 800 ML of dH_2O. The mixture was dissolved by magnetic stirrer if required.

1x TBST buffer preparation: first, prepare 100 mL of 10x stock of TBST by adding 2.42 g of Tris (Base), 8.77 g of NaCl, 500 µL of Tween 20 and topping up to 100 mL with dH2O. Second, prepare 500 mL of 1x TBST by adding 50 mL of 10x TBST into 450 mL of dH2O.

Preparation of 100 mL Ripa buffer:

Ripa buffer should be prepared according to the following order: first add 0.5g of 0.5% Na deoxycholate, 5 mL of 1M Tris HCL, 3 mL of 5M NaCL, 200 µl of 0.5M of EDTA, and dH_2O. Second, pH should be adjusted to 8.8. Then add 0.1g of SDS (Sodium dodecyl sulphate) and 1 mL of triton –x100.

2.2 Antibodies and supplier

Table 2 List of primary antibodies

Antibody	Cat. Number	Manufacture
Anti-PRCP	STJ25100	St John's laboratory
Anti-PRCP	15995-1-AP	Proteintech
Anti-ACE2	Ab15348	Abcam
Anti-TSG101	Ab125011	Abcam
Anti-CD63	Ab134045	Abcam

Table 3 List of secondary antibodies

Antibody	Cat. Number	Manufacture
Rabbit antimouse IgG Alexa Fluor 680	A21065	Thermo Fisher Scientific
Goat antirabbit IgG Alexa Fluor 680	A21076	Thermo Fisher Scientific

2.3 qRT-PCR probes and suppliers

Table 4 List of TaqMan probes and suppliers

Gene	Gene Name	Assay ID	Manufacturer	Dye/size
PRCP	Prolylcarboxypeptidase	Rn01511011_m1	Thermo Fisher Scientific	FAM-MGB
ACE2	Angiotensin converting enzyme 2	Rn01416293_m1	Thermo Fisher Scientific	FAM-MGB
ACE	Angiotensin converting enzyme	Rn00561094_m1	Thermo Fisher Scientific	FAM-MGB
Agtr1a	Angiotensin II receptor, type 1a	Rn02758772_s1	Thermo Fisher Scientific	FAM-MGB
Agtr2	Angiotensin II receptor, type 2	Rn00560677_s1	Thermo Fisher Scientific	FAM-MGB
Mas1	MAS1 proto-oncogene, G protein-coupled recepto	Rn00562673_s1	Thermo Fisher Scientific	FAM-MGB
Nppb	natriuretic peptide B (BNP)	Rn00580641_m1	Thermo Fisher Scientific	FAM-MGB

2.4 Cell culture

Human embryonic kidney (HEK) 293 cells (explained in section 2.1.3), rat cardiomyocytes (H9c2) (explained in section 2.1.2), and HeLa cells (human cancer cell line) (explained in section 2.1.4) (LGC STANDARDS- ATCC, Middlesex, UK) were used in this experimental work. All cell culture work was performed under sterile conditions to prevent any contamination by using a vertical laminar flow hood cleaned with 70% ethanol and sterile ddH_2O. Cell lines were taken from liquid nitrogen and 1 mL of Gibco minimum essential media (MEM) (Thermo Fisher, Paisley, UK) containing 10% fetal bovine serum (FBS), 200mM of L-glutamine, 10,000 units/mL Penicillin, 10,000µg/mL streptomycin, and 1 mM of sodium pyruvate (Thermo Fisher, Paisley, UK) (Table 5), was added drop by drop . The cells were then subjected to centrifugation, re-suspended in 1 mL of fresh media, and transferred into a T150 cm^2 flask with 25 mL total volume of media. The cells were incubated in 37°C and5% CO2, and media was changed every 48 hr or as required. The desired confluence for healthy cell maintenance was 80% for 293 cells and HeLa cells, while H9c2 cells were cultured until approximately 70% confluence. Cells were detached and harvested via washing with Dulbecco's phosphate-buffered saline (DPBS) and incubated for 5 minutes at 37°C with 4 mL of 1x citric saline, for 293 cells, or 1x trypsin- EDTA for HeLa cells and H9c2 cells. To inactivate the citric saline or trypsin EDTA, double the volume of media was added, and the cells were then subjected to centrifugation at 500 g for 5 minutes at room temperature and re-suspended in fresh media as required.

Table 5 Buffers and equipment used in tissue culture.

Material/equipment	Manufacture	Lot or REF number
Minimum essential media (MEM)	Gibco	2255196
Phosphate buffer saline (PBS)	Gibco	2293689
L-Glutamine 200mM	Gibco	2165253
Pen Strep	Gibco	2321114
Sodium pyruvate 100mM	Gibco	2088876
HERA CELL CO2 incubator	Thermo scientific	51030286
Cell culture hood	Thermo scientific	51025635

2.4.1 H9c2 cells

The rat H9c2 cardiomyocyte cell line was purchased from Sigma Aldrich (Irvine, UK). This cell is a subclonal line of the original clonal cell line derived from embryonic BD1X rat heart myoblast by Kimes and Brandt (Kimes & Brandt, 1976). H9c2 cells have been shown to be a good model for differentiation studies, hypertrophy, protein and gene expression as well as toxicity assessment (Watkins, Borthwick, & Arthur, 2011; Zevolis, Philippou, Moustogiannis, Chatzigeorgiou, & Koutsilieris, 2022). Complete minimum essential media was used to culture H9c2 and trypsin-EDTA used to detach them and was passaged into 3 or 5 T150 cm^2 flasks according to confluence of the original flask. In comparison to neonatal rat cardiomyocyte, H9c2 cells do not present contractile activity (Branco et al., 2015).

2.4.2 HEK293 cell culture

HEK293 cells are Human embryonic kidney cell line that was first generated by Frank Graham via transfection of those cells with sheared fragments of serotype adenovirus 5 DNA (Graham et al., 1977). This led to selection of a clone that had integrated DNA containing the E1 region which is essential for adenoviral replication (Graham et al., 1977). The name of HEK293 came from Graham's experiment number 293 as he used to number his experiments (Graham et al.,

1977). HEK293 cells were cultured in complete MEM and detached using 1x citric saline and could be passaged up to 1:5 of T150 cm^2 flasks.

2.4.3 Hela cells

HeLa cells were derived from cervical cancer cell line of African American lady named Henrietta Lacks in 1951(Masters, 2002). Hela cells are cultured in complete MEM media containing 10% FBS and detached using trypsin-EDTA (Kanzawa et al., 2004) .

2.5 Construction of a replication-deficient adenovirus serotype 5 vector expressing rat prolylcarboxypeptidase

2.5.1 Design of a flexible cloning vector encoding rat prolylcarboxypeptidase

The rat prolylcarboxypeptidase (PRCP) cDNA sequence was obtained from a PubMed nucleotide search. To facilitate sub-cloning of PRCP into a range of gene transfer vector systems including adenoviral, adeno-associated viral (AAV) and lentivirus a modified sequence was designed to incorporate flanking unique restriction endonuclease recognition sites including *Neh*I, *Not*I, *Sal*I, *EcoR*I, *HinD*III, *Xho*I, and *Mlu*I. A plasmid cloning vector incorporating this sequence (pEX-A258-Rat PRCP) was purchased from (Eurofins Scientific, Luxembourg, Germany). Detailed for the plasmid map was mentioned in (section 3.2.1). A stock of 100ng/µL was prepared by adding the calculated volume of nucleotide free water to the plasmid for storage at -20°C. A further stock with 10 ng/µL was prepared to use for the transformation of competent *E. coli*.

2.5.2 Plasmid DNA transformation

DH5 alpha cells Max Efficiency kits (Invitrogen Thermo Fisher Scientific, Paisley, UK) were used for the transformation. The cells were taken from -80°C and thawed on ice. Next, 50 µL of cells were transferred to a 1.5 mL Eppendorf tube and 1 µL of DNA was added and left on ice for 30 minutes. Then, heat shock was applied by placing the tube in a 42°C water bath for 45 seconds. The tube was returned back to the ice for 2 minutes. Next, 450 µL SOC (Super Optimal broth with Catabolite repression (New England BioLabs (Ipswich, UK)) medium was added and the tube was incubated in a rotator incubator for 1 hr and 225 rpm at 37°C. Then, 10 µL of cells was added to an agar plate containing 100 µg/mL ampicillin and incubated overnight at 37°C. On the following day, colonies were

picked and transferred into 10 mL of Luria broth containing 100 µg/mL of ampicillin, and incubated overnight at 37°C in a shaking incubator at 180 rpm. Miniprep and colony screening were performed on the following day as explained in the following section.

2.5.3 Screening by small scale miniprep for plasmid DNA

Miniprep plasmid DNA was purified using PureYield™ Plasmid Miniprep System (Promega, Madison, USA). Three mL of bacterial culture was transferred into an Eppendorf tube and was subjected to centrifugation at 12,000 x g, the supernatant discarded, and the pellet was re-suspended in nuclease free water. The cells were then lysed by cell lysis buffer and incubated for 5 min followed by adding 350µL cold neutralization solution and performing centrifugation at 12,000 × g for 3 minutes. The supernatant was transferred carefully to a pure-Yield Mini-column placed into a collection tube. The tubes were then subjected to centrifugation in a micro-centrifuge at 12,000 x g for 15 seconds and the flow through was discarded. The column was then washed via centrifugation at maximum speed for 15 seconds with 200 µL of Endotoxin removal wash followed by another centrifugation with 400 µL of column wash solution for 30 seconds at 12,000 x g. Then, the mini-column was moved to new labeled Eppendorf tube and 30 µL of elution buffer or nuclease free water added and the plasmid DNA eluted by centrifugation for 2 min at 12,000 × g. The eluted DNA was stored at -20 °C. The DNA concentration was then quantified by NanoDrop as detailed in (section 2.2.5).

2.5.4 Glycerol stock for bacterial culture

To store the bacterial culture at this stage, 200 µL of sterile glycerol was added into 800 µL of culture in a cryovial tube, mixed and stored at -80 °C. To re-establish the culture, from -80 °C, the cryovial content was thawed on ice and a small volume added to an agar plate containing the required antibiotic to allow single colonies to grow.

2.5.6 Maxi preparation for the plasmid DNA

To produce large scale of the plasmid DNA preparation, approximately 7 mL of bacterial culture was transferred to a large conical flask and 500 mL Luria Broth containing the appropriate antibiotic was added to grow a large-scale culture for maxi preparation and incubated overnight at 37°C with shaking at180 rpm.

Then, the plasmid was isolated and purified using PureLink™ HiPure Plasmid Filter Maxiprep Kit (Invitrogen™). According to manufacture protocol, the culture was transferred to bug pots and harvested by centrifugation at 6000 x g for 15 minutes at 4°C and resuspended in 10 mL of resuspension buffer (R3) containing 100 µg/mL RNase A, and transferred to small centrifuge tubes. Cell lysis and precipitation were done using lysis buffer (L7) and precipitation buffer (N3) respectively and the tubes were subjected to centrifugation at 20,000 x g for 20 minutes at room temperature. The supernatant was transferred to the PureLinkHiPure maxi-column and clarified by allowing the lysate to filter through by gravity flow. The lysate was washed by adding 60mL of washing buffer (W8) and left to filter through by gravity. Then, 15mL of elution buffer (E4) was added to the column and the eluted samples were collected into clear centrifuge tubes. Precipitation was performed by adding 10.5mL of2-propanolol and centrifugation was performed at 15,000 x g for 30 minutes at 4°C. The pellet then was resuspended in 4 mL of 70 % ethanol, transferred to Eppendorf tubes, and subjected to centrifugation 16000 x g for 5 min at 4°C in a microcentrifuge. The supernatant was discarded, and the tubes were left for 15-20 minutes at room temperature to dry out. Next, 200 µL of nuclease free water was added and tubes subjected to centrifugation for 1 minute. The supernatant containing the DNA was transferred to new labeled Eppendorf tube.

2.5.7 Determination of Nucleic acid concentration by NanoDrop

The DNA and RNA concentration and purity were determined using NanoDrop™ 1000 Spectrophotometer (ThermoFisher Scientific). Initially, a sample volume of 1.4µL was added into the receiver fibre obtic cable and the upper arm was lowered into the sample. Next, an xenon flash lamp allow the light to pass through the sample and the absorbance at different wave length was measured via spectrometer. DNA absorbance light at 260 nm which therefore can be utilized to calculate the concentration of the sample using the beer-lambert equation as follow:

$$C=(A*e)/b$$

Where **C** is the concentration in ng/µL.

A is the absorbance in absorbance unit (AU)).

e is the wavelength-dependent extension coefficient in ng-cm/µL.

b is the path length in cm.

a ratio of 260/280 is used to determine the purity of the DNA and RNA where a ratio of 1.8-2.2 was considered pure.

2.5.8 Restriction endonuclease-mediated digestion of plasmid DNA

Restriction endonucleases digests were applied to verify the presence of the DNA restriction sites and to prepare the DNA fragments for subclone into the backbone vector. The digestion process was performed according to manufacturer protocol (England BioLabs (NEB) (Ipswich, UK). The tubes were labelled and the calculated volume of DNA, buffer, restriction enzymes and dH2O were added to each tube with a total volume of 20 µL for small volume or 250 µL for large quantity. Sample were then incubated at 37°C in water bath for 2 hours for small digest or overnight for large digest. Samples were then run in agarose gel electrophoresis to verify/checking the successful of the digestion. The digested plasmid DNA was purified using phenol:chlorophorm purification method, while the pRat-PRCP was gel purified.

2.5.9 Agarose gel electrophoresis

To prepare (0.7%) agarose gel, 1.4 g UltraPure™ Agarose (Thermo Fisher Scientific) was added to 200 mL of 1 x TBE buffer Thermo Fisher Scientific) and dissolved by heating in the microwave. The agarose/TBE solution was then allowed to cool down for approximately 5 min and brought to the hood and 4 µL of ethidium bromide (Millipore Sigma, MO, USA) to allow DNA imaging. The solution was poured into gel mould and allowed to solidify (about 30 min). the gel was then placed in an electrophoresis tank containing proper volume of TBE buffer. Loading dye (6x blue/orange) (Promega, Southampton, UK) was added to the samples. Next, proper amount of 1kb ladder (Promega) and samples were loaded into the wells of the gel and subjected to 130 V for 45 min to allow separation for DNA fragments. DNA bands were imaged using (ChemiDocTM XRS+, Bio-Rad, CA, USA).

2.5.10 Phenol/chloroform purification of DNA

For phenol/chloroform purification, an equal amount of phenol:chloroform:isoamyl alcohol(Sigma, Irvine, UK) was added gently to DNA

1:1 mix. The tube was vortexed for 30 sec until the mixture becamewhite in color and then subjected to centrifugation at 13000 x g for 2 minutes. The upper aqueous layer was transferred to another tube and an equal volume of chloroform was added to remove the phenol followed by centrifugationat16,100g. The upper layer containing plasmid DNA was transferred into a fresh tube and 1/10th volume 3M sodium acetate (pH 5.2) and 2 volumes 100% of ethanol were added. The tube then was placed in dry ice for 10-15 minutes and subjected to centrifugation for 10 minutes at 16,100g. The supernatant was discarded, and the pellet was re-suspended in 100 µL of 70% ethanol and subjected to centrifugation for 2 minutes at 16,100g. The supernatant was removed and the tube left to air dry for 5-10 minutes and the pellet was re-suspended in a sterile nuclease free water. Agarose gel electrophoresis was performed using approximately 300 ng DNA to ensure the complete digest for DNA.

2.5.11 DNA gel extraction and purification

DNA gel extraction and purification was performed as per the kits manufacture construction (The WizardR SV Gel and PCR Clean-up System (Promega)). DNA was imaged via UV transilluminator and the slice of agarose gel containing the required DNA band excised from the gel weighed in a sterile 1.5 mL microcentrifuge tube. A guanidine isothiocyanate containing solution (Membrane Binding Solution) was added to the gel segment at a ratio of 10 µL to 10 mg gel slice and incubated at 50-56°C for 10 min to allow complete dissolve of the gel. Samples were the transferred into SV mini-column and incubated for 1 min before subjected to centrifugation at 16000 x for 1 min. The flow-through was discarded and 700 µL of ethanol containing membrane wash solution (MWS) was added to the columns and subjected to centrifugation for 1 min at 16000 g x. Next, 500 µL of MWS was added and subjected to centrifugation for at 16000 x g for 5 min. A further centrifugation was applied to columns at 16000 g x for 1 min without the centrifuge lid to allow maximum ethanol evaporation. The columns were the placed into fresh sterile 1.5 mL Eppendorf tubes and 40 µL of nuclease-free water was added directly to the membrane for DNA elution. The sample incubated for 5 min prior to centrifugation for 1 min at 16000 x g. The DNA concentration was determined via NanoDrop (section 2.2.6).

2.5.12 Ligation reaction for plasmid DNA into the backbone vector

Ligation reactions for cloning PRCP were set up using a 96 well PCR plate according to the following insert to vector ratios (in ng) (0:1, 3:1, and 5:1). The calculated volume of buffer, dH_2O, and 1 µL of T4 DNA ligase (New England Biolabs, Ipswich, MA) was added, and the plate was covered by adhesive film and incubated at 16°C in MJ Research Tetrad PTC-225 Thermal Cycler (Global Medical Instrumentation Inc, MN, USA) overnight. The following day heat inactivation was performed at 65°C for 10 minutes followed by cooling down to 4°C. The transformation was then performed using 2 µL of ligation reaction and 100 µL of XL10-Gold ultracompetent cells (Agilent Technologies, Sydney). The cells were plated in LB agar plates containing 50 µg/mL of kanamycin and incubated at 37°C overnight. Colonies were picked the following day and screened using miniprep and diagnostic restriction endonuclease digest.

2.5.13 Designing primers for sequencing

Ten primers were designed for sequencing the recombinant plasmid (pShuttle-CMV-pRat-PRCP) as shown in Table 3. The designed primers sites on the plasmid were shown in (Figure 2.1). Plasmids were aliquoted into sterile Eppendorf tubes at a concentration of 50-100ng/µL in total volume 15µL. Sequencing primers were aliquoted separately at a concentration of 10pmol/µL to a total volume 10µL for each primer. Samples were then sent to Eurofins Genomics (Germany) for sequencing.

Table 6 Forward and reverse primers designed for plasmid sequencing.

Forward primers	Reverse primers
5'CATTGACGCAAATGGGCGGTAG 3	5'GTAAAACCTCTACAAATGTGG3'
5'C AAC AGA AGG TTG ACC ACT TTG3'	5'GTGTCTGTGATGTCTTTGGTG3'
5'CAG AGT TAA TCA GGC ACT TG3'	5'CATTGGGATTCCTCAAGTATC3'
5'CTG AAA CCT GGG TGA ACC TG3'	5'GATATTTCATCCTGAACCAGG3'
5'GA TGA CTA CCA TGT ATG GTG GC3'	5'GTGTGTTAGTTGACAAGTGCG3'

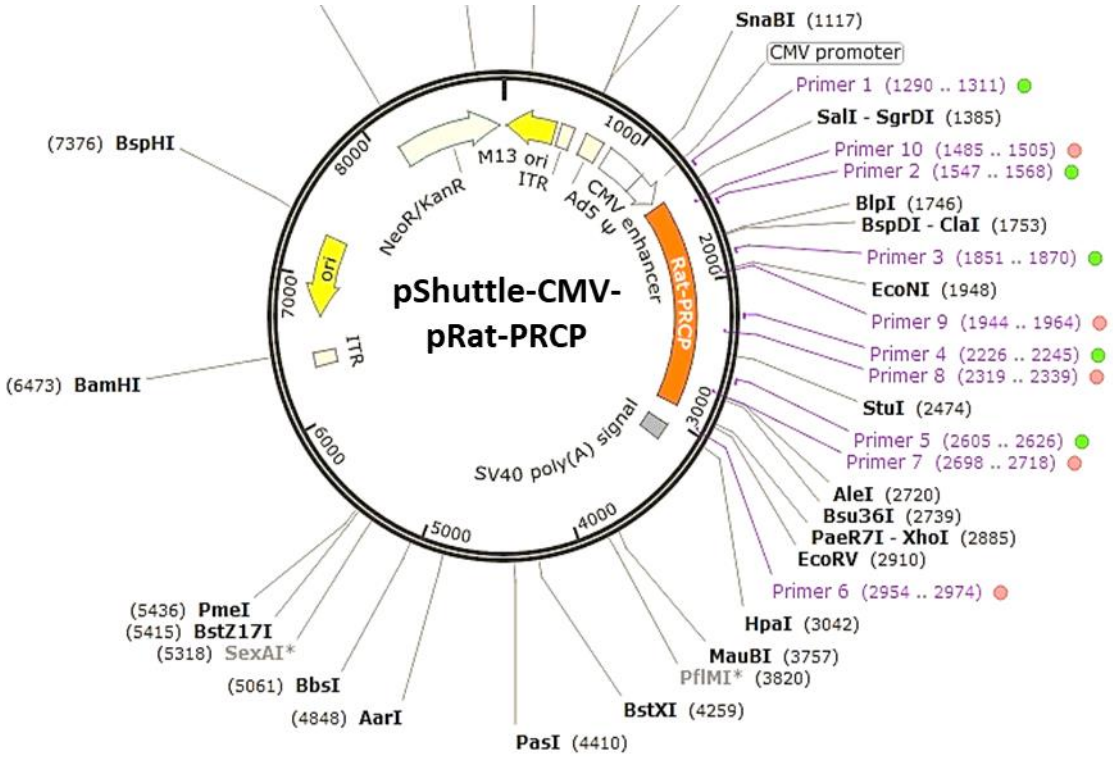

Figure 2.1 Primer sites distribution on the DNA plasmid.

2.5.14 Homologous recombination between pShuttle-CMV-pRat-PRCP and pAdEasy-1 system

Pshuttle-CMV-PRCP were digested overnight with *Pme*I and purified by Phenol/chloroform method (section 2.2.9). BJ5183 cells (Addgene, Teddington, UK) that are pre-transformed with linearized pAdEasy were aliquoted into 50□L and kept on ice. One microgram of the digested DNA (pshuttle-CMV-pRat-PRCP) or uncut (control) DNA was prepared in 6µL of nuclease-free water and maintained in ice as well. The total volume of prepared DNA was added to 50□L of cells and mixed by gentle pipetting. Next, the mixture was transferred to a 0.2 cm pre-chilled electroporator cuvette (Cell Project, EP-102, Staffordshire, UK). The cuvette was carefully tapped 2 to 4 times to remove the air bubbles and left on ice for 2-3minutes. The electroporation was performed usingEc2 mode for a 1-second pulse using an electroporator (Bio-Rad, Hercules, CA, USA).

Then, the cuvettes were removed and 500 µL of cold SOC medium was added immediately. The samples were transferred to Eppendorf tubes and incubated for 1hr at 37°C using a shaking incubator. Following centrifugation for 1 minute the pellets were plated on agar plate, using a sterile spreader to spread the mixture, containing 50 µg/mL of kanamycin and incubated overnight at 37°C with shaking at 180rpm. Small colonies were picked the following day and screened via miniprep (section 2.2.3) and diagnostic restriction endonuclease digestion (section 2.2.5).

2.5.15 Transfection of recombined pAdEasy-pShuttleCMV-pRat-PRCP into HEK293 cells

100 µg of the intact recombinant pAdEasy-1 vector encoding PRCP was digested with *Pac*I and purified by adding 2 volumes of 100% ethanol and 1/10th volume 3M sodium acetate (pH 5.2) and freezing the samples in dry ice for 10-15 minutes. Next the sample was subjected to centrifugation at 16,100 x g, the pellet washed via adding 70 % ethanol and subjected to a further centrifugation step for 2 minutes at 16,100 x g. The supernatant was removed, and the tube left to air dry for 5-10 minutes and the pellet was re-suspended in 100 µL of sterilized water. Transfection into HEK293 cells was performed using the Xfect transfection reagent protocol (Clontech Laboratories, Inc. A Takara Bio Company, Mountain View, CA, USA). Low passage HEK293 cells were seeded into a 6 well plate at$6x10^5$cells/well to become 70-80% confluent the following day. For each well, five microgram of the digested recombinant plasmid was added into 1.5 µL of Xfect Polymer and the volume brought to 100 µL with Xfect reaction buffer. The mixture was vortexed and incubated for 10 minutes at room temperature before the total volume was added to the well. Three wells were transfected with the recombinant plasmid (pAdEasy-pShuttleCMV-pRat-PRCP), and one well with pEGFP plasmid. The remaining two wells were left un-treated (-ve control) or treated with Xfect polymer alone. The plate was incubated at 37°C/ 5% CO2 and the media was replaced after 4hr with pre-warmed fresh complete media. The plate was incubated for 7-10 days, and the media were changed every 2-3 days or when required. The well transfected with GFP plasmid was assessed after two days under a fluorescence microscope to evaluate the transfection efficiency. Once cytopathic effect (CPE) was evident in pAdEasy-1 transfected wells, the media was not changed and the well was monitored until

CPE was complete. At this point the media containing the cells was collected into a Falcon tube and subjected to centrifugation at 250g for 10 minutes at room temperature. The supernatant was discarded, and the pellet was re-suspended in 1 mL of PBS. Next, an equal amount of ArkloneP (trichlorotrifluoroethane, Sigma, Irvine, UK) was added and mixed by inverting for 10 sec, followed by shaking for 10-15 sec and this step was repeated for 1 minute. Next. the mixture was subjected to centrifugation for 10 min at 750g and the upper layer containing the virus was pipetted carefully into Eppendorf tubes (100□L/tube) and stored at -80°C.

2.5.16 Production of high titer stock of recombinant adenoviral vectors

First, one confluent T150 cm^2 flask of HEK 293 cells was passaged into 5 x T150 cm^2 flasks. Once flasks become confluent, they were further expanded into 22 T-150 cm^2 flasks for infection preparation. Once cells became approximately 80% confluent, they were transduced with Ad-R-PRCP to generate large scale preparations of the vector for experimentation. First, 50 μL of the seed stock virus was added into 550 mL of complete MEM. Then, the media in 21 flasks were replaced with 25 mL of Ad-R-PRCP containing media and incubated at 37°C for approximately 5 days. One flask was retained as a negative control. The cells were checked daily, and the media were changed every 3 days with fresh complete MEM. Once CPE started no more media changes were performed and cells were monitored daily until CPE was complete (typically within 5 days when cells started to detach from the flask. At this point, the cells were collected into 50 mL Falcon tubes and subjected to centrifugation at 850g for 10 minutes at room temperature. The media was removed, and the pellet was re-suspended in 6 mL of PBS and stored at -80°C until purification.

2.5.17 Adenoviral vector purification

The cells were removed from -80°C, thawed and the cell lysis was performed by adding an equal volume (6mL) of ArkloneP to the Falcon tube containing the cells and then invert the tube for 30 s followed by shaking (not too vigorously) for 10 s. Cells were then subjected to centrifugation at 1900 x g for 10 minutes at room temperature. Three layers were formed following centrifugation and the upper/aqueous layer that contained the adenoviral vector was removed and transferred into a fresh sterile tube.

Next CsCl gradient ultracentrifugation was performed to remove any remaining cell debris. First, sterile SW40 ultracentrifugation tubes (Beckman Coulter Ltd, Buckinghamshire, UK) were pre-sterilized with 70% ethanol and rinsed with distilled water. Next, 2.5mL of low density (1.25 g/mL) CsCl was added to the tube and then 2.5mL of high density (1.40 g/ml) was added carefully below the first layer. Next, the crude adenovirus preparation was added gently on the top of the CsCI layers by touching the wall of the tube with the pipette tip so as to not disturb the gradient layers. The tube was then filled with PBS. Subsequently, ultracentrifugation was performed at 217,874g for 1.5hr at room temperature with maximum acceleration and minimum deceleration. Three layers were formed following ultracentrifugation and the bottom layer, or the small white band is the one that contains the mature virus. The adenovirus was collected carefully using a 2mL syringe (Injekt®-F Solo, B. Braun, Germany) + 21 G sterile green needle (Becton Dickinson, NJ, USA) by inserting the needle directly underneath the virus layer and collecting the band of mature adenovirus using a sweeping motion in the tube. The purified adenovirus was then transferred to a fresh tube. For the second CsCl gradient 5 mL of 1.34 g/mL density CsCl solution was added to a fresh ultracentrifuge tube and the adenovirus solution was added very gently. The tube was then filled with PBS prior to subjected to ultracentrifugation for 1.5 h at 217,874 x g. The virus band was then collected from the ultracentrifuge tube gently as aforementioned and the adenovirus was then subjected to dialysis using a Slide-A-lyser cassette (10,000 molecular weight cut off (MWCO), 0.5–3.0 mL capacity) (Thermo Fisher Scientific, MA, USA) to remove contaminating CsCl. The dialysis buffer was 200 mL of 1X Tris EDTA (T/E) and 1800 mL of sterile H_2O for 2 hr and this step was repeated followed by overnight dialysis in 10% autoclaved glycerol and 1X TE buffer and 1600mL of sterile H_2O. The virus was then collected by syringe, aliquoted and stored at -80°C.

2.5.18 Sequencing for the Adenovirus Product

Sequencing for the adenovirus was performed using four primers, two forward and two reverse primers. 100ng/µL of Ad-PRCP was prepared into Eppendorf tubes in 20µL total volume and eurofins tube labels were used to identify the tube. The sequencing primers were aliquoted separately at a concentration of 10 pmol/µL in 15µL total volume.

2.5.19 Micro BCA protein assay to measure viral particle titer

Adenoviral vector viral particle (vp) concentration was measured by micro-BCA protein assay following the manufacturer's protocol (Pierce Biotechnology, Rockford, lL USA). Nine bovine serum albumin (BSA) standards were prepared with concentration ranging between 0 µg/µL to 200 µg/µL. Next, 150 µL of standards were added into a 96 well plate in duplicate. Three different volumes of virus stock were added: (1 µL, 3µL, and 5µL) in duplicate and then each well made up to 150 using PBS. Next, 150 µL of the microBCA working reagent, prepared by mixing 25 parts of Micro BCA Reagent MA and 24 parts Reagent MB with 1 part of Reagent MC, was added to each well and the plate was incubated at 37°C for 2 hours. The plate was then read at 562nm absorbance using SpectraMax M2 micro-plate reader (Molecular Device LLC, San Jose, CA) and a standard curve was generated, and protein values of the virus samples were calculated from the standard curve equation. The final vp/mL titer was calculated where 1 µg protein = 1 x 10^9 vp.

2.6 Titration of Adenovirus by End-Point Dilution

The infectious virus titer as plaque forming unit was determine by end point dilution assay using 96 well plate. The titer plate was prepared using an 80% confluent flask of HEK293 cells. The cells were harvested from the flask and suspended in 25 mL of fresh media. Next, 3 mL of cell suspension was transferred into a fresh tube and 17.5 mL media was added. The cells were then seeded into 96 well plate with 200µL/well. The cells were transduced with 100 µL of Ad-PRCP the following day using serial dilution starting from 1 x 10^{-2} to 1 x 10^{-11}. The bottom row was left un-transduced as a control. Media was changed on the next day and then every three days with fresh media. After 8 days the plate was analysed, and the pfu/mL was calculated by the following formula.

The proportionate distance (PD) =
% positive wells above 50% -50 / (% positive wells above 50%) – (% positive below 50%)

and log ID50=

log dilution above 50% + (proportionate distance x dilution factor)

For example, for a plate with 7 positives well at 10^{-10} dilution and 2 positives well at 10^{-11}dilution the calculation would be as follow:

PD = 70% - 50% /70% - 20% = 0.4

Log ID 50= -10 +(0.4* -1) = -10.4

Final titre = 1.76 $x10^{11}$ Pfu/mL.

2.7 Transducing Cardiomyocyte with adenoviral vector for mRNA evaluation

H9c2 cells were seeded into a 6 well plate at $3x10^5$ cells/well. After 24 hr, the cells were transduced with 10,000 viral particle (VP)/cell of Ad-R-PRCP or left untreated (control) and incubated for 48 hr. Cells were washed with PBS and lysed with Qiazol lysis reagent (Qiagen, Manchester, UK) and RNA extraction was performed using miRNeasy mini-Kit (Qiagen, Manchester, UK).

2.8 RNA extraction for gene expression assessment

Chloroform was added to lysed cells and samples subjected to centrifugation for 15 minutes at 12000 x g and 4°C. The aqueous layer was transferred to a new collection tube and 100% of ethanol was added before mixing thoroughly. Next, the samples were transferred to an RNeasy Mini column placed in collection tubes and centrifugation was performed at 8000 x g for 15 seconds at room temperature. Then, 700 µL RWT buffer was added, and samples subjected to centrifugation for 15 seconds at 8000 x g followed by adding 500 µl RPE buffer centrifugation at 8000 x g for 15 s. The last step was repeated with centrifugation for 2 minutes. Next, the RNase mini column was transferred to new labelled Eppendorf tubes and 50 µL of RNase-free water was added for elution and subjected to centrifugation at 8000 x g.

2.9 Reverse transcription to generate cDNA.

The cDNA was generated by reverse transcriptase in a 96 well plate. Calculated volume of RNA and H_2O (usually 7.7µl) was added and then the master mix was prepared by adding 4.4 µL MgCl, 2 µL of RT buffer, 4 µL of dNTPs, 1 µL of random primer, 0.4 µL of RNAse inhibitor, and 0.5µl of reverse transcriptase for each well. The thermal cycle was performed as follow; 25°C for 10 minutes, 37°C for 30 minutes, 95°C for 5 minutes, and 4°C indefinitely.

2.10 Gene expression analysis by TaqMan

TaqMan gene expression analysis was then performed using a 384 well plate. 0.5µl of gene of interest probe was added to 5µl of master mix (Thermo Fisher Scientific, MA, USA) and RNAse-free water was added to get 8 µL final volume for each well then, 8 µL was added to selected wells followed by 2 µL of cDNA. The plate was run in QuantStudio 12K flex software.

2.11 Measurement of Ang II and Ang-(1-7) levels by ELISA

2.11.1 Sample preparation

100 nM Ang II was added to cell culture media and levels measured at specific time points in both Hela and H9c2 cells transduced with Ad-PRCP, Ad-GFP or control (untreated). Cells were seeded into 12 well plates with 1.5x10^5 cells/well and incubated for 24h at 37°C. Then, cells were transduced with 10,000 viral particles (vp) for Hela cells, and 100pfu/cell for H9c2 cells, of Ad-PRCP, Ad-GFP or left untreated, and incubated for 24h at 37°C. Following 24hrs of adenoviral transduction or EV treatment Ang II was added to cells and culture media were collected at 5min, 10min, 15min, 30min, 60min, and 24hr for Hela cells. For H9c2 cells, samples were collected at 24hr and 48hr following treating with Ang II and stored at -80°C.

2.11.2 Measurement of Ang II by ELISA

Ang II was assessed using Ang II enzyme immunoassay kit #A05880 (Bertin Pharma, Montigny le Bretonneux, France), according to the manufacturer's protocol. First, 100 µL of standard, samples, non-specific binding (NSB) and quality control were added to appropriate wells in duplicate or triplicate. The plate was covered with cover sheet and incubated for 1hr at room temperature (RT) with gentle agitation. Next, 50 µL of glutaraldehyde was dispensed to each well, except blank (BK) wells, and incubated for 5min at RT with gentle agitation. Next, 50 µL of Borane trimethylamine was added to each well except BK and incubated at RT for 5 min. The plate was then inverted, and wells washed five times with washing buffer. At the end of the last wash, buffer was removed by inverting the plate and shaking out the last drop using paper towel. Then, 100 µL of Ang II tracer was added to each well except BK and plate was covered and incubated at 4°C overnight. On the following day, the plate was emptied and rinsed 5 times with washing buffer, as mentioned earlier, followed

by dispensing 200 µL of Ellman's reagent into each well. The wells were covered with aluminium sheet and incubated in the dark at RT. The reading was performed every 30 min at a wavelength between 405-414 nm using a Victor micro-plate reader.

Table 7 Standard for Ang II ELISA 1

Standard	Volume of Standard	Volume of assay buffer	Standard concentration pg/mL
S1	1000µL	-	125
S2	500µL of S1	500µL	62.5
S3	500µL of S2	500µL	31.25
S4	500µL of S3	500µL	15.63
S5	500µL of S4	500µL	7.81
S6	500µL of S5	500µL	3.91
S7	500µL of S6	500µL	1.95
S8	500µL of S7	500µL	0.98

2.11.3 Ang-(1-7) ELISA protocol

Ang-(1-7) was measured using ANG1-7 ELISA Kit # OKEH02599 (Aviva system Biology, San Diego, USA). The same samples prepared for AngII detection was used to assess Ang-(1-7) levels. According to manufacturer's protocol, 50µL of standard, samples or blank were added into appropriate wells in two or three replicates. Then, 50 µL of 1xANG1-7-Biotin Complex was added to each well (except absolute Blank) and the plate was covered and incubated for 60min at 37°C. The liquid was discarded by inverting the plate and gently blotted any remaining liquid from the wells by tapping onto paper towel. Wells were then washed three times using 1x washing buffer and any remaining liquid was removed gently by tapping onto paper towel. Next, 100µL of 1X Avidin-HRP Conjugate was dispensed into each well and the plate was covered and incubated for 45min at 37°C. The liquid was discarded, and wells were washed again 3 times with 1x washing buffer. Next, 90 µL of TMB Substrate was added to each well and the plate was covered and incubated at 37°C in the dark for 15-30min. The color of the well should change to gradient blue and the incubation time could be adjusted according to the color intensity. Finally, 50 µL of stop solution was added to each well and the reading was performed within 5 minutes at 450nm.

Table 8 Standards for Ang-(1-7) ELISA

Standard	Standard to dilute	Volume of standard to dilute	Volume of diluent added	Final concentration (pg/mL)
1	500pg/mL	300 µL	0	500
2	500pg/mL	300 µL	300 µL	250
3	250pg/mL	300 µL	300 µL	125
4	125pg/mL	300 µL	300 µL	62.5
5	62.5pg/mL	300 µL	300 µL	31.2
6	31.2pg/mL	300 µL	300 µL	15.6
7	15.6pg/mL	300 µL	300 µL	7.8
8	blank	300 µL	300 µL	blank

2.12 Hypertrophy assay for cardiomyocytes in response to Ang II stimulation

H9c2 cardiomyocytes were seeded into a 6 well plate using coverslips 22x22 mm with $3x10^4$ cells/well and incubated for 24hr at 37°C and 5% CO2. The cells were then transduced with 300 pfu/cell of Ad-PRCP, Ad-GFP or untreated (control) and the media changed to serum free media and incubated at 37°C/ 5% CO2 for 24hr. The cells were then treated with 100nM of Ang II and incubated for 96hr. Media was removed, cells washed gently with PBS and fixed using 4% paraformaldehyde (PFA) on ice for 15 min. Cells were then washed twice and permeabilization was performed via incubation in PBS containing 0.1% Triton-X-100 for 10 minutes at room temperature. Next, cells were washed twice and stained with 5 µg/mL phalloidin/FITC in 1% bovine serum albumin (BSA)/PBS for 1 hr at room temperature. Next, cells were washed and coverslips removed from wells and mounted using ProLong Gold Antifade Mountant with DAPI (Thermo Fisher Scientific, Paisley, UK) and incubated in the dark for 24hr at 4°C.

Images were taken for 3+ fields of view for each coverslip using a live cell microscope (Zeiss, Germany) at a magnification of 20x. Cell area was measured using ImageJ by calibrating scale bar and selecting the area of interest and the average was determined for each condition.

2.13 In-vivo assessment of PRCP gene transfer on Cardiac Function

2.13.1 In-vivo assessment of adenovirus dose on Wistar Kyoto (WKY) Rats

All animal surgical procedures were performed in accordance with the Animal Scientific Procedures Act (1986) and licensed by the UK Home Office (under the project licence held by Dr Delyth Graham, PPL 70/9021).

WKY rats (10 weeks old) were purchased from (ENVIGO Bicester, Oxon,UK) and housed for one week acclimatisation. Two animals were assigned to receive adenovirus and one animal for saline solution. Surgery room was prepared for surgery procedure. To assess liver transduction Ad-LacZ was prepared at $1x10^{11}$ viral particle/animal in a total volume of 150 µL sterile saline.

Osmotic minipumps were prepared with required volume of saline and soaked in saline for 24hr before use. Induction of anaesthesia was performed with 5% isoflurane and maintained at 1.5 L/min medical oxygen. Osmotic minipumps were implanted subcutaneously in the upper back of animals. The femoral vein

was exposed and Ad-LacZ was injected using microscope. Pain relief (Carprieve 50 mg/mL, Norbrook, NewryIreland) was administered in the post-operative recovery phase. Animals were housed for 5 days under 12h light/dark cycle at constant temperature of 21°C with free access to food and water and monitored daily. Rats were humanely killed using terminal anaesthesia and liver, heart, kidney were collected.

2.13.2 Minipump implantation

Anaesthesia was induced with 5 % isoflurane in 1.5 L/min oxygen and maintained at 2.5% isoflurane and 1.5L/min oxygen. The hair was shaved from the target area at the back of the rat and iodine antiseptic was applied for sterilization. Pain relief, Carprieve was injected to minimize pain after surgery. An incision was made on the skin at the target area using sharp autoclaved sterile scissor. Once the cut has been mad, the sterile scissor was inserted underneath the skin very carefully to create space for the minipump. The minipump was inserted subcutaneously using sterile forceps. Finally, the skin was sutured using polyglactin 910 Coated VICRYL Plus Antibacterial suture (Ethicon, NU-CARE, Bedfordshire, UK).

2.13.3 Femoral vein injection of adenoviral vectors

Following minipump implantation, rats were immediately flipped over and legs were sterilized, and a small cut was performed carefully using sharp blade to expose the femoral vein. A syringe (BD Micro-Fine 1ml Syringe 0.33mm) containing the adenoviral vector was prepared and the needle was adjusted/angled to almost 90 degree so as to be parallel to the vein upon injection. The required saline or virus were injected while looking at the vein through a light microscope to enhance vein visibility.

2.13.4 Detection of B-Galactosidase enzyme expression in the liver

Livers were collected and chopped into several pieces and rinsed twice with saline. Next, livers were immediately fixed with 2% paraformaldehyde (PFA) and placed at 4°C overnight. On the following day, livers were washed twice with PBS and submerged in X-Gal stain and incubated at 37°C overnight. Positive B-Galactosidase staining appeared dark blue. For 20 mL of x-GAL stain preparation: 1.54 mM Na_2HPO_4, 0.46 mM NaH_2PO_4, 26.00 µM $MgCl_2$, 60.00 µM

$K_3Fe(CN)_6$, 60.00 µM $K_4Fe(CN)_6$, and 1 mg/mL X-gal and top up to 20 mL with dH_2O. The stain was filtered before use and stored at 4 ºC.

2.13.5 Blood Pressure measurement

Systolic blood pressure was measured via non-invasive tail cuff plethysmography using Visitech BP-2000 Series II Blood Pressure Analysis System (Visitech Systems, North Carolina, USA). All animals were acclimatized for the new environment and trained for BP via applying the procedure for at least one time before starting the actual experiment. Animal were warmed by placing them in a heated box with exposure to a heat lamp for approximately 30°C for about 15-20 minutes to allow vasodilation (less than 15 minutes might not provide enough vasodilation for WKY rats). Animal were then moved to a heated mat to maintain body temperature and covered with a soft, dry cloth with the tail exposed. A blood pressure occlusion cuff was placed first at the base of the tail and the transducer cuff were then inserted to detect the pulse and measure systolic blood pressure. The machine was connected to a programmed electro-sphygmomanometer which was calibrated prior to the beginning of the BP session. For calibration, the machine was set in calibration mode and connected to an air source. Once the program started, calibration was performed via selecting calibration and then accepting the new reading. The program ensures consistent inflation-deflation rates of 1 mmHg and registers pressure changes detected by the transducer. Upon inflation, peak SBP was measured and on deflation base DBP (Figure). An average of at least three blood pressure reading were taken for each rat to get the mean systolic BP. Measurements were taken in the morning to minimize diurnal variation.

2.13.6 Echocardiography

Assessment of heart function was performed using an echocardiography machine (Siemens, Surrey, UK) with a fifteen-megahertz transducer that allows enhanced images in small animals. Rats were isolated in a small chamber and anaesthesia was induced using 5% isoflurane in 2L/min oxygen. Rats were then moved to a warm pad to maintain normal body temperature and isoflurane was adjusted to 2% in 1.5L/min oxygen for anaesthesia maintenance during the procedure using a nose cone. The hair was removed from the chest area by shaving and alcohol swab was applied for sterilization. A pre-warmed ultrasound gel was applied to

the target area and the transducer was manipulated until the required image was achieved (usually when the probe was directed/pointed to be between the 2 and 3 o'clock position for quick imaging). A three second video clip for short axis and long axis view were recorded and 2D M-mode image for left ventricular(LV) parameters were acquired (Figure 2.2). LV wall parameters including the left ventricular end diastolic diameter (LVEDD), end systolic diameter (LVESD), ventricular anterior wall thickness (AWT), and posterior wall thickness (PWT) were measured. Analysis of M-mode images was performedusing ImageJ software.

Following taking measurement, the heart parameters were calculated as follow,

Stroke volume (mL) = $EDV\text{-}ESV$

Cardiac output (mL/min) = $SV \times HR$

Ejection Fraction (%) = $(SV/EDVol) \times 100$

Fractional shortening (%) = $(EDD{-}ESD/EDD) \times 100$

Left ventricular mass (g) = $(0.8 \times ASEcube) + 0.6/1000$

Where ASEcube = $1.04 \times (IVSTd + LVIDd + PWTd)3 - LVIDd3$

LVIDd = average EDD x 10

IVSTd = average AWTd x 10

APWTd = average PWTd x 10

EDVol = $1.047 \times LVIDd3$

ESV = $1.047 \times (AverageEDDs)3$

HR = Determined by counting the number of peaks observed in 1000msec during M-mode imaging.

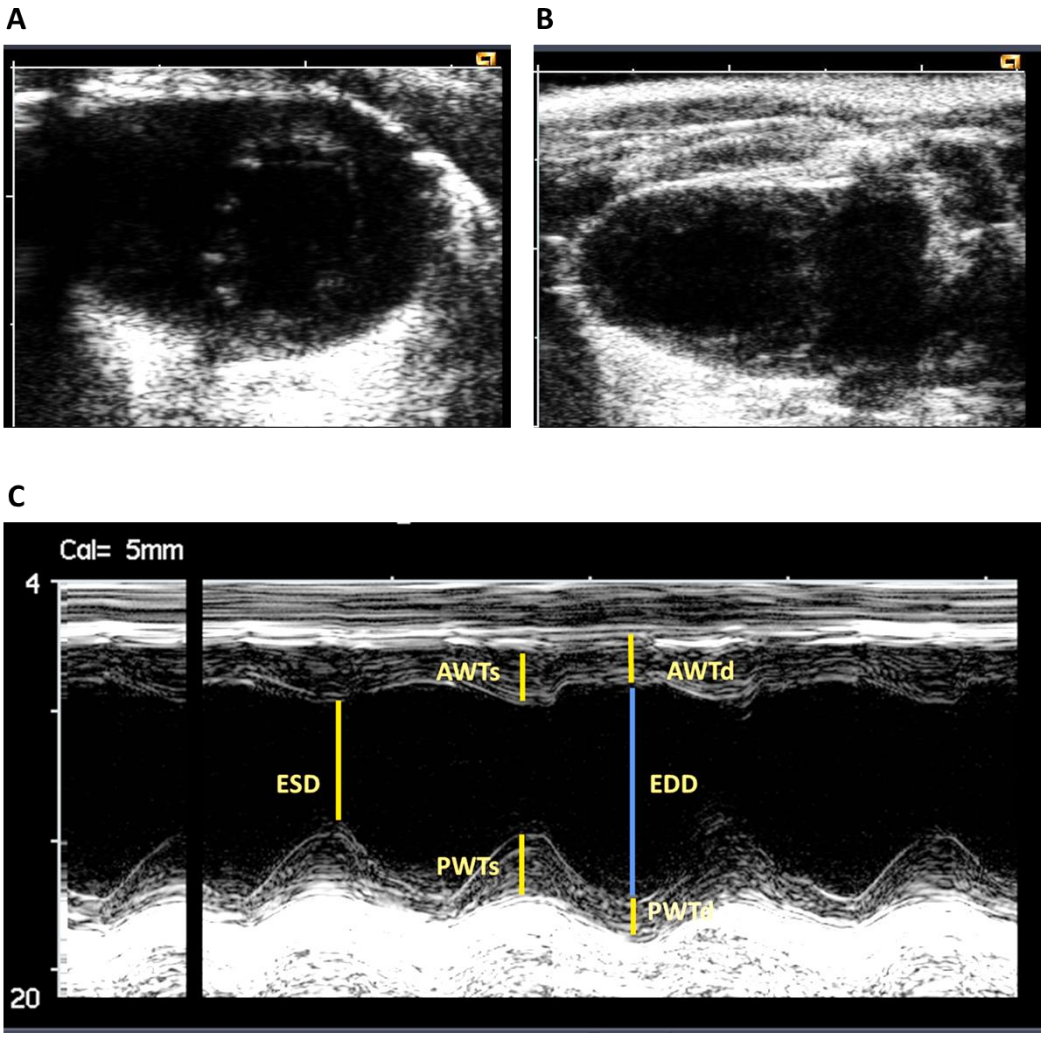

Figure 2.2 Representative image of echocardiography parameters

(A) Short axis view (B) Long axis view (C) 2D-M-mode where: ESD: end systolic diameter, EDD: end diastolic diameter, AWTs: anterior wall thickness at systole, AWTd: anterior wall thickness at diastole, PWTs: posterior wall thickness during systole, PWTd: posterior wall thickness during diastole.

2.13.7 Collection and fixation of animal tissues

Rats were humanly killed by placing them in a small chamber and were fully anesthetised with 5% isoflurane in 2L/min oxygen and then they were moved to the surgery table for tissue collection. Animals were checked via pinching tail and legs to ensure the complete anaesthesia before starting the cut. Then, scissor was used to cut just underneath the diaphragm and remove the skin to expose the heart. Aorta was collected first to avoid loss upon exsanguination. Next, heart, kidneys, liver, and lung were collected. Heart weights were measured before hearts and other tissues were either fixed immediately in 4% PFA for immunohistochemistry or placed into liquid nitrogen and then stored at -80 for protein and RNA expression analysis.

2.14 Preparing tissue sections.

Sectioning for heart tissues was performed using a LEICA RM2235 manual rotatory microtome (Leica Microsystems, Breckland, Linford Wood, UK). This system allows sectioning ranging in size between 1 and 10 micrometre. Tissues were placed in the freezer for one hour prior to each sectioning session to avoid folding or non-smooth cutting. Tissue was fixed safely on the microtome and cutting began with larger thickness to remove unwanted paraffin wax/tissues. Next the microtome was adjusted to 5µm for cutting of histological sections. Once the required section was obtained, sections were placed into a water bath at 37°C for approximately 1 minute to and then removed by immersing a microscope slide in the water bath to capture the section. Slides were left to dry out.

2.15 Picrosirius red staining

Picrosirius red is used to stain type I and III collagen in heart tissues. Five-micron paraformaldehyde-fixed aorta sections were de-paraffinized using xylene and ethanol at several concentrations (xylene for 7 minutes, 100% ethanol for 5 minutes, 95 % ethanol for 5 minutes, 70% ethanol for 5 minutes, and dH_2O for 5 minutes). Next, the sections were stained with VFM Harris Haematoxylin stain (CellPath Ltd, UK) for 10 minutes and washed in running tap water for 10 minutes. The slides were stained with picrosirius red solution F3B (Sigma Aldrich, Irvine, UK) for 90 minutes and washed with acidified water followed by dehydration with 100% ethanol. Finally, slides were washed with xylene and mounted with coverslips in DPX mounting medium (Sigma Aldrich, Irvine, UK).

2.16 Ad-ACE2 and Ad-GFP virus amplification and purification

Ad-ACE2 and Ad-GFP virus production and purification as well as micro-BCA were performed as previously prescribed (in sections 2.5.17, 2.5.16, and 2.5.19).

2.17 Protein expression in H9C2 cardiomyocytes following Ad transduction.

H9c2 cells were cultured as previously described until approximately 70% confluent. The cells were seeded into 6 well plates with cell density of $3x10^5$cells/ well. On the following day, the cells were transduced with 500 pfu/cell of Ad-ACE2 or Ad-LacZ and then incubated for 48hr. The cells were lysed in Radioimmunoprecipitation (RIPA) buffer for western immunoblotting analysis.

Lysis buffer was prepared by adding 5 mL of assay buffer (RIPA) + ½ tablet of protease inhibitor + 50µl of phosphatase inhibitor into a falcon tube kept on ice. The plates were removed from the incubator and placed on ice. The media were removed, and the cells were washed with cold PBS and 200 µL of lysis buffer was added to each well and cells were scraped using a 1mL syringe plunger. The lysate then was collected into Eppendorf tubes and placed on rotator wheel at 4°C for 30 minutes. Next, the lysate was spun at maximum speed for 10 minutes at 4 °C. The supernatant was moved to new labelled Eppendorf tubes and stored at - 80 °C.

2.18 Determination of protein concentration

Protein estimation was performed using BCA protein assay. It is similar to the micro-BCA protein assay. Briefly, nine BSA standards were prepared with concentration ranging between 0 µg/µl to 2000 µg/µl. Next, 25 µl of standards were added to a 96 well plate and then 5 µl of samples were added in duplicate and topped up to 25 µl by PBS. Then, the working reagent was added and the plate was read by plate reader and the volume of samples, loading dye and lysis buffer or water was calculated.

Table 9 BCA protein standards

Vial	Volume of diluent µL (PBS)	BSA stock (µL)	Final BSA concentration (µg/ML)
A	0	300	2000
B	125	375	1500
C	325	325	1000
D	175	175 of B	750
E	325	325 of C	500
F	325	325 of E	250
G	325	325 of F	125
H	400	100 of G	25
I	400	0	0=blank

2.19 SDS-polyacrylamide gel electrophoresis

Sodium dodecyl sulphate polyacrylamide gel electrophoresis (SDS-PAGE) and western blotting were used for protein detection. The electrophoresis tank was placed in ice and filled up with running buffer (recipe in section 2.1). The samples were denatured at 95˚C for 5 minutes and then loaded into the gel (NuPAGE 4-12% Bis-Tris Midi Protein 12+2-well gels (Thermo Fisher, Paisley, UK)) and electrophoresed for 1 hr at 150V. The gel was then removed and marked, and inserted into a cassette holder to transfer to a membrane. Filter papers and meshes were used to cover and protect the gel and the membrane from both sides. The cassette then inserted into a transfer tank at 4˚C containing transfer buffer (receipt in section 1.5.1) and electrophoresed for 90 minutes at 100V . Next, nonspecific site on the membrane were blocked by Seablock blocking buffer (Thermo Fisher, Paisley, UK) 1:1 dilution with 1X TBST for 1 hr at room temperature prior to antibody detection.

The membrane was then washed with 1X TBST and incubated with primary anti-antibody overnight at 4ºC . On the following day, the membrane was washed with 1X TBST and Incubated with secondary antibody for 1 hr at room temperature. Then, the membrane was washed with 1X TBST and was also washed and kept in PBS until ready for reading by Odyssey® CLx Imaging System (LI-COR, Nebraska USA).

2.20 Generation of ACE2 EVs in H9c2 Cells

The H9c2 cells were cultured in complete MEM and passaged into T75 cm^2 flasks (3 flasks/condition). Once they reached 70% confluence, the flasks were transduced with 50 pfu/cell of Ad-ACE2, Ad-GFP, or left untreated (control) with serum free media. After 48 hr, the media were collected for EVs isolation and the cells were lysed for western blot analysis.

2.21 ACE2 EVs isolation from H9c2 Cells culture media

The H9c2 cells were cultured in complete MEM and passaged into T75 flasks (3 flasks/condition). Once they reached 70% confluence, the flasks were transduced with 50 pfu/cell of Ad-ACE2 or Ad-GFP, or left untreated (control) with serum free media. After 48 hr, the media were collected for EVs isolation and the cells were lysed for western blot analysis. The conditioned media were subjected to centrifugation at 500g for 5 minutes, filtered and transferred to sterile ultra-clear centrifuge tubes. Ultracentrifugation was performed at 100,000 g and 4°C for 1.5 hrs. The pellet was re-suspended in 1 mL of PBS and subjected to another ultracentrifugation step at 100,000 g and 4°C for 1.5 hr. The EVs were re-suspended in 120uL of PBS and analysed using Nano-sight tracking analysis (NTA). A stock of the lysis buffer was prepared by adding 50 mM Tris-HCl (pH 7.4),50 mM NaF, 1 mM Na4P2O7,1 mM EDTA, and 1 mM EGTA. Then, the following materials were added to 5mL of the stock just before use; 50µl of 1% (v/v) Triton X-100, 227.71 mg of 250mM mannitol, 5µl of 1mM DTT, 5µl of 1mM Na3PO4, 5 µl of 0.1mM PMSF and ½ tablet Protease Inhibitor. Primary anti-ACE2 (ab108252), anti-TSG101 (ab125011), and anti-CD63 (ab108950) (Abcam, Cambridge, UK) were used to identify and confirm the expression of ACE2 EVs protein.

2.22 NanoSight tracking analysis (NTA)

EVs were characterised by Nanoparticle Tracking Analysis (NTA) by NanoSight (Malvern NanoSight LM10). The system detects and measures the Brownian motion of the nanoparticles in solution via light scattering. The particle solution was exposed to a focussed laser beam that cause particle illumination within that solution. The NTA software allowed to capture 5 videos for the particles with 60 s each to generate average particle size distribution and concentration for each sample. 10 µL of EVs samples were diluted in 1x PBS 1:100 and loaded

into the chamber of an LM10 NanoSight unit that an Andor DL-658-OEM-630 camera (Malvern Instruments, Malvern, UK) using 1 mL syringe. Five videos from different fields of view were recorded for 1 min each. Next, videos were analysed via NanoSight software NTA 3.1 that can detect particles with size up to 1000nm. The average concentration and particle size plot was then generated, and the determined concentration was adjusted by the dilution factor.

2.23 ACE2 activity assay in the isolated EVs

ACE2 activity assay was measured in the isolated EVs and in the cell lysate using SensoLyte ® 390 ACE2 Activity Assay Kit (Anaspec, Fremont, CA, USA). H9c2 cells were transduced with 50 pfu/cell of AdACE2 or AdGFP, or left untreated (control), and incubated for 48hr at 37°C and 5% CO2. Conditioned media were collected for EVs isolation and cells were lysed with 200µL assay buffer (component C) containing 0.1% of Triton-X-100. The lysed cells were then collected into Eppendorf tubes and incubated at 4°C for 10 minutes, and subjected to centrifugation for 10 min at 20,000g. The supernatant was moved to a fresh labelled tube and stored at -80°C until use. For enzymatic reaction, ACE2 substrate solution was diluted to the required concertation in assay buffer. Recombinant rat ACE2 (R&D Systems, Inc. Minneapolis,USA) was diluted to0.5ng in assay buffer and used as positive control. Black 96-well plates were utilized in this enzymatic reaction. Next, 50 µL of test samples and control samples were added to the wells followed by adding an equal volume of ACE2 substrate solution. The plate was protected from light and incubated for 30 minutes at room temperature. Stop solution was added to each well and the fluorescence intensity was measured for the endpoint at Excitation/Emission 330 nm/390 nm using SpectraMax M2 micro-plate reader (Molecular Device LLC, San Jose, CA).

2.24 Optimizing ACE2 EVs dose for treating Cardiomyocyte

ACE2 EVs and GFP EVs were isolated as previously prescribed. EVs concentration were determined using nanosight tracking analysis. H9c2 cells were seeded into 12 well plate with $1.5x10^5$ cells/well and incubated for 24h. Then, cells were treating with range of exosome concentration ($3.7x10^9$ particle/mL, $7.4x10^9$ particle/mL, and $1.48x10^{10}$ particle/mL) of ACE2 EVs, GFP EVs or control EVs

using NanoSight titer. Cells were incubated for 24h and then lysed using RIPA buffer and stored at -20°C until use for western blot analysis.

2.25 Statistical analysis

Statistical analysis was performed using GraphPad Prism Version 5 (GraphPad Software, CA, USA) and statistical significance was determined by one-way ANOVA with Bonferroni post-hoc analysis, unless otherwise stated. Bonferroni test helps in reducing the chance of type I error or false positive results when making multiple comparison test (Armstrong, 2014). Data are expressed as mean ± standard error and p value with <0.05 was considered to be statistically significant for all experiments.

Chapter 3 Construction of adenoviral vector expressing PRCP and in-vitro assessment of Ad-PRCP overexpression on cardiomyocyte hypertrophy.

3.1 Introduction

3.1.1 Methods for constructing Adenoviral vectors

Recombinant adenoviral vectors have been frequently used for a variety of purposes including gene transfer *in vitro* (Santin et al., 2016), *in vivo* studies (Crystal, 2014), clinically for vaccination (Mendonça, Lorincz, Boucher, & Curiel, 2021) and for gene therapy (McConnell & Imperiale, 2004). Multiple features of adenoviral vector biology have made it well suited for gene delivery such as the ability to mediate gene transfer to a broad spectrum of cell types including quiescent and actively dividing cells, the ability to produce high titer virus and high level of transgene expression (He et al., 1998). Furthermore, adenovirus can be easily manipulated to accommodate a relatively large foreign transgene, up to 7.5 kb, and has been safely used as a vaccine in humans (He et al., 1998; Mendonça et al., 2021).

There are three general methods used to generate recombinant adenoviral gene transfer vectors (Luo et al., 2007). The first approach involves direct cloning of the gene of interest into the adenoviral genome (Luo et al., 2007; Okada, Ramsey, Munir, Wildner, & Blaese, 1998). This method is less commonly used because of the difficulties of purifying large viral genomic DNA fragments, which also limits useful unique restriction endonuclease sites in the adenovirus genome to facilitate cloning, and the efficiency of large fragment DNA ligation is limited. The second approach involves using a site-specific recombinase system (Hallet & Sherratt, 1997; Luo et al., 2007). This method contains processes in which DNA molecules are rearranged by breaking and rejoining the strands at specific points. Site-specific recombination involves two short DNA sequences which might be present within the same molecule or may be in another molecule. This method utilizes a specialized recombinase enzyme that recognizes the sites and then promotes a rearrangement of the DNA (Hallet & Sherratt, 1997; Luo et al., 2007).

The third and most common used method to construct adenoviral vectors is cloning the gene of interest into a plasmid shuttle vector and then recombining the newly formed plasmid with a larger plasmid encoding the adenoviral genome backbone (e.g. pAdEasy-1, adenoviral plasmid contains all adenoviral 5 sequences except E1 and E3 genes) (He et al., 1998). A DNA molecule incorporating both the backbone and the shuttle vector sequences, will be

generated using bacterial cells. A regular shuttle vector usually carries the 5′ end of the adenoviral genome in which E1 and other non-essential genes are removed creating more space for insertion of up to 7.5 kb of foreign DNA fragment and up to 10.1 kb when pAdEasy-2 adenoviral vector, where E4 is removed in addition to E1 and E3 regions, is used (Choi & Chang, 2013; He et al., 1998; Luo et al., 2007). The recombinant adenoviral plasmid vector encoding the transgene expression cassette also includes the majority of the adenoviral genome but not the E1 genes required for virus replication and propagation in normal cells. E1-deleted adenoviral vectors are propagated in the HEK 293 cell line (Graham et al., 1977), which has the adenoviral E1 region integrated into its chromosomes providing E2 expression *in trans* and enabling the vector to replicate and therefore be amplified and produced at high titers. The cloned DNA can be transfected into HEK293 cell for virus production (Graham & Prevec, 1992; Luo et al., 2007). The AdEasy-1 cloning system consists mainly of 3 steps; First, subclone the gene of interest into a shuttle vector (e.g., pshuttle-CMV), and confirm the ligation process via diagnostic digest and/or sequencing of the recombinant plasmid. Upon conducting this step, it is recommended to avoid gel purification of the linearized shuttle vector as the purification process might affect the transformation efficiency, and it may introduce unwanted nicks in the DNA. Second, linearize the shuttle vector with specific restriction endonucleases and electroporate the vector into a strain of BJ5183 bacterial cells that contains the supercoiled backbone vector (AdEasier cells). BJ5183 bacterial cells lack some certain enzymes that mediate recombination in bacteria but still permit efficient generation of stable homologous recombinants(He et al., 1998). The last step involves digestion the formed recombinant DNA with *Pac*I restriction enzyme followed by transfection into HEK-293 cells and incubating for 6-10 days or until the cytopathic effect (CPE) is complete to harvest the viruses (Alba et al., 2012).

3.1.2 Gene transfer of RAS components using Adenoviral vectors.

Adenoviral vectors have been used widely in pre-clinical and clinical studies for gene transfer therapy, including delivery of several components of the RAS for targeting cancer, diabetes, and cardiovascular disease. In human prostate cancer cell lines, adenoviral-mediated overexpression of AT_2R induced apoptosis and inhibited cell proliferation as well as promoted significant reduction in S-

phase cell and enrichment in G1-phase cell, an effects involved activation of p38 mitogen-activated protein kinase (MAPK), caspase-8, and caspase-3, and partially p53 (H. Li et al., 2009). Similarly, *In vivo* administration of recombinant adenoviral vector mediating AT_2R gene transfer attenuated tumour growth of prostate cancer via inducing cell apoptosis and inhibiting proliferation in mice (J. Li et al., 2016). In diabetic (db/db) mice model, adenoviral vectors expressing human ACE2 (Ad-hACE2-eGFP) injected into the pancreas showed significant improvement in glucose tolerance, reduced B-cell proliferation and insulin content and enhanced islet function in comparison to db/db mice transduced with control adenovirus (Ad-eGFP) (Bindom et al., 2010).

Adenoviral vectors were developed to express Ang-(1-7) (RAdAng-(1-7) or Ang-(1-9) (RAdAng 1-9) into H9c2 rat cardiomyocytes and the anti-hypertrophic effect following Ang II stimulation was assessed (Flores-Muñoz, Godinho, Almalik, & Nicklin, 2012). The study showed gene transfer of either peptide significantly reduced Ang II-induced cardiomyocyte hypertrophy (Flores-Muñoz et al., 2012). Intramyocardial injection of adenoviral-mediated transfer of ACE2 (Ad-ACE2) shows antiapoptotic and anti-inflammatory effects against doxorubicin-induced cardiomyopathy in rats (Ma et al., 2017). The study also indicates that Ad-ACE2 overexpression in rats reduces oxidative stress, left ventricular volume, and cardiac fibrosis as well as enhancing the left ventricular ejection fraction following doxorubicin treatment (Ma et al., 2017). Ad-ACE2 treated rats maintain a greater survival rate in response to doxorubicin treatment (Ma et al., 2017).

Adenoviral gene transfer and overexpression also helps in understanding gene physiological and/or pathological functions. For instance, the relationship between AT_2R and prolylcarboxypeptidase has been reported in mouse coronary artery endothelial cells (ECs) (L. Zhu et al., 2010b). Transduction of ECs with adenoviral vector expressing AT_2R (Ad-AT_2R) increased PRCP mRNA expression by 1.7-fold and protein expression by 2.5-fold (L. Zhu et al., 2010b). Bradykinin protein expression was also increased by 2.2-fold in Ad-AT_2R transduced mouse coronary artery ECs. Blocking of AT_2R with PD123319 significantly abolished bradykinin levels, while AT_1R blocker (valsartan) showed no effect on bradykinin release in Ad-AT_2R transduced ECs (L. Zhu et al., 2010a). Inhibition of PRCP via small interfering RNA (siRNA) significantly reduced bradykinin release by 35%,

which suggested that AT_2R-induced bradykinin release is mediated at least partially by PRCP (L. Zhu et al., 2010b).

Furthermore, adenoviral delivery of the AT_1R promoted direct neonatal rat cardiomyocyte hypertrophy, following Ang II stimulation of 100 nM/L for 72h, as shown by upregulation of the immediate-early response genes, *c-jun and* c-*fos* as well as ANP (Thomas et al., 2002). The hypertrophic effect mechanism of AT_1R involved the activation of MAPK and the epidermal growth factor receptor (EGFR)(Thomas et al., 2002).

3.1.3 PRCP delivery to the heart for cardiac gene therapy

Adenoviral vectors contains either prolylcarboxypeptidase (Ad-PRCP) with 4×10^9 PFU/200µL for PRCP overexpression, or shRNA PRCP(sh-PRCP) to knockdown PRCP with 1×10^{10} PFU/200µL, have been delivered via tail vein injection to Wistar rats in order to assess the protective role of PRCP against myocardial ischemia reperfusion (I/R) injury induced by ligation of the left anterior descending coronary artery (LAD) (Hao et al., 2020). First, the study demonstrated that the myocardium protein expression and the activity of PRCP were significantly increased in Ad-PRCP group in comparison to sham (underwent the same surgical procedure, but the suture was not tied) and Ad-control (empty adenovirus vector). Conversely, the protein expression and activity of PRCP were significantly lower in sh-PRCP animal compared to sham and scramble shRNA (sh-Con), which suggested that adenoviral vector is efficient in overexpression and knocking down PRCP gene (Hao et al., 2020). Second, the plasma and heart levels of Ang-(1-7) and Bradykinin-(1–9) were significantly higher in Ad-PRCP treated animals and lower in sh-PRCP group. The Ang II level in the plasma and myocardium was significantly reduced in Ad-PRCP group, while it increased in sh-PRCP during both ischemia and reperfusion (Hao et al., 2020). Echocardiography data showed significant suppression of left ventricular (LV) fractional shortening (FS) following I/R injury, which was further reduced in sh-PRCP group. However, Adenoviral delivery of PRCP significantly increased FS compared to Ad-control and vehicle groups after I/R injury. Left ventricular function, assessed by maximal LV systolic pressure (LVSP), LV end-diastolic pressure (LVEDP), and maximal ascending and descending rate of LV pressure ($\pm dp/dt$), was significantly deteriorated in I/R rats compared to sham and worsen in PRCP knockdown group. PRCP overexpression significantly improved LV

functional parameters in comparison to Ad-Control following I/R (Hao et al., 2020). However, no significant effect of PRCP was observed on mean arterial BP and heart rate in this study (Hao et al., 2020). Furthermore, infarct size was significantly lower in response to PRCP overexpression compared to Ad-control group. PRCP knockdown showed significantly greater infarct size than rats treated with scramble shRNA (Hao et al., 2020). Adenoviral-mediated PRCP overexpression significantly reduced I/R-induced mitophagy in the myocardium and reversed the decreased in cardiomyocyte cell viability resulting from hypoxia/reoxygenation injury (Hao et al., 2020). The cardioprotective effects of PRCP were reported to be mediated mainly via upregulation of Ang-(1–7) and Bradykinin-(1–9) (Hao et al., 2020). These data suggested that PRCP gene transfer elicits a protective role against myocardial I/R injury by modulating RAS activity.

3.2 Hypothesis and aims

Hao et al reported that delivery of PRCP via adenoviral gene transfer vector was protective against myocardial ischemia reperfusion (I/R) injury (Hao et al., 2020). In this study here similar therapeutic approach was used to investigate hypertensive cardiac remodelling using in vitro cardiomyocyte model and in vivo model of essential hypertension. It was hypothesised that overexpression of PRCP via adenoviral gene transfer vector can prevent Ang II-dependent cardiomyocyte hypertrophy in vitro.

The aims of this chapter were to:

- Clone rat PRCP into the AdEasy-1 shuttle and generate a recombinant adenoviral gene transfer vector encoding PRCP.
- To determine whether in vitro gene transfer of Ad-PRCP altered Ang II and Ang-(1-7) levels in cardiomyocytes.
- Assess the effects of adenoviral gene transfer of PRCP on Ang II-induced hypertrophy in rat H9c2 cardiomyocytes.

3.3 Results

3.3.1 Plasmids design and preparation

Rat PRCP protein sequence was obtained from PubMed nucleotide search and was flanked with unique restriction endonuclease recognition sites including *Neh*I, *Not*I, *Sal*I, *EcoR*I, *HinD*III, *Xho*I, and *Mlu*I. This design was then synthesized into pEX-A carrier plasmid by (Eurofins Scientific, Luxembourg) and named pEX-A258-Rat PRCP (pRat-PRCP) plasmid Figure 3.1.1A. pShuttle-CMV sequence was obtained from https://www.addgene.org/16403/ and was provided by (Prof. Stuart Nicklin lab) Figure 3.1.1B.

A **B**

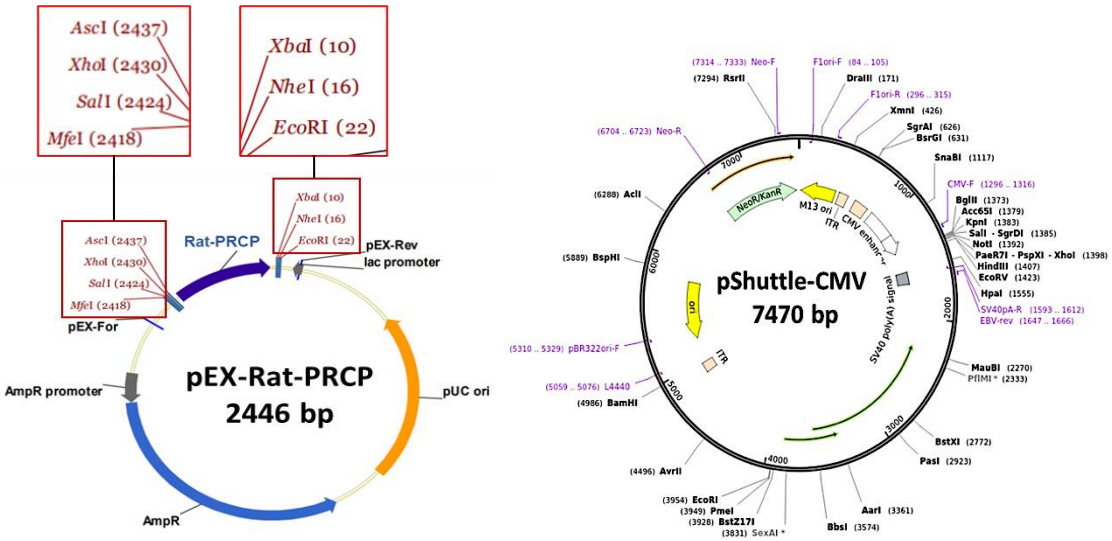

Figure 3.1.1 Plasmids design for pRat-PRCP and pShuttle-CMV

(A) The backbone vector for pRat-PRCP showing the plasmid flanked with endonuclease restriction enzymes (highlighted) that could be utilized for cloning into pShuttle-CMV vector **(B)**The plasmid map for pShuttle-CMV.

3.3.2 Plasmids Analysis via endonuclease restriction enzymes digest

Next, the plasmids were subjected to endonuclease restriction enzyme analysis to confirm the presence of the insert gene as well as the restriction enzymes that can facilitate the subcloning into pShuttle-CMV vector backbone. pRat-PRCP was subjected to single or double digest with *Not*I and *HinD*III Figure 3.1.2A. The ethidium bromide agarose gel electrophoresis showed the release of PRCP gene (lane 3) from the backbone vector following double digest as shown by the DNA fragment band at~1562 bp. A single band at ~7470 bp was observed following digest of the pShuttle-CMV with *Not*I or *Hind*III, or *Xho*I Figure 3.1.2B. pRat-PRCP was also double cut with *Sal*I and *Xho*I as shown in lane 5 of Figure 3.1.2C. Pshuttle-CMV was also subjected to double digest with *Sal*I and *Xho*I (lane 1) and to a single digest with *HinD*III (lane 3) Figure 3.1.2C.

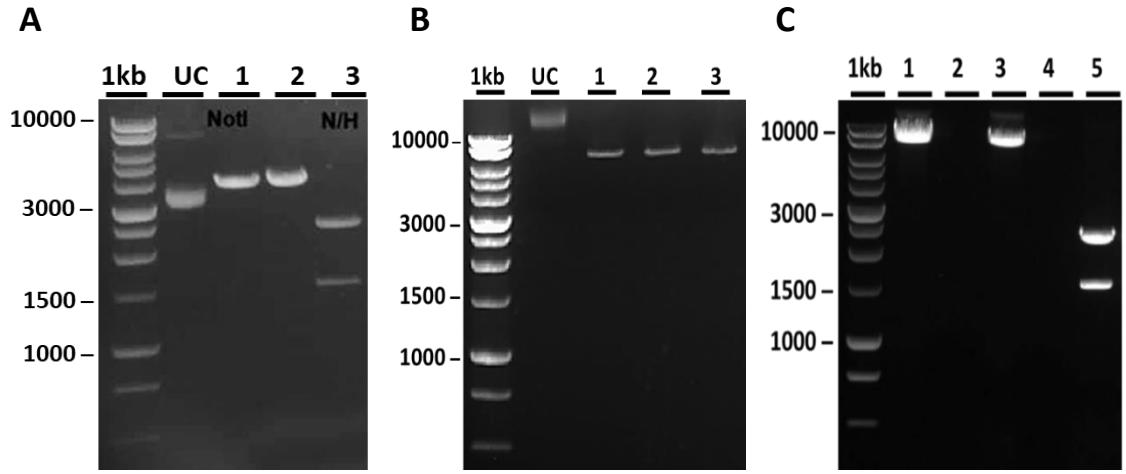

Figure 3.1.2 Analysis of pShuttle-CMV and pRat-PRCP plasmids with restriction endonuclease enzymes..

(A) Ethidium bromide agarose gel electrophoresis showing the uncut pRat-PRCP or digested with *Not*I (lane 1*), HinD*III (lane 2), and double digest with *Not*I and *HinD*III (lane 3) which shows the separation of DNA fragment of PRCP at~1526 bp and another band at ~2446 bp.**(B)** Agarose gel electrophoresis showing the single digest of pShuttle-CMV with restriction endonuclease enzymes *Not*I (lane 1), *HinD*III (lane 2), and *Xho*I (lane 3) which show single DNA band at ~7470 bp. **(C)** Agarose gel showing the double digestion with *Sal*I and *Sho*I for pShuttle-CMV (lane 1) and pRat-PRCP (lane 5), and single cut with *HinD*III for pShuttle-CMV(lane 3) UC=uncut.

3.3.3 Steps for generation adenoviral vector expressing rat PRCP

The working plan/steps for constructing adenoviral vector expressing rat PRCP(Ad-PRCP) was summarized in (Figure 3.1.3). Ad-PRCP was then amplified in HEK 293 cells and purified using cesium chloride density gradient ultracentrifugation.

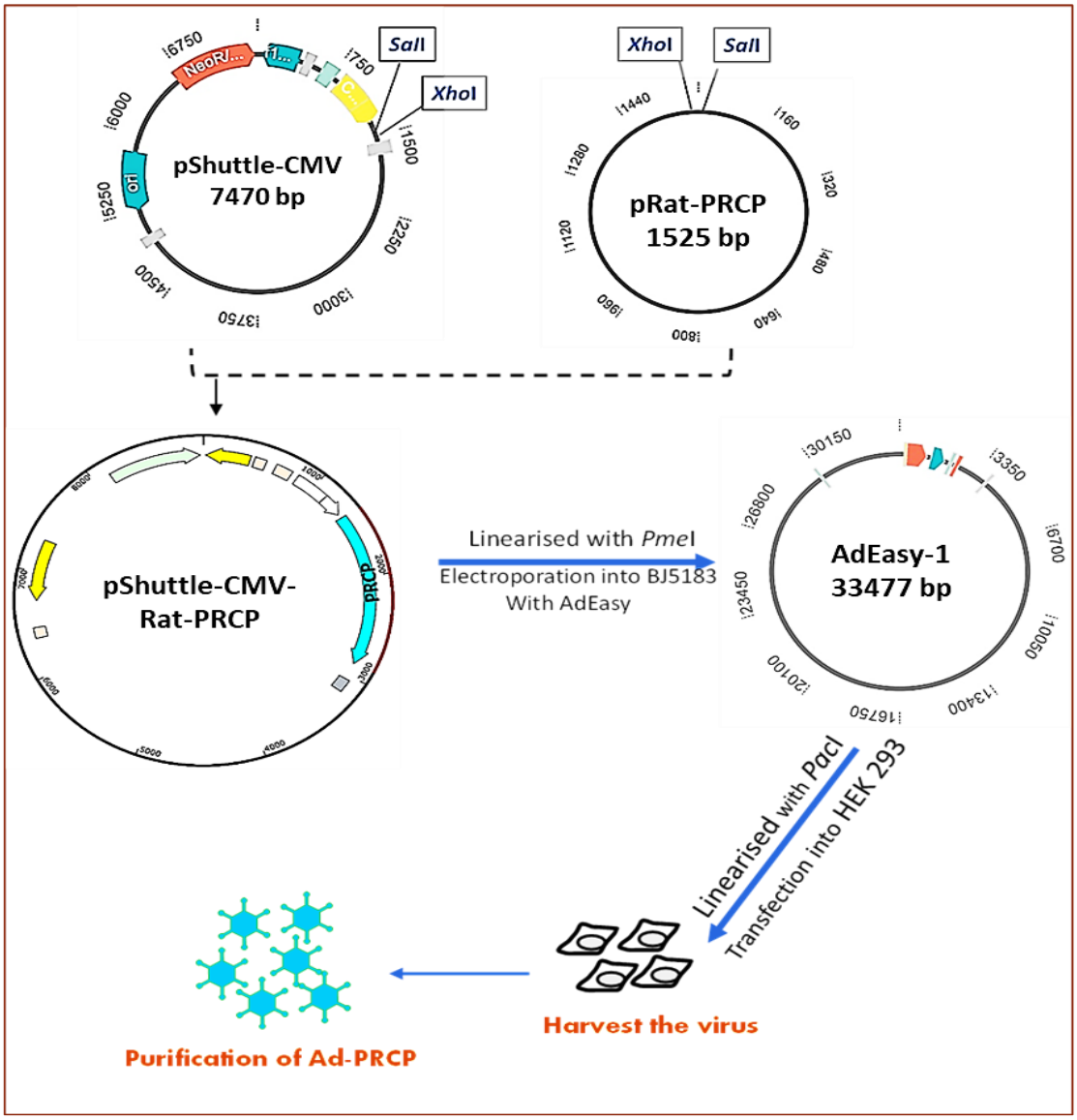

Figure 3.1.3 A schematic representation of the process for generation of adenoviral vector expressing Rat-PRCP.

First, pRat-PRCP plasmid was sub-cloned into pshuttle-CMV using *Xho*I and *Sal*I restriction endonuclease sites. Next, the formed DNA (pShuttle-CMV-Rat-PRCP) was linearized with *Pme*I and co-transformed into BJ583 cells containing pAdEasy-1. Finally, the recombinant plasmid was digested with *Pac*I and transfected into HEK 293 cells to produce recombinant Ad-PRCP.

3.3.4 Subcloning of pRat-PRCP into pShuttle-CMV

pShuttle CMV and pRat-PRCP were digested with *Sal*I and *Xho*I restriction enzymes overnight and run in agarose gel electrophoresis (Figure 3.2A). Both plasmids were then purified and run in agarose gel electrophoresis and showed that a single DNA fragment band at approximately 1526 bp for pRat-PRCP and 7470 bp for pShuttle-CMV which are the expected banding sizes for both DNAs (Figure 3.2B). Next, the pRat-PRCP was subcloned to pShuttle-CMV via ligation reaction and followed by transformation into XL10-Gold ultracompetent cells. The ligated plasmid DNA (pShuttle-CMV-Rat-PRCP) was amplified and purified from individual colonies and screened for successful insertion of PRCP. The agarose gel electrophoresis showed that only 3 colonies (7,9, and 11) out of 18 were positive as shown by separation of pRat-PRCP DNA fragment from pShuttle-CMV after double digestion with *Sal*I and *Xho*I restriction endonuclease enzymes (Figure 3.2C). The separated bands were visualized at approximately 1526 bp, while the pShuttle-CMV band was visualized at ~7470 bp. For confirmation purpose, the three positive plasmids were run again in agarose gel and provided the same observation for the initial screening which indicated successful insertion of the PRCP gene into pShuttle-CMV (Figure 3.2D). The insertion of pRat-PRCP into pShuttle-CMV was further confirmed by DNA sequencing (data not shown).

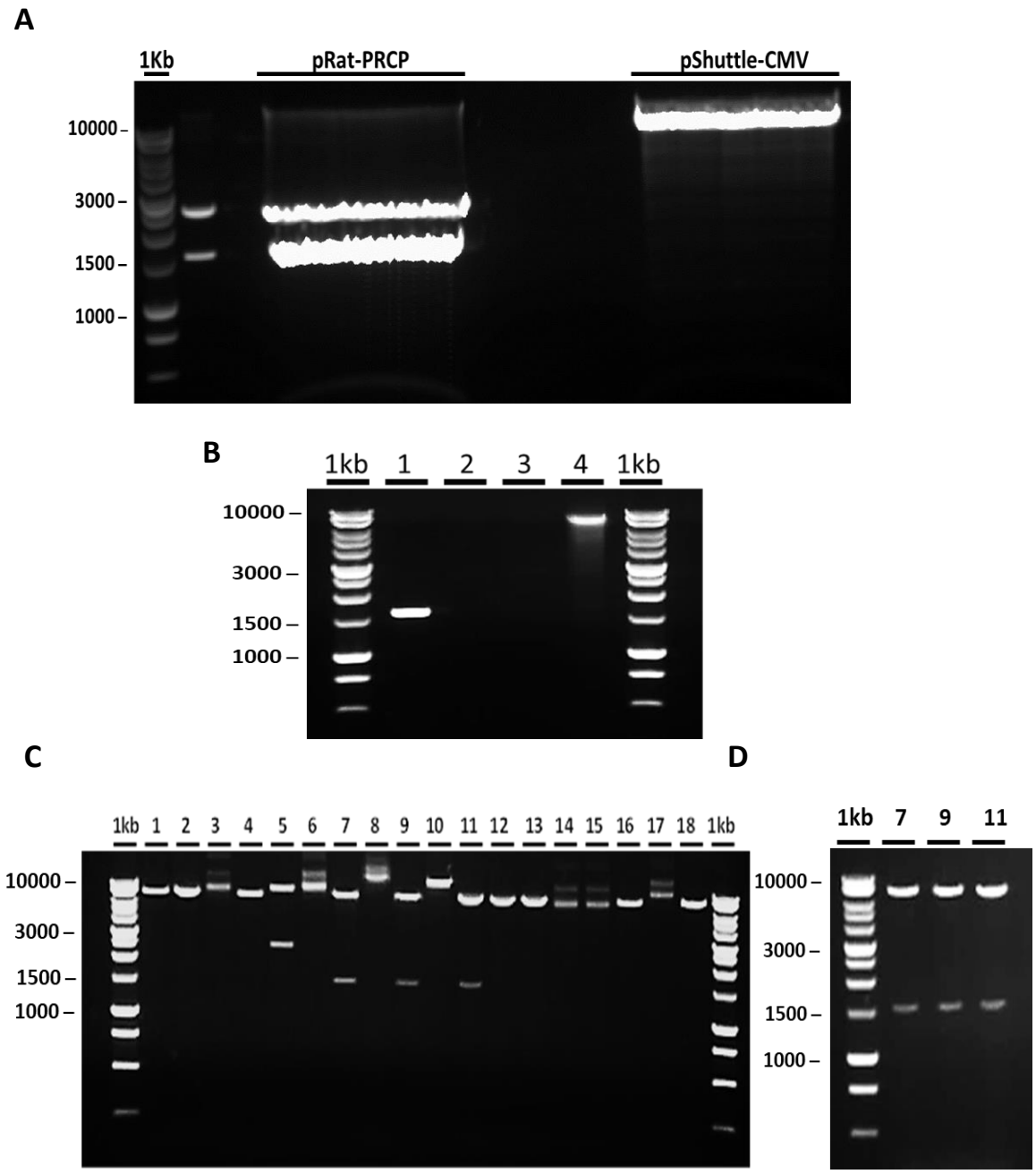

Figure 3.2 Cloning of pRat-PRCP plasmids into pShuttle-CMV.

(A) Ethidium bromide agarose gel electrophoresis (0.7 %) showing the overnight digest with double restriction endonuclease enzymes, *Sal*I and *Xho*I, for both pRat-PRCP and pShuttle-CMV before gel-extraction and purification. **(B)** Ethidium bromide agarose gel electrophoresis showing the purified pRat-PRCP as indicated by a DNA band at the expected size of 1526 bp (lane1), and for the purified pShuttle-CMV at the expected band size at 7470 bp(lane 4).**(C)** Ethidium bromide agarose gel (0.7 %) showing the successful insertion of pRat-PRCP into pShuttle-CMV as shown by separation of PRCP from pShuttle-CMV following double *Sal*I

and *Xho*I restriction digest in 3 positive colonies (7, 9, and 11) out of 18 screened by mini preparation. The positive separated bands of PRCP were visualized at ~1526 bp, while the pShuttle-CMV band was visualized at~7470 bp. **(D)** The positive colonies (7, 9, and 11) were run again in a separate agarose gel for verification purpose and yielded the same observation for the initial screening. 1kb; 1 kb ladder.

3.3.5 Homologous recombination and co-transformation into pAdEasy-1 system

The recombinant plasmid pShuttle-CMV-pRat-PRCP was digested with restriction endonuclease *Pme*I overnight and purified (Figure 3.3A). Next, homologous recombination between pAdEasy-1 and Pshuttle-CMV-pRat-PRCP was performed using BJ5183 cells, that already transformed with pAdEasy-1, via electroporation and following plating and overnight incubation individual colonies were picked and screened. A diagnostic restriction endonuclease digestion was performed using *Pac*I and the gel electrophoresis showed one positive colony (lane 2), out of 8 screened, as visualized by the presence two DNA bands; one at 30kb and another at 3 Kb (Figure 3.3B). The positive sample was amplified by maxi preparation, purified and linearized with *Pac*I restriction endonuclease to liberate both inverted terminal repeats (ITR) and to be transfected into HEK293 cell for the production of final recombinant adenoviral containing PRCP (Figure 3.3C). The final product of Ad-PRCP was also verified via DNA sequencing (data not shown).

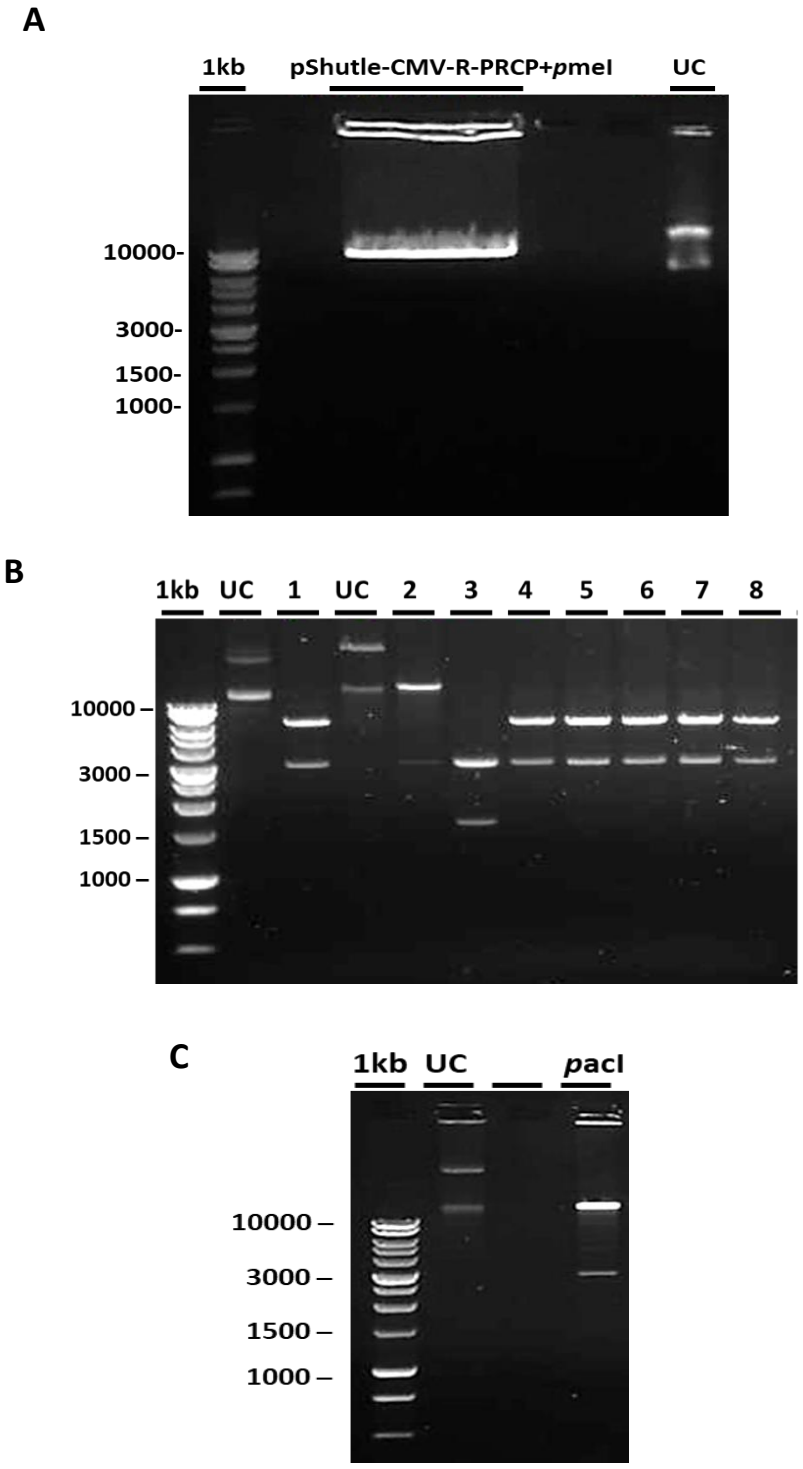

Figure 3.3 Cloning of the recombinant pShuttle-CMV-PRCP into pAdEasy-1.

(A) Ethidium bromide agarose gel electrophoresis showing the linearized pShuttl-CMV-R-PRCP with *P*meI restriction enzyme. **(B)** Diagnostic digest showing successful recombination of pShuttle-CMV-R-PRCP and pAdEasy-1 system shown in one positive colony (lane 2) following cut with *P*acI and mini preparation screening. **(C)** The positive colony was amplified by maxi preparation and digested with *P*acI. 1kb; 1 kb ladder, UC; uncut.

3.3.6 Transfection of the recombinant AdEasy-pShuttle-pRat-PRCP into HEK 293

The transfection process was performed using Xfect transfection (Figure 3.4A) and was shown to be successful as indicated by visualization of eGFP fluorescence expression from the HEK 293 cells transfected with the positive control pEGFP 48h post transfection compared to control (un-transfected cells) (Figure 3.4B).

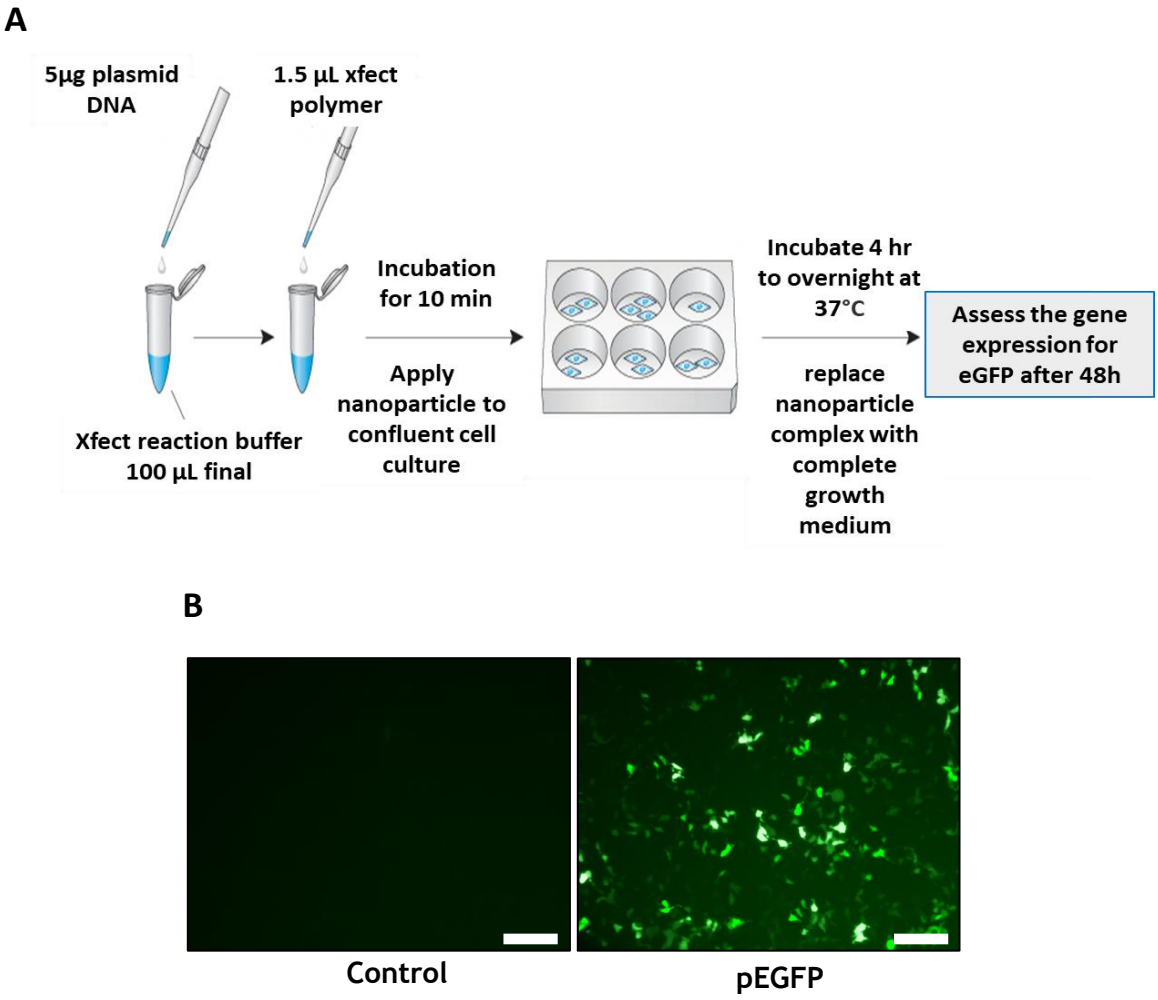

Figure 3.4 Transfection process for the recombinant AdEasy-pShuttle-pRat-PRCP into HEK 293 cell

(**A)** Schematic representing the transfection steps using Xfect transaction reagent (Clontech). Five microgram of DNA plasmid was added to 1.5 µL of the polymer in 100 µL of buffer. The sample was incubated at room temperature for 10 min and applied to the assigned wells. (B) Representative images for control (un-transfected) and pEGFP transfected HEK 293 cells following 48h of transfection (10x magnification). Scale bar=100 µm.

However, for pAdEasy-pShuttle-pRat-PRCP transfected cells, plaques started to appear after 7-11 days which indicated that Ad-Rat-PRCP(Ad-PRCP) was produced and replicating in the HEK293 cells. Once cytopathic effect (CPE) begins, media was not changed to allow CPE to complete and expand through the well. The media/cells were then collected and subjected to centrifugation at 300 x g for 10 minutes, and the pellet was resuspended in 1 mL of PBS. An equal volume (1mL) of Arklone P (1,1,2-Trichlorotrifluoroethane) was added, followed by inversion for 10 s and shaking for 5 sec, a step that was repeated gently. Next, the crude virus was purified as detailed in (section 2.2.10). Then, seed stock of Ad-PRCP was prepared as previously described in (section 2.2.11). Seed stock was used to produce large scale of recombinant Ad-PRCP using HEK 293 cells and purified using cesium chloride (CsCl) density gradient as detailed in section (2.2.12). The final purified Ad-PRCP is shown in (Figure 3.5). Ad-PRCP was then confirmed via DNA sequencing (data not shown).

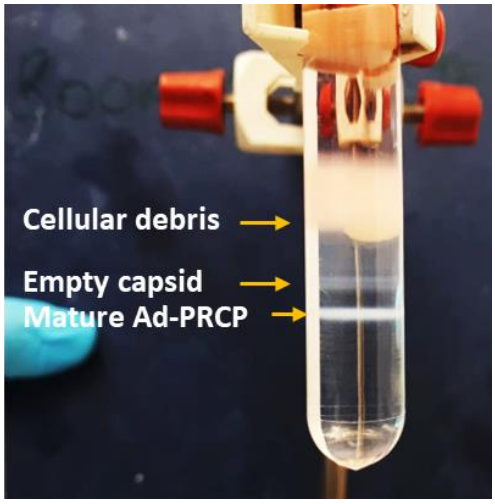

Figure 3.5 Representative image for purified Ad-PRCP using cesium chloride (CsCl) density gradient.

Two layers of CsCl (1.25 g/mL and 1.40 g/mL) were added into SW40 ultracentrifugation tube and the virus preparation was added afterward, and subjected to ultracentrifugation at 217,874g for 1.5 hr. The ultracentrifugation yielded three layers, from the bottom; mature virus, empty capsids, and cellular debris.

3.3.7 Assessment of Ad-GFP transduction efficiency in H9C2 cardiomyocyte

Initially, the efficiency of adenoviral-mediated delivery of pEGFP (Ad-GFP) into cardiomyocytes was assessed. H9C2 cardiomyocytes were transduced with MOI of 2000 viral particle/ cell or untreated (control) and the expression of eGFP was assessed following 48 h of transduction. High expression of eGFP was observed in Ad-GFP transduced cardiomyocytes, while there was no eGFP expression detected in the control group (Figure 3.6).

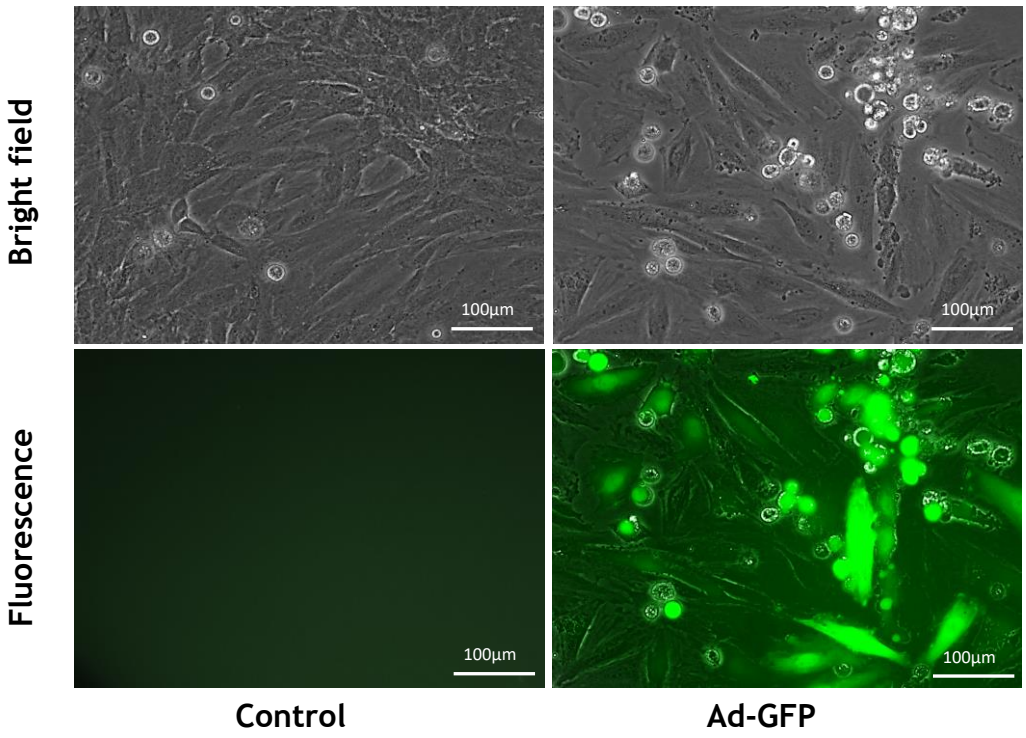

Figure 3.6 Representative images of H9C2 cardiomyocytes transduced with Ad-GFP.

Ad-GFP was added to cultured H9C2 cardiomyocyte at multiplicity of infection (MOI) of 2000 viral particle/ cell. Control cells remained uninfected. The bright field and the fluorescence images are shown. 20x magnification. Scale bar= 100 µm.

3.3.8 PRCP mRNA expression in H9c2 cardiomyocyte in response to Ad-PRCP transduction

The mRNA of PRCP was evaluated in H9C2 cardiomyocytes following transduction with Ad-PRCP. The data revealed adenoviral delivery of rat PRCP produced a significant increase in PRCP gene expression compared to untransduced (control) and Ad-GFP transduced cells (mean fold change was 87.8±7.6 for Ad-R-PRCP compared to control (1.0±0.01) and Ad-GFP transduced cardiomyocyte (0.87±0.04), (***p<0.001; n=3) (Figure 3.7). The sequencing of the the expression cassette of Ad-PRCP was performed using four primers designed previously as indicated in section (2.3.3) and confirmed to be correct in the Ad-PRCP vector (data not shown).

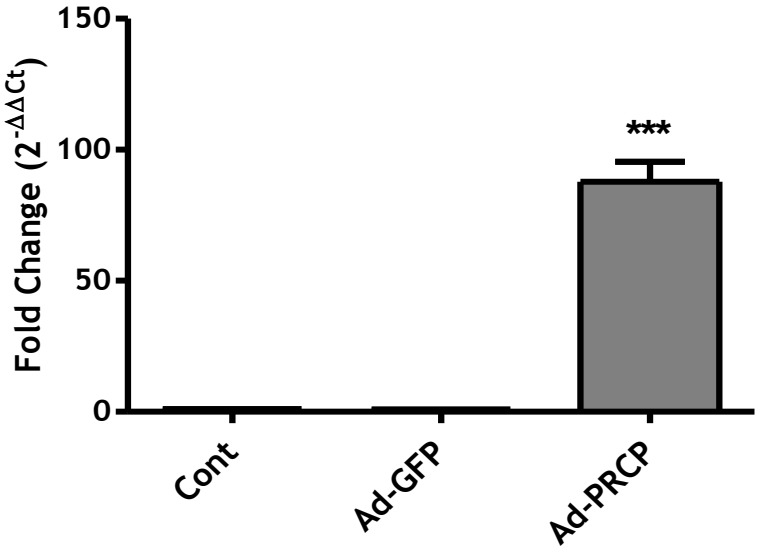

Figure 3.7 TaqMan analysis for PRCP gene expression following Ad-PRCP transduction.

Analysis of PRCP gene expression in H9C2 cardiomyocyte transduced with 10,000 vp/cell Ad-PRCP, Ad-GFP, or untreated (control) at 48 hr, ***p<0.001 vs control and Ad-GFP, n=3.

3.3.9 Endogenous PRCP gene expression in control H9C2 cardiomyocyte and in response to different pathogenic stimuli

Endogenous PRCP mRNA expression was assessed in control H9C2 cardiomyocyte or stimulated with Ang II, TGFß1 or PDGF (platelet-derived growth factor) at 24 hr (Figure 3.8A). The results showed that endogenous PRCP was detectable in all conditions but did not significantly change following exposure to Ang II (0.99±.0.07), TGFß1(1.3±0.05) or PDGF (1.4±0.16) fold changes compared to control (1.1±0.11) (Figure 3.8B).

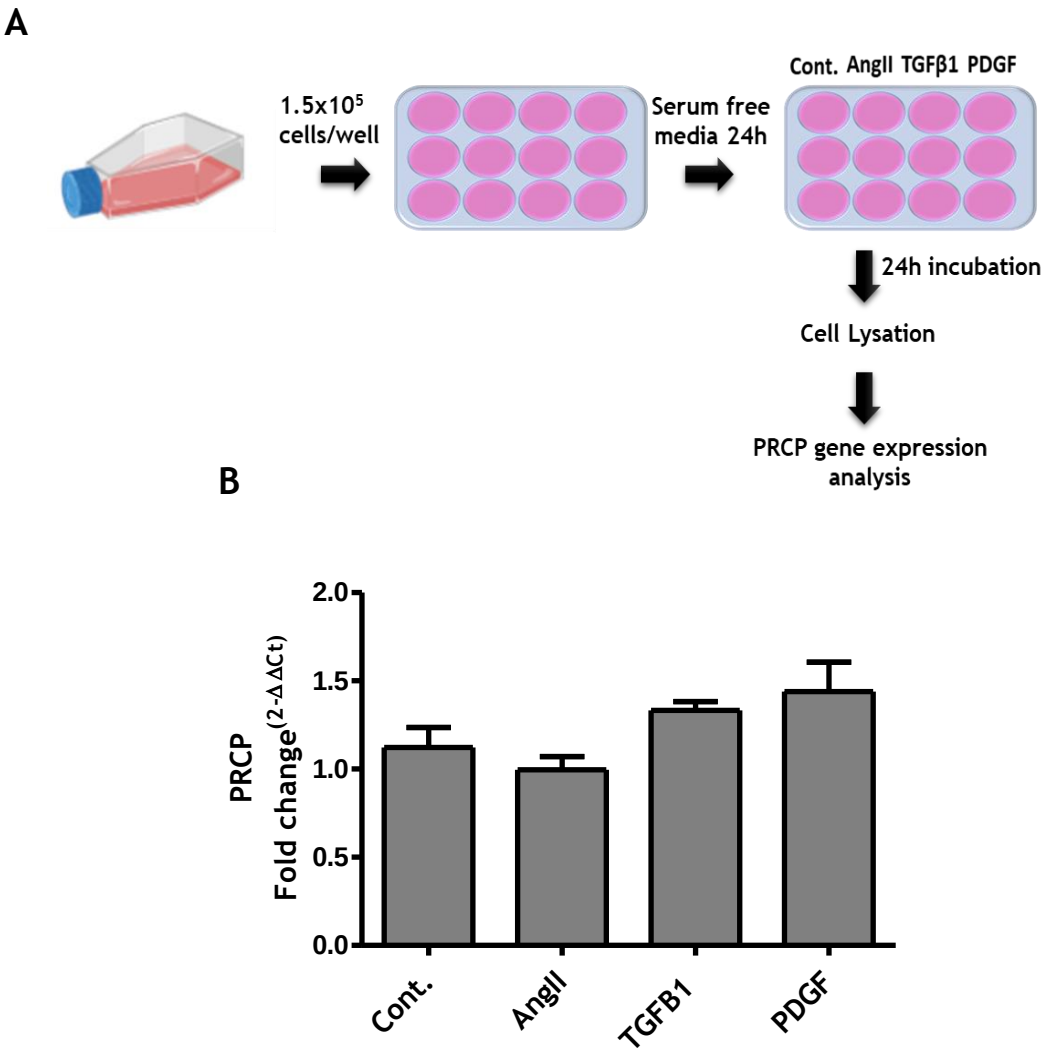

Figure 3.8 TaqMan analysis for endogenous PRCP gene expression in H9c2 cardiomyocyte following stimulation with Ang II, TGFß1 and PDGF.

(A) Schematic representing the work plan for the assessment of endogenous PRCP expression in control H9c2 and in response to stimulation with Ang II,

TGFß1 and PDGF. **(B)** Analysis for PRCP gene expression under each condition, n=3.

3.3.10 Assessment of Ang II levels in HeLa cells transduced with Ad-PRCP

Ang II levels were assessed in HeLa cells transduced with MOI of 10,000 vp/cell of Ad-PRCP or Ad-GFP or left untransduced (control). Following 24 h transduction cells were exposed to cell culture media containing 100 nM of Ang II (Flores-Muñoz et al., 2012) and culture media were then collected at specific time points for measurement of Ang II levels by ELISA. Analysis showed degradation of Ang II levels in Ad-PRCP group at 24h of Ang II stimulation (14.39 ± 2.1-fold change) compared to Ad-GFP 24h (47.4 ± 0.1-fold change) and Ang II only treated (44.4 ± 3.3-fold change) groups. Furthermore, among all Ang II treated groups, Ang II level was markedly reduced only in Ad-PRCP 24h group (Figure 3.9).

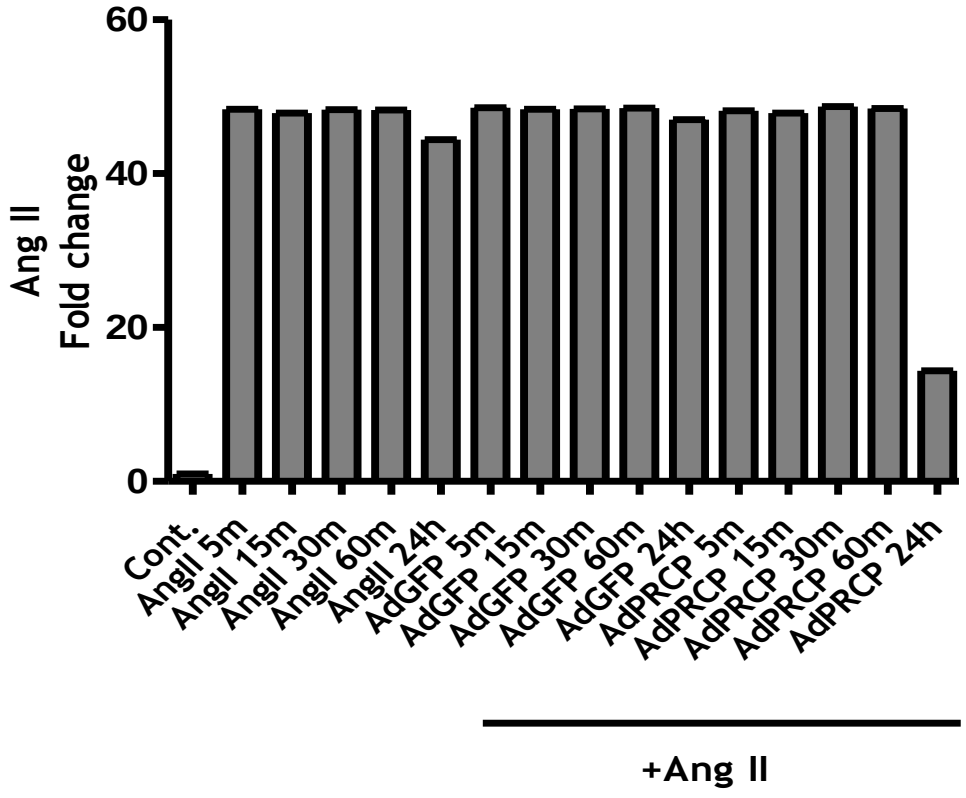

Figure 3.9 The ELISA analysis of Ang II levels in Hela cells following Ad-PRCP transduction.

Ang II was added to cell culture media and levels measured at specific time points (5, 15, 30, 60 min and 24h) in HeLa cells transduced with Ad-PRCP, Ad-GFP or un-transduced. Control group remained untreated, n=1

3.3.11 Effect of Ad-PRCP on Ang II metabolism by rat H9C2 cardiomyocytes

Next, experiments were performed in the rat H9c2 cardiomyocyte model which has previously been utilized to investigate the RAS and effects on cell phenotypes such as hypertrophy (K. Peng et al., 2016). H9c2 cardiomyocytes were transduced with 100 pfu/ cell of Ad-PRCP, Ad-GFP or left un-transduced and following 24 h transduction cells were incubated with cell culture media containing 100 nM Ang II and then media collected at 24 h and 48 h timepoints. Ang II and Ang-(1-7) levels were then quantified using ELISA. Analysis showed significantly higher Ang II levels in Ang II 24 h (5.14±1.1 fold change) and Ad-GFP 24h (4.8±1.0 fold change) groups compared to control. Ad-PRCP 24 h showed a tendency for reduced Ang II level (3.16 ± 0.9 fold change) compared to Ang II at 24 h and Ad-GFP at 24 h, however the reduction did not reach significance. By 48h Ang II levels had returned to equivalent levels in all groups, suggesting the cells were able to metabolize Ang II following this time incubation. ***** $p<0.05$ vs control, n=3 (Figure 3.10)

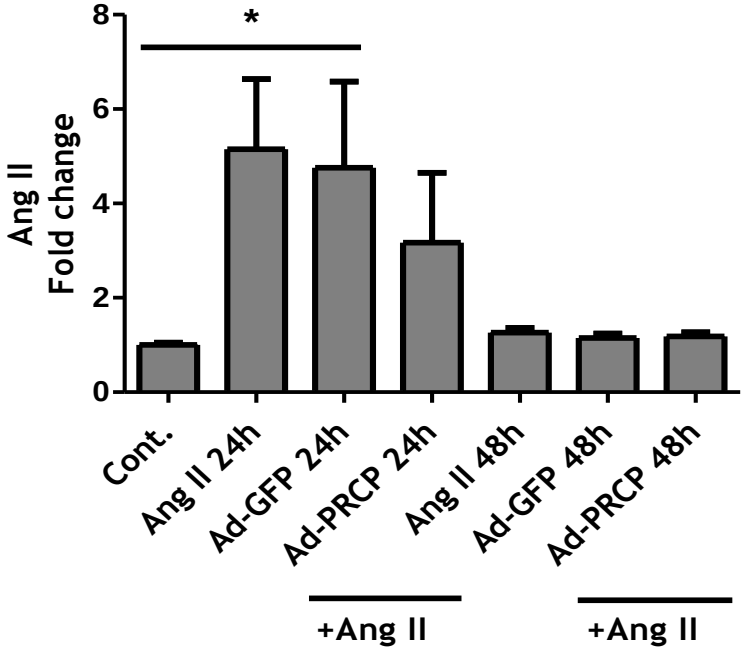

Figure 3.10 Ang II levels in H9c2 cardiomyocyte in response to Ad-PRCP transduction.

Ang II was added to cell culture media of H9c2 cardiomyocyte transduced with Ad-PRCP, Ad-GFP or un-transduced and incubated at 37ºC. Control group remained untreated (neither Ang II nor adenoviral were added to control). Culture media were collected at 24h and 48h for Ang II analysis by ELISA, * p<0.05 vs control, n=3.

3.3.12 Assessment of Ang-(1-7) levels in H9C2 cardiomyocyte transduced with Ad-PRCP

Conversely, when measuring Ang-(1-7) equivalent levels were observed in all groups at 24h, however they were significantly increased in the Ad-PRCP transduced cardiomyocyte at 48h (1.48±0.1-fold change) compared to control (non-treated) group (1.0±0.04-fold change). This significant formation of Ang-(1-7) was observed even though there was no exogenous Ang-(1-7) added to the cells in this experiment (*p<0.05, n=3) (Figure 3.11).

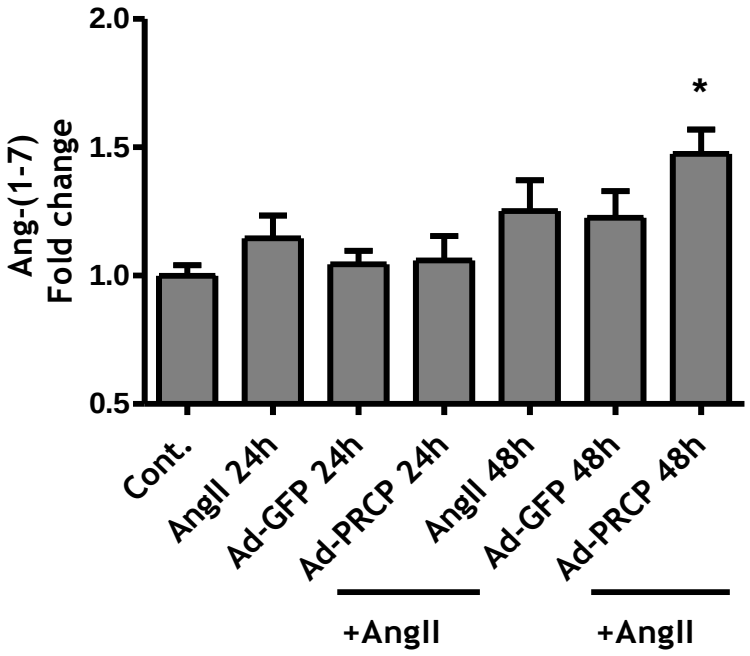

Figure 3.11 Analysis of Ang-(1-7) levels in H9c2 cardiomyocytes transduced with Ad-PRCP

Ang II was added to cell culture of H9c2 cardiomyocyte transduced with Ad-PRCP, Ad-GFP or un-transduced and incubated at 37ºC. Control group remained untreated (neither Ang II nor adenoviral were added to control). Culture media were collected at 24h and 48h for Ang-(1-7) analysis, * p<0.05 vs control, n=3.

3.3.13 Effect of Ad-PRCP on Ang-(1-7)/Ang II ratio in H9C2 cardiomyocyte

Following Ang II and Ang-(1-7) levels evaluation, Ang-(1-7)/Ang II ratio was also assessed for the same samples explained in (section 3.4). The analysis revealed that Ang-(1-7)/Ang II ratio in Ang II 48h (1.07), and Ad-GFP 48h (1.04) remain equivalent to control (1.0). However, there was a significant increased Ang-(1-7)/Ang II ratio in Ad-PRCP 48h group (1.4) compared to control which indicated more conversion of Ang II to Ang-(1-7) in response to Ad-PRCP transduction at this time point. Furthermore, it was also observed that Ang-(1-7)/Ang II ratio was reduced significantly in both Ang II 24h (0.27) and Ad-GFP 24h (0.36) groups, but not Ad-PRCP 24h (0.5), in comparison to control. *****p<0.05 vs control, n=3 (Figure 3.12).

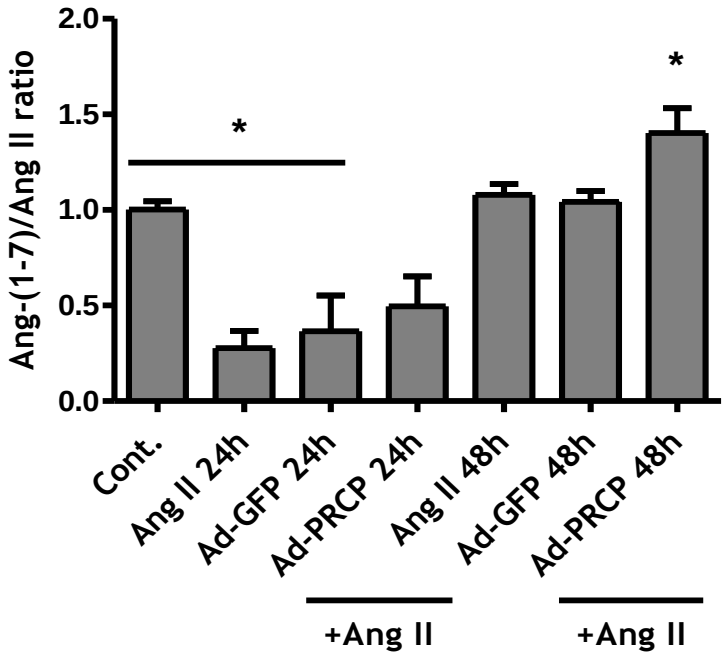

Figure 3.12 Analysis of Ang-(1-7)/Ang II ratio in Ad-PRCP-transduced cardiomyocyte.

Ang-(1-7)/Ang II ratio was calculated for samples analysed in figures 3.10 and 3.11, *p<0.05 vs control, n=3.

3.3.14 Investigating the effect of Ad-PRCP on Angiotensin II-induced Cardiomyocyte hypertrophy

H9c2 cardiomyocytes were either untreated (control) or transduced with Ad-PRCP or Ad-GFP and stimulated with 100 nM Ang II for 96h to induce hypertrophy (Flores-Muñoz et al., 2012) (Figure 3.13A). Cardiomyocytes were stained and imaged and cell size measured for hypertrophy analysis (Figure 3.13B). Results revealed significant increase in cardiomyocyte surface area in both Ang II and Ad-GFP groups (6029 ± 410.5 μm^2 and 5960 ± 557.7 μm^2 respectively) in comparison to control (4253 ± 263.3 μm^2). Ad-PRCP transduced cardiomyocytes showed reduced cell size (4712 ± 319.6 μm^2) compared to Ang II and to Ad-GFP groups even though it did not reach significance. Furthermore, there was no significant difference between control and Ad-PRCP transduced cardiomyocytes, n=5 (Figure 3.13C).

A

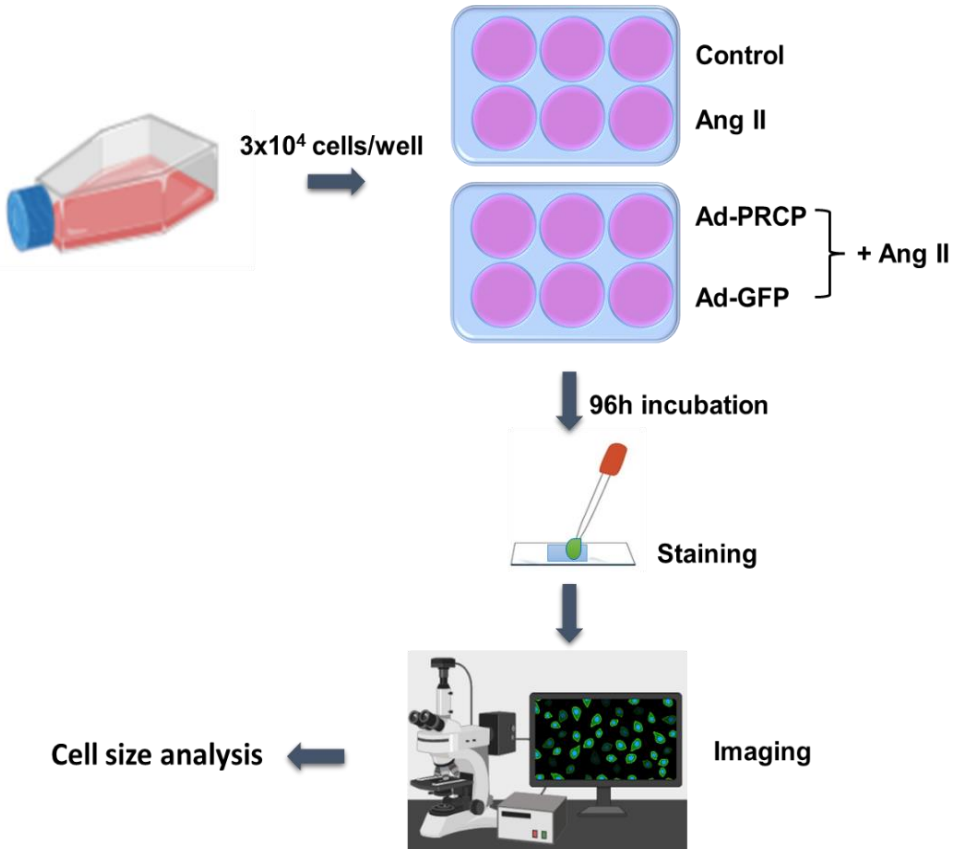
3x10⁴ cells/well
Control
Ang II
Ad-PRCP
Ad-GFP
+ Ang II
96h incubation
Staining
Imaging
Cell size analysis

B

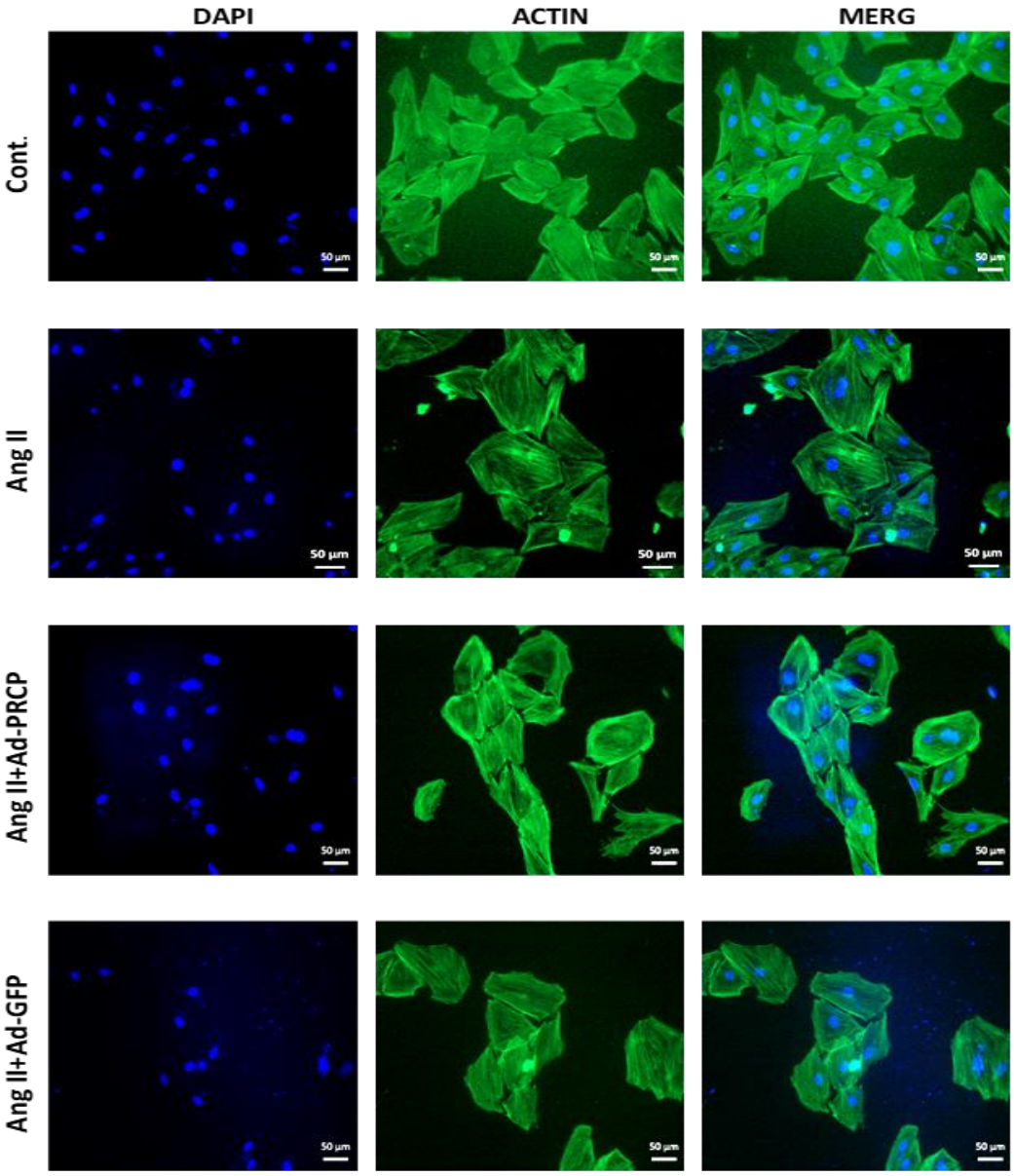

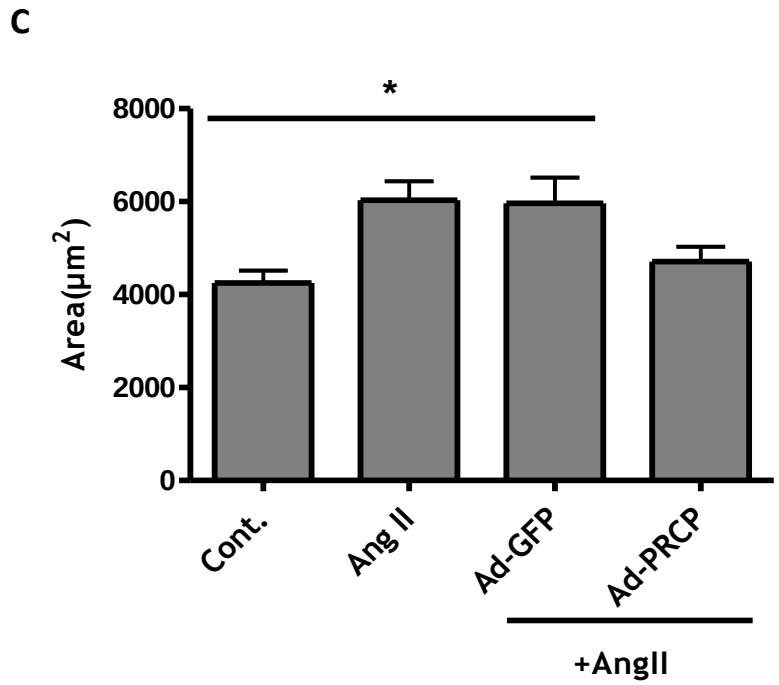

Figure 3.13 Investigating the protective role of PRCP overexpression on Ang II-induced cardiomyocyte hypertrophy.

(A) Schematic representation of the work plan for investigating the role of Ad-PRCP on Ang II-induced H9c2 cardiomyocyte hypertrophy. H9c2 cardiomyocytes transduced with Ad-PRCP, or Ad-GFP or un-transduced and stimulated with Ang II. **(B)** Representative images for H9c2 cardiomyocytes under each condition (20x magnification, scale bar=50μm)**. (C)** Analysis of H9c2 cardiomyocyte cell size for each condition (**p*<0.05 vs control) n=5.

3.3.15 Assessment of TGFß1 gene expression in Ad-PRCP transduced cardiomyocyte

TGFß1 has been linked to cardiac hypertrophy and considered an important mediator of cardiac hypertrophy induced by angiotensin II (Schultz et al., 2002). Therefore, the gene expression for TGFß1 was assessed in this study for the conditions explained in section 3.3.6. The data revealed that TGFß1 was detectable under each condition. However, there was no significant change observed between groups, control (1.0±0.00), Ang II (1.1±0.03), Ad-GFP (0.84±0.05), Ad-PRCP (0.98±0.06) (Figure 3.15), n=3.

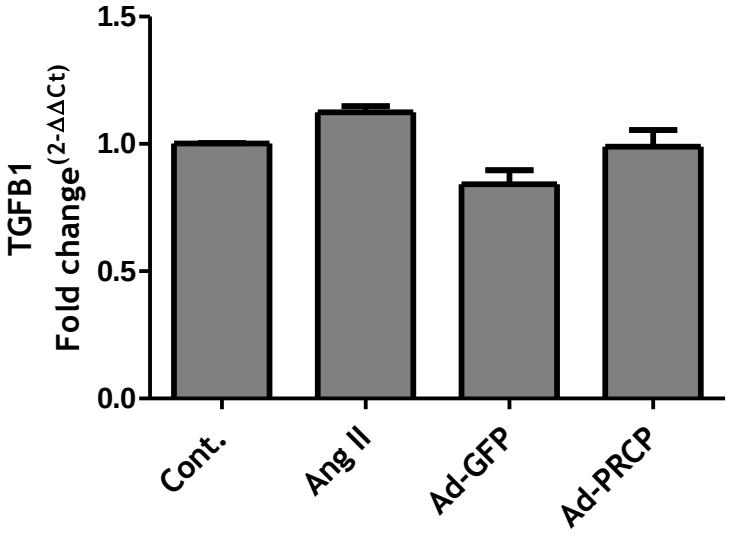

Figure 3.14 Gene expression of TGFß1 in response to Ad-PRCP transduction in Ang II treated cardiomyocyte.

Ang II was added to H9C2 cardiomyocyte that untreated or transduced with Ad-GFP or Ad-PRCP and TGFß1 expression was assessed at 24h, n=3.

3.2.16 **Effect of Ad-PRCP on RAS receptors gene expression following Ang II stimulation**

H9c2 cardiomyocytes were seeded into 6 well plates and transduced with Ad-PRCP, Ad-GFP or control (non-transduced), followed by 1 μM Ang II stimulation in 5% serum media for 24 h and the gene expression for AT_1R, AT_2R and MasR were assessed.

The data showed that the gene expression of AT_1R in Ad-PRCP transduced cardiomyocytes (1.15 ± 0.57-fold change) was equivalent to control (1.25 ±0.13). However, there was a trend toward higher AT_1R expression in Ang II (1.53±0.73-fold change) and Ad-GFP (1.75 ±0.57-fold change) in comparison to control although it did not reach significant (Figure 3.16A, n=3).

Similarly, AT_2R gene expression analysis revealed no significant difference between groups, control (1.12±0.07), Ang II (1.18±0.43-fold change), Ad-GFP (1.5±0.27- fold change) and Ad-PRCP (1.03±0.32-fold change) Figure 3.16B, n=3).

The expression of MasR was also assessed and showed that its detectable in all conditions, but no significant change was observed between groups, control (1.1±0.01), Ang II (0.98±.21-fold change), Ad-GFP (0.99±.07-fold change), and Ad-PRCP (0.71±0.18 fold change) (Figure 3.16C, n=3).

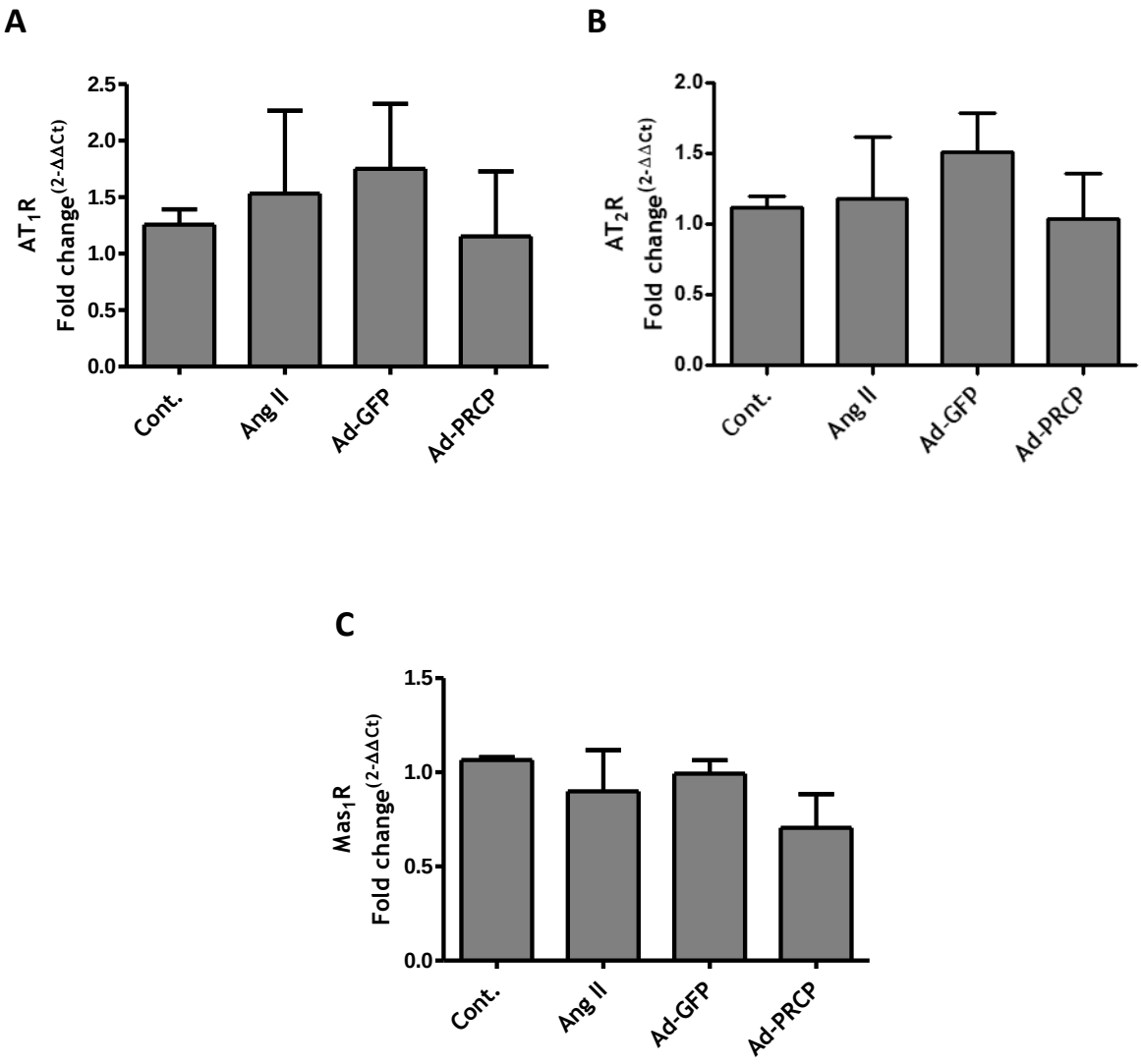

Figure 3.15 Evaluating RAS gene expression following Ad-PRCP overexpression in Ang II-stimulated cardiomyocyte.

H9c2 cardiomyocytes were untreated or transduced with Ad-GFP or Ad-PRCP and 1 μM Ang II was added. **(A)** Analysis of AT_1R gene expression under each condition, n=3. (B) Analysis of AT_2R gene expression under each condition, n=3. (C) Assessment of the gene expression for MasR under each condition, n=3.

3.4 Discussion

Prolylcarboxypeptidase (PRCP) contributes to counteract the harmful effects of the renin angiotensin system (RAS) via converting Ang II to Ang-(1-7)(J. Mallela et al., 2009; Odya et al., 1978). In this chapter, the cDNA for rat PRCP was cloned into the AdEasy-1 adenoviral gene transfer vector system (He et al., 1998), and a replication deficient human adenovirus serotype 5 gene transfer vector expressing rat PRCP (Ad-PRCP) was generated, amplified, purified and titered. The features and/ or characteristics that have made the adenoviral vector the choice of this study were explained in (section 1.3.5.5) and (section 3.1.1). Next, Ad-PRCP was assessed for its effects on metabolism of Ang II and cardiomyocyte hypertrophy following exogenous Ang II stimulation.

pRat-PRCP plasmid and pshuttle-CMV were digested with two restrictions endonucleases. Pshuttle-CMV was purified, and a ligation reaction and bacterial transformation performed successfully and pShuttle-CMV-pRat-PRCP positive colonies identified. pShuttle-CMV vector is important for gene expression and contains a polylinker for the insertion of the foreign transgene between a cytomegalovirus (CMV) promoter and polyadenylation site (He et al., 1998). The Pshuttle-CMV-pRat-PRCP was then linearized and subjected to electroporation into AdEasy-1 competent cells and colonies were screened by mini prep and diagnostic digest. Next the homologous recombinant AdEasy-1-*P*shuttle-CMV-pRat-PRCP was linearized and transfected into HEK 293 cells for virus production. Recombinant Ad-Rat-PRCP (Ad-PRCP) was then purified using ArkloneP and cesium chloride density gradient ultracentrifugation and titered using standard protocols (Alba et al., 2012) .

Before assessment of Ad-PRCP gene expression and function *in vitro*, Ad-GFP transduction efficiency was assessed in H9c2 cardiomyocytes. Ad-GFP has been frequently used as a control adenoviral vector for several studies including studies using the H9c2 cardiomyocyte model (Saeedi et al., 2009). In this study, the delivery of eGFP via adenoviral vector was efficient as observed by high expression of eGFP in Ad-GFP transduced cardiomyocyte which was consistent with previous studies using a similar viral vector and cell model (T. Chen, Ding, Jin, Wagner, & Yuan, 2012; Saeedi et al., 2009).

Following transduction of Ad-PRCP into H9c2 cells significantly higher gene expression of PRCP was observed, compared to untransduced or to Ad-GFP transduced cells confirming the successful generation of Ad-PRCP and that it is efficient in transducing H9c2 cardiomyocytes.

It has been previously reported that PRCP plays a protective role to the heart and blood vessels via degrading Ang II to Ang-(1-7) (Adams et al., 2013; Hao et al., 2020), and the depletion of PRCP induces vascular and cardiac dysfunction accompanied with hypertension (Adams et al., 2011; Maier, Schadock, Haber, Wysocki, Ye, Kanwar, Flask, Yu, Hoit, et al., 2017). The maximum in vitro activity of PRCP was reported at acidic environment, particularly at pH 5.0 (Maier, Schadock, Haber, Wysocki, Ye, Kanwar, Flask, Yu, Hoit, et al., 2017) using the fluorogenic substrate MCA-APK-(Dnp) in a test tube (not in a cell culture model) and this activity declined with higher pH (N. Grobe et al., 2013; Maier, Schadock, Haber, Wysocki, Ye, Kanwar, Flask, Yu, Hoit, et al., 2017). However, it has also been demonstrated that PRCP has enzymatic activity at normal pH (N. Grobe et al., 2013; Zia Shariat-Madar, Mahdi, & Schmaier, 2002). In the studies presented here a different approach was taken where adenoviral overexpression of PRCP in cardiomyocytes to test whether it could metabolise Ang II was assessed. Ang II levels were assessed by specific ELISA in vitro at specific time points in response to Ad-PRCP overexpression in HeLa cells and H9c2 cardiomyocytes. In the conditioned media of HeLa cells that had been stimulated with Ang II for 24hr degradation of Ang II was only observed following Ad-R-PRCP transduction compared to Ad-GFP and to Ang II only treated groups. However, no marked change was observed on Ang II levels on other selected time points (5, 15, 30, and 60 min) of stimulation between groups. HeLa cells have been previously utilized to study the function of the renin angiotensin system components e.g. AT_1R and AT_2R, following stimulation with Ang II, and reported that AT_2R counteract the AT_1R action, in part, via inactivation of Extracellular signal-regulated kinase/mitogen-activated protein kinase (ERK/MAPK) (Inuzuka et al., 2016). However, no studies for investigating PRCP function or expression in HeLa cells have been reported.

Following the observation in HeLa cells, the effects of Ad-PRCP transduction in metabolizing Ang II in H9c2 cardiomyocytes were assessed. H9c2 cardiomyocytes are a widely utilised cell model to investigate aspects of abnormal cardiac

remodelling in an in vitro context including hypertrophy (Ayyappan Prathapan, Vineetha, & Raghu, 2014; Watkins et al., 2011; Yan et al., 2013) and oxidative stress (B. Li, Kim, Yadav, Kim, & Chae, 2015) and hypoxia/reoxygenation injury (WenHua Li et al., 2019). In this study, H9C2 cardiomyocyte Ang II levels were significantly greater in Ang II treated and in Ad-GFP groups at 24 h of Ang II stimulation compared to (control) non-treated group. Furthermore, there were reduced Ang II levels in Ad-PRCP 24h transduced cardiomyocyte, although this did not reach significance in comparison to Ang II and Ad-GFP groups at similar time point. Also, there was no significant differences between Ad-PRCP 24h and control group. These data suggest that Ad-PRCP degraded Ang II in cardiomyocytes. Following 48h incubation, Ang II was reduced to minimal levels in all groups. Not observing significant degradation of Ang II could be related to the pre-selected incubation times for collecting the samples, alongside the specific cell model chosen. Ang II levels were initially assessed at incubation time points between 5 minutes to 1h, and then at 24h and 48h in HeLa cells. These data were then used to inform the design of the studies in H9c2 cardiomyocytes. Ang II levels were therefore not evaluated at incubation times between 1h and 24h. It is plausible that Ang II levels could have started to decline in the culture media (either degradation or through uptake into the cells) at sometimes between 1h and 24h in H9c2 cardiomyocytes. A previous in vitro study reported almost complete hydrolysis of Ang II in response to recombinant PRCP within less than 4h of incubation at 37°C and under constant shaking (850rpm) in a centrifuge tube with highest degradation rate between 1-3h (Maier, Schadock, Haber, Wysocki, Ye, Kanwar, Flask, Yu, Hoit, et al., 2017). However, this observation might not be comparable to the study presented here as it was conducted in a test tube, not in a cell culture model.

To investigate whether the degradation of Ang II led to increased levels of Ang-(1-7), next Ang-(1-7) levels were measured using a specific ELISA in the same samples. These data revealed significantly increased Ang-(1-7) levels in Ad-PRCP transduced cardiomyocyte at 48h of Ang II stimulation compared to non-treated (control) cells. There was no significant change in Ang-(1-7) levels between groups following 24h of Ang II treatment, suggesting that there was a delay in the Ang-(1-7) levels accumulating at a level detectable by the ELISA. Adding to that, the optimal activity of PRCP was reported at acidic pH (Maier, Schadock,

Haber, Wysocki, Ye, Kanwar, Flask, Yu, Hoit, et al., 2017; Odya et al., 1978). It is interesting to note that cells transduced with adenoviral vectors become more acidic at 48 h through the infection process (TOLLEFSON, RYERSE, SCARIA, HERMISTON, & WOLD, 1996) which might clarify, in part, the significant formation of Ang-(1-7) at this time point compared to control. Another ex-vivo study showed that incubation of Ang II with wild type mouse serum led to formation of Ang-(1-7) that peaked at 15 minutes and was no longer detectable at 2h of incubation (P. Serfozo et al., 2020) which further confirm the importance of selected time points for measuring the peptides.

The trend toward lower levels of Ang II in response to Ad-PRCP overexpression were consistent with previous studies that suggested a role for PRCP in degrading Ang II into Ang-(1-7) (N. Grobe et al., 2013). Previously it was shown that hydrolysis of AngII into Ang-(1-7) in human umbilical vein endothelial cells (HUVEC) and human aortic endothelial cells (HAoEC) was mainly PRCP dependent and occurred at 2h incubation time with maximum degradation rate at 24h of incubation under normal physiological pH (De Hert, Bracke, Lambeir, Van der Veken, & De Meester, 2021). In these studies no involvement of ACE2 or PRCP in metabolising Ang II was observed in both HUVEC and HAoEC. It has previously been reported that Ang II is a substrate for both ACE2 and PRCP (De Hert, Bracke, Lambeir, et al., 2021). Previous work has also concluded that PRCP is responsible for converting bradykinin (1–8) to bradykinin (1–7) in HUVEC while PRCP and ACE2 together contributed to Ang II hydrolysis in HAoEC from 2h and longer incubation (De Hert, Bracke, Lambeir, et al., 2021). Degradation of Ang III into Ang-(2-7) in HUVEC was also reported to be PRCP dependent and achieved after 8h of incubation. Furthermore, PRCP also degraded Ang III in HAoEC at a 4h time point (De Hert, Bracke, Lambeir, et al., 2021). Moreover, PRCP cleaved the C-terminal of (pyr)-apelin-13, another regulator peptide for the cardiovascular system, to form (pyr)-apelin-13(1–12) in vitro using HUVEC and HAoEC at 8h and 24h incubation times (De Hert, Bracke, Pintelon, et al., 2021). These data highlight that PRCP has broader substrates than Ang II alone and indicate a range of timepoints that PRCP is reported to have effects on peptide metabolism *in vitro* at incubation up to 24h (De Hert, Bracke, Pintelon, et al., 2021) of Ang II stimulation.

With regard to formation of Ang-(1-7) from Ang II by another RAS enzyme, ACE2, it has been reported that this was observed within less than 24 h in vitro (Ye et al., 2012). Recombinant mouse ACE2 (mrACE2) and recombinant human (hrACE2) was evaluated in vitro for the ability of forming Ang-(1-7) from exogenous AngII in test tubes. Both mrACE2 and hrACE2 led to formation of Ang-(1-7) after 4h of exposure to or/incubation with Ang II, and there was no spontaneous formation of Ang-(1-7) without rACE2 (Ye et al., 2012). In contrast to these in vitro data, formation of Ang-(1-7) from exogenous Ang II occurred at a faster time point of Ang II stimulation. *In vivo* studies revealed rapid formation of Ang-(1-7) following exposure to exogenous Ang II infusion (P. Serfozo et al., 2020). Blood was drawn by cardiac puncture from mice at 5 minutes of Ang II injection and Ang II levels were about a hundred-fold greater in the plasma of Ang II infused mice at 5 minutes of Ang II infusion compared to the control (no Ang II) group (P. Serfozo et al., 2020). Ang-(1-7) was significantly elevated at 5 minutes in Ang II infused animals compared to the control (non-treated) group (P. Serfozo et al., 2020). Plasma Ang II and Ang-(1-7) measurements were conducted using ELISA and further confirmed on the same samples by RIA and liquid chromatography tandem mass spectrometry (LC/MS-MS) (P. Serfozo et al., 2020). These data provided evidence for rapid formation of Ang-(1-7) from exogenous Ang II in vivo compared to in vitro and highlighted that there are other available methods to measure the peptides.

Recently, it has been reported that overexpression of PRCP via adenoviral gene transfer significantly increased Ang-(1-7) and bradykinin-(1-9) levels in plasma and myocardium in a rat model of I/R injury compared to the Ad-control group (Hao et al., 2020). Conversely, plasma and myocardium Ang II concentration was lower in Ad-PRCP animals compared to Ad-control following myocardial I/R injury (Hao et al., 2020). Ang II, Ang-(1-7) and bradykinin-(1-9) levels were assessed in this study using high-performance liquid chromatography (HPLC)-based radioimmunoassay (RIA) (Hao et al., 2020).

Although previous in vitro data suggested PRCP was maximally active at acidic pH (Maier, Schadock, Haber, Wysocki, Ye, Kanwar, Flask, Yu, Hoit, et al., 2017), this work was performed with recombinant protein in test tubes and the data presented in this thesis supports the assertion that PRCP actively metabolises Ang II at normal physiological pH in cell culture models which is consistent with

other studies (De Hert, Bracke, Lambeir, et al., 2021). Grobe et al, suggested that PRCP is abundant in the kidney collecting tubule and provides a reno-protective effect via degrading local Ang II into Ang-(1-7)(Grobe et al., 2015). The study also demonstrated that in the kidney tubules PRCP catalyses Ang II into Ang-(1-7) at an acidic pH≤ 6(Grobe et al., 2015; N. Grobe et al., 2013), while ACE2 was reported to degrade Ang II in the kidney at normal or basic pH. Furthermore, another in vivo study using a murine model with combined genetic ACE2 and PRCP deficiency (ACE2-/- PRCP-/- mice) indicated that Ang-(1-7) could also be formed from exogenous Ang II in the circulation and kidney independently of ACE2 or PRCP activity (P. Serfozo et al., 2020). The study revealed that prolyl endopeptidase (POP), another enzyme known to degrade Ang II, is the main enzyme responsible for Ang-(1-7) formation in the circulation as well as in the lung in the absence of ACE2 or PRCP following infusion of Ang II in ACE2-/- PRCP-/- mice (P. Serfozo et al., 2020). In contrast to the lung, ACE2 is the main enzyme that converts Ang II to Ang-(1-7) in the kidney (P. Serfozo et al., 2020). These finding further showed the complexity of RAS and indicated that it's a compensatory mechanism so that when the activity of one or more enzymes are removed another can maintain the regular balance. However, in these studies a minimal role for formation of Ang-(1-7) by PRCP in the kidney was reported under normal physiological pH suggesting that PRCP plays a role in degrading Ang II in certain regions e.g. kidney collecting tubule, where the pH is low (P. Serfozo et al., 2020). Research has also been undertaken to explore a role for PRCP in the heart, focused on cardiac functional and structural changes in global PRCP-deficient mice that generated using gene trap technology (Baygenomics) (Maier, Schadock, Haber, Wysocki, Ye, Kanwar, Flask, Yu, Hoit, et al., 2017). Left ventricular hypertrophy (LVH) was observed in PRCP-deficient mice at baseline in comparison to wild type (WT)mice (Maier, Schadock, Haber, Wysocki, Ye, Kanwar, Flask, Yu, Hoit, et al., 2017). However, following infusion of Ang II, LVH was increased in PRCP-deficient mice and in WT mice without any significant difference observed between the groups (Maier, Schadock, Haber, Wysocki, Ye, Kanwar, Flask, Yu, Hoit, et al., 2017). In addition, fractional shortening assessment revealed no significant difference between PRCP-deficient mice and WT mice in response to Ang II infusion (Maier, Schadock, Haber, Wysocki, Ye, Kanwar, Flask, Yu, Hoit, et al., 2017). Ang II and Ang-(1-7) levels were measured in plasma, heart, and kidney in PRCP-deficient and WT

mice and no significant difference was observed between the groups suggesting that the cardiac structural and functional changes in PRCP-deficient mice occurs independently of circulating Ang II and Ang-(1-7)(Maier, Schadock, Haber, Wysocki, Ye, Kanwar, Flask, Yu, Hoit, et al., 2017).

In the studies reported here we investigated whether overexpression of PRCP might provide a protective effect against Ang II-induced cardiomyocyte hypertrophy. H9c2 cardiomyocytes were transduced with Ad-PRCP, Ad-GFP or left untreated followed by Ang II incubation to stimulate hypertrophy. The data indicated significantly greater cardiomyocytes surface area in Ang II only treated group and in Ang II and Ad-GFP transduced cells compared to control non-stimulated group. This observation was consistent with previously published data used Ang II as a pro-hypertrophic agonist in H9c2 cardiomyocytes (Flores-Muñoz et al., 2012). The study suggested that stimulating H9c2 cardiomyocyte with 100 nm Ang II for 96h induced significant hypertrophy, an effect that was significantly reduced by adenoviral gene transfer of either Ang-(1-7) (RAdAng-(1-7)) and Ang-(1-9) (RAdAng-(1-9))(Flores-Muñoz et al., 2012). The antihypertrophic effect of Ang-(1-7) and Ang-(1-9) was mediated via their receptors, Mas and AT_2R respectively (Flores-Muñoz et al., 2012). Similar to H9c2 cardiomyocyte, RAdAng-(1-7) and RAdAng-(1-9) were efficient in reducing the hypertrophic effect of Ang II, particularly concentric hypertrophy, in adult rabbit left ventricular primary cardiomyocytes (Flores-Muñoz et al., 2012). Other studies indicated that 100 nM Ang II can produce hypertrophy in H9c2 cardiomyocyte within shorter incubation time e.g., 48 hour (A Prathapan & Raghu, 2018; Ayyappan Prathapan et al., 2014), while other investigators used higher Ang II dose (1μM) (Heng Zhou et al., 2014), or (200nM) (Watkins et al., 2011) to stimulate H9c2 hypertrophy at 48h. However, there are other hypertrophic agonists that can also be utilized to induce cardiomyocyte hypertrophy including endothelin-1 (Watkins et al., 2011), isoproterenol or arg-vasopressin (Flores-Muñoz et al., 2012), and high glucose (hyperglycemia) (K.-C. Cheng et al., 2019)

In this study, the hypertrophic effect of Ang II was diminished in response to Ad-PRCP overexpression compared to Ang II only treated group. These data suggest that *in vitro* models of cardiomyocyte hypertrophy PRCP overexpression might protect the cells from undergoing Ang II-dependent hypertrophy. There are

currently limited published data that have investigated the role of PRCP on cardiomyocyte hypertrophy *in vitro*. Our data is consistent with a current, non-peer reviewed, study indicated an antihypertrophic role of PRCP on adult rat cardiomyocyte (ARCM) following 48h of Ang II stimulation (Nguyen, 2020). First, the study showed that knockdown of PRCP expression via siRNA caused significantly more hypertrophy response to 1μM angiotensin II stimulation, as shown by greater cell surface area and upregulation of ANP and BNP mRNA gene expression, compared to Ang II only treated group (Nguyen, 2020). Second, the investigator indicted that overexpression of PRCP via adenoviral gene transfer vector (Ad-PRCP) significantly prevented Ang II-induced ARCM hypertrophy in comparison to control virus (Ad-GFP) treated group. However, the study did not mention the pH status of the experiment which indicated that the work was more likely conducted under normal physiological pH (Nguyen, 2020).

In this study, the exact mechanism of how prolylcarboxypeptidase diminished the Ang II hypertrophic effect needs further investigation. However, with the knowledge that PRCP metabolise Ang II and increases Ang-(1-7) it suggests that this may underly the reason of the observed anti-hypertrophic effect. Thus, PRCP could reduce the amount of Ang II uptake into cells in addition to forming the cardioprotective Ang-(1-7) (J. L. Grobe et al., 2007). It has been previously reported that Ang-(1-7) can provide protective effects for H9c2 cardiomyocytes against high glucose-induced injury and inflammation via inhibition of the reactive oxygen species –leptin–p38 MAPK/ERK1/2 pathways (Ccai et al., 2017). Furthermore, Ang-(1-7) is a ligand of the Mas receptor via which mediates anti-hypertrophic, anti-fibrotic, vasodilation and antioxidant effects (V. B. Patel, Zhong, Grant, & Oudit, 2016). Following Ang II stimulation, Mas receptors mediated the cardioprotective role of Ang-(1-7) against Ang II-induced neonatal rat cardiomyocyte autophagy and cardiac structural changes in an animal model (mice), via inhibition of oxidative stress. The selective Mas receptor blocker, A779, abolished the protective actions of Ang-(1-7) against Ang II-dependent autophagy, oxidative stress and cardiac remodelling both in vitro and in vivo indicating the beneficial role of Ang-(1-7) mediated mainly by Mas receptors (L. Lin et al., 2016). In the work here, regulation of Mas receptor gene expression following PRCP overexpression was not significantly affected although there was a significant formation of Ang-(1-7) at 48h compared to control. In

Sprague-Dawley rats with MI, Olmesartan and telmisartan (both are angiotensin receptor blockers, ARBs) significantly reduced Ang II and upregulated ACE2, Ang-(1-7) and MasR expression in the myocardium and attenuated cardiac fibrosis and remodeling compared to MI group (J. Wang et al., 2017). Other studies reported the protective role of Ang-(1-7) via Mas1 receptors using Mas1 inhibition or blocking mechanism both in vitro and in vivo. Indeed, Gaidarov et al, suggested a non-direct interaction between Ang-(1-7) and Mas1 receptor and that the protective effect of Ang-(1-7) might be achieved through potently antagonizing angiotensin II type I receptor signaling (Gaidarov et al., 2018). This further highlights the complexity of RAS and the multiple ways for it to provide biological function.

It has been repeatedly shown that angiotensin II enhanced the gene and protein expression of AT_1R and AT_2R both *in vitro* and *in vivo* (D. Liu, Gao, Roy, Cornish, & Zucker, 2008; Mitra, Gao, & Zucker, 2010; Vázquez et al., 2005). In the data presented here, the regulation of both receptors was not detectable at the gene expression level by Ang II and the reason behind that was not clear and needs further investigation.

Ang II can also promote cardiac structural changes indirectly via activating transforming growth factor beta 1 (TGFß1) cytokine (Rosenkranz, 2004). It has been reported that human atrial tissue stimulated with Ang II led to significant upregulation of TGFß1 mRNA expression (Schultz et al., 2002). TGFß1 can induce the proliferation of cardiac fibroblasts and their phenotypic conversion to myofibroblasts as well as promote changes to extracellular matrix proteins such as proteoglycan, fibronectin and collagen (Rosenkranz, 2004). It was previously reported that Ang II caused increased TGFß1 mRNA and protein expression in the H9c2 cardiomyocyte model (M. Wang et al., 2022). In the study presented here, the regulation of TGFß1 mRNA expression in response to Ang II was not observed and thus, the effect of PRCP overexpression on TGFß1 expression could not be determined.

Together the hypertrophy, and Ang II, and Ang-(1-7) ELISA data reported in this work support the assertion that the antihypertrophic effect of PRCP overexpression may be via activation of a PRCP/Ang-(1-7)-Mas1/axis and inhibition of Ang II/AT1R axis.

3.5 Limitation of the studies:

Presently there is insufficient information regarding the optimal time points for PRCP catalyzing Ang II into Ang-(1-7) using cell culture (particularly cardiomyocytes). This therefore made it challenging to choose the best time points to collect samples for measuring peptide levels via ELISA. In the future selecting more time points between 1h and 24h might have revealed more detailed information on the effects of PRCP on both Ang II degradation and Ang-(1-7) formation. Furthermore, since it has been reported in some tissues that the preferred working environment for PRCP is at low pH (pH=6 or below) it would be interesting to assess the effects of PRCP overexpression on Ang II degradation and cardiomyocyte hypertrophy and viability under low pH conditions e.g. ischemic/hypoxic conditions that can be modelled in the laboratory setting using a hypoxic chamber (Kuznetsov, Javadov, Sickinger, Frotschnig, & Grimm, 2015) . Studies such as this might further enhance understanding of PRCP function. Moreover, we did plan to investigate PRCP overexpression further in primary neonatal rat cardiomyocytes (NRCM) however, due to multiple lockdowns resulting from the current pandemic, this plan was cancelled.

NRCM is a well established cell model to study the cellular and molecular changes as well as the hypertrophy response and its underly mechanism including hypertrophic-specific gene markers, cell size and the reorganization of the contractile proteins (Watkins et al., 2011). Furthermore, NRCM show a very stable phenotype and comparable contractile profile to *in situ* hearts during ischemia-reperfusion injury (Chlopcikova, Psotová, & Miketová, 2001). In comparison to H9c2 cells, NRCM might be more suitable to study autophagy during hypoxia/reoxygenation (Cao et al., 2014).

3.6 Summary

An Ad vector expressing rat PRCP was successfully constructed and showed it metabolizes Ang II leading to increased Ang-(1-7) with antihypertrophic effects on H9c2 cardiomyocytes *in vitro*.

Chapter 4 In vivo assessment of adenoviral vector-mediated overexpression of PRCP in WKY rats

4.1 Introduction

4.1.1 Animal models in experimental cardiovascular research

The use of experimental models to investigate disease processes and assess novel therapies is fundamental in biological research and in new drug development. The basic and pre-clinical research for a new therapeutic agent requires animal research models, if there is no alternative techniques can deliver the answer, to study several aspects including efficacy, safety, pharmacokinetics, and pharmacodynamics (Hollands, 1986; Robinson et al., 2019). Animal studies have markedly contributed to improving human health and lifestyle as well as reducing mortality rate linked to some diseases. For instance, before insulin discovery in 1921, it was uncommon for patients with type I diabetes to live for more than a year or two (Bliss, 2013). However, the discovery of insulin by Frederick G Banting and Charles Best via isolating material from pancreatic extract of a dog to treat another diabetic dog model, have saved millions of people's lives since that time (Barré-Sinoussi & Montagutelli, 2015; Bliss, 2013; Vecchio, Tornali, Bragazzi, & Martini, 2018). Animals could also provide valued information about specific diagnostic or therapeutic tools. For instance, the first electrocardiogram recording was also reported on a dog model by Augustus Waller using capillary electrometer (Waller, 1909). Willem Einthoven's developed sensitive string galvanometer electrocardiograph and suggested that the electrocardiogram could be useful in studying heart conditions in animal and human subjects (Waller, 1909). Furthermore, the first blood dialysis via "artificial kidney" was performed by Abel, Rowntree, and Turner using dogs and rabbits under general anesthesia (Gottschalk & Fellner, 1997). However, the Scottish chemist Thomas Graham was called the "Father of Dialysis" as he was the first scientist to introduce the concept of dialysis supported by the discovery of the Graham's law (Cameron, 2012).

It is estimated that more than 115 million animals are used annually throughout the world in experimental research and to supply the biomedical industry (Mueller, Tippins, & Stewart, 2017). In the United Kingdom, it has been reported that 3.06 million scientific procedure involving living animal were conducted in 2021 according to the Home Office annual report (Annual statistics of scientific procedures on living animals, Great Britain 2021). Rodents, particularly mice

and rats, are among the most widely used model in biological research due to their biological processes being very close to humans e.g., rats, mice and human each have about 30,000 genes of which approximately ninety-five percentage are shared by all three species (Barré-Sinoussi & Montagutelli, 2015; Bryda, 2013). Mouse and rat share most of the breakpoints and usually have the same types of rearrangements when compared to the human genome (S. Zhao et al., 2004). Furthermore, rodents have lower maintenance costs as they require little space or resources to maintain, are easy to breed and to handle compared to large animals beside the fact that their generation time is short (Camacho, Fan, Liu, & He, 2016). However, rodent models may fail to meet the exact human diseases characteristics and long-term studies are not possible because of their limited lifespan, and therefore, very low numbers of research could be successfully translated from animal to human(Perlman, 2016). Indeed, generally, approximately 92% of medicines that passed the preclinical animal research fail to proceed to human clinical trial and benefit patients (Bailey, Owen, & Hutchinson, 2022). This low translational rates from pre-clinical animal study to human could be mainly attributed to the fact that human and animal are very complex systems with significant physiological, genetical, molecular biological, and epigenetic differences between species which make them always unpredictable in term of safety and efficacy (Leenaars et al., 2019). It is understandable that even human react/ or respond differently to disease and drugs and therefore one human cannot completely predict what a medicine can do for another human (Shanks, Greek, & Greek, 2009). Thus, it's unlikely for other species model to be completely extrapolative for humans and the clinical translation might be always restricted to some extent (Pound & Ritskes-Hoitinga, 2018; Shanks et al., 2009). Other reasons for the low animal-to-human translational rate might be attributed to the internal validity of the animal research (e.g. inappropriate study design, insufficient measures to control bias) (Pound & Ritskes-Hoitinga, 2018). However, recent debate about this topic (pre-clinical-to–clinical translational rate) has been increasing and questioning the factors affecting the translational success (Ferreira, Veening-Griffioen, Boon, Moors, & van Meer, 2020; Schulz, Cookson, & Hausmann, 2016).

4.1.2 Rat model of hypertension and cardiovascular disease

Choosing an appropriate animal model for conducting specific research is very critical (Camacho et al., 2016). Rodents (mainly mouse and rats) have been widely used to study essential hypertension and other cardiovascular diseases. Researchers have established genetically modified rats and mice model for hypertension and knockout technology to investigate several cardiovascular conditions. However, in the study here the focus will be on rat model because it's the one that has been investigated.

Spontaneously hypertensive rats (SHR) are one of the well-established models for high blood pressure that have been used extensively as a pathophysiological models for essential hypertension in humans (Takata & Kato, 1995). The SHR were first generated by Okamoto and Aoki I 1963 via selective inbreeding of Wistar Kyoto rats with high blood pressure (Conn, 2017; Hewitson, Ono, & Becker, 2008). Thus, WKY rats have been used as a normotensive control for SHR (Zhang-James, Middleton, & Faraone, 2013). Essential hypertension (systolic blood pressure of 140 mm Hg and diastolic blood pressure of 90 mm Hg or greater (McGee, 2021)) begins to develop in SHR between week 5-6 of age and peaks at around 50-60 days of age (Conn, 2017). At this point blood pressure remains stable or slightly decreased (Conn, 2017). Male SHR shows greater hypertension than female of similar age (Reckelhoff, Cardozo, & Fortepiani, 2018) which is consistent with gender-associated differences in blood pressure in humans (Reckelhoff, 2001). However, SHR develop hypertension in young adulthood while most hypertensive humans are in the middle age or older (Doggrell & Brown, 1998). The exact gene/s responsible for the development of inherited high blood pressure in SHR have not been identified (Rapp, 2000; Yoshida et al., 2014). It has been well accepted that the activation of sympathetic nervous system plays an important role in increased blood pressure in SHR (Iriuchijima, 1973). Administration of hexamethonium bromide (a nicotinic acetylcholine receptor (nAChR) blocker in autonomic ganglia) inhibits both sympathetic and parasympathetic activity (Ascher, Large, & Rang, 1979)), and brings the elevated blood pressure in SHR to normal levels (Iriuchijima, 1973). Electrical stimulation of paraventricular nucleus (PVN) of hypothalamus contributes to sympathetic hyperactivity-induced hypertension in SHR without increasing vasopressin release, an antidiuretic hormone that increase water

reabsorption (Takeda et al., 1991). Cardiac output increases at the early stage of hypertension, affected by sympathetic overactivity (Beevers, Lip, & O'Brien, 2001), with normal or little change in total peripheral resistance (Doggrell & Brown, 1998) . However, when hypertension stabilizes, cardiac output returns to normal levels despite having lower ejection fraction compared to normotensive WKY (Wilson et al., 2017), and more total peripheral resistance emerges (Conn, 2017). This is similar to human essential hypertension as most hypertensive patients have normal cardiac output but high peripheral resistance (Beevers et al., 2001). Elevated peripheral vascular resistance might be mediated by both $alpha_1$- and $alpha_2$-adrenergic receptors that promote vasoconstriction in humans and rats (Timmermans, Chiu, & Thoolen, 1987). In SHR kidney, higher density of $alpha_1$- adrenoceptor was reported, an observation that precedes the elevation of blood pressure, in comparison to WKY (Michel, Brodde, & Insel, 1990). The ability of SHR to maintain normal cardiac output at this stage is due to the development of larger end diastolic volume (EDV) as a compensatory mechanism to keep normal stroke volume, while there was no change of the heart rate in comparison to WKY (Wilson et al., 2017). This compensatory effects might lead to increase myocardial fibrosis from 12 months of age in SHR and the subsequent increased in left ventricular stiffness as well as end diastolic pressure which promotes eccentric hypertrophy (LeGrice et al., 2012). This cardiac remodelling will eventually progress to heart failure as SHR age, approximately at 18 months of age, which shows similarity to human heart failure development in the context of aging (Boluyt & Bing, 2000). Furthermore, the main stimulus for cardiac remodelling and heart failure in SHR is hypertension, which comes second only to MI as a precursor of heart failure in humans (Boluyt & Bing, 2000).

Generation of the stroke-prone spontaneously hypertensive rat (SHRSP) from a sub-strain of spontaneously hypertensive rats in 1974 by Okamoto et al also participated in investigating cardiovascular disease particularly hypertension-dependant stroke (Nabika, Ohara, Kato, & Isomura, 2012). Hypertension develops at 5 weeks of age in SHRSP and they have higher systolic blood pressure (250 mmHg in male) compared to SHR (200 mmHg) (Doggrell & Brown, 1998).

Other rats models that have been used to study cardiovascular disease include: mineralocorticoids (DOCA–salt) rats (DE CHAMPLAIN, Krakoff, & AXELROD, 1967), NO synthase inhibition (L-NAME administration) rats (G. Zhong, Chen, Cheng,

Tang, & Du, 2003), transgenics (TGR(mREN2)27 rats) (Albrecht, Nitschke, Von Bohlen, & Halbach, 2000), diabetic hypertensive rats (STZ-SHR, Zucker) (Van Zwieten et al., 1996), renal artery occlusion (1K1C, 2K1C) rats (Zeng, Zhang, Mo, Su, & Huang, 1998), hypertensive HF prone rats (Doggrell & Brown, 1998) angiotensin II-induced hypertension in rats (M.-S. Zhou, Schulman, & Raij, 2004) etc..

4.1.3 The pressor dose of angiotensin II in rat model

The renin angiotensin system plays a major role in cardiovascular hemostasis and structural change i.e., in vivo increased blood pressure and the subsequent vascular fibrosis, increased in left ventricular mass, cardiomyocyte hypertrophy, fibroblast proliferation and fibrosis, (Kim & Iwao, 2000; Williams, 2001). Both sympathetic nervous system and RAS are involved in complex relationship in inducing hypertension. Some reports suggested that the sympathetic nervous system contributes to Ang II-induced hypertension (Lohmeier, 2012), while others indicated that infusion of Ang II in Sprague-Dawley rats causes excitation of pre-autonomic neurons in the PVN which leads to elevated sympathetic outflow and the subsequent hypertension (Sharma et al., 2021). Intracerebroventricular (i.c.v.) injections of Ang II into male Wistar rats caused significant release of noradrenaline into the PVN in a dose-dependent manner (Stadler, Veltmar, Qadri, & Unger, 1992). Exposing vascular smooth muscle cells of Sprague-Dawley rats to 100 nM of Ang II led to increased alpha$_{1-}$ adrenergic receptor mRNA expression (Hu, Shi, Okazaki, & Hoffman, 1995). More details about the mechanism of Ang II in mediating hypertension and cardiovascular remodelling can be found in sections (1.2.3 – 1.2.5).

Ang II infusion has been repeatedly utilized to investigate hypertension and myocardial remodelling (fibrosis and hypertrophy) in rats (Justin L. Grobe et al., 2007; Takemoto et al., 1997). However, species, dose, and duration of Ang II infusion as well as the routes or the site of administration/delivery are critical to produce the expected peptide effect on blood pressure and cardiovascular remodelling. For instance, it has been reported that infusion of Ang II into rats via carotid artery exerts higher pressor response than Ang II infused via abdominal aorta (Lappe & Brody, 1984). Furthermore, previous literature suggested that the threshold pressor dose of Ang II in rats is 150-200 ng/kg/min when administered subcutaneously, and 250 ng/kg/min when Ang II is delivered

intraperitoneally (Simon, Abraham, & Cserep, 1995). Another report suggested that the pressor dose of Ang II is (>200 ng/kg/min) and the subpressor dose is (<200 ng/kg/min) (Cassis, Marshall, Fettinger, Rosenbluth, & Lodder, 1998). Subcutaneous infusion of non-pressor dose (200 ng/kg/min) Ang II via osmotic minipump into Sprague–Dawley rats for 72 h showed no significant difference in hemodynamic parameters (systolic, diastolic or mean blood pressure and heart rate), urine volume, urinary protein excretion and kidney weight/body weight ratio compared to vehicle (saline) group (Sugawara et al., 2021). The dose of 200 ng/kg/min was also prescribed as a "sub-pressor dose" when administered into Sprague–Dawley rats subcutaneously via osmotic minipump and failed to induce high blood pressure response over 7 to 14 days of treatment despite producing endothelium dysfunction (Szabó et al., 2004). Similarly, infusion of a subpressor dose (150 ng/kg/min) Ang II into male Wistar rats over 7 days did not elicit acute increase of systolic or diastolic blood pressure (Pavel, Oroszova, Hricova, & Lukacova, 2013). Another study reported that infusion of low dose (200ng/kg/min) of Ang II into male Wister rats for 7 days caused gradual increase of blood pressure with significantly higher blood pressure at day 3 and 7 but not at 24 h in comparison to saline-infused group (S. Kim et al., 1995). This study also demonstrated that low dose of Ang II can significantly induce mRNA expression of left ventricular hypertrophy markers such as ß-myosin heavy chain (ß-MHC), skeletal α-actin and ANP as well as increased left ventricular weight at day 3 and 7 of Ang II infusion (S. Kim et al., 1995). Blood pressure significantly increased in Sprague Dawley rats received 350 ng/kg/min Ang II by day 3 and day 7, while rats received 200 and/or 500 ng/kg/min showed significant elevated blood pressure at day 7 with significantly higher blood pressure in the group received the higher dose (500 ng/kg/min) (Cassis et al., 1998).

However, different rat strains might respond variously to exogenous Ang II infusion. For example, Fischer 344 (F344) rats showed significantly greater systolic blood pressure in response to Ang II injection compared to WKY received similar dose (Herin et al., 2003).

Despite the fact that rats are bigger in size than mice, rats are more sensitive to high Ang II dose that might cause significant body weight loss and the consequent illness that might end up having the animal excluded from the study. For instance, infusion of 500 ng/kg/min Ang II into Sprague Dawley rats resulted

in significant reduction in body weight within 7 days independently of elevated blood pressure (Cassis et al., 1998), while mice are able to tolerate up to 1000 ng/kg/min of continuous Ang II infusion (Iulita et al., 2018). Infusion of (1.4 mg/kg/day) Ang II into PRCP knockout and wild type (control) mice showed significant elevated blood pressure to baseline without marked difference between groups (Maier, Schadock, Haber, Wysocki, Ye, Kanwar, Flask, Yu, Hoit, et al., 2017). Ang II and Ang-(1-7) levels did not significantly change between PRCP knockout mice and control following Ang II infusion (Maier, Schadock, Haber, Wysocki, Ye, Kanwar, Flask, Yu, Hoit, et al., 2017). Infusion of (0.2 µg/g body weight) Ang II into wild type mice led to fast, within 5 minutes, increase of plasma Ang II and Ang-(1-7) levels, an observation that was similar to cross ACE2/PRCP knockout ($ACE2^{-/-}/PRCP^{-/-}$) mice infused with Ang II (P. Serfozo et al., 2020).

4.2 Hypothesis and aims

In the previous chapter of this work, delivery of PRCP via adenoviral vector diminished the hypertrophic effect of Ang II in vitro. Here it was hypothesized that Ad-PRCP can protect against Ang II-induced cardiac remodeling, dysfunction, and high blood pressure in WKY rats.

Aims

- To assess the effect of 400 ng/kg/min of Ang II on induce hypertension in WKY rats.

- To determine the correct dose of adenovirus serotype 5 to mediate liver transduction in the WKY rat following intravenous delivery.

- To assess the effects of adenoviral gene transfer of PRCP on BP and cardiac function and remodelling in the WKY rat.

4.3 Results

4.3.1 Assessment of subcutaneous infusion of (400ng/kg/min) Ang II on BP and body weight of WKY rats

Considering reports suggested that different rat strains might respond to exogenous Ang II differently (Herin et al., 2003) and the importance of choosing the correct pressor dose for rats (Cassis et al., 1998), two male WKY rats were used to determine the effect of osmotic minipump-mediated infusion of (400 ng/kg/min), a dose that has been used previously in Wistar rats (Figure 4.1A) (Ceravolo et al., 2014). One rat received normal saline (control) and the other received Ang II. The rats were monitored daily for body weight, and blood pressure was assessed weekly over 4 weeks (28 days). The baseline (before minipump implantation) body weights were 237g and 242g for control and Ang II infused animal respectively. The control rat maintained stable body weight that increased gradually with the time to reach 287g after 28 days. However, the Ang II-infused rat showed fluctuation in body weight the days following minipump implantation (239 g, 234 g, 241 g, and 228 g in the days 2,3,4, and 5 respectively). At day 6 of Ang II-infusing rat started to develop stable body weight that increased gradually until reaching 275 g at the end of the study (Figure 4.1B).

A

B

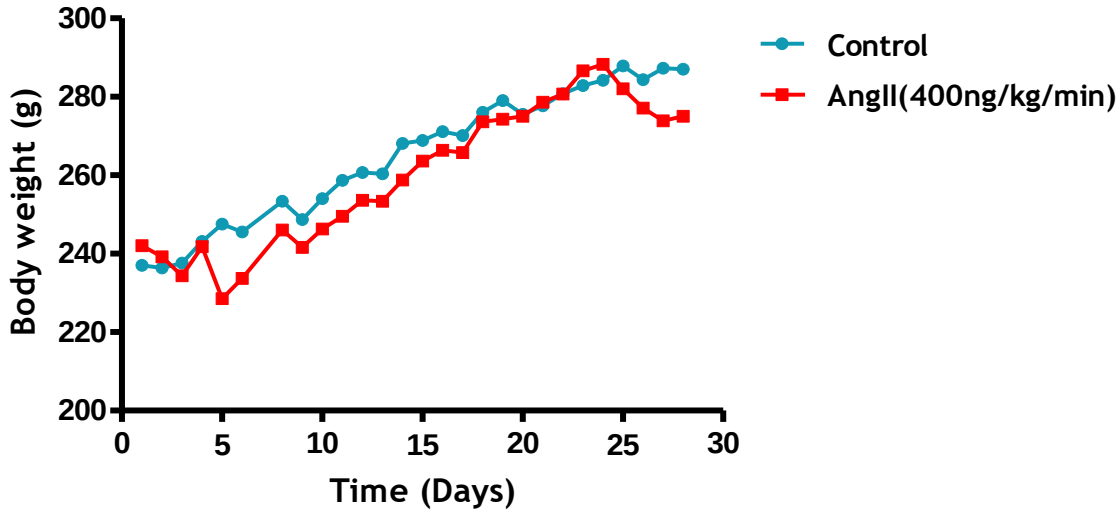

Figure 4.1 Evaluating the effect of (400 ng/kg/min) Ang II infusion on body weight of WKY.

(A) Representative image of subcutaneous osmotic minipump implantation. **(B)** Body weight for rats received either Ang II or saline (control) over 4 weeks, n=1 rat/group.

Blood pressure was also evaluated via tail-cuff plethysmography for the same rats mentioned above. Results showed that at baseline BP was 153.1 mmHg for control and 109.8 mmHg for Ang II assigned rats. Following one week of minipump implantation BP was slightly lower in the control rat (146.6 mmHg) and continue to decrease by time until reaching 125.4 mmHg at the 4th week. In contrast to control, BP was markedly increase in Ang II-infused rat (130.7 mmHg) after one week of minipump implantation and continue to gradually increases until become (206.1 mmHg) at week four of Ang II infusion (Figure 4.1.1).

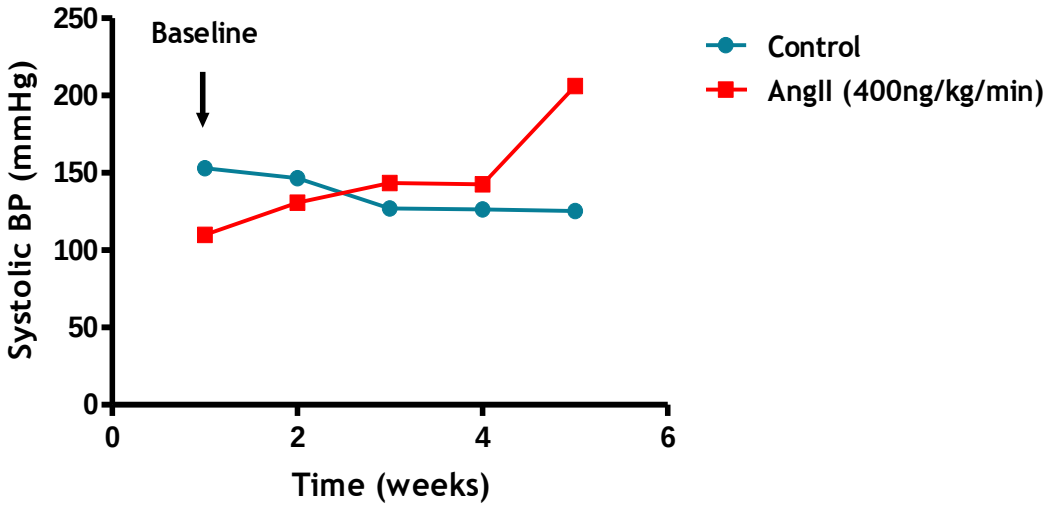

Figure 4.1.1 Assessment the effect of (400 ng/kg/min) Ang II infusion on BP of WKY.

BP at baseline (before surgery) and over 4 weeks for rats received osmotic minipump containing either normal saline(control) or Ang II, n=1 rat/group.

Heart weight and heart weight/body weight ratios were also assessed in rats receiving Ang II or normal saline (control). Results revealed that the heart weight for control was 0.93g and for Ang II rat was 1.01g. Similarly, the heart weight/body weight ratio was higher in Ang II-infused rat (0.37) in comparison to control (0.32) (Figure 4.1.2).

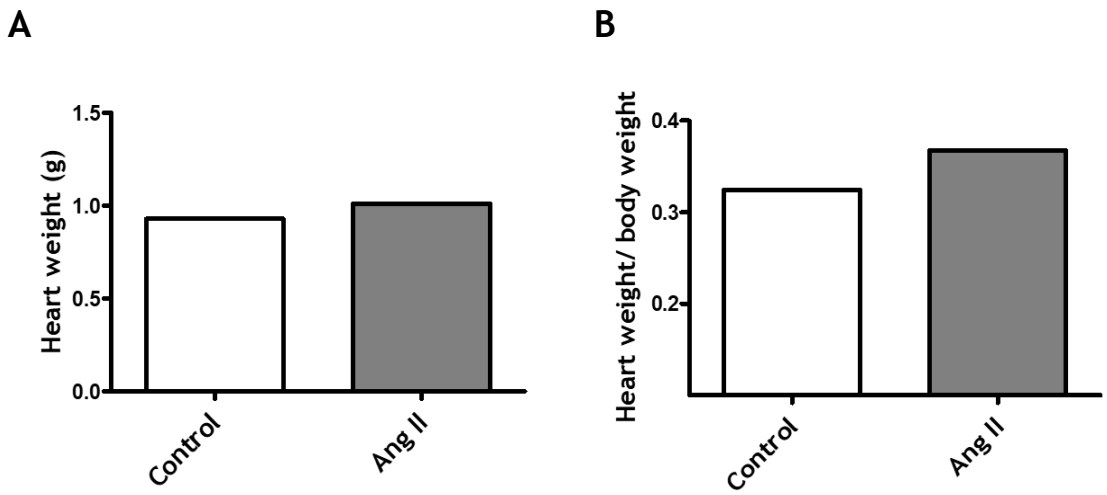

Figure 4.1.2 The effect of Ang II infusion of (400 ng/kg/min) on heart weight of WKY rats.

(A) Heart weight for rat received either Ang II over 4 weeks or control. **(B)** Heart weight/body weight ratio for the same rats, n=1 rat/group.

4.3.2 Determination of the efficiency of adenoviral-gene transfer of LacZ into WKY

The efficiency of human adenovirus serotype 5 to deliver LacZ gene (Ad-LacZ) into WKY rat was assessed as explained in (sections 2.5.3-2.5.4). Ad-LacZ ($1x10^{11}$ vp/animal) or saline were delivered via femoral vein injection. The rats also received saline via osmotic minipump (Figure 4.2A). Results indicated no change of liver's colour of the control group following X-gal staining for B-Galactosidase activity. However, Ad-LacZ group showed dark blue colour of the stained liver which indicated successful delivery of the virus (Figure 4.2B).

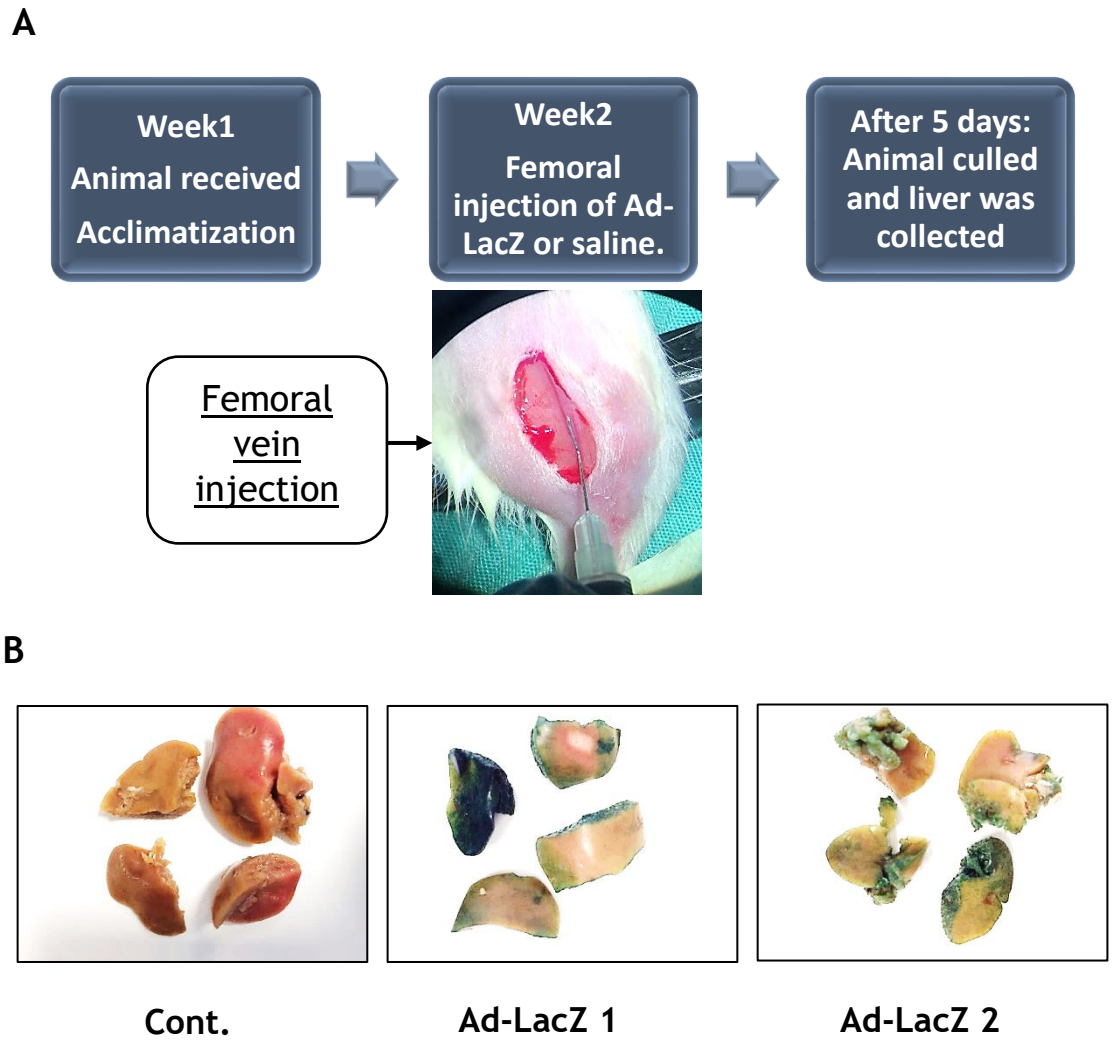

Figure 4.2: Assessment of the efficiency of adenoviral gene transfer of LacZ into WKY.

(A) Schematic representative of the plan for evaluating the efficiency of Ad-LacZ transduction. Rats left for a week for acclimatization and then received either Ad-LacZ or saline via femoral vein and monitored for 5 days. **(B)** Representative images of liver tissues stained for B-Galactosidase activity in each group**.** n=1-2/group.

4.3.3 Assessment of the effect of Ad-PRCP on Ang II-induced hypertension and cardiac structure and functional changes in WKY rats

12-week-old mail WKY rats were assigned randomly to receive either Ang II (400ng/kg/min) via osmotic minipump with or without Ad-PRCP or Ad-LacZ ($1x10^{11}$vp/animal), or) or receive normal saline (control) for 21 days (Figure 4.3).

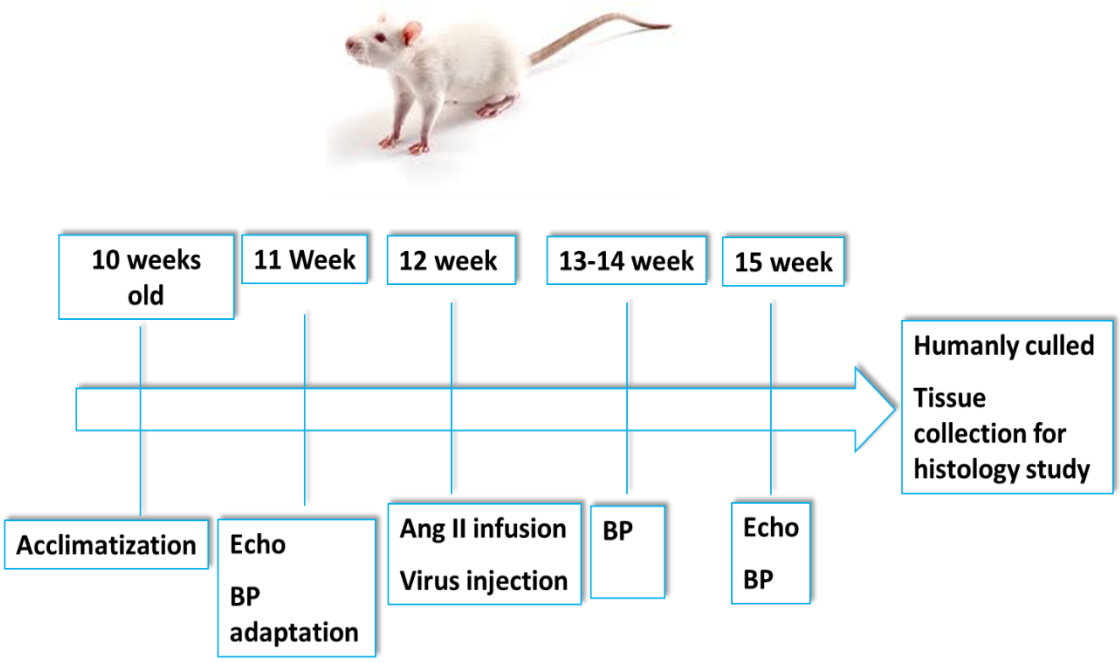

Figure 4.3 Schematic representative of the process for studying the role of Ad-PRCP on WKY rats following Ang II infusion.

Rats received Ang II subcutaneously via osmotic minipump implantation with or without Ad-LacZ or Ad-PRCP, via femoral vein, over 3 weeks. Control rats underwent the same surgical procedure but received normal saline via minipump or femoral vein injection. Blood pressure was measured at baseline (before surgery) and weekly via tail-cuff and echocardiography was performed at

baseline and before animals were humanely killed at the end of the study. After 3 weeks of Ang II infusion or adenovirus injection, the rats were humanely culled and tissues were collected for histological analysis.

4.3.4 Effect of PRCP overexpression on AngII-induced high blood pressure in WKY rats.

Systolic blood pressure was measured in rat groups as explained in (section 4.3.3). Results revealed that baseline BP was similar between groups with 106.1±4.4, 100.6±6, 100.1±7.6, and 110.8±6.2 mmHg for control, Ang II, Ad-LacZ, and Ad-PRCP groups, respectively. After 3 weeks, no significant different in BP of control group was reported (121.3±3.8 mmHg) compared to baseline. However, significant elevation of BP was observed after three weeks in Ang II group (158.5±5 mmHg) compared to baseline (p<0.001) and to control at 3 weeks (p<0.05). Similarly, Ang II infusion caused significantly higher BP in Ad-LacZ (150.4±14.3 mmHg) and Ad-PRCP (156.1±11.1 mmHg) in comparison to baseline (p<0.01) and to control at 3 weeks (p<0.05). However, there was no significant difference on systolic BP between groups after 3 weeks as shown by One Way ANOVA which suggested no effect of Ad-PRCP on Ang II-induced hypertension (Figure 4.4).

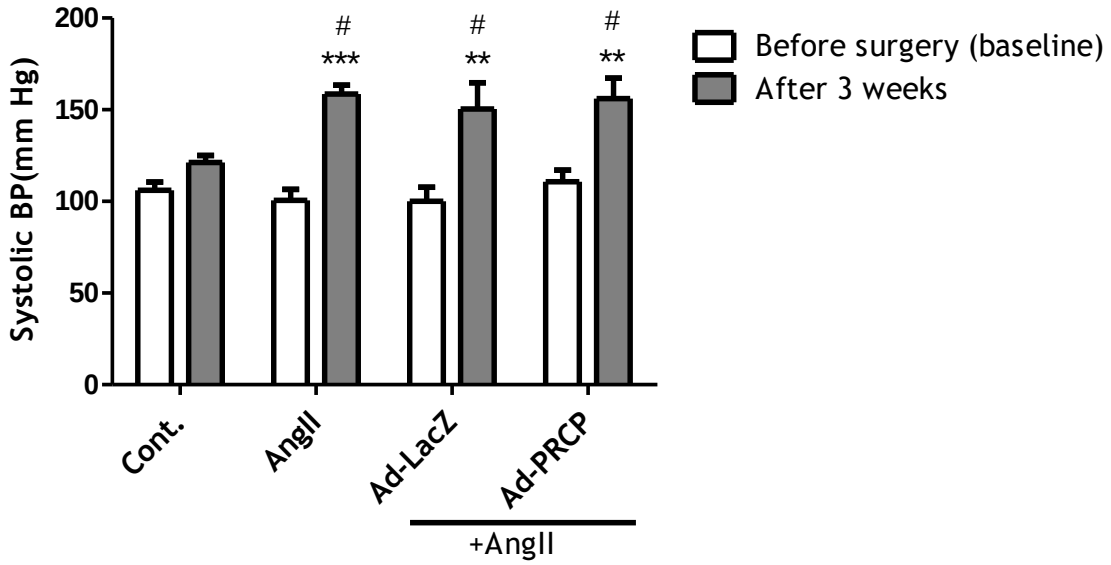

Figure 4.4 Evaluating the effect Ad-PRCP overexpression on Ang II-dependent hypertension.

Systolic blood pressure was measured at baseline and after 3 weeks via tail cuff plethysmography for each group of rats received Ang II alone or with Ad-LacZ or Ad-PRCP. Control group received normal saline. (n=5-8/group) *** $p<0.001$ vs **$p<0.01$ vs baseline, #$p<0.05$ vs control at 3 weeks.

4.3.5 Role of Ad-PRCP overexpression on Ang II-induced cardiac hypertrophy in vivo

In chapter three, it was indicated that PRCP might be protective against Ang II-induced cardiomyocyte hypertrophy *in vitro*. Here, the antihypertrophic effect of PRCP was assessed *in vivo*. After 3 weeks of Ang II infusion and/or adenoviral vector injection, rats were humanely culled via unrecovered anesthesia and hearts were collected and weighed immediately post culling (Figure 5.5A). Results showed heart weight for control group was (0.98±0.02g). Significantly higher heart weight was observed in Ang II group (1.14±0.07g) compared to control ($p<0.05$). Ad-LacZ and Ad-PRCP showed no significant difference in heart weight (1.018±0.03g and 1.08±0.04g, respectively) compared to control (Figure 5.5B).

Similarly, Heart weight/tibia length ratio analysis showed significantly greater values in Ang II group (0.29±0.01g) compared to control (0.24±0.01g) *(*$p<0.05$), but no significant changes were observed in Ad-LacZ (0.24±0.00g) or Ad-PRCP (0.26±0.00g) transduced groups compared to control or to Ang II only treated group (Figure 5.5C).

A

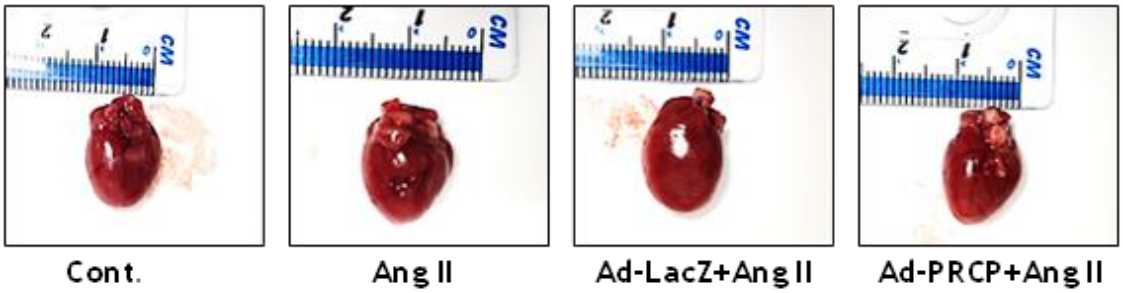
Cont.
Ang II
Ad-LacZ+Ang II
Ad-PRCP+Ang II

B

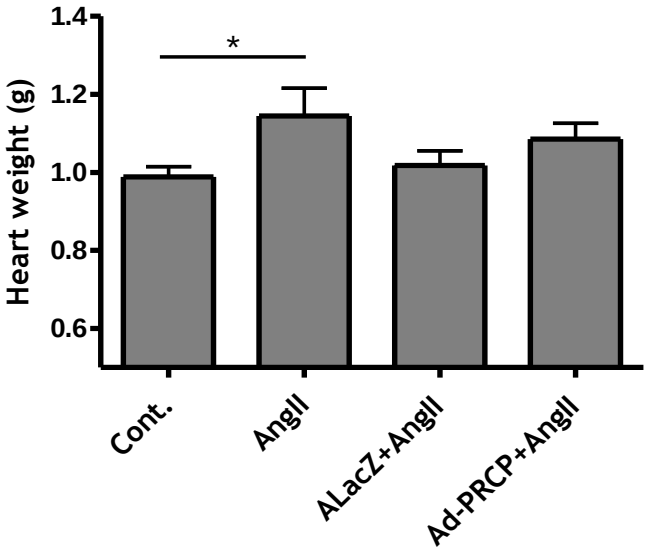
Heart weight (g)
1.4
1.2
1.0
0.8
0.6
*
Cont.
AngII
ALacZ+AngII
Ad-PRCP+AngII

C

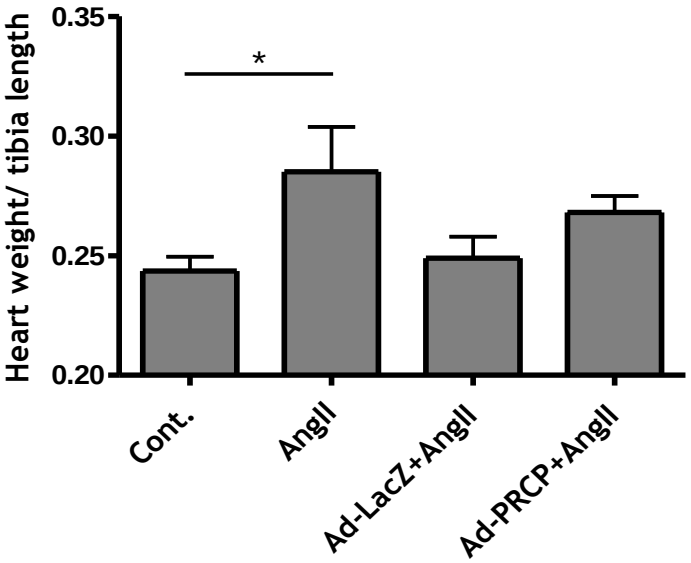
Heart weight/ tibia length
0.35
0.30
0.25
0.20
*
Cont.
AngII
Ad-LacZ+AngII
Ad-PRCP+AngII

Figure 4.5. Effect of Ad-PRCP on Ang II-induced cardiac hypertrophy.

(A) Representative heart images for the experimental groups (Control, Ang II, Ad-LacZ+Ang II, and Ad-PRCP+Ang II) **(B)** Heart weight for each group **(C)** Heart weight/tibia length ratio for each group. * $p<0.05$ vs Control, n=5-8 animal/group.

Following analysis whole heart hypertrophy, next the cardiomyocyte size was assessed via WGA staining of heart tissue sections (Figure 4.6A).

Results showed significantly higher cardiomyocytes surface area in Ang II infused group compared to control (562.6±27 μm^2 vs 475.4±23.9 μm^2 respectively $p<0.05$). No significant changes were observed in Ad-LacZ (453.0±24.3 μm^2) or Ad-PRCP (520.6± 31.5 μm^2) groups in comparison to control. n=5-8/group (Figure 4.6B).

A

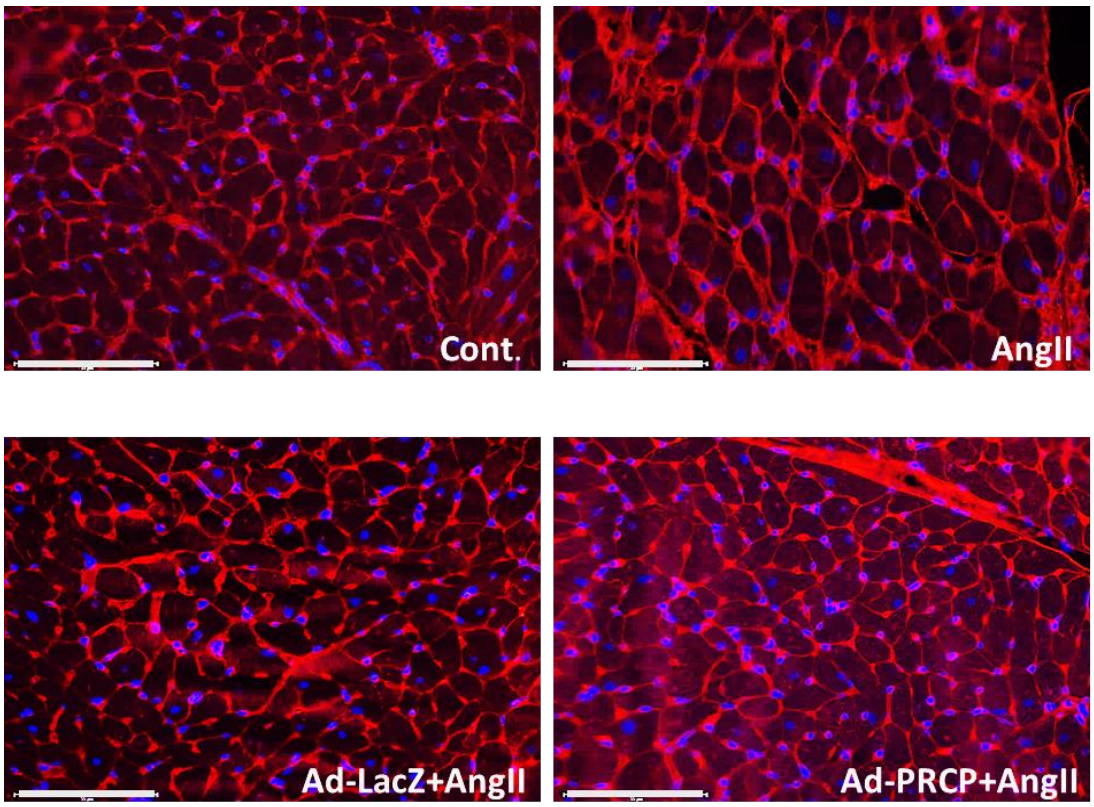

B

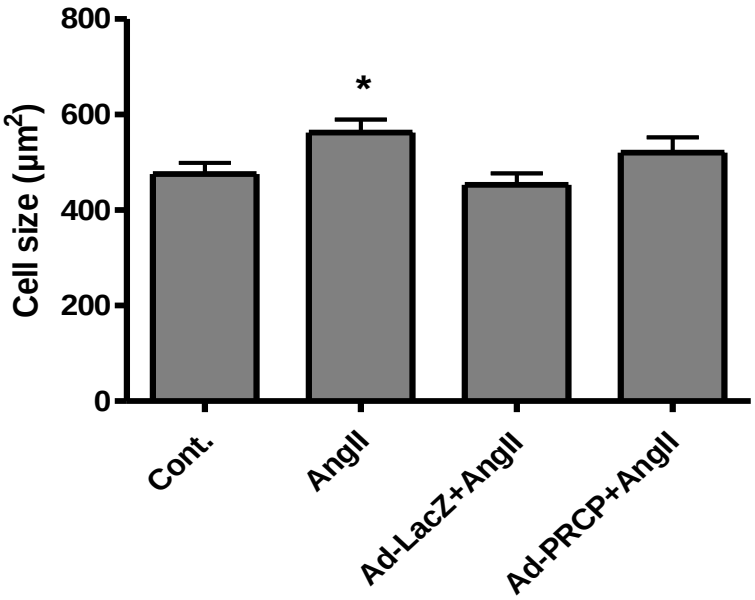

Figure 4.6 Histological assessment of Cardiomyocyte size.
(A) Representative Images for cardiomyocytes stained with WGA for experimental groups (Control, Ang II, Ad-LacZ+AngII, Ad-PRCP+AngII),20x magnification, Scale bar= 100µm (**B**) Measurement of cardiomyocyte cell surface area for each experimental group. *p<0.05 vs control. n=5-8 rats/group, 8 images per animal.

4.3.6 Assessment of PRCP overexpression on Ang II-induced myocardial fibrosis in WKY rats

To investigate whether Ad-PRCP is protective against Ang II-induced cardiac fibrosis, heart sections were stained with picrosirius red to quantify type I and type III collagen content (Figure 4.7A). Picrosirius red is a very common stain for detecting collagen fiber due to its ability to specifically isolate collagen contrast with linear polarizers on a brightfield microscope (Whittaker, Kloner, Boughner, & Pickering, 1994).

Quantifying of myocardium collagen showed significantly higher collagen content in Ang II (35.95 ±7.2 %) and Ad-LacZ (35.76± 9.3 %) rats compared to control (11.01± 2.4 %) $P<0.05$. However, it was observed that collagen contents were slightly, albeit non-significantly reduced in Ad-PRCP group (26.90±7.8 %), 3 images were analysed/animal (Figure 4.7B).

A

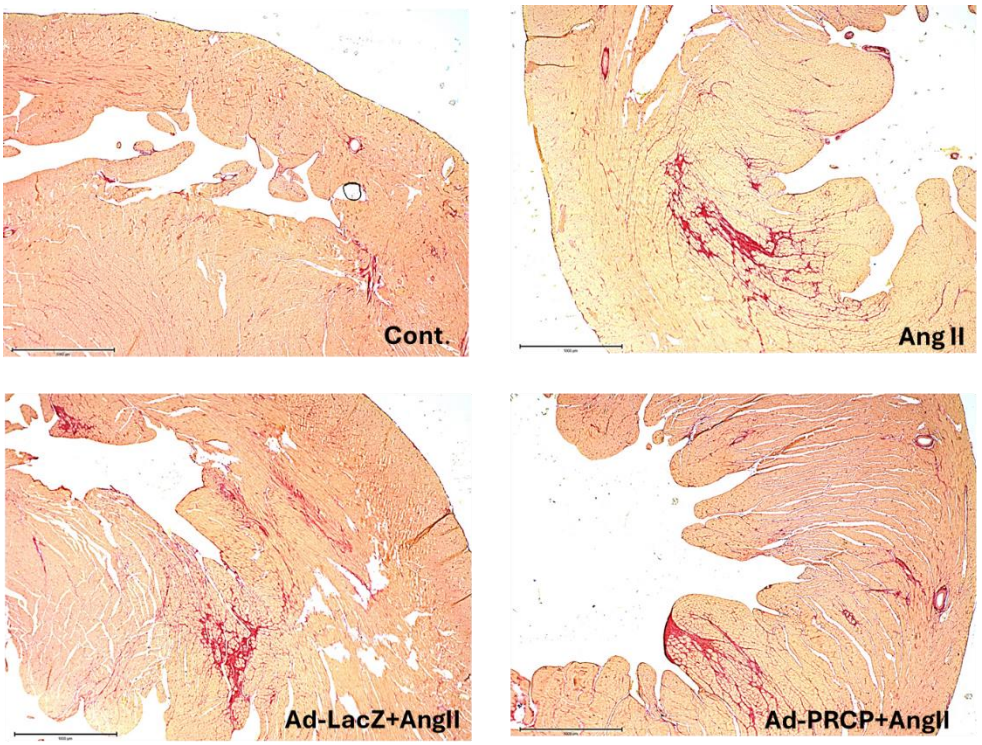

B

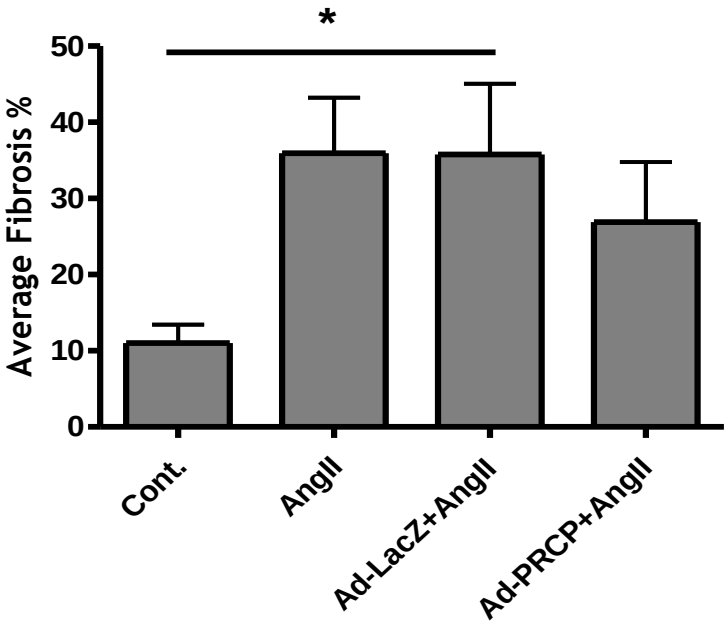

Figure 4.7 Analysis of cardiac fibrosis via picrosirius red staining for each experimental group.

(A) Representative images for heart sections stained with picrosirius red for each group, 4x magnification, Scale bar = 1000μm. **(B)** Analysis of fibrosis percentage for each group, *p<0.05 vs control.

4.3.7 Effect of PRCP overexpression on cardiac function in response to Ang II infusion in WKY rats

Assessment of heart function was performed via echocardiography. 2D M-mode images were captured for each animal as shown in Figure 4.8 A. A Paired t-test was used to compare the EF % values for each individual animal within the same group at baseline vs after three weeks of treatment. The result showed no significant changes (p>0.05) in EF % values between baseline and after 3 weeks in control group (88.62 ± 2.4 vs 87.3 ± 2.1), in Ang II group (92.75 ± 3.0 vs 80.81 ± 1.8), in Ad-LacZ group (93.99 ± 2.0 vs 89.97 ± 2.6), and in Ad-PRCP group (92.28 ± 1.7 vs 95.06 ± 1.9). Analysis by One-Way ANOVA comparing the different groups after 3 weeks revealed that the EF % of the Ad-PRCP group was significantly higher (p<0.01) in comparison to the Ang II group. There were no significant differences between other groups at the 3 week time point (Figure 4.8B).

A

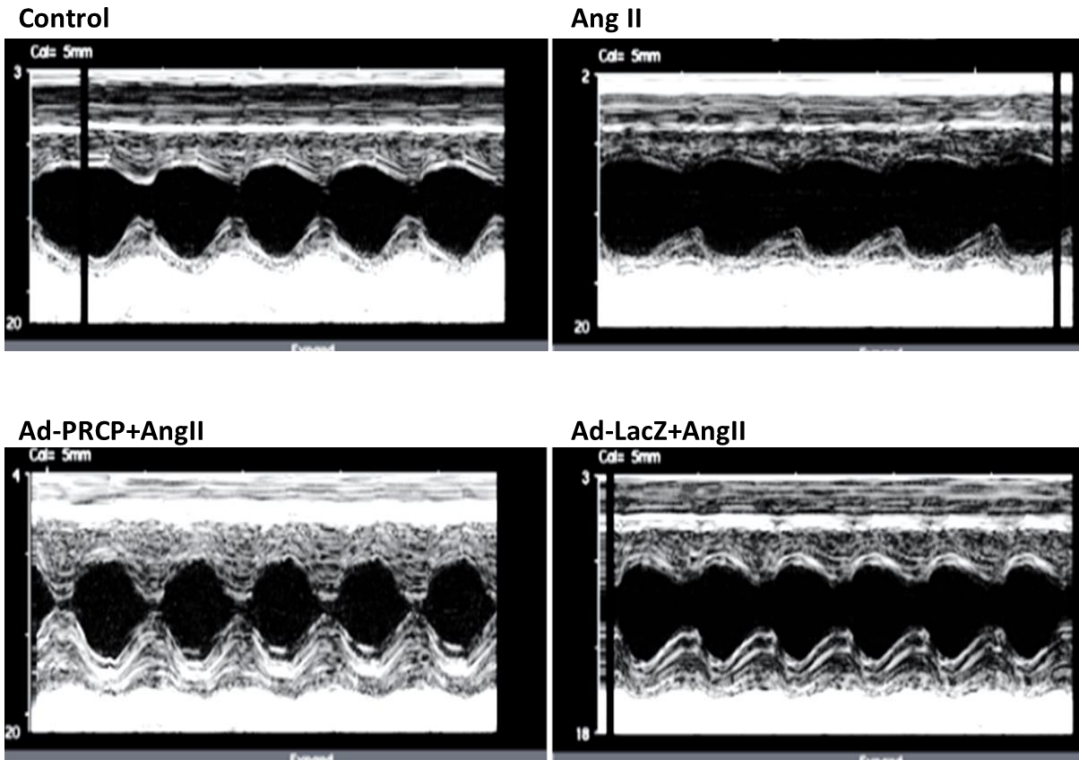

B

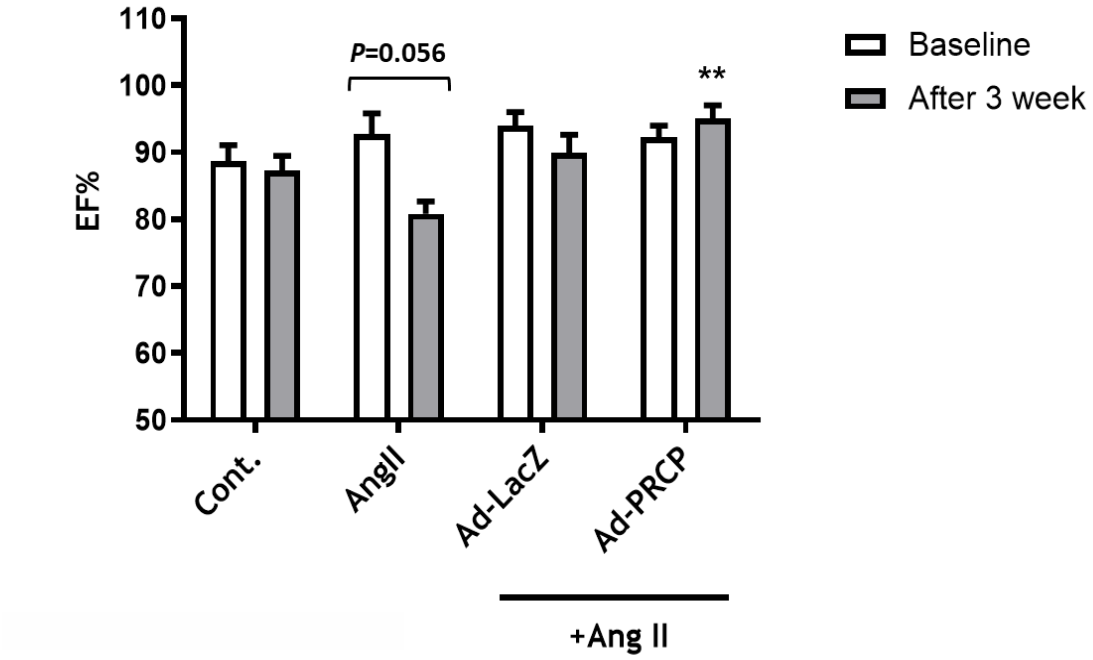

Figure 4.8 Role of Ad-PRCP overexpression on EF% following Ang II infusion

(A) Representative 2D m-mode images for experimental groups after 3 weeks of Ang II infusion and/or virus injection. **(B)** Ejection fraction % (EF%) at baseline and after 3 weeks for each group. Paired t-test (two-tailed) was used to compare values within each individual group between baseline and after 3 weeks. One-way ANOVA with Bonferroni post-hoc test was used to compare values after 3 weeks across different treated groups. ***P*<0.01 vs Ang II at 3 weeks, n=5-8/group.

A paired T test also showed no significant FS % values for each animal within each group at baseline vs after 3 weeks in control group (53.1 ± 4 vs 50.6 ± 2.4), in the Ang II group (60.95 ± 6.0 vs 42.6 ± 1.718), in the Ad-LacZ group (61.75 ± 4.151 vs 55.4 ± 4.5), and in the Ad-PRCP group (58.40 ± 3.2 vs 66.0 ± 4.357). However, One-way ANOVA analysis after 3 weeks showed significantly greater (p<0.001) FS % in the Ad-PRCP group compared to the Ang II group, Figure 4.9.

(Figure 4.9)

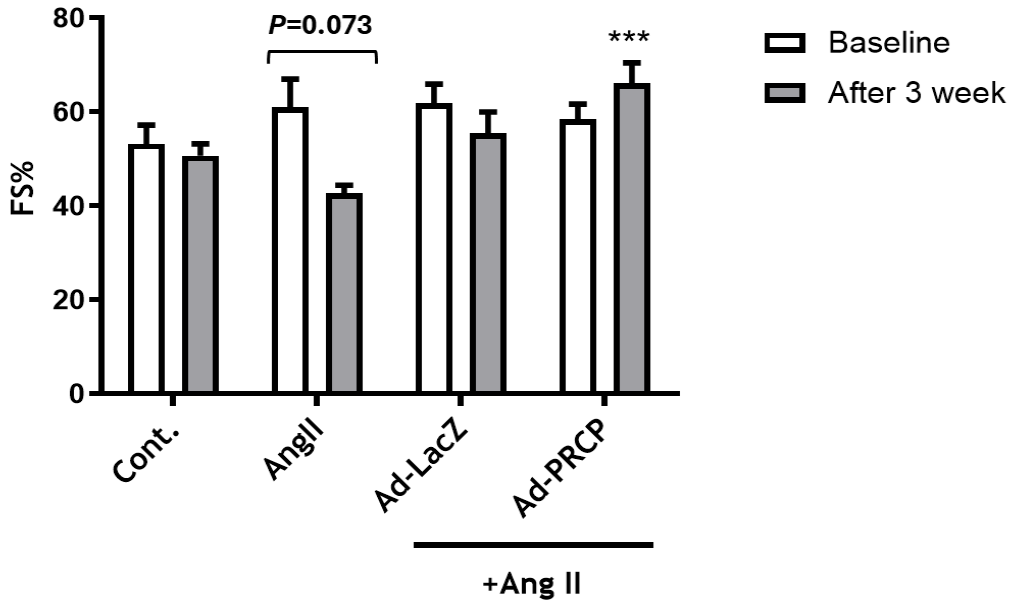

Figure 4.9 Role of Ad-PRCP overexpression on FS% following Ang II infusion.

FS% for each experimental group at baseline and after 3 weeks. Two-tailed paired t-test was performed to compare values within each individual group at baseline vs after 3 weeks. One-Way ANOVA with Bonferroni post-hoc analysis was used to compare values after 3 weeks across different treated groups. ***P<0.001 vs Ang II at 3 weeks, n=5-8/group.

4.3.8 Assessment of cardiac output for experimental group

Evaluating cardiac output revealed no significant changes between groups after 3 weeks as the mean values were: (66.50±8.1mL, 60.10±10.1mL, 53.54±5.6mL, and 55.53±5.3mL) for control, Ang II, Ad-LacZ, and Ad-PRCP, respectively. (Figure 4.10).

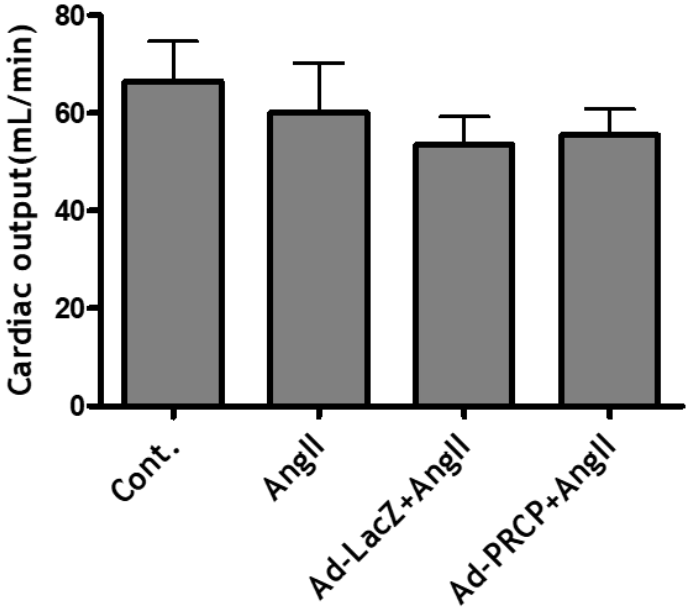

Figure 4.10 Effect of Ad-PRCP on cardiac output in Ang II-infused WKY rats.

Cardiac output analysis after 3 weeks for each experimental group. n=5-8/group.

4.3.9 Assessment of left ventricular mass (LVM) via echocardiography for the experimental groups.

Further echocardiography analysis for LVM/tibia length after 3 weeks of treatment showed significantly greater ratio in Ang II group (14.52±0.4) compared to control (11.12±0.9). No marked change was observed in Ad-LacZ

group (11.73±1.5) compared to control. LVM/tibia length for Ad-PRCP group (13.04±0.9) did not significantly change compared to control (Figure 4.11).

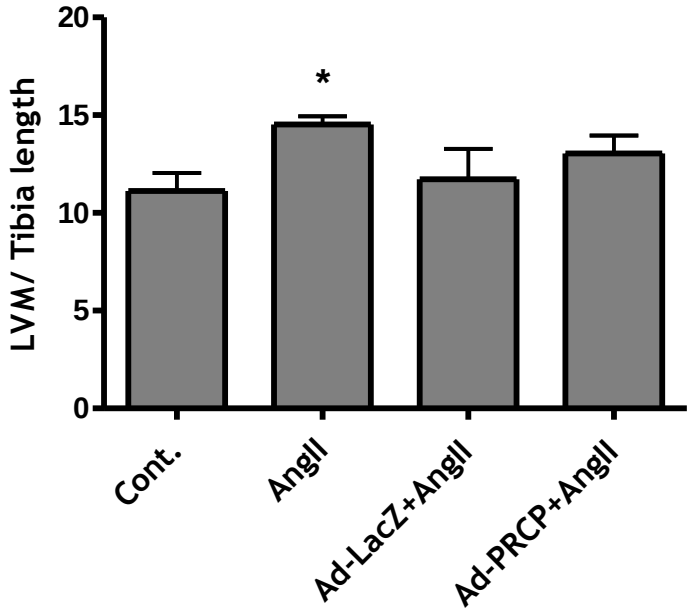

Figure 4.11 Assess the role of PRCP overexpression in Ang II-induced LV hypertrophy in WKY rats.

Analysis of left ventricular mass/tibia length ratio for each group. *P<0.05 vs control, n=5-8/group.

4.3.10 Assessment ANP mRNA expression in rat hearts for the experimental groups.

mRNA gene expression of ANP was analysed via TaqMan for each group. Results showed no significant changes in myocardium ANP gene expression in Ang II group (6.85±4.2 Fold change) compared to control (1.1±0.17). Similarly, ANP gene expression in Ad-LacZ group (4.39±2.8 fold change) and in Ad-PRCP group

(2.76±1.3 fold change) were not significantly different in comparison to control (Figure 4.12).

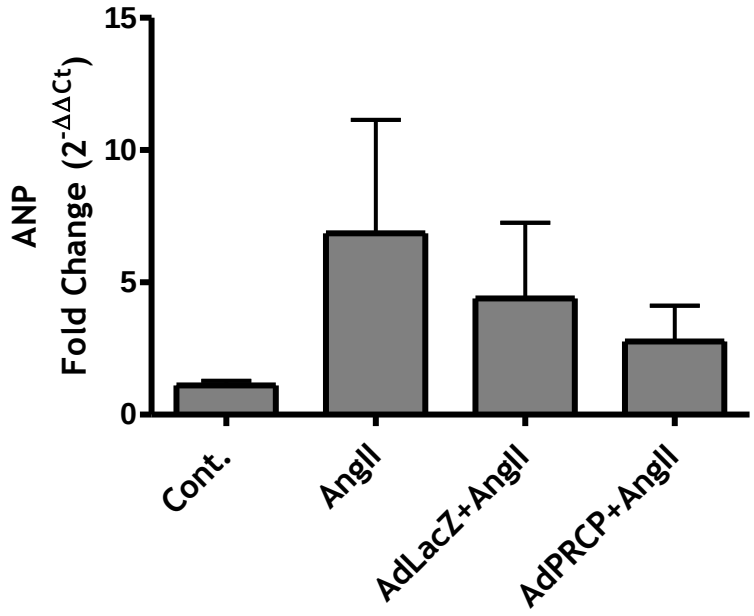

Figure 4.12 Evaluating mRNA expression of ANP in the heart tissues for the experimental group.

ANP gene expression was assessed via TaqMan gene expression assay for each group, n=5-8/group.

4.3.11 Effect of Ad-PRCP on RAS receptors expression in heart tissues following Ang II infusion

AT_1R gene expression for Ang II group was (1.86±1.0-fold change), and for Ad-LacZ was (1.80±0.5-fold change), and for Ad-PRCP was (1.15±0.2 fold change). However, none of these values were significantly different from control (1±0.1) Figure 4.13A.

Analysis of MasR gene expression in heart tissues also revealed no significant change between groups compared to control: (1.37±0.2, 1.65±0.4, and

1.191±0.3-fold change) for Ang II, Ad-LacZ, and Ad-PRCP groups respectively, compared to control (1.0±0.1) Figure 4.13B.

PRCP gene expression was also assessed in myocardial tissues and showed that Ang II (1.05±0.1 fold change), Ad-LacZ (1.16±0.5 fold change), and Ad-PRCP (0.86±0.07 fold change), compared to control. However, these values were not significantly different from control (1.0±0.1) Figure 4.13C.

A

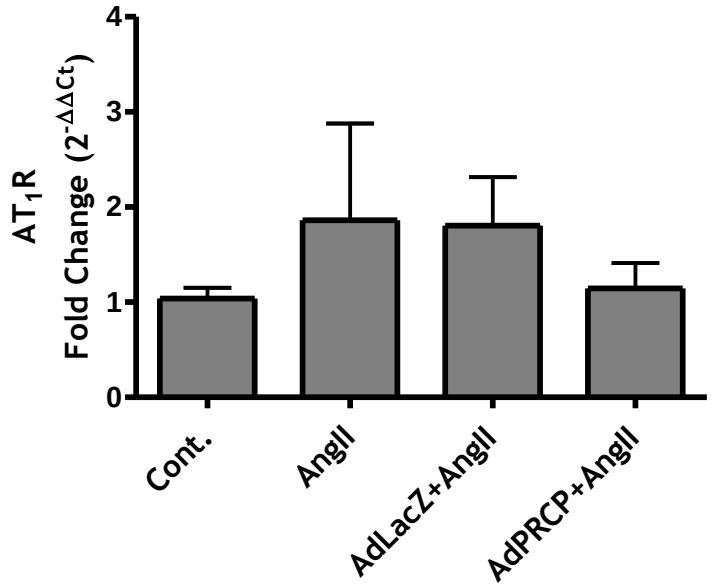

B

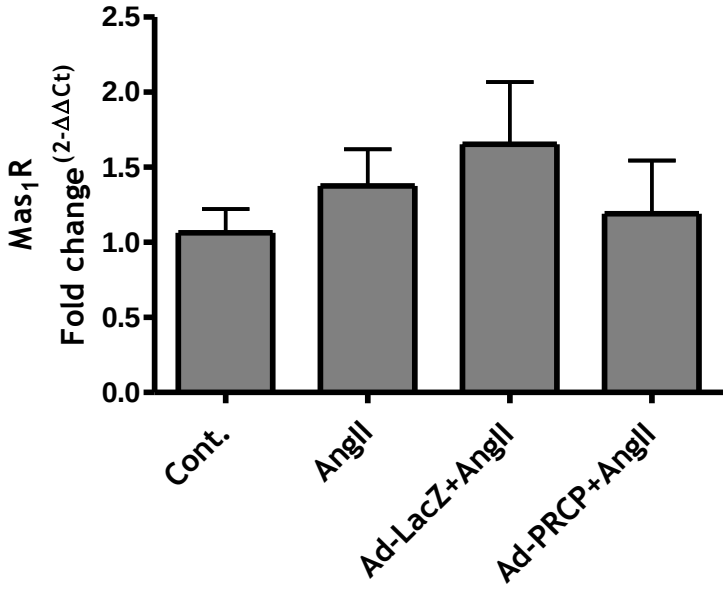

C

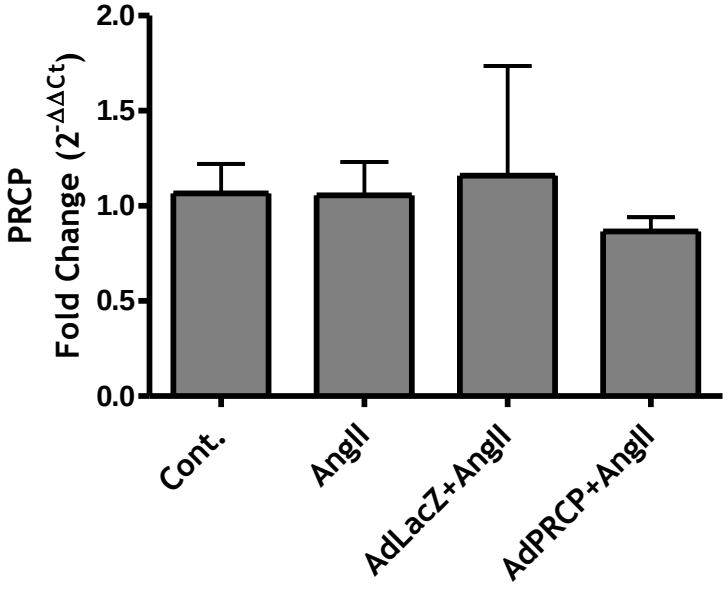

Figure 4.13 Assessment of RAS gene expression in heart tissues

(A) Analysis of AT_1R gene expression for each group. (B) Analysis of Mas1 receptors gene expression for each group (C) Analysis of PRCP gene expression for each group. n=5-8/group.

4.3.12 Assessment of TGFβ1 mRNA expression in heart tissues of the experimental groups

Analysis of TGFB1 gene in expression showed no significant change in Ang II (1.18±0.06 fold change), Ad-LacZ (1.2±0.17 fold change), or Ad-PRCP (1.32±0.12 fold change) groups in comparison to control.

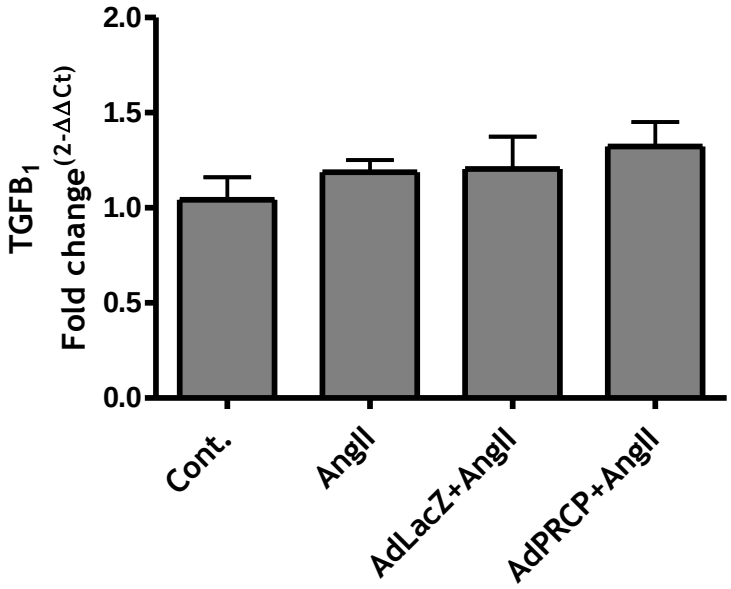

Figure 4.14 Evaluating TGFβ1 gene expression in heart tissues of WKY rats.

Analysis of Transforming Growth Factor Beta 1 (TGFβ1) gene expression in heart tissues for each group. n=5-8/group.

4.4 Discussion

In the previous chapter, an adenoviral vector to express rat prolylcarboxypeptidase was generated and its protective effects against Ang II-induced cardiomyocyte hypertrophy *in vitro* was assessed. In this chapter these studies were expanded to assess the role of PRCP overexpression after intravenous delivery of Ad-PRCP on blood pressure and cardiac functional and structural changes resulting from chronic exposure to Ang II *in vivo*. First, a tolerated dose of Ang II was determined for Wistar Kyoto rat via monitoring blood pressure and body weight for a single rat received continuous infusion of 400ng/kg/min Ang II over 28 days following subcutaneous implantation of an osmotic mini pump. Ang II-infused rats showed a marked elevation in blood pressure over time, stable body weight as well as increased heart weight/body weight ratio compared to vehicle infused rats. These data suggested that the selected dose was effective and well tolerated in WKY rats. This data agreed with a previous study that reported significantly higher systolic arterial pressure response in male Wistar rats after seven days and fourteen days of continuous infusion of similar dose of Ang II (400 ng/kg/min) (Ceravolo et al., 2014). Losartan, AT_1R antagonist, was effective in reducing the high blood pressure resulting from Ang II-infusion (Ceravolo et al., 2014).

However, using higher Ang II dose e.g. 500ng/kg/min, might have put the rats at high risk of losing significant body weight, as for example it has been reported that they can lose up to 26% body weight, within the 1^{st} week of Ang II infusion (Brink, Wellen, & Delafontaine, 1996). That level of body weight loss is considered a sign for dose intolerance and ill health. In addition, it would also surpass the limit of the body weight loss allowed within the project license for this work. However, using lower doses of Ang II e.g 200ng/kg/min, might not produce the expected cardiovascular response to Ang II in WKY rats within specific time as this dose was prescribed as a non-pressor dose in some studies (Sugawara et al., 2021; Szabó et al., 2004).

Second, the therapeutic adenoviral vector dose was also optimized by delivering $1x10^{11}$ vp/animal of control virus, Ad-LacZ, via femoral vein for five days. Histological analysis of the liver showed successful delivery of safe and effective adenovirus dose as indicated by blue staining. Intravenous administration of adenoviral vectors is widely accepted to result in the majority of transgene

expression being found in the liver, the major site of adenoviral sequestration (Smith, Tian, Lozier, & Byrnes, 2004). The technique uses the bacterial (*Escherichia coli*) LacZ gene which encodes ß-galactosidsae enzyme. Staining with X-gal (5-bromo-4-chloro-3-indolyl-beta-D-galactopyranoside) produces galactose and 5-bromo-4-chloro-3-hydroxyindole when cleaved by the ß-galactosidase enzyme (Burn, 2012). The second compound is then undergo oxidation reaction to form the final stable precipitate in blue colour (Cooper & Zhou, 2013). Thus, ß-galactosidsae staining of liver is used as an indicator for successful delivery of the adenoviral vector (Z. Zhong et al., 2002). In the work presented here, the expression of X-gal stain was detected robustly in all rats received Ad-LacZ. There was no expression detected in control rat. Therefore, the exact expression levels were not measured as it was only one adenoviral dosage used in this experiment. It has been well known that higher doses of adenoviral vectors may lead to immediate activation of the innate and adaptive immune system and can cause dose-dependent toxicity in rodent models (Varnavski, Calcedo, Bove, Gao, & Wilson, 2005), which may lead to death within minutes to hours. Interestingly, the systemic administration route of adenoviral vectors into animals, particularly rats, might play a role in virus-mediated toxicity and mortality (Boquet, Wonganan, Dekker, & Croyle, 2008). Tail vein injection of human adenoviral vector serotype 5 (Ad-lacZ) was associated with a significant mortality rate with up to forty two percent in comparison to a catheter surgically implanted in the jugular vein of Sprague Dawley rats (Boquet et al., 2008). In this published study all deaths of the rats happened within four hours of tail vein viral injection (Boquet et al., 2008). Thus, it was decided that as the dose of Ad (1x10e11 vp) chosen in our study was safely administered via femoral vein and well tolerated in the rats, this dose was selected for the therapeutic study.

Following determination of effective and safe doses of Ang II and adenoviral vector, rats were randomly assigned into 4 groups: control (vehicle), AngII, Ad-PRCP+AngII, and Ad-LacZ+AngII. Results showed significantly higher blood pressure at week 3 in all groups receiving Ang II compared to baseline and to control vehicle group. No marked effect for Ad-PRCP overexpression on blood pressure was observed in this work. There is very limited data regarding the effect of PRCP overexpression on blood pressure *in vivo*. Some available studies

indicated that overexpression of PRCP via adenoviral vector in male Wistar rats did not affect heart rate nor the mean arterial pressure after ischemic/reperfusion injury (Hao et al., 2020). Some studies reported marked drop in blood pressure in PRCP $^{gt/gt}$ mice compared to WT mice (Adams et al., 2011; Maier, Schadock, Haber, Wysocki, Ye, Kanwar, Flask, Yu, Hoit, et al., 2017), but the differences in blood pressure between the two groups was no longer observed after Ang II infusion (Maier, Schadock, Haber, Wysocki, Ye, Kanwar, Flask, Yu, Hoit, et al., 2017). However, the renin angiotensin system plays a pivotal role in regulating blood pressure, and PRCP belongs to the counter regulatory axis of the RAS (Sachetelli et al., 2006). It has been previously reported that chronic infusion of Ang-(1-7) , for 4 weeks, into Sprague-Dawley rats did not affect basal blood pressure nor attenuated the Ang II-induced hypertension despite being protective against Ang II-dependent cardiac hypertrophy (Guo et al., 2017). In addition, ACE2 also can degrade Ang II into the cardioprotective Ang-(1-7) (Basu et al., 2017). However, while there are some data suggested reduced blood pressure in response to recombinant human ACE2 (rhACE2) within six minutes of Ang II infusion and stabilized after 18 minutes in rodent model (Lo et al., 2013), ACE2 knockout mice showed similar blood pressure response to wild type group after 4 week of Ang II infusion despite exhibiting marked cardiac functional and structural changes between groups (Alghamri et al., 2013). Moreover, Ang-(1-9), is another cardioprotective peptide that also belongs to the counter regulatory axis of RAS, which has also shown no beneficial effect on blood pressure after chronic infusion via osmotic minipump into stroke-prone spontaneously hypertensive rats despite mediating an antifibrotic effect on the heart (Flores-Munoz et al., 2012). Grobe et al reported that infusion of Ang-(1-7) provided significant reduction in myocyte hypertrophy and interstitial fibrosis without marked change on blood pressure (J. L. Grobe et al., 2007). Therefore, activation of counter regulatory RAS does not always lead to reduction in blood pressure, even when reduction in tissue remodelling is observed. PRCP contributes to blood pressure regulation via two mechanisms; converting Ang II into the protective peptide Ang-(1-7), and activating plasma prekallikrein causing liberation of bradykinin, that can then act as a vasodilator, via increasing NO bioavailability from high molecular weight kininogen(J. Wang et al., 2014). However, the exact mechanism on how PRCP

might regulate blood pressure through the kallikrein/kinin system is not yet well understood.

In chapter three of this current study PRCP overexpression diminished Ang II-induced cardiomyocyte hypertrophy *in vitro*. Here, Ang II induced significant cardiac hypertrophy as shown by heart weight/tibia length. However, both Ad-PRCP and Ad-LacZ groups were not significantly different from control. Similarly, cardiomyocyte cell size analysis revealed higher cell surface area in Ang II group, but not in Ad-PRCP or Ad-LacZ groups, compared to vehicle. Left ventricular mass normalized to tibia length also showed greater values in Ang II infused animal, but not Ad-PRCP or Ad-LacZ groups, compared to vehicle. These data suggested that there might be limited effects of Ad-PRCP overexpression on minimizing the hypertrophic effect of Ang II. Additionally, the control vector Ad-LacZ produced almost similar effects to Ad-PRCP, made it challenging for these data to be explained. Further work to increase group sizes and to also consider delivering PRCP via adeno-associated virus serotype 9 mediated gene transfer to achieve direct gene delivery to the heart may affect cardiac remodelling more effectively. Overexpression of PRCP via adenoviral vector (Ad-PRCP) has been shown to be effective in reducing infarct size in male SPF Wistar rats with ischemia/reperfusion injury (Hao et al., 2020). This protective effect was mediating via increasing myocardial Ang-(1-7) and bradykinin-(1-9) and reducing Ang II levels (Hao et al., 2020). LV fractional shorting was significantly reduced after ischemia/ reperfusion injury and Ad-PRCP significantly enhanced fractional shortening in comparison to Ad-Control rats (Hao et al., 2020). Furthermore, left ventricular hypertrophy has been reported previously in PRCP deficient mice at baseline compared to WT mice, however, this effect was no longer significant between groups after chronic Ang II infusion (Maier, Schadock, Haber, Wysocki, Ye, Kanwar, Flask, Yu, Hoit, et al., 2017). Some enzymes of the counter regulatory axis of RAS have been shown to be effective in reducing cardiac hypertrophy in vivo, for example through ACE2 activity generating the protective peptide Ang-(1-7) (Basu et al., 2017; Y. Li et al., 2009). However, Ang-(1-9) did not elicit an antihypertrophic effect in stroke-prone spontaneously hypertensive rats (Flores-Munoz et al., 2012) over 4 week of Ang-(1-9) treatment. It is also possible that the adenoviral dose of PRCP might not be high enough to promote antihypertrophic effects in the heart of WKY rats especially when considering

the high dose of Ang II infusion. For instance, a dose of $1x10^9$ pfu of Ad-ACE2 was delivered directly via intramyocardial injection into Wistar Kyoto rats and shown to be protective against left ventricular dysfunction and remodelling resulting from myocardial infarction (Y. X. Zhao et al., 2010).

Baseline cardiac ejection fraction and fractional shortening were similar to the end point (after 3 weeks) within the same group. However, after 3 weeks of Ang II infusion or/and viral injection, echocardiography data analysis revealed that left ventricular ejection fraction was significantly reduced in Ang II infused animals in comparison to Ad-PRCP group. Similarly, fractional shortening was significantly reduced in the Ang II group compared to Ad-PRCP group after 3 weeks. These data suggested that PRCP overexpression via adenoviral gene transfer showed some potential protective effect in WKY rats against Ang II-induced impaired cardiac function. However, considering that EF% and FS% did not change significantly in Ang II group at 3 week time point compared to baseline and to control, it is suggested that cardiac dysfunction did not occur in these animals, and further studies are needed to reach a final conclusion. A previous study suggested impaired cardiac function in KST302-derived *prcp* $^{gt/gt}$ mice, housed for 6 months, as shown by significantly reduced LV fractional shortening compared to WT mice (Maier, Schadock, Haber, Wysocki, Ye, Kanwar, Flask, Yu, Hoit, et al., 2017). In a previous report overexpression of PRCP via adenoviral vector-mediated gene transfer injected into tail vein of SPF Wistar rats improved left ventricular fractional shortening following myocardial ischemia/reperfusion injury (Hao et al., 2020). Knockdown of PRCP via adenoviral vector carrying shRNA led to further reduction in fractional shortening compared with the sham control rats (Hao et al., 2020). Moreover, left ventricular function assessed by left ventricular systolic pressure (LVSP) and left ventricular end diastolic pressure (LVEDP) was significantly improved in response to PRCP overexpression following myocardial I/R injury compared to control adenovirus which came in agreement with the study presented here that delivery of PRCP via adenoviral vector is effective in improving cardiac function in response to different pathological stimuli (Hao et al., 2020). Another RAS protective enzyme, ACE2, has also promoted significant improvement in cardiac function after myocardial infarction in WKY rats (Y. X. Zhao et al., 2010). Overexpression of ACE2 via adenoviral vector-mediated gene

transfer (Ad-ACE2) injected directly into the myocardium (intramyocardial) with a dose of 1×10^9 pfu showed higher left ventricular ejection fraction and reduced left ventricular volumes as well as decreased expression of Ang II, collagen I and ACE in the myocardium compared to the control group (Y. X. Zhao et al., 2010). As both ACE2 and PRCP degrade Ang II to Ang-(1-7), this data (Y. X. Zhao et al., 2010) might agree with the results presented here in this chapter in regard of the protective effect of Ang-(1-7) against Ang II-induced cardiac dysfunction and fibrosis. Exogenous Ang-(1–7) injection improved the heart function and remodelling of the left ventricle in mice with 5/6 nephrectomy (NC) and minimized cardiac interstitial fibrosis (Y. Li et al., 2009). Therefore, in future work measuring Ang-(1-7) in the heart following Ad-PRCP injection and Ang II infusion might be beneficial in providing more information about the underlying mechanism of PRCP.

In order to assess the role of Ad-PRCP overexpression on cardiac fibrosis resulting from chronic Ang II infusion, cardiac sections were stained with picrosirius red and collagen content quantified by image analysis. The data revealed significantly greater collagen content in Ang II infused group and in Ad-LacZ group in comparison to control vehicle group. In contrast, Ad-PRCP transduced rats showed no significant difference in collagen content in comparison to control vehicle group. However, since there were no significant differences in cardiac fibrosis between all groups received Ang II, it was challenging to conclude that PRCP exerted antifibrotic effect.

However, it has been previously reported that PRCP is protective against cardiac fibrosis via degrading Ang II in the myocardium (Nguyen et al., 2023). Furthermore, Ang-(1-7) could alleviate cardiac fibrosis and remodelling mediated via Ang II (J. L. Grobe et al., 2007). Since PRCP metabolises Ang II to Ang-(1-7) it is plausible that the antifibrotic effect might be achieved via this mechanism. It was previously reported that Ad-ACE2 significantly reduced cardiac fibrosis in WKY rat model of myocardial infarction and that Ang-(1-7) antagonist, A779, abolished the therapeutic effect of Ad-ACE2 (Y. X. Zhao et al., 2010). In the study presented here, Ang-(1-7) level was not measured and the effect of its antagonist was not studied. Hao et al suggested another mechanism of the cardioprotective effect of PRCP which is via upregulation of bradykinin-(1–9) in

the myocardium of SPF Wistar rats with ischemic/reperfusion injury (Hao et al., 2020).

Renin angiotensin system receptors were assessed in this project to further understand the effects of PRCP delivery. It has been reported that Ang II-induced cardiac hypertrophy and remodelling effects are mediated mainly via AT_1R (Baker & Dostal, 1992). Some studies indicated that Ang II infusion into Sprague-Dawley rats led to increased AT_1R expression (Zhuo et al., 2002). However, in the study here, no significant change in AT_1R expression was observed between groups so that it was not possible to determine the role of PRCP on regulating this receptor. It was previously reported that PRCP gene trap ($^{gt/gt}$) mice (generated by microinjecting embryonic stem cell line GST090 into blastocysts of 129P2/OlaHsd mice and transplanting these cells into pseudo pregnant C57BL/6 foster mothers) showed no significant change in AT_1R mRNA expression in both the heart and kidney compared to WT (Maier, Schadock, Haber, Wysocki, Ye, Kanwar, Flask, Yu, Hoit, et al., 2017).

It has been also known that Mas receptor mediates the cardio protective effect of Ang-(1-7) (L. Lin et al., 2016), and therefore its expression was assessed in this study. However, MasR was detectable in all experimental groups, but no significant change was observed between groups. Maier et al reported no significant different in MasR gene expression between $PRCP^{gt/gt}$ mice and WT mice in the heart and the kidney (Maier, Schadock, Haber, Wysocki, Ye, Kanwar, Flask, Yu, Hoit, et al., 2017).

Atrial natriuretic peptide (ANP) expressing cells increases markedly when the ventricle is pressure loaded and hypertrophied such as the case of chronic hypertension (Kessler-Icekson et al., 2002) or during hypoxia (Pfeifer et al., 1997). Therefore, ANP is considered an important marker for cardiac hypertrophy and heart failure (Langenickel, Pagel, Hӧhnel, Dietz, & Willenbrock, 2000) . In the study of this chapter, ANP mRNA gene expression was measured but showed no significant changes between groups despite the hypertrophy effect of Ang II. This observation needs further investigation.

1.6 4.5 Limitation of the study

The initial number of animals participated in this project was 32 rats with 8 animal/group. However, this number was reduced due to several deaths and due

to changing the adenoviral dose after toxicity observed in the first batch of animals. Having multiple lockdowns due to the pandemic meant there was insufficient time for further studies. It is important to mention that the power estimation and sample size were not performed in advance for this work. Thus, it is plausible that the study conducted here is not sufficiently powered to prevent type I error (occurs when the null hypothesis is incorrectly rejected which lead to a false-positive result) and type II error (occurs when the null hypothesis is incorrectly accepted causes a false-negative result) (Columb & Atkinson, 2016). Prior power calculation is used to estimate the probability of correctly rejected the null hypothesis (when the null hypothesis is falls) in a larger population by observing the effects in the available sample size (Serdar, Cihan, Yücel, & Serdar, 2021). In future studies, power estimation and sample size should be performed in advance. In addition, assessment of cardiac and plasma Ang II and Ang-(1-7) and bradykinin levels as well as the protein expression of Mas1 receptors in the heart might enhance our understanding of the underlying mechanism of PRCP role on the cardiovascular system. Also, trying higher adenoviral doses to assure the therapeutic/effective dose delivered to the animal e.g $2x10^{11}$ VP/animal.

1.7 4.4 Summary

An effective and well tolerated dose of Ang II was established in Wistar Kyoto rats that led to increased blood pressure and cardiac remodelling. Overexpression of PRCP via adenoviral vector-mediated gene transfer had no effects on blood pressure or cardiac hypertrophy following Ang II infusion but showed some potential protective effects on cardiac function that needs further studies.

Chapter 5 Generation of ACE2 Loaded Extracellular Vesicles and assessment of their effects on Cardiomyocyte hypertrophy in vitro.

5.1 Introduction

5.1.1 The role of EVs in transporting components of the renin angiotensin system and signaling in CVD

Extracellular vesicles (EVs) are endogenous vesicles that are released from most cell types and can transport a range of biological mediators, including DNA, RNA and proteins, and thus can contribute to cell-cell signaling. It has recently been demonstrated that components of the RAS are amongst the cargo that EVs can transport and that this can affect RAS signaling in both local and distant recipient cells of the cardiovascular system. For example, a study has shown that exosomes can mediate transfer of the AT_1R which then elicits functional effects *in vivo* and *in vitro* (Pironti et al., 2015). This study first demonstrated that exosome concentration was markedly elevated in the conditioned media from wild type HEK293 cells in response to osmotic stretch compared to isotonic media (Pironti et al., 2015). Next, it was found that both osmotic stretch and Ang II stimulation significantly increased exosome release into the conditioned media of a cell line that stably expressing the AT_1R (HEK293 cells transfected with pCDNA3.1 expressing plasmid encoding hemagglutinin (HA) epitope-tagged AT_{1A} receptor (pcDNA3.1-HA-$AT_{1A}R$) (Wei et al., 2003), which was inhibited by the addition of dimethyl amiloride (an inhibitor of exosome release (C. Chen et al., 2023; Savina, Furlán, Vidal, & Colombo, 2003))(Pironti et al., 2015). Whether or not released exosomes contain AT_1R was investigated using a saturation radioligand binding assay. Exosomes derived from AT_1R stable cell line stimulated with either Ang II or osmotic stretch showed a more than 10-fold increase in AT_1R density compared to unstimulated cells (Pironti et al., 2015). In vivo investigation also revealed that AT_1R exosomes were detected at 100-fold greater levels in serum of WT mice exposed to cardiac pressure overload, induced via transverse aortic constriction (TAC), compared to sham controls (Pironti et al., 2015). YFP-tagged AT_1R and mCherry-tagged Alix fluorescence were used to trace the exosomes in the recipient cells. AT_1R (YFP) and Alix-mCherry enriched vesicles were added to HEK293 cells and incubated for 12 hours. Confocal microscopy analysis revealed transfer of Alix-mCherry to the inside of cells and AT_1R-YFP to the plasma membrane (Pironti et al., 2015). Furthermore, AT_1R exosomes were able to increase phosphorylation of ERK1/2 in HEK293 cells, an effect which was inhibited by the AT_1R receptor blocker

Telmisartan (Pironti et al., 2015). The study also indicated that AT_1Rs encapsulated in exosomes mediated physiological effects through altering blood pressure in vivo. AT_1R-knockout (KO) mice were injected with either AT_1R exosomes or with control exosomes or PBS and blood pressure was monitored following Ang II stimulation. Following Ang II infusion, there was no elevation in blood pressure in AT_1R knockout mice received exosome free saline solution (Pironti et al., 2015). However, AT_1R-KO mice injected with AT_1R enriched exosomes restored the Ang II-dependant increased systolic blood pressure (Pironti et al., 2015). Furthermore, AT_1R expression were markedly higher in the heart and skeletal muscle of AT_1KO mice infused with AT_1R-enriched exosomes compared to untreated mice (Pironti et al., 2015).

Another study also highlighted the role of exosomes in cardiac fibroblast-induced cardiomyocyte hypertrophy via modulation of the levels of RAS components. The study first showed that neonatal rat cardiac fibroblast-conditioned medium, but not HEK293 cell-conditioned medium, promoted pathological hypertrophic effects on neonatal rat cardiomyocytes which was determined to be mainly mediated mainly via exosomes (Lyu et al., 2015). Next, the exosome secretion from cardiac fibroblasts was assessed in response to several pathological stimuli including: Ang II, TGFß1, endothelin 1(ET-1), insulin, lipopolysaccharide (LPS), and hydrogen peroxide (H_2O_2). Interestingly, exosome released from cardiac fibroblasts were markedly higher after Ang II stimulation, and there was no significant change in exosome secretion in response to other conditions compared to control treatment (Lyu et al., 2015). Telmisartan and PD123319 (an AT_2R antagonist) inhibited Ang II-induced exosome release from cardiac fibroblasts. Similarly, the exosome inhibitors GW4869 (Y. Peng et al., 2022) and dimethyl amiloride (DMA) markedly attenuated Ang II-induced exosome release from cardiac fibroblasts. In turn this inhibited [^{3}H]-Leucine uptake in the cardiomyocytes (Lyu et al., 2015). Cardiac fibroblast exosomes also significantly enhanced the mRNA expression of renin, angiotensinogen, AT_1R, and AT_2R and reduced the expression of ACE2 in neonatal rat cardiomyocytes (Lyu et al., 2015). The upregulation of RAS components by cardiac fibroblast exosomes was attained via activation of Mitogen-activated Protein Kinases (MAPKs) and the Akt pathway, an effect which was inhibited by using kinase specific inhibitors (Lyu et al., 2015). Therefore, the study concluded

that cardiac fibroblast-derived exosomes can upregulate RAS components via activation of MAPKs and the Akt pathway and promote cardiomyocyte hypertrophy in vitro (Lyu et al., 2015). To further confirm the effect of exosomes in mediating cardiac hypertrophy, Ang II and exosome inhibitors (GW4869 and DMA) were administered into C57BL/6N mice for five days and cardiac hypertrophy and fibrosis were investigated (Lyu et al., 2015). The study showed that Ang II-induced cardiac hypertrophy and fibrosis were significantly reduced in both of the exosome inhibitor-treated groups compared to mice treated with Ang II alone (Lyu et al., 2015). The in vivo investigation also indicated that exosome inhibitors blocked Ang II-induced exosomes release from cardiac fibroblasts in the murine heart (Lyu et al., 2015).

Moreover, it has also been reported that exosomes are involved in regulating vascular homeostasis and structure via transfer of RAS components. Vascular adventitial fibroblast (AFs) are the main cell type in the vascular adventitia that participates in maintaining vascular function and structure (Tong et al., 2018). The number of vascular smooth muscle cells (VSMC) migrating and the overall migration distance increased when treated with conditioned medium from cultured AFs that had been isolated from spontaneously hypertensive rat (SHR), an effect blocked by adding 20 μmol/L of the exosome inhibitor GW4869 (Tong et al., 2018). Exosomes were isolated from AFs (AFE) of SHR and WKY rats and were added to VSMCs from both strains to assess migration effects (Tong et al., 2018). It was observed that AFE isolated from SHR induced migration of VSMCs from WKY and SHR while AFE isolated from WKY rats showed no measurable migration effect (Tong et al., 2018). Blocking the AT_1R via Losartan attenuated AFE-induced VSMC migration in VSMCs of SHR but not in VSMCs from WKY rats. Also, the ACE inhibitor, captopril, decreased AFE-induced VSMC migration in WKY and SHR VSMCs (Tong et al., 2018). ACE was knocked down in AFs of SHR via transfection of ACE-siRNA for 5 days, and it was subsequently demonstrated that the ACE content and activity were reduced in the AFE (Tong et al., 2018). Consequently, AFE-induced VSMC migration was reduced in response to AFE isolated from ACE-knockdown SHR AFs. These data demonstrate that AFs from SHR induce VSMC migration via exosome-mediated transfer of ACE (Tong et al., 2018).

Another investigation conducted by the same research group assessed the mechanism of AFE's effects on VSMC proliferation and vascular remodelling in SHR and WKY rats (Ren et al., 2020). The study showed that EVs isolated from AFs of WKY rats (WKY-EVs) had no effect on WKY-VSMC proliferation but in contrast reduced SHR-VSMC proliferation (Ren et al., 2020). In contrast, EVs isolated from AFs of SHR rats (SHR-EVs) promoted proliferation in both WKY and SHR VSMCs but with a more pronounced proliferative effect on SHR-VSMCs. It was further reported that miR155-5p affected the differentiation of AFs and miR155-5p levels negatively correlated with blood pressure in SHR (Ren et al., 2020). WKY-EVs were enriched with miR155-5p while SHR-EVs contained lower levels of miR155-p (Ren et al., 2020). In order to determine whether or not miR155-5p was involved in the effect of EVs on VSMC proliferation, a miR155 inhibitor was used. The proliferation effect of SHR-EVs on VSMCs were increased following administration of a miR155-5p inhibitor, while the inhibitory effect of WKY-EVs was preserved (Ren et al., 2020). WKY-EVs attenuated ACE mRNA and protein expression, while SHR-EVs enhanced ACE protein expression in both WKY and SHR VSMCs. The study also showed that SHR-EVs induce VSMC proliferation via EV-mediated ACE transfer (Ren et al., 2020).

EVs have also been reported to be involved in regulating the counter regulatory axis of the RAS and the consequential effects on blood pressure. A recent study revealed that human acute monocytic leukemia (THP-1) cell- derived-EVs increased rat systolic blood pressure via downregulation of the Ang-(1-7)/Mas receptor axis and upregulation of the vasoconstrictor phenylephrine (Zou et al., 2020). Briefly, the study first indicated that blood pressure was markedly elevated in Sprague Dawley rats following THP-1 cell-derived EV administration twice a week via tail vein over 4 weeks (Zou et al., 2020). Next, the main candidate microRNAs (miR-27a and miR-181a(Marques et al., 2015; Suzuki et al., 2022)) that might be responsible for hypertension caused by EVs were determined via several investigation steps involving three types of cells: HEK-293 cells, THP-1 cells, and HUVECs. Animals treated with pre-miR-27a EVs, but not pre-miR-181a EVs, showed impaired Ang-(1-7)-mediated vasodilation and causes high blood pressure (Zou et al., 2020). Injecting pre-miR-27a EVs into Sprague–Dawley rats also reduced the protein expression of the Mas receptor and p-eNOS (phosphorylated endothelial nitric oxide synthase) in mesenteric arteries (Zou et

al., 2020). Moreover, next THP-1 cells were transfected with either a miR-27a mimic or miR-27a inhibitor and EVs were isolated and added to HUVECs to assess Mas receptor expression *in vitro* (Zou et al., 2020). Mas receptor expression increased in response to the miR-27a inhibitor, while the miR-27a mimic reduced the protein expression of Mas receptors in HUVECs (Zou et al., 2020).

Another study indicated that EVs isolated from AT_1R transfected HEK293 cells increased the mRNA and protein expression of AT_1R in recipient HEK293 cells (J. Cai et al., 2013). For example; EVs derived from VSMCs elevated AT_1 receptor protein expression in HEK293 cells which further increased when adding higher concentrations of EVs (J. Cai et al., 2013). The transferred AT_1 receptors promoted functional effects in HEK 293 cells via enhancing the stimulatory effect of Ang II on Na^+–K^+ ATPase activity (J. Cai et al., 2013). Taken together, these studies indicated that RAS components can be regulated by EVs and EVs can also be affected by RAS and cause the consequence functional or structural effect.

5.2 Hypothesis and aims

It has been repeatedly reported that EVs can transport therapeutic protein to cardiomyocyte and elicit functional effect. ACE2 plays a crucial role in countering cardiac hypertrophy. Therefore, it was hypothesized that EVs-mediated ACE2 delivery might be protective against Ang II-dependent cardiomyocyte hypertrophy.

The aims of this chapter were to:

- Production of Ad-ACE2 and Ad-GFP and verification via western blot and immunofluorescence
- Generation and characterization of ACE2-loaded extracellular vesicles (ACE2 EV)
- Determine the role of ACE2 EV in altering Ang II and Ang-(1-7) in H9c2 cardiomyocyte.
- Determine whether ACE2 EV is protective against Ang II-induced cardiomyocyte hypertrophy.

5.3 Results

5.3.1 Production and purification of Ad-ACE2 and Ad-GFP

Ad-GFP and Ad-ACE2 were produced and purified as previously illustrated in section 2.2.11 (Figure 5.1)(Luo et al., 2007).

Figure 5.1 Representative image for purified Ad-ACE2 and Ad-GFP using cesium chloride (CsCl) density gradient.

Two layers of CsCl (1.25 g/mL and 1.40 g/mL) were added into SW40 ultracentrifugation tubes and the virus preparations were added drop by drop afterward, and subjected to ultracentrifugation at 217,874g for 1.5hr. each image showed three layers from the bottom; mature virus, empty capsids, and cellular debris.

5.3.2 Evaluating the transduction efficiency for the Ad-GFP preparation.

The expression of eGFP was detected in H9C2 cardiomyocyte transduced with a range of MOI of Ad-GFP (1000, 2500,5000, 10,000 and 20,000 VP/cell) using fluorescence microscopy. Data indicated that the expression of eGFP protein increased in a dose dependent manner. Control cardiomyocyte did not transduce and showed no eGFP expression (Figure 5.2).

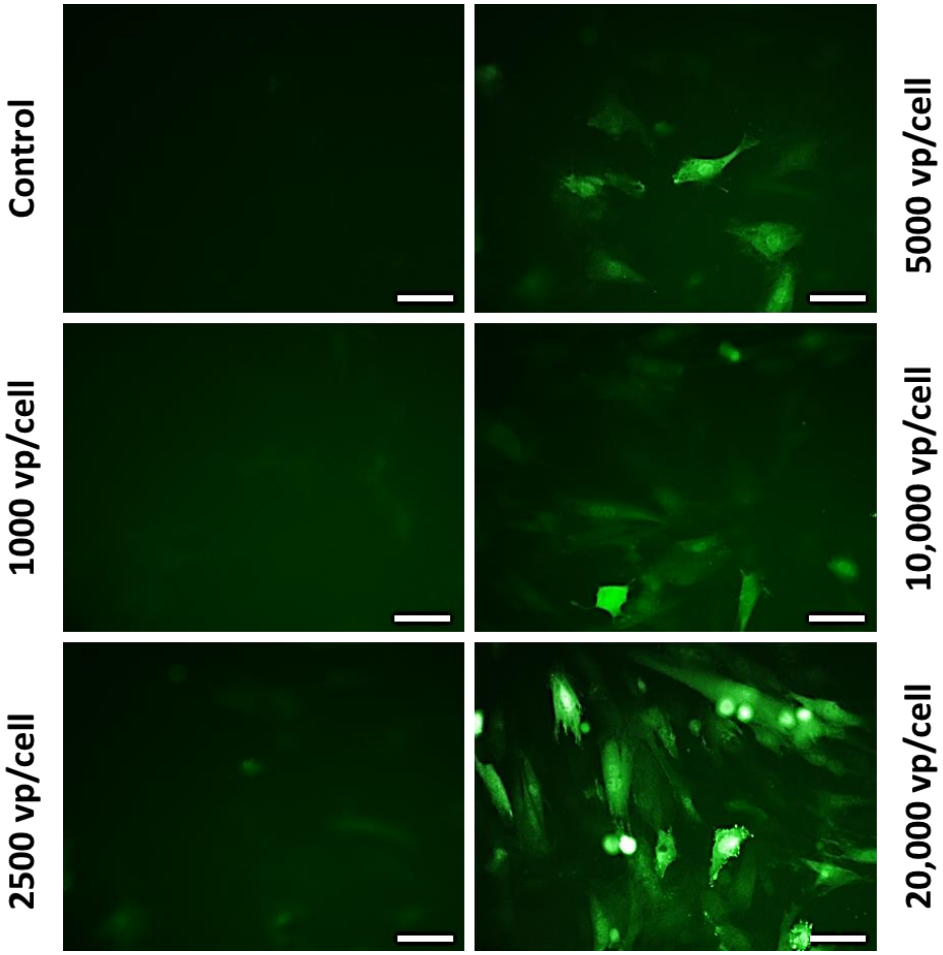

Figure 5.2 Representative images for eGFP expression in cardiomyocytes

H9c2 cardiomyocyte were seeded into 6 well plate at 3x10^5 cells/well. The cells were then un-transduced (control) or transduced with a range of Ad-GFP (1000VP/cell- 20,000VP/cell) and incubated at 37°C for 48hr. The images were taken using fluorescence microscopy at 20x magnification. Scale bar=100µm.

5.3.3 Assess the protein expression of ACE2 in cardiomyocyte followed Ad-ACE2 transduction.

Protein expression of ACE2 was detected by western immunoblotting in H9c2 cardiomyocyte transduced with 50 pfu/cell of Ad-ACE2 or Ad-GFP for 48h or left un-transduced (control). ACE2 protein was observed at ~110 KDa band size (predicted band size is ~92 KDa) (lane 4 and 5). This observation agreed with the manufacture for the Anti-ACE2 antibody. There was no ACE2 expression detected in control (lane 1) or Ad-GFP transduced cells (lane 2) (Figure 5.3).

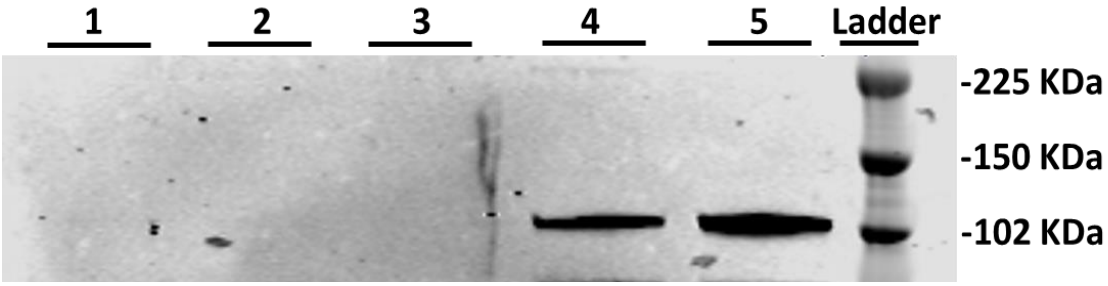

Figure 5.3 Detection of ACE2 protein by western immunoblotting

Representative image for western immunoblotting showed the ACE2 protein at expected band size ~110KDa (lane 4 and 5). No ACE2 protein detected in control (lane 1) or Ad-GFP (lane 2) groups (n=3).

5.3.4 Generation and isolation of extracellular vesicles

EVs were isolated from conditioned media of un-transduced H9c2 cardiomyocytes (Cont. EV) or transduced with 50 pfu/cell Ad-ACE2 (ACE2 EV) or Ad-GFP (GFP EV) using ultracentrifugation as explained in (section 2.6.4) and summarized in (Figure 5.4).

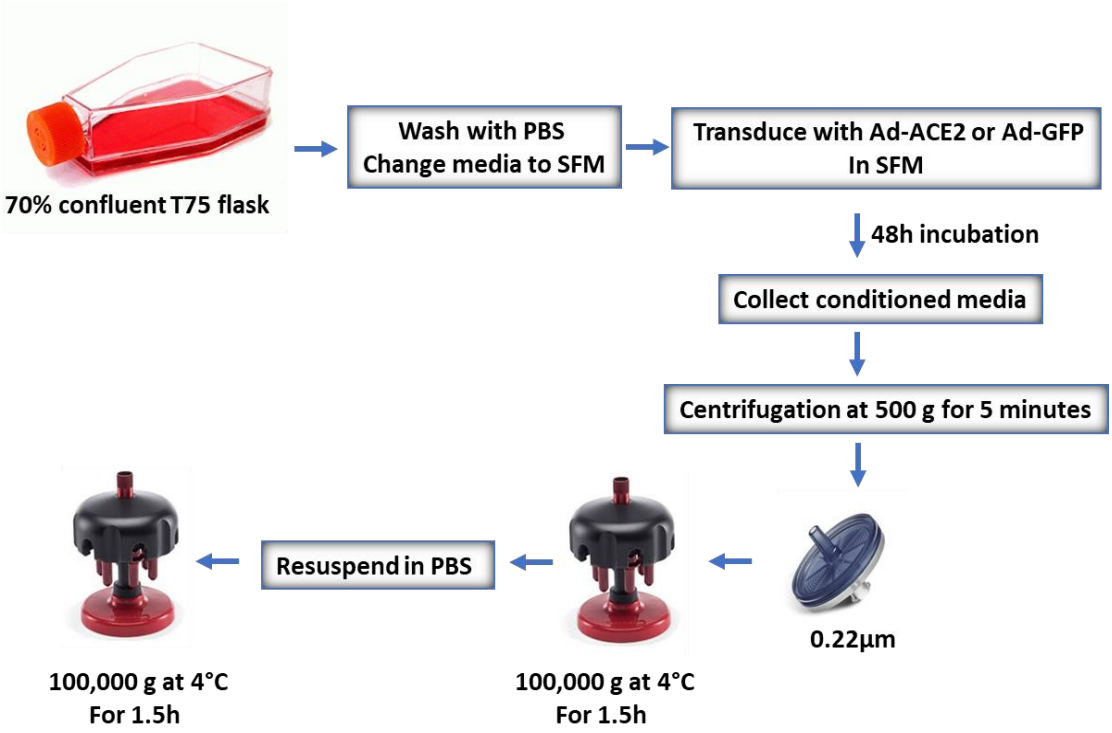

Figure 5.4 A schematic representation of the process for production and isolation of extracellular vesicles.

H9c2 cardiomyocyte was cultured in T75 flasks until 70% confluent. Cells were washed with PBS and transduced with 50 pfu/cell of Ad-ACE2 or Ad-GFP and incubated for 48h. Control cells were left un-transduced. Conditioned media collected and subjected to centrifugation at 500 g for 5 minutes and supernatant passed through a 0.22 µm filter, to further remove any remaining cell debris and large particles and subjected to ultracentrifugation at 100,000 g for 90 minutes. Pelleted EVs were resuspended in PBS and washed in PBS via another ultracentrifugation at 100,000 g for 90 minutes (Théry, Amigorena, Raposo, & Clayton, 2006).

5.3.5 Characterization of extracellular vesicles by NanoSight

Nanoparticle Tracking Analysis (NTA) was utilized to analyse EVs and a plot representing the EV size and concertation was generated for control EV, GFP EV and ACE2 EV (Figure 5.5 A, B and C).

A

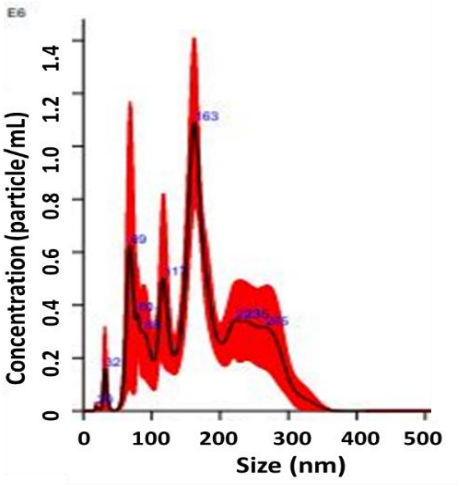

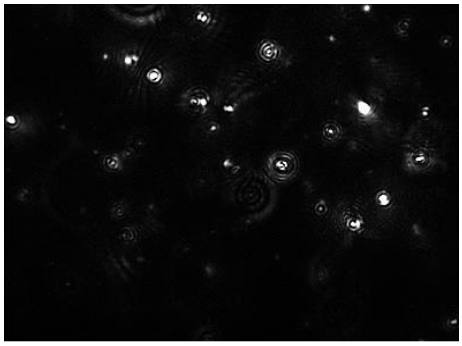

Control EV

B

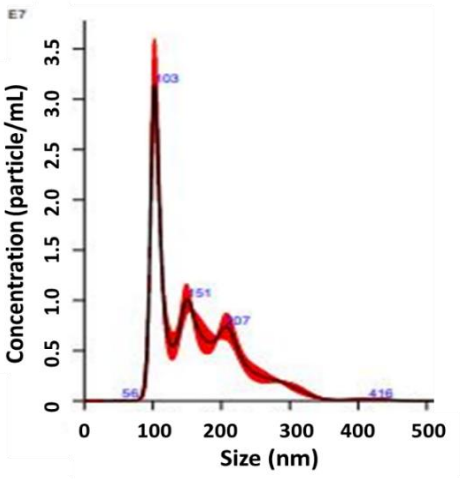

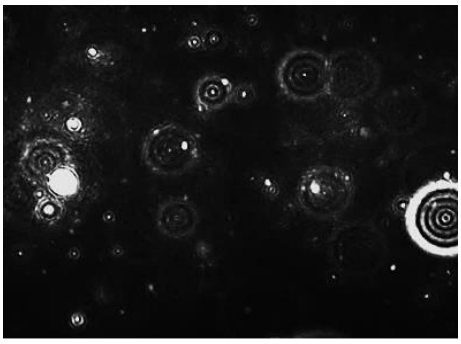

GFP EV

C

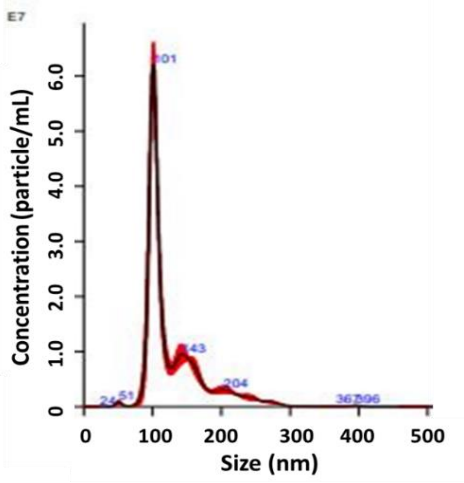

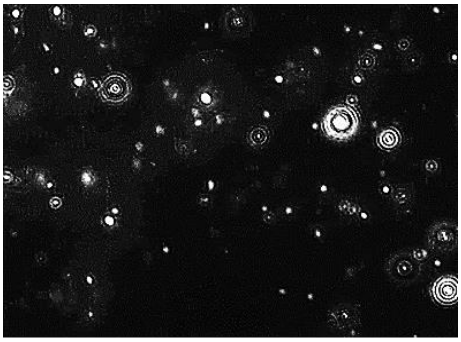

ACE2 EV

Figure 5.5 Representative nanosight plots and images for EVs in each condition.

(A) Representative size and concentration plot and image for control EV. **(B)** Representative size and concentration plot and image for GFP EV. **(C)** Representative size and concentration plot and image for ACE2 EV.

The NTA data showed that the concentration for control EV was ($2.9x10^8 \pm 6 x10^7$ particles/mL) and for the GFP EV was ($8.6 x10^8 \pm 2.6x10^8$ particles/mL) without significant different between these two groups. However, significantly higher concentration of ACE2 EV ($2.4 x10^9 \pm 3.1x10^8$ particles/mL) was observed compared to control EV ($p<0.001$) and to GFP EV ($p<0.01$) (Figure 5.6 A), n=5.

Analysis of the EVs particle size revealed that the measured mode size of control EV was (140.6±18.9 nm), (102.6± 2.3 nm) for ACE2 EV, and (103±0.5nm) for GFP EV without significant different between groups. n=5/group (Figure 5.6 B). These data indicated that the size of the isolated particles is within the exosome size range(30-150 nm) (Doyle & Wang, 2019).

However, the average mean size for the control EV was (165.2±12.1 nm) and (150.8±5.4) for GFP EV and (135.8±3.9 nm) for ACE2 EV (Figure 5.6 C).

A

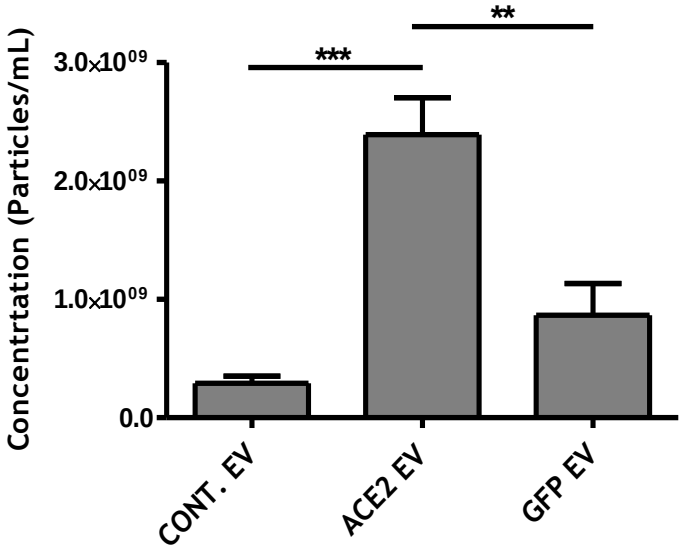

B

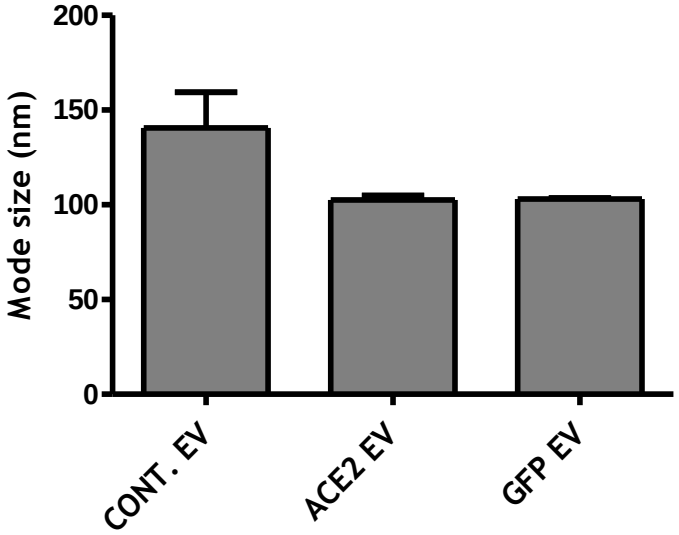

C

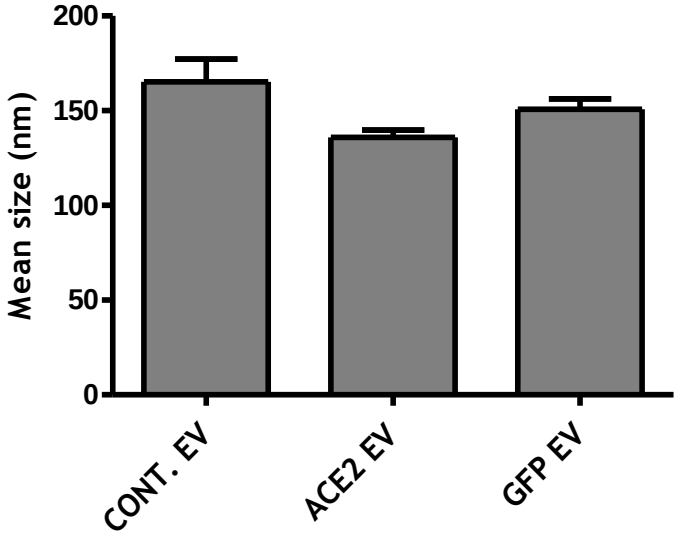

Figure 5.6 Analysis of the concentration and size for EVs under each condition.

(A) Analysis of EV concentration for each group **(B)** Analysis of mode size for each group. **(C)** Analysis of average mean size in each group, n=5

5.3.6 Assessment of ACE2 protein levels and EV markers in the isolated EVs via western immunoblotting

Next EV were further characterised by assessing the EV associated markers CD63 and TSG101 via western immunoblotting. The isolated EVs were lysed and a concentration of 4.5µg/ml was loaded for electrophoresis. Both EV markers were detected at approximate sizes of 53 kDa for (CD63) and 50 kDa for (TSG101), as expected, in ACE2 EV and GFP EV, further supporting the conclusions that populations of EV had been successfully isolated. However, EV markers were not detected in control EVs, n=3.

Furthermore, assessment ACE2 levels in the isolated EV showed successful detection of ACE2 protein as a band was observed at ~97KDa. Importantly, ACE2 was only detected in EVs isolated from Ad-ACE2 transduced H9c2 cardiomyocytes, while no band was detected in either control EV or GFP EV. These data demonstrated that cells transduced with Ad-ACE2 secreted EVs which contained ACE2 protein, n=3 (Figure 5.7).

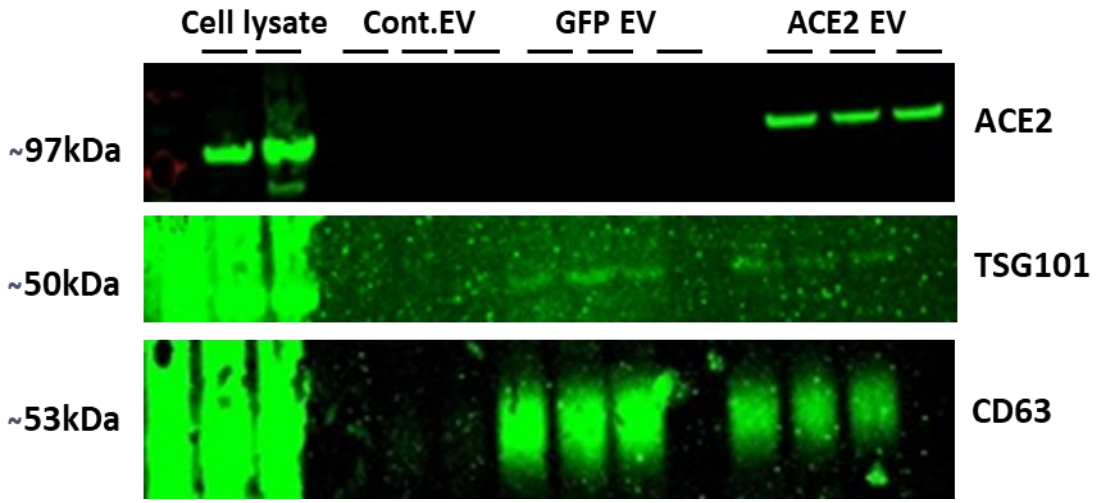

Figure 5.7 Characterization of EVs via western immunoblotting

Protein expression of ACE2 ~110KDa, and EVs associated markers (TSG101) ~50KDa and (CD63) ~53KDa for EVs isolated from untreated H9C2 cardiomyocyte (Cont. EV) or transduce with 50 pfu/cell of Ad-ACE2 (ACE2 EV) or Ad-GFP (GFP EV) for 48h, n=3.

5.3.7 ACE2 activity measurement for the isolated EVs

To determine if the ACE2 detected in EVs was functional, an ACE2 activity assay was performed as detailed in (section 2.6.10). Results demonstrated that there was significantly higher relative ACE2 enzymatic activity in ACE2 EV (172.8± 31.6 RFU) compared to Cont. EV (36.2±5.8 RFU) $P<0.05$, and to GFP EV and (21.7 ±15.9 RFU) $p<0.01$. There was no significant difference between GFP EV and control EV, n=3 (Figure 5.8).

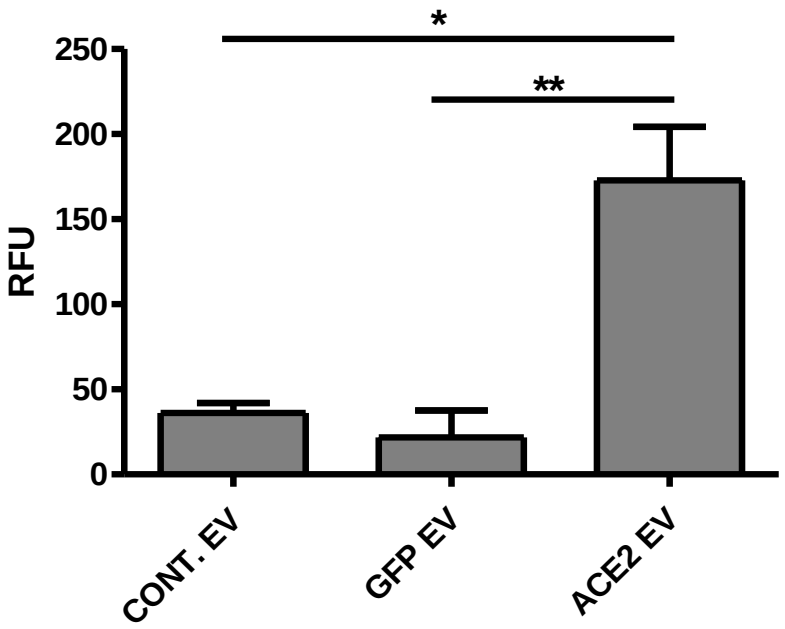

Figure 5.8 Measurement of ACE2 catalytic activity in the isolated EVs.

EVs isolated from untreated H9C2 cardiomyocyte (Cont. EV) or transduce with 50 pfu/cell of Ad-ACE2 (ACE2 EV) or Ad-GFP (GFP EV) for 48h, and ACE2 enzymatic activity was measured in EVs of each condition. *$p<0.05$ vs control EV, **$p<0.01$ vs GFP EV, RFU=relative fluorescence unit, n=3.

5.3.8 Assessment of ACE2 protein expression in cardiomyocyte following treatment with ACE2 EV

To further investigate whether the ACE2 EV can transfer ACE2 into cardiomyocyte and enhance its' protein expression, H9c2 cell were treated with ACE2 EV, GFP EV or left untreated (control) and protein expression assessed via western immunoblotting.

Due to challenges in detecting or quantitation EVs via BCA protein assay, Nanosight titer was utilized as a treatment unit. Therefore, cells were treated with range of ACE2 EV or GFP EV concentrations, based on NanoSight titer($3.7x10^9$ particles/mL, $7.4x10^9$ particles/mL, and $1.48x10^{10}$ particles/mL) and incubated for 24h before cells were lysed and samples prepared for western immunoblot. Results showed that ACE2 protein expression was detected at the expected band size ~110KDa in a dose dependent manner in all three utilized doses (lane 1, lane 2, and lane 3, for $3.7x10^9$, $7.4x10^9$, and $1.48x10^{10}$ particles/mL respectively). There was no band detected in either GFP EV group (lanes 4,5 and 6) or in control group. These observations indicated successful transfer of ACE2 EV into H9c2 cardiomyocyte. Lane 8 represents positive control for ACE2 (figure 5. 9).

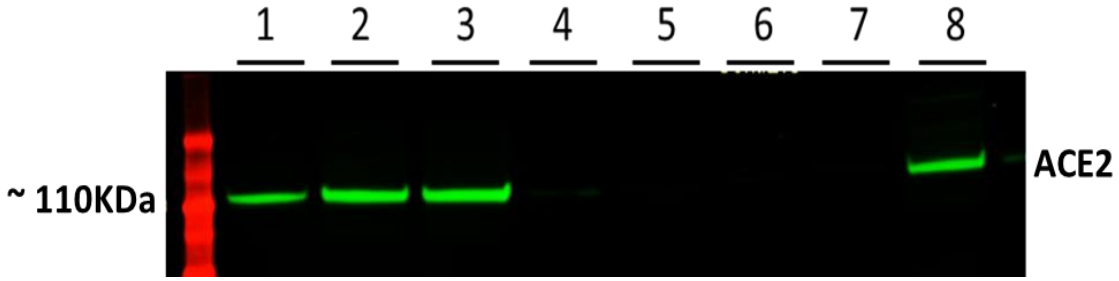

Figure 5.9 Western immunoblotting for ACE2 protein in H9c2 cardiomyocyte treated with ACE2 EV.

H9c2 cells were untreated (control) (lane 7) or treated with ($3.7x10^9$ p/mL, $7.4x10^9$ p/mL, and $1.48x10^{10}$ p/mL) of ACE2 EV (lane 1, 2, and 3) or GFP EV (lane 4,5, and 6) for 24h and cells lyased for western immunoblotting analysis. p/mL=particles/mL, lane 8 represent ACE2 +ve control, (n=2).

5.3.9 Assessment of Ang II levels following treatment of H9c2 cardiomyocytes with EVs

In order to determine whether ACE2 activity in EVs could promote a biological effect in cardiomyocytes, Ang II levels were measured by ELISA in unstimulated H9c2 cardiomyocytes, or following stimulation with 100 nM Ang II and treatment with either ACE2 EV or GFP EV for 24h (Figure 5.10A).

Analysis showed that Ang II level in control group was (0.49 ± 0.01 pg/mL), in Ang II-only treated group was (1.25 ± 0.65 pg/mL), in GFP EV group was (1.12 ± 0.44 pg/mL), and in ACE2 EV treated group was (0.58 ± 0.03 pg/mL) without significant differences between groups (Figure 5.10B).

A

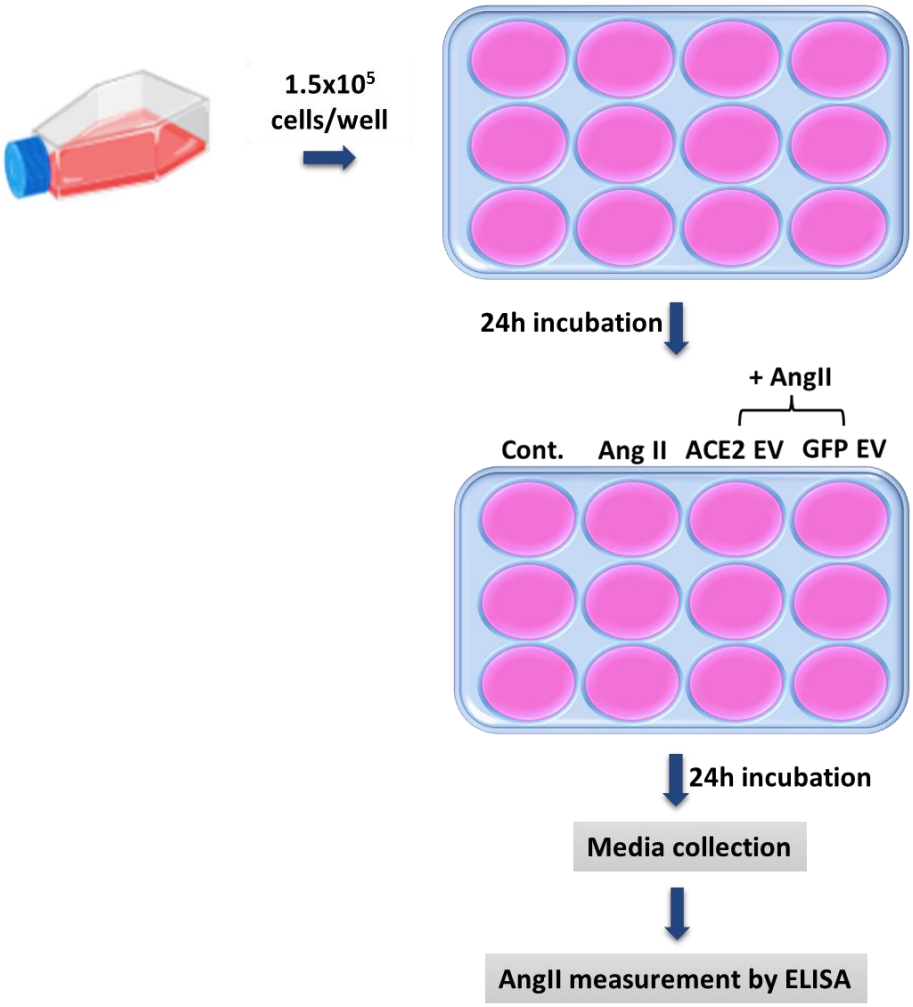

B

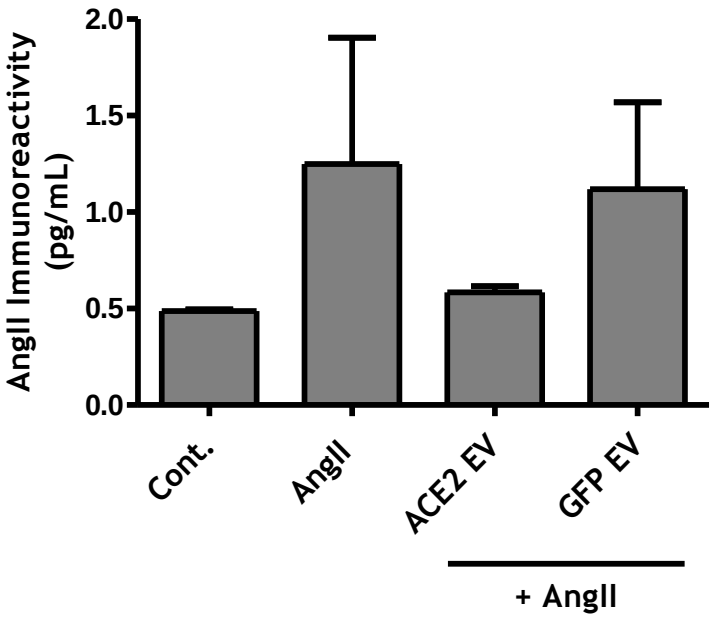

Figure 5.10 Assessment of Ang II levels in response ACE2 EV treatment in H9c2 cardiomyocyte

(A) Schematic representative of the work plan for measuring Ang II levels in untreated H9c2 cells or stimulated with 100nM Ang II and treated with ACE2 EV or GFP EV for 24h. **(B)** ELISA analysis for Ang II levels in each group (n=4).

5.3.10 Assessment of Ang-(1-7) levels in H9c2 cardiomyocytes following EV treatment.

Ang-(1-7) was measured by ELISA at two time points (24h and 48h) following Ang II and/ or EV treatment as explained in (section 5.2.6). Results showed a trend towards higher Ang-(1-7) level at 24h in ACE2 EV treated group (3.1± 1.2 pg/mL) compared to control (1.1 ± 0.8 pg/mL) and Ang II (0.75 ± 0.8pg/mL) groups, but this difference was not significant. Ang-(1-7) level in GFP EV group was also higher (2.274 ± 0.51 pg/mL) compared to control and to Ang II groups but it was also non-significant, n=3-4 (Figure 5.11 A).

At 48h, there were no significant differences in Ang-(1-7) levels between control (2.9 ± 0.03 pg/mL) and other groups; Ang II (2.01 ± 0.59 pg/mL), ACE2 EV (2.82 ± 0.28 pg/mL) and GFP EV (3.49 ± 1.48 pg/mL), n=3 (Figure 5.11 B).

A

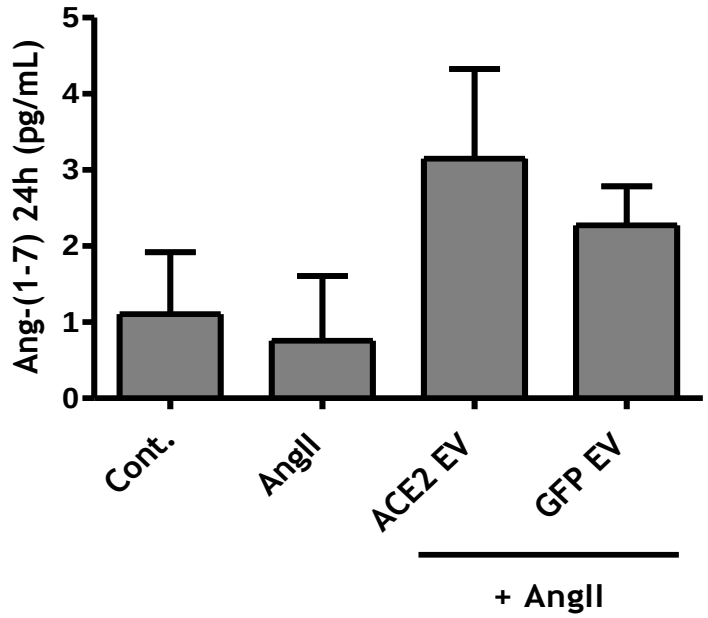

B

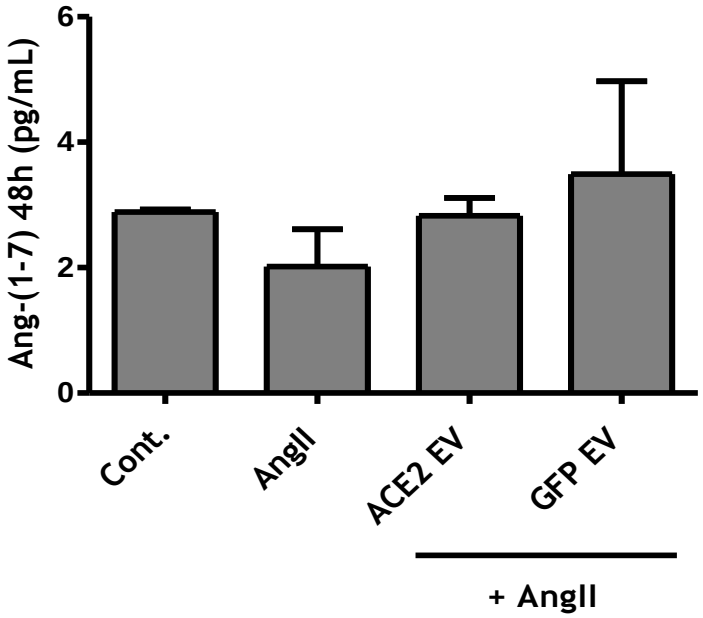

Figure 5.11 Evaluation of Ang-(1-7) levels in response to ACE2 EV treatment in H9c2 cardiomyocyte.

Cells were untreated (control) or stimulated with Ang II and treated with ACE2 EV or GFP EV and culture media collected for Ang-(1-7) ELISA analysis. **(A)** Ang-(1-7) level at 24h for each group, n=3-4 (**B)** Ang-(1-7) level at 48h for each group, n=3.

5.3.11 Evaluation of the effects of EVs on Ang II-Induced Cardiomyocyte hypertrophy

H9c2 cardiomyocytes were left untreated or stimulated with 100nM Ang II alone or Ang II and either ACE2 EV or GFP EV and incubated for 48h (Figure 5.12 A). Next, cells were fixed and stained, and images were taken for cell size analysis (Figure 5.12 B).

A

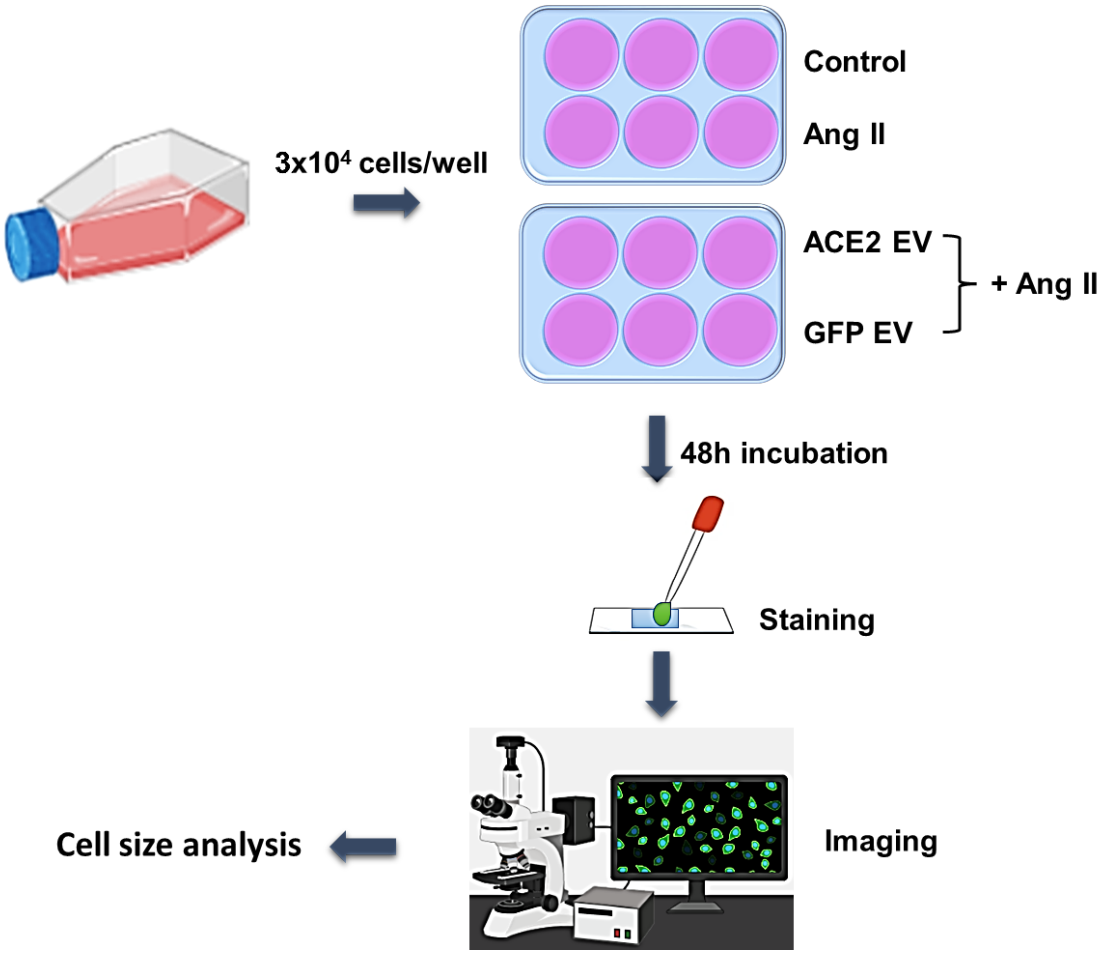

B

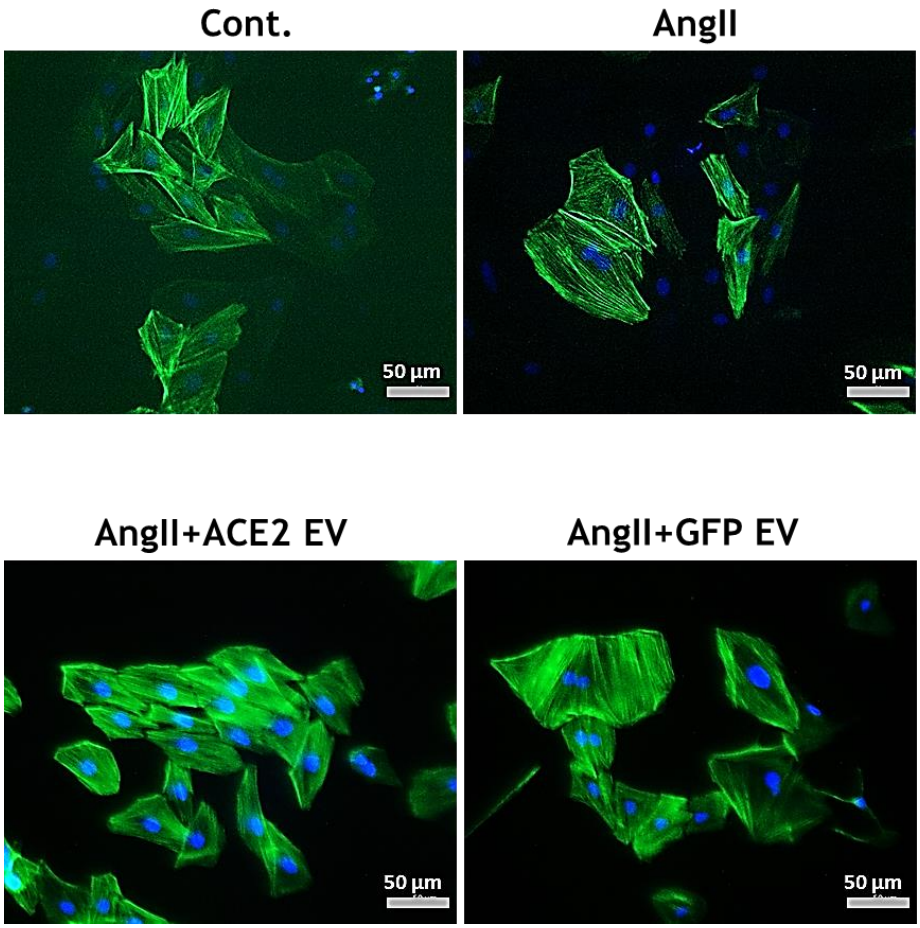

Results revealed that the cardiomyocyte surface area for control was (3453±195.8 µm^2). Ang II only treated group showed significantly greater cell size (5513±320.2 µm^2) in comparison to control (p<0.05). GFP EV group showed no statistical difference in cell size (5112±974.9 µm^2) compared to control. ACE2 EV treated cardiomyocytes surface area was (3916±268.1 µm^2), without significant difference in comparison to control, n=3(Figure 5.12 C)

C

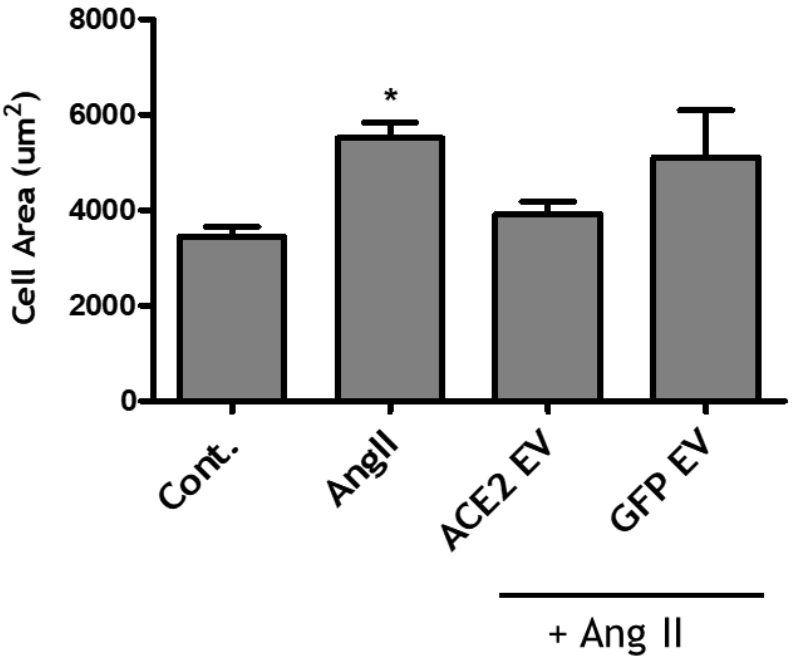

Figure 5.12 Assessing the effects of ACE2 EV on Ang II-induced cardiomyocyte hypertrophy.

(**A)** Schematic representing the work plan for evaluating the effect of ACE2 EV on Ang II-dependent hypertrophy: H9c2 cardiomyocyte were left untreated or stimulated with 100nM Ang II and treated with ACE2 EV or GFP EV for 48h for cell size measurement **(B**) Representative images for each experimental group **(C)** analysis of cardiomyocyte surface area under each condition (**p*<0.05 vs control), n=3.

5.3.12 Effect of EV treatment on RAS receptor gene expression following Ang II stimulation of H9c2 cardiomyocytes

Gene expression of the AT_1R, AT_2R, and MasR were quantified in untreated cells, Ang II stimulated cells and/or stimulated with Ang II and treated with either ACE2 EVs or GFP EVs.

Analysis of AT_1R gene expression showed a trend towered higher values in the Ang II treated group (2.29±0.6 fold change) compared to the control group (1.28± 0.4) and the ACE2 EV group (1.66± 0.5 fold change), although due to the low n values no statistical comparison could be made. GFP EV group showed no markedly different values (2.45 ±0.6) to Ang II group, n=2 (Figure 5.13 A).

Analysis of AT_2R gene expression showed no significant change between treatment groups (Ang II 1.2±0.2, ACE2 EV 0.96±0.13, GFP EV 1.23±0.1 fold change) in comparison to control (1.0±0.1), n=2 (Figure 5.13 B).

Similarly, analysis of MasR gene expression suggested no marked change between groups (1.3±0.2, 1.2±0.2, and 1.5±0.2) for Ang II, ACE2 EV, and GFP EV respectively compared to control (1.0±0.1), n=2 (Figure 5.13 C).

A

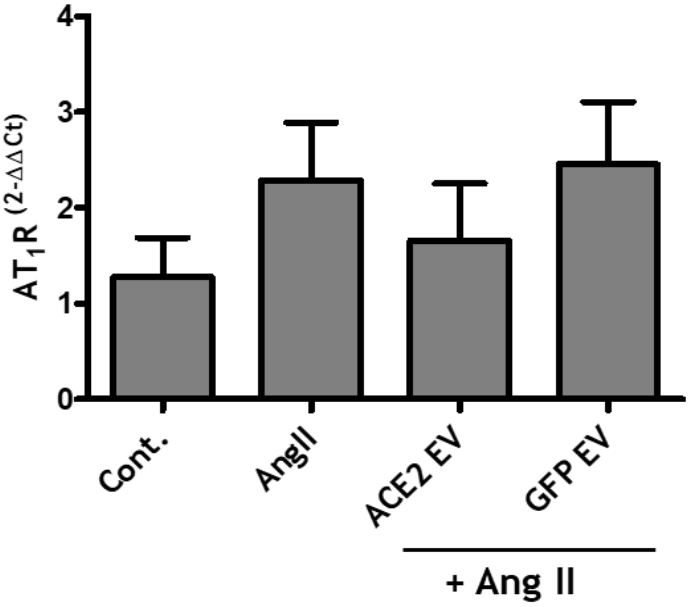

B

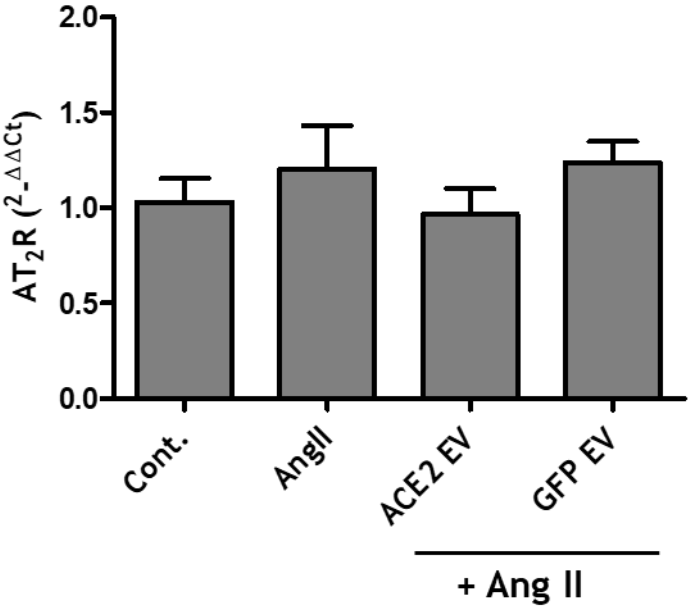

C

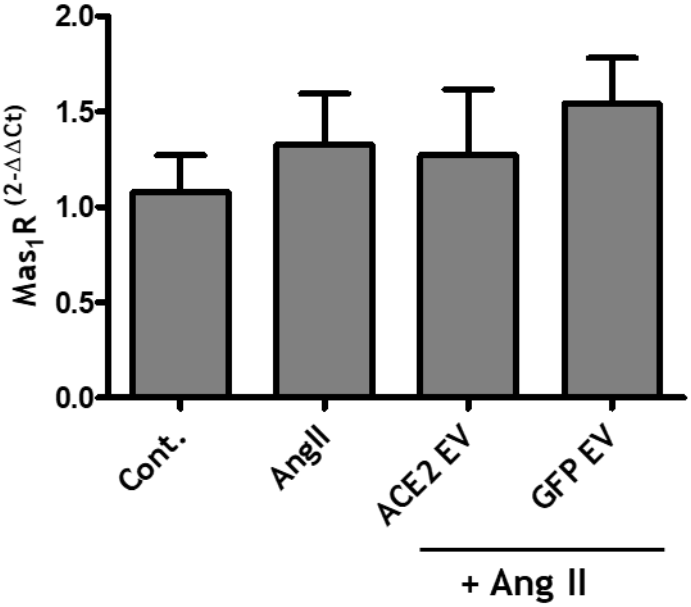

Figure 5.13 Gene expression of the AT1R, AT2R, and MasR in response to Ang II in EV-treated H9c2 cardiomyocytes

Cells were untreated (control) or stimulated with 1μM Ang II alone or Ang II and treated with ACE2 EV or GFP EV for 24h. **(A)** Analysis of AT1R for each group **(B)** Analysis of AT2R for each group**(C)** analysis of MasR under each condition, n=2.

5.3.13 Effect of ACE2 EV on TGFβ1 gene expression in response to Ang II stimulation

Previous reports indicated that TGFβ1 plays a role in mediating Ang II-induced cardiac hypertrophy (Schultz et al., 2002). Therefore, the gene expression of TGFβ1 has been evaluated in this project. Results showed no marked change between experimental groups (0.99±.09, 1.0±0.04, and 0.9±0.08) for Ang II, ACE2 EV and GFP EV respectively in comparison to control (1.0±0.04), n=1 (Figure 5.14).

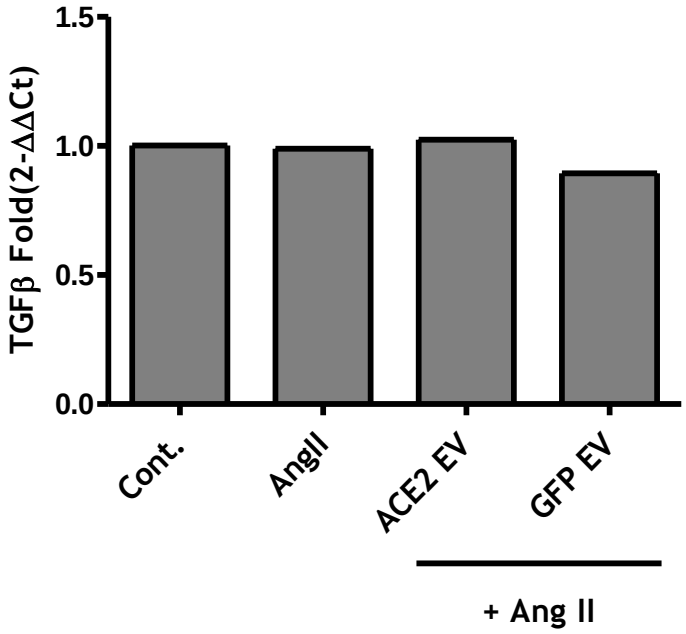

Figure 5.14 Evaluating TGFβ1 gene expression for the experimental groups

TGFβ1 gene expression was analysed for untreated cardiomyocyte or stimulated with Ang II alone or Ang II plus ACE2 EV and GFP EV, n=1

5.4 Discussion

The effects of ACE2 on the heart have been well studied using gene therapy approaches (Huentelman et al., 2005; Tikellis & Thomas, 2012), but the ability of EVs to deliver functional ACE2 to the heart has not been well understood. Here, whether EVs could transfer functional ACE2 to cardiomyocytes was assessed. EVs were successfully isolated from the conditioned media of un-transduced H9c2 cardiomyocytes or from H9c2 cardiomyocytes transduced with Ad-ACE2 or Ad-GFP using ultracentrifugation. The mode size for the isolated EVs were below 150 nm for all conditions, which indicated that the EVs were within the exosome size range (Brennan et al., 2020; C. Chen et al., 2023; Gurung, Perocheau, Touramanidou, & Baruteau, 2021; Kalluri & LeBleu, 2020; Malloci et al., 2019; Rajput, Varshney, Bajaj, & Pokharkar, 2022; X. Wang, Xia, Yang, Dai, & He, 2023). However, some reports suggested lower upper size for exosome i.e it has been described with size range of 40-100nm (Yi Zhang et al., 2020) or 30-140nm (Kruse, Schneider, Reger, Kampmann, & Reif, 2022) or less than 150nm in diameter (Liang et al., 2022). The average mean size for the isolated EVs in this study here gave higher values than the mode size with the control EV more than 150nm in dimeter. This could be due to the lower concentration of the control EV which might shift the average mean to greater values. However, according to the minimal information for studies of extracellular vesicles 2018, EVs were classified as small EVs with diameter size of <200nm and medium or large EVs with size of >200nm in diameter (Théry et al., 2018).

The concentration of EVs isolated from Ad-ACE2 transduced H9c2 cardiomyocytes (ACE2 EV) was significantly higher than the concentration isolated from either the control untreated cells (control EV) or those from the Ad-GFP transduced cells (GFP EV). Further characterization was performed using western immunoblotting for the EV-associated surface marker CD63 (Kowal et al., 2016) and the cytosolic EV marker TSG101 (Kowal et al., 2016). Both markers were detected in ACE2 EV and GFP EV, but not in control EV. The reason for not detecting the EV markers in control EV was not known. Via western immunoblotting ACE2 protein expression was only detected in the ACE2 EVs evidencing that Ad-ACE2 transduction led to overexpression of ACE2 and its incorporation into secreted EVs.

Assessment of ACE2 catalytic activity showed that the ACE2 incorporated into the EV (ACE2 EV) had catalytic activity. Together, these data suggest that functional ACE2 can be loaded into EVs using adenoviral transduction of cells and ACE2 over-expression.

Overexpression of specific molecule into parent cells is one of the effective methods to load the required EVs into that cell (Pedrioli, Piovesana, Vacchi, & Balbi, 2021). Furthermore, overexpression of a target protein or RNA is also sufficient to enhance EVs secretion of that specific protein or RNA from the host cells (Pedrioli et al., 2021). For instance, recent work has demonstrated that ACE2 could be loaded into EVs via a cell line which expressed ACE2 endogenously (Cocozza et al., 2020). The human lung epithelial cell line (Calu3) and the epithelial colorectal cell line (Caco2g) both produce ACE2 naturally (Cocozza et al., 2020). When EVs were isolated from the conditioned media of Calu3 and Caco2g cells, ACE2 protein was detected in the EVs along with EV- specific markers including CD63, CD81 and ADAM10 (Cocozza et al., 2020). However, it was observed that the concentration of the EVs product (ACE2 EV) was not sufficient. Hence, the investigators produced higher levels of ACE2 and a combined approach with packaging of ACE2 and the transmembrane serine protease 2 [TMPRSS2; a protein that cleaves the spike (S) protein of the SARS-CoV-2 and allow virus entry into cells (Fraser et al., 2022)], via overexpression of the target proteins in 293FT cells (a fast-growing variant of HEK 293 cell line) using lentiviral vector-mediated gene transfer (Cocozza et al., 2020). It was subsequently reported that this approach led to production of ACE2 enriched EVs or ACE2-TMPRSS2-EVs which were effective in reducing the infection of SARS-CoV-2-spike-pseudotyped virus into cells via working as a decoy agent to bind the S protein pseudotyped vector (Cocozza et al., 2020).

Another study utilised HEK293T cells which were transduced with a lentiviral vector expressing ACE2 in order to generate a cell line with stable ACE2 expression (Canhao Wu et al., 2022). ACE2-EVs were produced and isolated from cell culture supernatant of the engineered HEK293-ACE2 cells using differential ultracentrifugation and their ability to attenuate SARS-CoV-2 infection was assessed (Canhao Wu et al., 2022). EV characterization demonstrated that the concentration of ACE2-EVs was higher than that found for the control-EVs (isolated from non-transduced cells). This finding was consistent with the

findings reported in this chapter and the fact that this was observed following both adenoviral and lentiviral transduction may suggest that ACE2 over-expression affects EV release. In the published study it was also reported that the mean diameter size of the control EVs showed a trend to be larger than ACE2-EVs, although this did not reach significance (Canhao Wu et al., 2022). Again, this finding was in agreement with the data reported in this thesis chapter. (Canhao Wu et al., 2022) also showed that ACE2-EVs significantly antagonised SARS-CoV-2 infection in three different cell lines including HeLa, the human colon cancer cell line (HCT116), and the human prostate cancer cell line (PC3)(Canhao Wu et al., 2022). Since ACE2 is abundant in nasal epithelial cells, this may make the nasal cavity a primary host or incubator for SARS-CoV-2 infection and further assess the ability of ACE2-EVs to prevent SARS-CoV-2 infection *in vivo*, BALB/c mice received either ACE2-EVs, control EVs or PBS via nasal administration followed by 30 minutes exposure to S-pseudovirus (Canhao Wu et al., 2022). Next, mice were humanely killed, and the nasal mucosa tissues were collected for S-pseudovirus infection rate analysis. The data showed that the infection rate of S-pseudovirus was more than hundred times greater in mice treated with control EVs or PBS compared to the ACE2-EVs group,indicating that ACE2-EVs were effective in preventing SARS-CoV-2 entry via nasal cavity(Canhao Wu et al., 2022). In the data on this thesis chapter the effects of ACE2 EVs isolated from ACE2 overexpressing H9c2 cardiomyocytes in functional oucomes in cardiomyocyte hypertrophy in vitro was assessed (see later) but further work is required to assess whether these effects might also be observed in vivo.

EVs have also been shown to be effective therapeutic vectors for other molecules such as RNA. RNA-enriched exosomes were also engineered via an overexpression strategy and were shown to be effective in promoting functional effects in the cardiovascular system (Jiwen Liu et al., 2018). MiR-93-5p was introduced to adipose-derived stromal cells (ADSCs) via transfection with miR-93-5p mimic for 48h to enhance exosome secretion (Jiwen Liu et al., 2018). MiR-93-5p enriched exosomes significantly reduced infarct size in Sprague-Dawley rat subjected to a myocardial infarction via inhibiting autophagy and inflammatory markers such as the inflammatory factors IL-6, IL-1ß, and TNF-α (Jiwen Liu et al., 2018).

Utilizing adenoviral vector-mediated gene transfer to over-express proteins in cells with the aim to engineer EVs is not as frequently used as alternative approaches such as lentiviral gene transfer or transfection methods (B. Wu et al., 2018). A previous study reported that adenoviral vector was effective in enhancing EVs release of glutaminase 1(GLS1), a mitochondrial enzyme that is involved in metabolizing glutamine into glutamate, in HeLa cell via overexpression of the two isoforms of GLS1: kidney-type glutaminase (KGA) and glutaminase C (GAC) (B. Wu et al., 2018). The study also indicated that levels of EVs markers: tTG and flotillin-2 were significantly increased in EVs isolated from KGA- and GAC-overexpressed HeLa cells (B. Wu et al., 2018). This study is in agreement with the data presented in this chapter that indicated that human adenoviral gene transfer is effective in producing and enhancing the release of specific EVs (B. Wu et al., 2018)

Previous studies have highlighted the role of exosomes in facilitating the entry of adenoviral vectors into cells with negligible CAR expression (the main cell attachment entry receptor for Ad5 (Freimuth, Philipson, & Carson, 2008)) (Sims, Gu, Krendelchtchikov, & Matthews, 2014). The murine B cell line, A20, which has negligible CAR, were transduced with Ad5 in the presence or absence of exosomes derived from neural stem cells (Sims et al., 2014). Exosomes significantly enhanced the Ad5 entry into A20 cells in a dose-dependent manner (Sims et al., 2014).

Furthermore, It has been found that exosomes plays a dual role in Hepatitis A virus (HAV) and Hepatitis C virus (HCV) infections and immune activation (Longatti, 2015). Both viruses utilized exosomes for viral transmission and hence, evading antibody-mediated immune response (Longatti, 2015). Paradoxically, viral exosome were detected in plasmacytoid dendritic cells (pDCs) which cause innate immune activation and type I interferon production (Longatti, 2015).

It is well accepted that ACE2 is the major counter regulator of the classical RAS through its role in converting Ang II to Ang-(1-7), and Ang I into Ang-(1-9)(Donoghue et al., 2000; Justin L. Grobe et al., 2007). Loss of ACE2 leads to Ang II accumulation in plasma and heart leading to reduced metabolism of plasma Ang II in mice (Gavin Y. Oudit et al., 2010). In contrast, mice treated with recombinant human ACE2 (rhACE2) had reduced plasma and myocardial Ang II

levels and decreased cardiac hypertrophy, myocardial fibrosis, and oxidative stress following 14 days of Ang II infusion (Gavin Y. Oudit et al., 2010). Furthermore, overexpression of ACE2 was demonstrated to significantly attenuate cardiac hypertrophy and fibrosis resulting from 4 weeks of Ang II infusion in Sprague Dawley rats (Huentelman et al., 2005), while inhibition of ACE2 exaggerated the hypertrophic and fibrotic effects of Ang II in (mRen2)27 hypertensive rats (Trask et al., 2010). ACE2 promotes the protective cardiac effect not only via the Ang-(1-7)/Mas axis, but also by converting Ang I into the protective peptide Ang-(1-9)(Donoghue et al., 2000).As we verified that ACE2 could be loaded into EVs, it was of interest to investigate whether ACE2 EV can mediate functional protective effects in cardiomyocytes in vitro. Therefore, H9c2 cardiomyocytes were first treated with ACE2 EV or GFP EV and ACE2 protein expression was successfully detected by western immunoblotting in the cell lysates in cells treated with the ACE2 EVs only, demonstrating that the EVs were taken up into the cells and that ACE2 was delivered. Next, Ang II levels in the cell media of H9c2 cardiomyocytes was evaluated in response to ACE2 EV treatment and the data suggested that ACE2 EV treatment led to reduced Ang II levels, however there was variable levels across each replicate and a conclusive statistical effect was not achieved. This may suggest further optimisation of the protocol to measure Ang II levels is required in this experimental design, for example, since Ang II might be degraded or taken up by the cells between 1h and 24h following exposure, assessment at different time points may reduce variability and provide more conclusive data. The same conclusion might be made for measuring Ang-(1-7) levels where a trend for increased levels was observed in the ACE2 EV group at 24h, however no statistically significant change could be observed between groups at 24h or 48h of sample collection. Therefore, again assessing other time points for assessment and/ or higher Ang II concentrations might be required to better assess Ang II and Ang-(1-7) levels in H9c2 cardiomyocytes following exposure to ACE2 EVs. Another option that worth to tested is to change the treatment time points of ACE2 EV i.e pre-treat the cells for specific times before Ang II stimulation.

A growing range of evidence suggest that EVs can mediate transfer of ACE2 and promote functional effects, including degrading Ang II to Ang-(1-7) (Jinju Wang, Chen, & Bihl, 2020). Human endothelial progenitor cells (EPC) were transduced

with a lentiviral vector expressing ACE2 (ACE2-EPCs) or left un-transfected (control)(Null-EPC), and the culture media were used for coculture experiments. ACE2-EPCs-cultural media (CM) increased ACE2 mRNA expression and reduced Ang II/Ang-(1-7) ratio in Ang II-stimulated endothelial cells (Jinju Wang et al., 2020), the effects were abolished when exosomes were depleted from CM. These data suggesting that exosome-mediated ACE2 transfer to endothelial cells may be responsible for catalysing Ang II to Ang-(1-7). Similarly, endothelial cells treated with ACE2-EPCs-CM demonstrated a reduction in the percentage of mitochondrial fragmentation as well as decreased Nox2 and Nox4 expression levels resulting from Ang II exposure in comparison to Null-EPC-CM treated group. These effects were reduced when exosomes were removed from the culture media (Jinju Wang et al., 2020). In vivo assessment also confirmed the protective role of ACE2-EPCs-exosomes against Ang II-induced endothelial cell apoptosis and dysfunction in R+ mice (mice with high level of Ang II in the plasma)(Jinju Wang et al., 2020). Furthermore, it was demonstrated that the ACE2 inhibitor (DX600), prevented the protective effect of ACE2-EPCs-exosome in Ang II-induced endothelial cell injury, further confirming that the transferred ACE2 was responsible for the protective effect (Jinju Wang et al., 2020).

Whether ACE2 EV could prevent or minimise Ang II-induced cardiomyocyte hypertrophy was investigated in this thesis chapter using the H9c2 cardiomyocyte model of Ang II-induced hypertrophy (Ayyappan Prathapan et al., 2014). H9c2 cells were left untreated or stimulated with AngII and then incubated with either ACE2 EV or GFP EV and the hypertrophy response was assessed. Significantly greater cardiomyocyte cell surface area was observed in the Ang II alone treatment group compared to control unstimulated cells, in agreement with previous studies (A Prathapan & Raghu, 2018; Ayyappan Prathapan et al., 2014). In contrast, in the Ang II and ACE2 EV treated group there was no significant increase in cell size compared to control unstimulated cardiomyocytes. In the Ang II and GFP EV treated group greater cardiomyocyte size was observed in comparison to control, although it did not reach significance. These data suggested that ACE2 EV may diminish the hypertrophic response in Ang II stimulated cardiomyocytes and therefore that they may be protective against Ang II-induced cardiomyocyte hypertrophy. These data are consistent with previous research that have suggested functional protective roles

of ACE2 EV/exosomes in recipient cells in different disease models (Jinju Wang et al., 2020; Canhao Wu et al., 2022). It remains to be determined in studies with ACE2 EVs as to whether both Ang-(1-7) and Ang-(1-9) can contribute to the therapeutic effects. For example, Ang-(1-9) is also reported to elicit an anti-hypertrophic effect against Ang II-induced H9c2 cardiomyocyte hypertrophy (Flores-Muñoz et al., 2012) and that it is also protective in vivo. However, whether the cardiac protective effects of ACE2 EVs are mediated mainly via Ang II reduction or Ang-(1-7) or Ang-(1-9) production or both requires further investigation. It also remains to be investigated whether any endogenous protective effects of ACE2 are mediated through its transport in EVs.

Next, AT_1R mRNA gene expression as well as AT_2R and Mas1 were assessed to further understand the possible mechanisms of the anti-hypertrophic effect of ACE2 EV. The finding revealed a trend for downregulation of AT_1R expression in ACE2 EV treated cardiomyocytes in comparison to the Ang II group. However, these studies require further n's to be conclusive. No differences in AT_2R or Mas1 gene expression were observed between groups. It has previously been reported that Ang II treatment significantly increases the mRNA expression of the AT_1R in a neuronal cell line (CATH.a), an effect that was inhibited by the AT_1R blocker (Losartan)(D. Liu et al., 2008). Some reports also indicated that Ang II can increase the protein expression of AT_1R in CATH.a cell line (Mitra et al., 2010). Both protein and mRNA expressions of AT_2R was significantly increased in rat kidney in response chronic Ang II infusion independently of the elevated blood pressure(Vázquez et al., 2005) .

TGFβ1 role in mediating Ang II-induced cardiomyocyte hypertrophy was mentioned in (section 3.3) (Schultz et al., 2002) and therefore its' gene expression was also evaluated for the experimental groups. There was no marked change in TGFβ1 observed between group and more n's required to reach final conclusion.

5.5 Limitations of the Study

As indicated in a previous chapter of this project regarding Ang II and Ang-(1-7) measurements, using higher Ang II and ACE2 EV concentration and selecting more time points between 1h and 24h for sample collections might provide better understanding of the role of ACE2 EV in degrading Ang II to Ang-(1-7).

Moreover, Ang-(1-9) is also another cardioprotective peptide produced from Ang I by ACE2 and therefore that could be measured in response to exogenous Ang I stimulation and this may further enhance understanding of the protective role of ACE2 EVs. Also, more n's for RAS receptors and TGFβ1 gene expression should be considered for future work.

A further limitation is that the in vivo effects of ACE2 EVs on Ang II-induced cardiac functional and structural change were not investigated. The Ang II infusion model of hypertension and cardiac remodelling would be an ideal model to assess the effects of ACE2 EVs as explained in (section 4.1.3) (J. L. Grobe et al., 2007), although it is likely that this would require selection of an appropriate concentration of EVs, and consideration as to whether single dose or continuous infusion would be required.

5.6 Summary

In summary, using adenoviral gene transfer of ACE2, ACE2 EVs were successfully isolated, and purified from H9c2 cardiomyocytes and characterized. The data suggest that this approach can be used to load ACE2 into EVs/exosomes. Protein expression was detected in ACE2 EV treated cardiomyocyte which indicated that the EVs were taken up by the cells and that ACE2 EVs diminished the hypertrophic effect resulting from Ang II treatment of H9c2 cardiomyocytes. Further work is required to determine whether ACE2 EV could be therapeutic in vivo in the setting of cardiac disease.

Chapter 6. General discussion

It is estimated that there are more than 900,000 people living with heart failure in the UK according to BHF report 2021 (BHF analysis of ONS Nomis (England & Wales), NRS (Scotland) and NISRA - 2021 mortality data). Heart failure is caused by continuous exposure to long term cardiac stress or injury that includes pressure or volume overload (e.g., high blood pressure), myocardial infarction, and inherited diseases (Tham, Bernardo, Ooi, Weeks, & McMullen, 2015). It is accepted that Ang II release increases with the progression of heart failure (Serneri et al., 2001) and chronic exposure to Ang II leads to hypertension, left ventricular hypertrophy, contractile dysfunction and eventually development of heart failure (Wollert & Drexler, 1999). Thus, despite the availability of ARBs and ACE inhibitors, agents that have been used extensively in various cardiovascular disease, finding other therapeutic agents that can counteract the harmful effect of the classical RAS is still in high demand. The counterregulatory RAS therefore remains a novel target to investigate to better characterized components and understand the best therapeutic approach for them. Therefore, in this experimental work, the protective role of two enzymes (PRCP and ACE2) that belong to the counter-regulatory arm of RAS has been assessed using different approach.

6.1 Ad-PRCP degraded Ang II and increased Ang-(1-7) in H9c2 cardiomyocyte and attenuated cardiac hypertrophy in vitro and cardiac dysfunction in vivo.

Previous studies investigated the role of PRCP on cardiac hypertrophy, remodelling, and function focused on using genetically modified animals such as the spontaneously hypertensive rat (Jinyao Liu, Hakucho, & Fujimiya, 2015; Marangoni, Santos, & Piccolo, 2014) and PRCP knockout mice (Maier, Schadock, Haber, Wysocki, Ye, Kanwar, Flask, Yu, Hoit, et al., 2017). However, none of these studies evaluated the effect of PRCP overexpression on cardiac hypertrophy via a gene therapy approach. Recently, (Hao et al., 2020) assessed the role of PRCP overexpression via adenoviral mediated gene therapy on heart function and remodelling in an ischemic/ reperfusion rat model, but not in response to exogenous angiotensin II stimulation.

In this work, the role of PRCP overexpression via adenoviral-mediated gene therapy on Ang II-induced cardiac dysfunction and remodelling was studied both in vitro and in vivo. Therefore, the first goal was to generate an adenoviral

vector mediated-gene transfer of PRCP and study its effect on cardiac hypertrophy in response to exogenous Ang II stimulation.

Initially, adenoviral gene transfer vector expressing rat prolylcarboxypeptidase (Ad-PRCP) was generated, purified and titered using standard techniques (Luo et al., 2007). Enhanced mRNA expression of PRCP in cardiomyocyte as well as protein expression in rat's liver were observed in response to Ad-PRCP treatment. Next, PRCP overexpression on HeLa cells via adenoviral vector showed marked decreased in Ang II levels at 24 h of stimulation, but not at time points between 5-60 minutes, compared to Ad-GFP and to Ang II only treated groups. Based on this observation, the effect of Ad-PRCP on Ang II levels was assessed in H9c2 cardiomyocyte at 24h and 48h of Ang II stimulation. The data revealed a trend, that was however not significant, toward reduced Ang II levels following 24h of Ang II stimulation in Ad-PRCP transduced cardiomyocyte in comparison to to Ad-GFP and Ang II only treated cardiomyocytes. Considering multiple reports suggesting that PRCP metabolises Ang II into the cardioprotective Ang-(1-7) (Karamyan & Speth, 2007; J Mallela et al., 2008; J. Mallela et al., 2009), Ang-(1-7) levels were also evaluated in the same samples. The data showed significantly greater Ang-(1-7) levels in Ad-PRCP transduced cardiomyocytes following 48h of Ang II stimulation compared to control (non-treated) group. PRCP activity has acidic pH optima of (~ 5.0)(Maier, Schadock, Haber, Wysocki, Ye, Kanwar, Flask, Yu, Hoit, et al., 2017) , however, it has also retained significant activity at natural pH(Kumamoto et al., 1981) and can hydrolyse Ang II into Ang-(1-7) at 63% of the rate at pH 5.0 (Skidgel & Erdös, 1998). Furthermore, it has been reported that at acidic pH, PRCP cleaved Ang II and Ang III faster than an N-blocked dipeptide derivative representing their COOH terminal end (Odya et al., 1978). Another study indicated that PRCP activity favoured acidic pH when metabolizing short synthetic peptide substrates, but showed significant activity at neutral pH when hydrolysing longer naturally occurring peptides such as Ang II, Ang III, and bradykinin (Karamyan & Speth, 2007). However, the data presented in this work showed significantly greater Ang-(1-7)/Ang II ratio in H9c2 cardiomyocyte in response to Ad-PRCP overproduction which might suggest a potential cardioprotective role of PRCP.

Next, the effect of PRCP overexpression on cardiomyocyte hypertrophy following Ang II stimulation was assessed. The finding showed that Ang II induced cardiomyocyte hypertrophy in Ang II and Ad-GFP groups, but not in Ad-PRCP group, in comparison to control. These data indicated an anti-hypertrophic role of PRCP against Ang II in H9c2 cardiomyocytes. Considering the ELISA results of this work that showed PRCP can convert Ang II into Ang-(1-7), which are consistent with previous reports (Maier, Schadock, Haber, Wysocki, Ye, Kanwar, Flask, Yu, Hoit, et al., 2017; J. Mallela et al., 2009), it suggests that this may underly the reason for the observed anti-hypertrophic effect. While there are limited data highlighting the role of PRCP on cardiac hypertrophy in vitro, there have been some studies that suggested a relationship between cardiac hypertrophy and PRCP deficiency. Posterior wall thickness/end-diastolic diameter (EDD) ratio was significantly higher in PRCP $^{gt/gt}$ (GST090) mice versus wild type control (Maier, Schadock, Haber, Wysocki, Ye, Kanwar, Flask, Yu, Hoit, et al., 2017). The heart weight/body weight ratio was also greater in PRCP $^{gt/gt}$ mice as compared to WT. However, following 3 weeks of Ang II infusion, the cardiac hypertrophy increased in both groups (PRCP $^{gt/gt}$ and WT mice) without significant difference between groups (Maier, Schadock, Haber, Wysocki, Ye, Kanwar, Flask, Yu, Hoit, et al., 2017). Furthermore, PRCP mRNA expression was significantly decreased in spontaneously hypertensive (SHR) rats with left ventricular hypertrophy, but not in hypertensive (2 kidney-1 clip) rats, at 5 and 16-week old as compared with age-matched Wistar controls (Marangoni et al., 2014). The protein expression of PRCP was also reduced in 16-week old SHR compared to Wistar rats at the same age (Marangoni et al., 2014). Both studies (Marangoni et al., 2014) and (Maier, Schadock, Haber, Wysocki, Ye, Kanwar, Flask, Yu, Hoit, et al., 2017) suggested that the association between PRCP and cardiac hypertrophy might be independent of angiotensin II. However, none of these in vivo studies overexpressed PRCP and assessed its effect of cardiac function and remodelling.

Therefore, the role of PRCP overexpression via adenoviral gene transfer on Ang II-dependent hypertension and cardiac hypertrophy has been evaluated on Wistar Kyoto rats. The major findings from this study demonstrated that significantly lower EF% and FS% in Ang II group after 3 week compared to Ad-PRCP treated animals at the same time point. There was no significant difference in cardiac

function between Ang II and Ad-LacZ groups. These data suggested that PRCP might be protective against Ang II-induced impaired cardiac function. Although this observation needs further studies as Ang II group at the end point did not significantly change compared to baseline and to control group.

However, this study also indicated that PRCP did not reduce systolic blood pressure or cardiac hypertrophy (as shown by heart weight/body weight ratio) resulting from long term infusion of Ang II. The cardiomyocyte analysis showed that PRCP diminished the hypertrophic effect of Ang II, however, a similar effect was observed in Ad-GFP treated animals. Another study using ischemia with reperfusion rat model reported that overexpression of PRCP via adenoviral vector increased left ventricular fractional shortening and improved other cardiac function parameters (left ventricular systolic pressure (LVSP), left ventricular end-diastolic pressure (LVEDP), and maximal ascending and descending rate of left ventricular pressure ($\pm dp/dt$), but did not affect the mean arterial blood pressure nor the heart rate (Hao et al., 2020). The exact mechanism of how PRCP prevents Ang II-dependant cardiac dysfunction needs further investigation. A theoretical explanation is that PRCP shuttles Ang II metabolism towered the cardioprotective Ang-(1-7) formation. Several reports have indicated that Ang-(1-7) improved heart function and attenuated cardiac fibrosis and hypertrophy resulting from Ang II infusion (McCollum et al., 2012; Vaibhav B Patel et al., 2015). Infusion of Ang-(1-7) also did not affect blood pressure in response to Ang II infusion in Sprague-Dawley rats despite being cardioprotective (McCollum et al., 2012), which comes in agreement with this study of PRCP effect. However, the heart and plasma levels for both peptides, Ang II and Ang-(1-7), have not been assessed in the in vivo part of this study.

PRCP has been linked to blood pressure regulation (Marangoni et al., 2014; Yan Zhang et al., 2009). In renovascular hypertensive Sprague-Dawley rats (Goldblatt two-kidney, one-clip (2K1C)) model, long term treatment with rutaecarpine attenuated high blood pressure and mesenteric artery remodelling which might be related to upregulation of PRCP expression in the circulation and small arteries (Qin et al., 2009). Furthermore, PRCP gene-trap $^{(gt/gt)}$ mice showed significant elevation in blood pressure, and their plasma analysis indicated high thrombin generation time (Adams et al., 2011). This was associated with increased uncoupled eNOS and higher reactive oxygen species (ROS) in kidney

and aortic tissues of PRCP $^{gt/gt}$ (Adams et al., 2011). Interestingly, inhibition of ROS activity in the mitochrondria via antioxidants (mitoTEMPO, apocynin, Tempol) abolished the hypertensive effect as well as the time to arterial thrombosis in PRCP $^{gt/gt}$ mice which suggest that the vascular dysfunction and the prothrombotic phenotype of these animal related to high ROS epression in the vascular cells and tissues (Adams et al., 2011).

Another possible mechanism for the cardioprotective role of PRCP is via degradation or inactivation of Ang III which has similar action to Ang II via binding to AT_1R and causing direct cardiac dysfunction and hypertrophy. Inactivation of Ang III can also lead to decrease aldosterone secretion and sodium reabsorption (De Hert, Bracke, Lambeir, et al., 2021).

To further investigate the mechanism of PRCP's protective role in cardiac function and fibrosis, the mRNA expression of angiotensin receptors (AT_1R, AT_2R, and Mas_1R) in rat's heart have been evaluated in this study. However, there was no marked effect of Ad-PRCP on the expression levels of these receptors in heart tissues. Currently, there is no data evaluated the mRNA expression of AT_1R, AT2R or Mas1R in response to PRCP overexpression. However, PRCP can form Ang-(1-7) and its expression could be altered via ARBs such as olmesartan, a selective AT_1R blocker. Levels of Ang-(1-7) as well as Mas1 mRNA expression were significantly increased in Lewis rats with heart failure treated with Olmesartan (Sukumaran et al., 2012). Overexpression of AT_2R via adenoviral vector (Ad-AT_2R) in coronary artery endothelial cells of mouse increased PRCP mRNA expression by 1.7-fold as well as protein expression of PRCP and bradykinin by 2.5-fold and 2.2-fold respectively in comparison to endothelial cells treated with Ad-GFP (control) (L. Zhu et al., 2010b). Blocking PRCP with a small interfering RNA (siRNA) significantly inhibited bradykinin release (L. Zhu et al., 2010b).

6.2 Future Perspectives for PRCP study

The in vitro investigation of cardiac hypertrophy has been conducted on H9c2 rat cardiomyocyte only. Even though these cardiomyocytes have been shown to be reliable animal-free alternative model and are widely used in cardiac research in vitro (Nuamnaichati, Parichatikanond, & Mangmool, 2022; Pang et al., 2004) , H9c2 cardiomyocyte are a proliferative cell line that lack the beating ability and

might not mimic the in vivo setting as primary cell culture (Kimes & Brandt, 1976). In addition, there were difficulties in detecting the mRNA of cardiac hypertrophy markers in H9c2 cardiomyocyte as well as ACE and ACE2 in consistent manner in this study. Therefore, studying the antihypertrophic effect of PRCP using another reliable cardiac cell should be considered in future investigation. Neonatal rat cardiomyocytes (NRCM) are non-proliferative, although they might perform a few divisions early in culture (Schwarzer, 2016), and can continue to beat up to 20h post plating (Ehler, Moore-Morris, & Lange, 2013). NRCM have been used extensively in the assessment of cardiac pathology such as hypertrophy, ischemia, hypoxia, electrophysiological characteristics of the heart and toxicity of various materials (Chlopcikova et al., 2001; Van Kesteren et al., 1997). NRCM can be isolated from the heart of 1- to 3-days old rats by several steps of enzymatic digestion with collagenase of cardiac tissue(Schwarzer, 2016). The contraction ability for NRCMs makes them a good candidate in vitro model for investigating the circadian rhythms of the heart. NRCM displayed functional rhythmicity which could be altered in response to foreign compounds treatment such as doxorubicin, an anticancer agent with cardiotoxic side effect (Bastiaan et al., 2017). Both NRCM and H9c2 showed significant hypertrophic response following 48h of angiotensin II stimulation (Watkins et al., 2011). Therefore, it will be interesting to study the antihypertrophic effect of PRCP on the primary NRCM as they reflect more characteristics of the in vivo heart study. Adult rat cardiomyocytes (ARCM) could also be another option to consider for investigating the cardiac hypertrophy as they could be cultured for longer time than NRCM and it might be isolated from hypertensive rat model (Ehler et al., 2013). However, ARCMc are more sensitive to calcium containing media and its isolation is difficult and time consuming as it takes longer time to breed rats to adulthood and it might yield small cell number due to the fact that they do not proliferate (Bastiaan et al., 2017).

The fact that there are multiple enzymes involved in converting Ang II into Ang-(1-7) demonstrates the complexity of the renin angiotensin system and the need for further investigations to reveal the role of each enzyme at local and circulating levels. In a kidney study of ACE2 gene deletion mice, it has been reported that Ang II degraded into Ang-(1-7) independently of ACE2 (Nadja Grobe et al., 2013). Another study reported that conversion of Ang II into Ang-(1-

7) in the kidney is mainly mediated by ACE2, while prolyl endopeptidase metabolized Ang II into Ang-(1-7) in the circulation and in the lung (Peter Serfozo et al., 2020).

It has been repeatedly reported that PRCP has optimal activity under acidic pH, therefore, it would be rational to investigate the role of PRCP on degrading Ang II to Ang-(1-7) as well as on preventing cardiomyocyte hypertrophy under hypoxic conditions. Hypoxia could be initiated in vitro via utilizing hypoxic chamber or an anaerobic glove box with no-glucose media and incubation at 37 °C with 1% O_2, 90-94% N_2, and 5% CO_2 to mimic hypoxic status (Y. Li, Ren, Xia, Wei, & Xi, 2020; L. Sun et al., 2018). However, NRCM might be more suitable for studying metabolic changes under hypoxic condition as they displayed more protein expression levels of autophagy markers (Beclin-1 and LC3II) than H9c2 cardiomyocyte in response to hypoxia/reoxygenation conditions (Cao et al., 2014). In addition, it would be interesting to study the role of other catalytic enzymes (ACE2 and prolyl endopeptidase) that are also reported to play a role in degrading Ang II into Ang-(1-7) and compare them to PRCP catalytic efficiency under both hypoxic and normoxic conditions. This might help in understanding the preferred therapeutic enzyme for heart specific heart condition. For instance, myocardial ischemia (occurs when the myocardial demand for substrates exceeds that of supply (De Lemos & Omland, 2017)) or myocardial hypoxia (reduced oxygen supply to myocardium (P.-S. Chen et al., 2020)) are perhaps among the most occurring metabolic disruption experienced by the heart, and are accompanied by marked reduce in cellular pH (Milliken, Ciesla, Nadtochiy, & Brookes, 2023). It has been reported that acute myocardial infarction is associated with the development of a considerable metabolic acidosis, about 66% of 50 patients with AMI developed significant acidosis) (Neaverson, 1966). In such cases, it will be interesting to investigate which enzyme of the counter regulatory axis of RAS can be more protective considering that the optimal activity of PRCP is at pH 5.0, while the activity of ACE2 was reported absent below pH 5.5 (Maier, Schadock, Haber, Wysocki, Ye, Kanwar, Flask, Yu, Hoit, et al., 2017). Furthermore, PRCP was found to be protective against myocardial I/R injury in rats, a condition that might accompanied with metabolic acidosis (Hao et al., 2020).

Nonetheless, in case of obesity PRCP might not be the preferred option, theoretically, to counteract the harmful RAS effects as it has been shown to induce food intake and promote obesity in mice which is a risk factor on development of CVD (Wallingford, Perroud, Gao, Coppola, Gyengesi, Liu, Gao, Diament, Haus, & Shariat-Madar, 2009). Furthermore, PRCP plasma levels were found to be higher in obese and diabetic patients and therefore, investigators targeting PRCP inhibitors as a candidate anti-obesity agent and to regulate food intake for diabetic patients (Xu et al., 2012).

However, there were no reported studies that assessed the interaction between those enzymes on the heart level and it would be interesting to evaluate their catalytic efficiency using a gene therapy approach.

Furthermore, in addition to evaluating mRNA levels of angiotensin receptors, it will be interesting to measure the protein expression for those receptors as well as other RAS peptides, such as ACE and ACE2, protein and mRNA expression following transducing with Ad-PRCP.

As previously mentioned, for any future in vitro assessment of the catalytic efficiency of PRCP it is important to consider more selected time points for collecting the samples for ELISA analysis taking in the account that PRCP showed catalytic activity on endothelial cells as early as 2h of stimulation and/or incubation (De Hert, Bracke, Pintelon, et al., 2021).

Whether or not the antihypertrophic effect of PRCP is mediated via Mas receptors could be determine by using Mas receptor antagonist (A779)(Flores-Muñoz et al., 2012) in Ad-PRCP transduced cardiomyocyte that might further enhance our understanding about the underying mechanism.

The in vivo data of this study suggested that PRCP overexpression is protective against angiotensin II-induced cardiac dysfunction and fibrosis and might be a potential therapeutic target for heart disease. However, these finding need to be confirmed with further investigation using larger size of animal in each group. For instance, the role of PRCP on mitigating myocardial ischemia/reperfusion injury has been studied in vivo using 20 rats in each group (Hao et al., 2020). Such large group of study would also provide sufficient samples to analyse Ang II and ang-(1-7) levels in the heart and in the circulation as well as protein and mRNA expression of cardiac Mas receptors and other RAS components such as

ACE2, ACE, AT1R, and AT2R (Klimas et al., 2015; J. Wang et al., 2017). Furthermore, blocking the left ventricle Mas receptors via A779 (R. A. Santos et al., 1994), and assessment of bradykinin levels in myocardial tissues and plasma (Hao et al., 2020) might be beneficial to reveal the underline mechanism of PRCP's cardioprotective role.

6.3 ACE2 can be loaded into EVs and exhibited cardioprotective effect in vitro

The capability of extracellular vesicles to transfer functional cargos (RNA, lipid, and protein) between cells has made them a potential therapeutic target for various types of disease including cardiovascular disease. Nonetheless, the use of EVs in clinical setting as a biomarkers vehicle for diagnostic application has been already established (Sonoda et al., 2009; Hua Zhou et al., 2006). Furthermore, it has been accepted that EVs can carry functional RAS components and elicit the consequent effect (Han et al., 2021).

The role of ACE2 on cardiovascular disease has been studied extensively using a gene therapy approach (Díez-Freire et al., 2006; Dong et al., 2012; Y. X. Zhao et al., 2010), but to date the role of ACE2 EVs on cardiac pathology has not been sufficiently investigated. Therefore, the aim of this part of the study was to generate ACE2 EVs and study their effect on cardiomyocyte hypertrophy following Ang II stimulation in vitro.

Extracellular vesicles have been generated from un-transduced H9c2 cardiomyocyte (control) or transduced with either Ad-ACE2, or Ad-GFP and isolated using ultracentrifugation (Momen-Heravi, 2017). Next, characterization of EVs via NTA showed that the size of all conditions were within the exosome size range (Konoshenko et al., 2018), with significantly higher EVs yield in Ad-ACE2 transduced cardiomyocyte compared to other groups. The protein expression of two EVs biomarkers (CD63 and TsG101) were detectable in ACE2 EVs and GFP EVs. ACE2 protein expression was also detected in EVs isolated from Ad-ACE2 transduced cardiomyocyte indicating that the secreted EVs encapsulating ACE2. Further characterization of ACE2 EVs revealed that they have greater ACE2 catalytic activity than other groups. In addition, ACE2 protein expression was also detected in H9c2 cardiomyocyte treated with ACE2 EVs only, indicating that the EVs were taken into the cells. These data suggested that

overexpression of ACE2 via adenoviral vector in a cell model might be potential method to produce ACE2 EVs secreted from the cells into the cell culture media for purification as therapeutic delivery vectors that omit the need to deliver viral gene therapy vectors in vivo to patients.

Next, the role of ACE2 EVs on Ang II metabolism was assessed and the data indicated that ACE2 EVs can reduce Ang II levels. However, there were variable responses from each replicate which suggested the need for further investigation. There was no marked change observed on the levels of Ang-(1-7) in this study. Finally, whether ACE2 EVs is protective against Ang II-dependent hypertrophy was investigated and revealed that ACE2 EVs diminished H9c2 cardiomyocyte hypertrophy resulting from Ang II. However, these studies were conducted during the pandemic.

6.4 Future Perspectives for ACE2 EVs study

The EVs isolation method used in this work is differential ultracentrifugation. Even though this was the first method utilized for EVs isolation and remain one of the most widely technique used for the isolation process, it's not without drawbacks (Doyle & Wang, 2019). Differential ultracentrifugation is time consuming and requires large volume of culture media or samples and longer centrifugation for more than 4h may results in significant contamination with soluble proteins (Doyle & Wang, 2019; Zaborowski, Balaj, Breakefield, & Lai, 2015). In addition, ultracentrifugation yields enrichment of exosome but it may also co-pellet some other larger proteins from the extracellular space such as lipoproteins, fatty acid synthase, viral particles and HSPG (Zaborowski et al., 2015). Therefore, looking for an alternative isolation method that could save time and allow more EVs concentration should be considered for future experiments. Size exclusion chromatography is another technique that can isolate exosomes from other EVs based on their size. An example of this approach is iZON science that provides qEV Exosome Isolation Kit which can isolate highly purified exosomes based on size exclusion chromatography within relatively shorter time (as short as 15 min) and smaller volume of samples (Vogel et al., 2016). However, the lack of standard method for isolation, analysis, and characterization of EVs is still an outstanding issue in EVs research filed that need further investigation.

Furthermore, although the ELISA results of Ang II showed reduced levels in response to ACE2 EVs treatment, this data cannot be concluded and needs to be confirmed by using more replicates in the future study. Moreover, using higher Ang II concentration, for example 1µm, might provide clearer Ang-(1-7) signalling and better understanding for the role of ACE2 EVs in Ang II metabolism. In addition, all the suggestions stated previously for the Ad-PRCP in vitro prospective work could be also applied to ACE2 EVs to further investigate their protective role of in cardiomyocytes hypertrophy in vitro.

Finally, as this study showed that ACE2 EVs prevented cardiomyocyte hypertrophy in vitro, it will also be interesting to study the protective role of ACE2 EVs in Ang II-dependent cardiac hypertrophy and dysfunction in animal model, for example ACE2 knockout mice (Gavin Y Oudit, Crackower, Backx, & Penninger, 2003). Furthermore, the protective effect of ACE2 EVs could be also assessed in response to other pressor stimuli such as epinephrine and norepinephrine (Rapacciuolo et al., 2001), transverse aortic constriction (TAC) animal model (Jian Wang & Yang, 2012), two-kidney, one clip and one-kidney, hypertensive animal model (Wiesel, Mazzolai, Nussberger, & Pedrazzini, 1997) as well as spontaneously hypertensive rat.

A study indicated that EVs isolated from human embryonic kidney cells showed very limited immunogenicity and toxicity when administered intravenously and intraperitoneally into mice for 3 weeks (X. Zhu et al., 2017). Such report indicated that EVs might be an important potential candidate for drug delivery(Meng et al., 2020).

6.5 Summary

The delivery of both enzymes, PRCP via adenoviral gene transfer vector and ACE2 via extracellular vesicles, exhibited potential protective effects against Ang II-induced cardiac remodelling. Further studies needed to determine the best cardioprotective enzyme for specific cardiac disease condition and the preferred approach for therapeutic protein delivery.

References

Adachi, Y., Saito, Y., Kishimoto, I., Harada, M., Kuwahara, K., Takahashi, N., . . . Tanimoto, K. (2003). Angiotensin II type 2 receptor deficiency exacerbates heart failure and reduces survival after acute myocardial infarction in mice. *Circulation, 107*(19), 2406-2408.

Adams, G. N., LaRusch, G. A., Stavrou, E., Zhou, Y., Nieman, M. T., Jacobs, G. H., . . . Schmaier, A. H. (2011). Murine prolylcarboxypeptidase depletion induces vascular dysfunction with hypertension and faster arterial thrombosis. *Blood, 117*(14), 3929-3937. doi:10.1182/blood-2010-11-318527

Adams, G. N., Stavrou, E. X., Fang, C., Merkulova, A., Alaiti, M. A., Nakajima, K., . . . Schmaier, A. H. (2013). Prolylcarboxypeptidase promotes angiogenesis and vascular repair. *Blood, 122*(8), 1522-1531. doi:10.1182/blood-2012-10-460360

Ainscough, J. F., Drinkhill, M. J., Sedo, A., Turner, N. A., Brooke, D. A., Balmforth, A. J., & Ball, S. G. (2009). Angiotensin II type-1 receptor activation in the adult heart causes blood pressure-independent hypertrophy and cardiac dysfunction. *Cardiovascular research, 81*(3), 592-600.

Alba, R., Baker, A. H., & Nicklin, S. A. (2012). Vector Systems for Prenatal Gene Therapy: Principles of Adenovirus Design and Production. In *Methods in molecular biology (Clifton, N.J.)* (Vol. 891, pp. 55-84). Totowa, NJ: Humana Press.

Albrecht, D., Nitschke, T., Von Bohlen, O., & Halbach, O. (2000). Various effects of angiotensin II on amygdaloid neuronal activity in normotensive control and hypertensive transgenic [TGR (mREN‐2) 27] rats. *The FASEB journal, 14*(7), 925-931.

Alenina, N., Böhme, I., Bader, M., & Walther, T. (2015). Multiple non-coding exons and alternative splicing in the mouse Mas protooncogene. *Gene, 568*(2), 155-164.

Alghamri, M. S., Weir, N. M., Anstadt, M. P., Elased, K. M., Gurley, S. B., & Morris, M. (2013). Enhanced Angiotensin II-Induced Cardiac and Aortic Remodeling in ACE2 Knockout Mice. *Journal of cardiovascular pharmacology and therapeutics, 18*(2), 138-151. doi:10.1177/1074248412460124

Aloul, B. A., LI, J. M., Benditt, D., & Tholakanahalli, V. (2006). Atrial fibrillation associated with hypokalemia due to primary hyperaldosteronism (Conn's syndrome). *Pacing and clinical electrophysiology, 29*(11), 1303-1305.

Alzhrani, G. N., Alanazi, S. T., Alsharif, S. Y., Albalawi, A. M., Alsharif, A. A., Abdel‐Maksoud, M. S., & Elsherbiny, N. (2021). Exosomes: Isolation, characterization, and biomedical applications. *Cell biology international, 45*(9), 1807-1831.

Ambühl, P., Felix, D., & Khosla, M. C. (1994). [7-D-ALA]-angiotensin-(1–7): selective antagonism of angiotensin-(1–7) in the rat paraventricular nucleus. *Brain research bulletin, 35*(4), 289-291.

Ames, M. K., Atkins, C. E., & Pitt, B. (2019). The renin‐angiotensin‐aldosterone system and its suppression. *Journal of veterinary internal medicine, 33*(2), 363-382.

Anand, S. S., Islam, S., Rosengren, A., Franzosi, M. G., Steyn, K., Yusufali, A. H., . . . Yusuf, S. (2008). Risk factors for myocardial infarction in women and men: insights from the INTERHEART study. *European heart journal, 29*(7), 932-940.

Ancion, A., Tridetti, J., Nguyen Trung, M.-L., Oury, C., & Lancellotti, P. (2019). A Review of the Role of Bradykinin and Nitric Oxide in the Cardioprotective Action of Angiotensin-Converting Enzyme Inhibitors: Focus on Perindopril. *Cardiology and therapy, 8*(2), 179-191. doi:10.1007/s40119-019-00150-w

Armstrong, R. A. (2014). When to use the B onferroni correction. *Ophthalmic and Physiological Optics, 34*(5), 502-508.

Arslan, F., Lai, R. C., Smeets, M. B., Akeroyd, L., Choo, A., Aguor, E. N., . . . Pasterkamp, G. (2013). Mesenchymal stem cell-derived exosomes increase ATP levels, decrease oxidative stress

and activate PI3K/Akt pathway to enhance myocardial viability and prevent adverse remodeling after myocardial ischemia/reperfusion injury. *Stem cell research, 10*(3), 301-312.

Ascher, P., Large, W., & Rang, H. (1979). Studies on the mechanism of action of acetylcholine antagonists on rat parasympathetic ganglion cells. *The Journal of physiology, 295*(1), 139-170.

Atasheva, S., & Shayakhmetov, D. M. (2022). Cytokine responses to adenovirus and adenovirus vectors. *Viruses, 14*(5), 888.

Atchison, R., Casto, B. C., & Hammon, W. M. (1966). Electron microscopy of adenovirus-associated virus (AAV) in cell cultures. *Virology, 29*(2), 353-357.

Atchison, R. W., Casto, B. C., & Hammon, W. M. (1965). Adenovirus-associated defective virus particles. *Science, 149*(3685), 754-756.

Averill, D. B., Ishiyama, Y., Chappell, M. C., & Ferrario, C. M. (2003). Cardiac angiotensin-(1-7) in ischemic cardiomyopathy. *Circulation, 108*(17), 2141-2146.

Bader, M. (2010). Tissue Renin-Angiotensin-Aldosterone Systems: Targets for Pharmacological Therapy. *Annual review of pharmacology and toxicology, 50*(1), 439-465. doi:10.1146/annurev.pharmtox.010909.105610

Bailey, J., Owen, C., & Hutchinson, I. (2022). Modernizing Medical Research to Benefit People and Animals.

Baker, K. M., & Dostal, D. E. (1992). Angiotensin II stimulation of left ventricular hypertrophy in adult rat heart: mediation by the AT1 receptor. *American journal of hypertension, 5*(5_Pt_1), 276-280.

Barré-Sinoussi, F., & Montagutelli, X. (2015). Animal models are essential to biological research: issues and perspectives. *Future science OA, 1*(4), FSO63-FSO63. doi:10.4155/fso.15.63

Barry, S. P., Davidson, S. M., & Townsend, P. A. (2008). Molecular regulation of cardiac hypertrophy. *The international journal of biochemistry & cell biology, 40*(10), 2023-2039.

Basso, N., & Terragno, N. A. (2001). History About the Discovery of the Renin-Angiotensin System. *Hypertension (Dallas, Tex. 1979), 38*(6), 1246-1249. doi:10.1161/hy1201.101214

Bastiaan, C., Dierickx, P., Crnko, S., Doevendans, P. A., Vos, M. A., Geijsen, N., . . . van Laake, L. W. (2017). Neonatal rat cardiomyocytes as an in vitro model for circadian rhythms in the heart. *Journal of molecular and cellular cardiology, 112*, 58-63.

Basu, R., Poglitsch, M., Yogasundaram, H., Thomas, J., Rowe, B. H., & Oudit, G. Y. (2017). Roles of angiotensin peptides and recombinant human ACE2 in heart failure. *Journal of the American College of Cardiology, 69*(7), 805-819.

Batty, C. J., Heise, M. T., Bachelder, E. M., & Ainslie, K. M. (2021). Vaccine formulations in clinical development for the prevention of severe acute respiratory syndrome coronavirus 2 infection. *Advanced drug delivery reviews, 169*, 168-189.

Beevers, G., Lip, G. Y., & O'Brien, E. (2001). The pathophysiology of hypertension. *Bmj, 322*(7291), 912-916.

Bellomo, R., Wunderink, R. G., Szerlip, H., English, S. W., Busse, L. W., Deane, A. M., . . . Young, P. J. (2020). Angiotensin I and angiotensin II concentrations and their ratio in catecholamine-resistant vasodilatory shock. *Critical Care, 24*(1), 1-8.

Bernstein, K. E., Ong, F. S., Blackwell, W.-L. B., Shah, K. H., Giani, J. F., Gonzalez-Villalobos, R. A., . . . Fuchs, S. (2013). A Modern Understanding of the Traditional and Nontraditional Biological Functions of Angiotensin-Converting Enzyme. *Pharmacological reviews, 65*(1), 1-46. doi:10.1124/pr.112.006809

Berry, C., Touyz, R., Dominiczak, A. F., Webb, R. C., & Johns, D. G. (2001). Angiotensin receptors: signaling, vascular pathophysiology, and interactions with ceramide. *American Journal of Physiology - Heart and Circulatory Physiology, 281*(6), 2337-2365. doi:10.1152/ajpheart.2001.281.6.H2337

Bertoldi, K., Cechinel, L. R., Schallenberger, B., Corssac, G. B., Davies, S., Guerreiro, I. C. K., . . . Siqueira, I. R. (2018). Circulating extracellular vesicles in the aging process: impact of aerobic exercise. *Molecular and cellular biochemistry, 440*(1), 115-125.

Bindom, S. M., Hans, C. P., Xia, H., Boulares, A. H., & Lazartigues, E. (2010). Angiotensin I–converting enzyme type 2 (ACE2) gene therapy improves glycemic control in diabetic mice. *Diabetes, 59*(10), 2540-2548.

Blaese, R. M., Culver, K. W., Miller, A. D., Carter, C. S., Fleisher, T., Clerici, M., . . . Tolstoshev, P. (1995). T lymphocyte-directed gene therapy for ADA− SCID: initial trial results after 4 years. *Science, 270*(5235), 475-480.

Bliss, M. (2013). *The discovery of insulin*: University of Chicago Press.

Blömer, U., Naldini, L., Kafri, T., Trono, D., Verma, I. M., & Gage, F. H. (1997). Highly efficient and sustained gene transfer in adult neurons with a lentivirus vector. *Journal of virology, 71*(9), 6641-6649.

Boluyt, M. O., & Bing, O. H. (2000). Matrix gene expression and decompensated heart failure: the aged SHR model. *Cardiovascular research, 46*(2), 239-249.

Boquet, M. P., Wonganan, P., Dekker, J. D., & Croyle, M. A. (2008). Influence of method of systemic administration of adenovirus on virus-mediated toxicity: Focus on mortality, virus distribution, and drug metabolism. *Journal of pharmacological and toxicological methods, 58*(3), 222-232. doi:10.1016/j.vascn.2008.07.003

Branco, A. F., Pereira, S. P., Gonzalez, S., Gusev, O., Rizvanov, A. A., & Oliveira, P. J. (2015). Gene expression profiling of H9c2 myoblast differentiation towards a cardiac-like phenotype. *PLoS One, 10*(6), e0129303.

Braun-Menendez, E., & Page, I. H. (1958). A Suggested Revision of Nomenclature-Angiotensin. *Nature (London), 181*(4615), 1061-1061. doi:10.1038/1811061b0

Brennan, K., Martin, K., FitzGerald, S., O'sullivan, J., Wu, Y., Blanco, A., . . . Mc Gee, M. (2020). A comparison of methods for the isolation and separation of extracellular vesicles from protein and lipid particles in human serum. *Scientific reports, 10*(1), 1039.

Brink, M., Wellen, J., & Delafontaine, P. (1996). Angiotensin II causes weight loss and decreases circulating insulin-like growth factor I in rats through a pressor-independent mechanism. *The Journal of clinical investigation, 97*(11), 2509-2516. doi:10.1172/JCI118698

Brosnihan, K., Neves, L., Anton, L., Joyner, J., Valdes, G., & Merrill, D. (2004). Enhanced expression of Ang-(1-7) during pregnancy. *Brazilian Journal of Medical and Biological Research, 37*, 1255-1262.

Bryda, E. C. (2013). The Mighty Mouse: the impact of rodents on advances in biomedical research. *Missouri medicine, 110*(3), 207.

Bujak, M., & Frangogiannis, N. G. (2007). The role of TGF-β signaling in myocardial infarction and cardiac remodeling. *Cardiovascular research, 74*(2), 184-195.

Bumpus, F. M., Schwarz, H., & Page, I. H. (1957). Synthesis and Pharmacology of the Octapeptide Angiotonin. *Science (American Association for the Advancement of Science), 125*(3253), 886-887. doi:10.1126/science.125.3253.886

Burn, S. F. (2012). Detection of β-galactosidase activity: X-gal staining. *Kidney Development: Methods and Protocols*, 241-250.

Burrell, L. M., Johnston, C. I., Tikellis, C., & Cooper, M. E. (2004). ACE2, a new regulator of the renin–angiotensin system. *Trends in Endocrinology & Metabolism, 15*(4), 166-169.

Burson, J. M., Aguilera, G., Gross, K. W., & Sigmund, C. D. (1994). Differential expression of angiotensin receptor 1A and 1B in mouse. *American Journal of Physiology - Endocrinology And Metabolism, 267*(2), 260-267. doi:10.1152/ajpendo.1994.267.2.E260

Busche, S., Gallinat, S., Bohle, R.-M., Reinecke, A., Seebeck, J., Franke, F., . . . Unger, T. (2000). Expression of angiotensin AT1 and AT2 receptors in adult rat cardiomyocytes after myocardial infarction: a single-cell reverse transcriptase-polymerase chain reaction study. *The American journal of pathology, 157*(2), 605-611.

Cai, J., Han, Y., Ren, H., Chen, C., He, D., Zhou, L., . . . Zeng, C. (2013). Extracellular vesicle-mediated transfer of donor genomic DNA to recipient cells is a novel mechanism for genetic influence between cells. *Journal of molecular cell biology, 5*(4), 227-238. doi:10.1093/jmcb/mjt011

Cai, W., Zhang, Z., Huang, Y., Sun, H., & Qiu, L. (2018). Vaccarin alleviates hypertension and nephropathy in renovascular hypertensive rats. *Experimental and therapeutic medicine, 15*(1), 924-932.

Camacho, P., Fan, H., Liu, Z., & He, J.-Q. (2016). Small mammalian animal models of heart disease. *American journal of cardiovascular disease, 6*(3), 70.

Cameron, J. S. (2012). Thomas Graham (1805–1869)—The "Father" of Dialysis. In *Dialysis: History, Development and Promise* (pp. 19-25): World Scientific.

Campbell, D. J., Kladis, A., & Duncan, A.-M. (1993). Nephrectomy, Converting Enzyme Inhibition, and Angiotensin Peptides. *Hypertension (Dallas, Tex. 1979), 22*(4), 513-522. doi:10.1161/01.HYP.22.4.513

Cao, X., Wang, X., Ling, Y., Song, X., Yang, P., Liu, Y., . . . Chen, A. (2014). Comparison of the degree of autophagy in neonatal rat cardiomyocytes and H9c2 cells exposed to hypoxia/reoxygenation. *Clin Lab, 60*(5), 809-814.

Carey, R. M. (2017). Update on angiotensin AT2 receptors. *Current opinion in nephrology and hypertension, 26*(2), 91.

Carretero, O. A., & Oparil, S. (2000). Essential hypertension: part I: definition and etiology. *Circulation, 101*(3), 329-335.

Cassis, L. A., Marshall, D. E., Fettinger, M. J., Rosenbluth, B., & Lodder, R. A. (1998). Mechanisms contributing to angiotensin II regulation of body weight. *American Journal of Physiology-Endocrinology And Metabolism, 274*(5), E867-E876.

Ccai, S. A., Chen, J. F., Chen, M. J., Lin, J. C., Feng, J. Q., Lin, K., . . . Wu, W. (2017). [Angiotensin-(1-7) protects cardiac myocytes against high glucose-induced injury by inhibiting ClC-3 chloride channels]. *Nan Fang Yi Ke Da Xue Xue Bao, 37*(7), 895-901. doi:10.3969/j.issn.1673-4254.2017.07.07

Ceravolo, G. S., Montezano, A. C., Jordao, M. T., Akamine, E. H., Costa, T. J., Takano, A. P., . . . Carvalho, M. H. C. (2014). An Interaction of Renin-Angiotensin and Kallikrein-Kinin Systems Contributes to Vascular Hypertrophy in Angiotensin II-Induced Hypertension: In Vivo and In Vitro Studies. *PLoS One, 9*(11), e111117. doi:10.1371/journal.pone.0111117

Cerniello, F. M., Carretero, O. A., Longo Carbajosa, N. A., Cerrato, B. D., Santos, R. A., Grecco, H. E., & Gironacci, M. M. (2017). Mas1 receptor trafficking involves ERK1/2 activation through a β-Arrestin2–Dependent pathway. *Hypertension, 70*(5), 982-989.

Chaurasiya, S., & Hitt, M. M. (2016). Adenoviral vector construction I: mammalian systems. In *Adenoviral Vectors for Gene Therapy* (pp. 85-112): Elsevier.

Chen, C., Zhang, Z., Gu, X., Sheng, X., Xiao, L., & Wang, X. (2023). Exosomes: New regulators of reproductive development. *Materials Today Bio*, 100608.

Chen, C. C., Liu, L., Ma, F., Wong, C. W., Guo, X. E., Chacko, J. V., . . . Ségaliny, A. (2016). Elucidation of exosome migration across the blood–brain barrier model in vitro. *Cellular and molecular bioengineering, 9*(4), 509-529.

Chen, P.-S., Chiu, W.-T., Hsu, P.-L., Lin, S.-C., Peng, I., Wang, C.-Y., & Tsai, S.-J. (2020). Pathophysiological implications of hypoxia in human diseases. *Journal of biomedical science, 27*(1), 1-19.

Chen, T., Ding, G., Jin, Z., Wagner, M. B., & Yuan, Z. (2012). Insulin ameliorates miR-1-induced injury in H9c2 cells under oxidative stress via Akt activation. *Molecular and cellular biochemistry, 369*, 167-174.

Cheng, J., Luo, X., Huang, Z., & Chen, L. (2019). Apelin/APJ system: A potential therapeutic target for endothelial dysfunction‐related diseases. *Journal of cellular physiology, 234*(8), 12149-12160.

Cheng, K.-C., Chang, W.-T., Kuo, F. Y., Chen, Z.-C., Li, Y., & Cheng, J.-T. (2019). TGR5 activation ameliorates hyperglycemia-induced cardiac hypertrophy in H9c2 cells. *Scientific reports, 9*(1), 1-11.

Chlopcikova, S., Psotová, J., & Miketová, P. (2001). Neonatal rat cardiomyocytes-a model for the study of morphological, biochemical and electrophysiological characteristics of the heart. *Biomedical Papers-Palacky University in Olomouc, 145*(2), 49-55.

Choi, Y., & Chang, J. (2013). Viral vectors for vaccine applications. *Clin Exp Vaccine Res, 2*(2), 97-105. doi:10.7774/cevr.2013.2.2.97

Chong, S. Y., Lee, C. K., Huang, C., Ou, Y. H., Charles, C. J., Richards, A. M., . . . Pastorin, G. (2019). Extracellular vesicles in cardiovascular diseases: alternative biomarker sources, therapeutic agents, and drug delivery carriers. *International journal of molecular sciences, 20*(13), 3272.

Claude, M., & Fauquet, M. (2004). *Virus taxonomy: eighth report of the International Committee on Taxonomy of Viruses*: Elsevier Science & Technology.

Clauser, E., Gaillard, I., Wei, L., & Corvol, P. (1989). Regulation of angiotensinogen gene. *American journal of hypertension, 2*(5_Pt_1), 403-410.

Clayton, A., Turkes, A., Dewitt, S., Steadman, R., Mason, M. D., & Hallett, M. B. (2004). Adhesion and signaling by B cell‐derived exosomes: the role of integrins. *The FASEB journal, 18*(9), 977-979.

Cocozza, F., Névo, N., Piovesana, E., Lahaye, X., Buchrieser, J., Schwartz, O., . . . Martin‐Jaular, L. (2020). Extracellular vesicles containing ACE2 efficiently prevent infection by SARS‐CoV‐2 Spike protein‐containing virus. *Journal of Extracellular Vesicles, 10*(2), e12050-n/a. doi:10.1002/jev2.12050

Cole, J., Ertoy, D., & Bernstein, K. E. (2000). Insights derived from ACE knockout mice. *Journal of the renin-angiotensin-aldosterone system, 1*(2), 137-141. doi:10.3317/jraas.2000.016

Columb, M., & Atkinson, M. (2016). Statistical analysis: sample size and power estimations. *Bja Education, 16*(5), 159-161.

Conn, P. M. (2017). *Animal models for the study of human disease* (Second ed.). London, United Kingdom: Academic Press is an imprint of Elsevier.

Conte, J. V., Baumgartner, W. A., Dorman, T., & Owens, S. G. (2007). *The Johns Hopkins Manual of Cardiac Surgical Care: Mobile Medicine Series*: Elsevier Health Sciences.

Cooper, M. A., & Zhou, R. (2013). β-Galactosidase staining of LacZ fusion proteins in whole tissue preparations. *Neural Development: Methods and Protocols*, 189-197.

Cosselman, K. E., Navas-Acien, A., & Kaufman, J. D. (2015). Environmental factors in cardiovascular disease. *Nature reviews cardiology, 12*(11), 627-642. doi:10.1038/nrcardio.2015.152

Crackower, M. A., Sarao, R., Oudit, G. Y., Yagil, C., Kozieradzki, I., Scanga, S. E., . . . Pei, Y. (2002). Angiotensin-converting enzyme 2 is an essential regulator of heart function. *Nature, 417*(6891), 822-828.

Crenshaw, B. J., Jones, L. B., Bell, C. R., Kumar, S., & Matthews, Q. L. (2019). Perspective on Adenoviruses: Epidemiology, Pathogenicity, and Gene Therapy. *Biomedicines, 7*(3), 61. doi:10.3390/biomedicines7030061

Crystal, R. G. (2014). Adenovirus: the first effective in vivo gene delivery vector. *Human gene therapy, 25*(1), 3-11.

Dai, S., Wei, D., Wu, Z., Zhou, X., Wei, X., Huang, H., & Li, G. (2008). Phase I clinical trial of autologous ascites-derived exosomes combined with GM-CSF for colorectal cancer. *Molecular therapy, 16*(4), 782-790.

Danilczyk, U., & Penninger, J. M. (2006). Angiotensin-converting enzyme II in the heart and the kidney. *Circulation research, 98*(4), 463-471.

Danser, A. H. J., van Kats, J. P., Admiraal, P. J. J., Derkx, F. H. M., Lamers, J. M. J., Verdouw, P. D., . . . Schalekamp, M. A. D. H. (1994). Cardiac Renin and Angiotensins: Uptake From Plasma Versus In Situ Synthesis. *Hypertension (Dallas, Tex. 1979), 24*(1), 37-48. doi:10.1161/01.HYP.24.1.37

Danthinne, X., & Imperiale, M. (2000). Production of first generation adenovirus vectors: a review. *Gene therapy, 7*(20), 1707-1714.

Dasgupta, C., & Zhang, L. (2011). Angiotensin II receptors and drug discovery in cardiovascular disease. *Drug discovery today, 16*(1), 22-34. doi:10.1016/j.drudis.2010.11.016

de Castilla, P. E. M., Tong, L., Huang, C., Sofias, A. M., Pastorin, G., Chen, X., . . . Wang, J.-W. (2021). Extracellular vesicles as a drug delivery system: A systematic review of preclinical studies. *Advanced drug delivery reviews, 175*, 113801.

DE CHAMPLAIN, J., Krakoff, L. R., & AXELROD, J. (1967). Catecholamine metabolism in experimental hypertension in the rat. *Circulation research, 20*(1), 136-145.

De Hert, E., Bracke, A., Lambeir, A. M., Van der Veken, P., & De Meester, I. (2021). The C-terminal cleavage of angiotensin II and III is mediated by prolyl carboxypeptidase in human umbilical vein and aortic endothelial cells. *Biochem Pharmacol, 192*, 114738. doi:10.1016/j.bcp.2021.114738

De Hert, E., Bracke, A., Pintelon, I., Janssens, E., Lambeir, A. M., Van Der Veken, P., & De Meester, I. (2021). Prolyl Carboxypeptidase Mediates the C-Terminal Cleavage of (Pyr)-Apelin-13 in Human Umbilical Vein and Aortic Endothelial Cells. *Int J Mol Sci, 22*(13). doi:10.3390/ijms22136698

De Lemos, J., & Omland, T. (2017). *Chronic Coronary Artery Disease: A Companion to Braunwald's Heart Disease E-Book: A Companion to Braunwald's Heart Disease*: elsevier Health Sciences.

Denby, L., Nicklin, S., & Baker, A. (2005). Adeno-associated virus (AAV)-7 and-8 poorly transduce vascular endothelial cells and are sensitive to proteasomal degradation. *Gene therapy, 12*(20), 1534-1538.

Der Sarkissian, S., Grobe, J. L., Yuan, L., Narielwala, D. R., Walter, G. A., Katovich, M. J., & Raizada, M. K. (2008). Cardiac overexpression of angiotensin converting enzyme 2 protects the heart from ischemia-induced pathophysiology. *Hypertension, 51*(3), 712-718. doi:10.1161/hypertensionaha.107.100693

Di Pasquale, E., Latronico, M., Jotti, G., & Condorelli, G. (2012). Lentiviral vectors and cardiovascular diseases: a genetic tool for manipulating cardiomyocyte differentiation and function. *Gene therapy, 19*(6), 642-648.

Díez-Freire, C., Vázquez, J., Correa de Adjounian, M. a. F., Ferrari, M. F., Yuan, L., Silver, X., . . . Raizada, M. K. (2006). ACE2 gene transfer attenuates hypertension-linked pathophysiological changes in the SHR. *Physiological genomics, 27*(1), 12-19.

Doggrell, S. A., & Brown, L. (1998). Rat models of hypertension, cardiac hypertrophy and failure. *Cardiovascular research, 39*(1), 89-105.

Dong, B., Yu, Q. T., Dai, H. Y., Gao, Y. Y., Zhou, Z. L., Zhang, L., . . . Zhang, Y. H. (2012). Angiotensin-converting enzyme-2 overexpression improves left ventricular remodeling and function in a rat model of diabetic cardiomyopathy. *Journal of the American College of Cardiology, 59*(8), 739-747.

Donoghue, M., Hsieh, F., Baronas, E., Godbout, K., Gosselin, M., Stagliano, N., . . . Acton, S. (2000). A Novel Angiotensin-Converting Enzyme–Related Carboxypeptidase (ACE2) Converts Angiotensin I to Angiotensin 1-9. *Circulation research, 87*(5), e1-e9. doi:10.1161/01.RES.87.5.e1

Doran, B., & Voora, D. (2016). Circulating extracellular vesicles containing miRNAs may have utility as early biomarkers for cardiac injury. *Annals of translational medicine, 4*(Suppl 1).

Dorer, F. E., Kahn, J. R., Lentz, K. E., Levine, M., & Skeggs, L. T. (1974). Hydrolysis of Bradykinin by Angiotensin-Converting Enzyme. *Circulation research, 34*(6), 824-827. doi:10.1161/01.RES.34.6.824

Dorn, G. W. (2007). The fuzzy logic of physiological cardiac hypertrophy. *Hypertension, 49*(5), 962-970.

Douglas, J. T. (2007). Adenoviral vectors for gene therapy. *Molecular biotechnology, 36*(1), 71-80.

Douglas, J. T., Rogers, B. E., Rosenfeld, M. E., Michael, S. I., Feng, M., & Curiel, D. T. (1996). Targeted gene delivery by tropism-modified adenoviral vectors. *Nature biotechnology, 14*(11), 1574-1578.

Doyle, L. M., & Wang, M. Z. (2019). Overview of extracellular vesicles, their origin, composition, purpose, and methods for exosome isolation and analysis. *Cells, 8*(7), 727.

Ehler, E., Moore-Morris, T., & Lange, S. (2013). Isolation and culture of neonatal mouse cardiomyocytes. *JoVE (Journal of Visualized Experiments)*(79), e50154.

Elased, K. M., Cunha, T. S., Gurley, S. B., Coffman, T. M., & Morris, M. (2006). New mass spectrometric assay for angiotensin-converting enzyme 2 activity. *Hypertension, 47*(5), 1010-1017.

Escola, J.-M., Kleijmeer, M. J., Stoorvogel, W., Griffith, J. M., Yoshie, O., & Geuze, H. J. (1998). Selective enrichment of tetraspan proteins on the internal vesicles of multivesicular endosomes and on exosomes secreted by human B-lymphocytes. *Journal of Biological Chemistry, 273*(32), 20121-20127.

Escrevente, C., Keller, S., Altevogt, P., & Costa, J. (2011). Interaction and uptake of exosomes by ovarian cancer cells. *BMC cancer, 11*(1), 1-10.

Esther, C. R., Marino, E. M., & Bernstein, K. E. (1997). The Role of Angiotensin-Converting Enzyme in Blood Pressure Control, Renal Function, and Male Fertility. *Trends in endocrinology and metabolism, 8*(5), 181-186. doi:10.1016/S1043-2760(97)00039-8

Falk, E. (1985). Unstable angina with fatal outcome: dynamic coronary thrombosis leading to infarction and/or sudden death. Autopsy evidence of recurrent mural thrombosis with peripheral embolization culminating in total vascular occlusion. *Circulation, 71*(4), 699-708.

Fattah, C., Nather, K., McCarroll, C. S., Hortigon-Vinagre, M. P., Zamora, V., Flores-Munoz, M., . . . Touyz, R. M. (2016). Gene therapy with angiotensin-(1-9) preserves left ventricular systolic function after myocardial infarction. *Journal of the American College of Cardiology, 68*(24), 2652-2666.

Femminò, S., Penna, C., Margarita, S., Comità, S., Brizzi, M. F., & Pagliaro, P. (2020). Extracellular vesicles and cardiovascular system: Biomarkers and Cardioprotective Effectors. *Vascular Pharmacology, 135*, 106790.

Ferrario, C., Italia, L. D., & Varagic, J. (2020). Molecular signaling mechanisms of the renin-angiotensin system in heart failure. In *HEART FAILURE A Companion to Braunwald's Heart Disease* (pp. 76-90): ELSEVIER, Philadelphia, PA.

Ferreira, G. S., Veening-Griffioen, D. H., Boon, W. P., Moors, E. H., & van Meer, P. J. (2020). Levelling the translational gap for animal to human efficacy data. *Animals, 10*(7), 1199.

Flores-Muñoz, M., Godinho, B. M., Almalik, A., & Nicklin, S. A. (2012). Adenoviral delivery of angiotensin-(1-7) or angiotensin-(1-9) inhibits cardiomyocyte hypertrophy via the mas or angiotensin type 2 receptor. *PLoS One, 7*(9), e45564. doi:10.1371/journal.pone.0045564

Flores-Munoz, M., Work, L. M., Douglas, K., Denby, L., Dominiczak, A. F., Graham, D., & Nicklin, S. A. (2012). Angiotensin-(1-9) Attenuates Cardiac Fibrosis in the Stroke-Prone Spontaneously Hypertensive Rat via the Angiotensin Type 2 Receptor. *Hypertension (Dallas, Tex. 1979), 59*(2), 300-307. doi:10.1161/HYPERTENSIONAHA.111.177485

Flores‐Muñoz, M., Smith, N., Haggerty, C., Milligan, G., & Nicklin, S. (2011). Angiotensin1‐9 antagonises pro‐hypertrophic signalling in cardiomyocytes via the angiotensin type 2 receptor. *The Journal of physiology, 589*(4), 939-951.

Fordjour, F. K., Guo, C., Ai, Y., Daaboul, G. G., & Gould, S. J. (2022). A shared, stochastic pathway mediates exosome protein budding along plasma and endosome membranes. *Journal of Biological Chemistry*, 102394.

Fraser, B. J., Beldar, S., Seitova, A., Hutchinson, A., Mannar, D., Li, Y., . . . Leopold, K. (2022). Structure and activity of human TMPRSS2 protease implicated in SARS-CoV-2 activation. *Nature Chemical Biology, 18*(9), 963-971.

Freimuth, P., Philipson, L., & Carson, S. (2008). The coxsackievirus and adenovirus receptor. *Group B Coxsackieviruses*, 67-87.

Friedmann, T. (1992). A brief history of gene therapy. *Nature genetics, 2*(2), 93-98.

Gáborik, Z., Szaszák, M., Szidonya, L., Balla, B., Paku, S., Catt, K. J., . . . Hunyady, L. (2001). Beta-arrestin- and dynamin-dependent endocytosis of the AT1 angiotensin receptor. *Molecular pharmacology, 59*(2), 239.

Gaidarov, I., Adams, J., Frazer, J., Anthony, T., Chen, X., Gatlin, J., . . . Unett, D. J. (2018). Angiotensin (1-7) does not interact directly with MAS1, but can potently antagonize signaling from the AT1 receptor. *Cell Signal, 50*, 9-24. doi:10.1016/j.cellsig.2018.06.007

Gao, L., Wang, W., Wang, W., Li, H., Sumners, C., & Zucker, I. H. (2008). Effects of angiotensin type 2 receptor overexpression in the rostral ventrolateral medulla on blood pressure and urine excretion in normal rats. *Hypertension, 51*(2), 521-527.

Gascón, A. R., del Pozo-Rodríguez, A., & Solinís, M. Á. (2013). Non-viral delivery systems in gene therapy. In *Gene therapy-tools and potential applications*: IntechOpen.

Gava, E., de Castro, C. H., Ferreira, A. J., Colleta, H., Melo, M. B., Alenina, N., . . . Kitten, G. T. (2012). Angiotensin-(1-7) receptor Mas is an essential modulator of extracellular matrix protein expression in the heart. *Regulatory peptides, 175*(1-3), 30-42.

Gavras, H., Lever, A. F., Brown, J. J., Macadam, R. F., & Robertson, J. I. S. (1971). ACUTE RENAL FAILURE, TUBULAR NECROSIS, AND MYOCARDIAL INFARCTION INDUCED IN THE RABBIT BY INTRAVENOUS ANGIOTENSIN II. *The Lancet (British edition), 298*(7714), 19-22. doi:10.1016/S0140-6736(71)90008-0

Gavras, I., & Gavras, H. (2002). *Angiotensin II as a cardiovascular risk factor*, Basingstoke.

Gavras, I., & Gavras, H. (2002). Angiotensin II as a cardiovascular risk factor. *Journal of human hypertension, 16*(S2), S2. doi:10.1038/sj/jhh/1001392

Gerhardt, T., Haghikia, A., Stapmanns, P., & Leistner, D. M. (2022). Immune mechanisms of plaque instability. *Frontiers in cardiovascular medicine, 8*, 797046.

Gho, Y. S., & Lee, C. (2017). Emergent properties of extracellular vesicles: a holistic approach to decode the complexity of intercellular communication networks. *Molecular Biosystems, 13*(7), 1291-1296.

Ghossoub, R., Lembo, F., Rubio, A., Gaillard, C. B., Bouchet, J., Vitale, N., . . . Zimmermann, P. (2014). Syntenin-ALIX exosome biogenesis and budding into multivesicular bodies are controlled by ARF6 and PLD2. *Nature communications, 5*(1), 3477.

Glasser, S. P., Selwyn, A. P., & Ganz, P. (1996). Atherosclerosis: risk factors and the vascular endothelium. *American heart journal, 131*(2), 379-384.

Goldblatt, H., Lynch, J., Hanzal, R. F., & Summerville, W. W. (1934). Studies on experimental hypertension I. The production of persistent elevation of systolic blood pressure by means of renal ischemia. *The Journal of experimental medicine, 59*(3), 347-U151. doi:10.1084/jem.59.3.347

Gomez, R. A., Cassis, L., Lynch, K. R., Chevalier, R. L., Wilfong, N., Carey, R. M., & Peach, M. J. (1988). FETAL EXPRESSION OF THE ANGIOTENSINOGEN GENE. *Endocrinology (Philadelphia), 123*(5), 2298-2302. doi:10.1210/endo-123-5-2298

Gottschalk, C. W., & Fellner, S. K. (1997). History of the science of dialysis. *American journal of nephrology, 17*(3-4), 289-298.

Graham-Brown, M. P., Patel, A., Stensel, D., March, D. S., Marsh, A.-M., McAdam, J., . . . Burton, J. O. (2017). Imaging of myocardial fibrosis in patients with end-stage renal disease: current limitations and future possibilities. *BioMed Research International, 2017*.

Graham, F. L., & Prevec, L. (1992). Adenovirus-based expression vectors and recombinant vaccines. *Biotechnology, 20*, 363-390. doi:10.1016/b978-0-7506-9265-6.50022-1

Graham, F. L., Smiley, J., Russell, W. C., & Nairn, R. (1977). Characteristics of a Human Cell Line Transformed by DNA from Human Adenovirus Type 5. *Journal of general virology, 36*(1), 59-72. doi:10.1099/0022-1317-36-1-59

Grobe, J. L., Mecca, A. P., Lingis, M., Shenoy, V., Bolton, T. A., Machado, J. M., . . . Katovich, M. J. (2007). Prevention of angiotensin II-induced cardiac remodeling by angiotensin-(1-7). *Am J Physiol Heart Circ Physiol, 292*(2), H736-742. doi:10.1152/ajpheart.00937.2006

Grobe, J. L., Mecca, A. P., Lingis, M., Shenoy, V., Bolton, T. A., Machado, J. M., . . . Katovich, M. J. (2007). Prevention of angiotensin II-induced cardiac remodeling by angiotensin-(1–7). *American Journal of Physiology - Heart and Circulatory Physiology, 292*(2), 736-742. doi:10.1152/ajpheart.00937.2006

Grobe, N., Elased, K. M., Salem, E. S., Gurley, S. B., Ong, F. S., Bernstein, K. E., . . . Morris, M. (2013). Discovery of new renal Ang II processing enzyme activity using mass spectrometry and gene deletion mouse models. In: Wiley Online Library.

Grobe, N., Leiva, O., Morris, M., & Elased, K. M. (2015). Loss of prolyl carboxypeptidase in two-kidney, one-clip goldblatt hypertensive mice. *PLoS One, 10*(2), e0117899. doi:10.1371/journal.pone.0117899

Grobe, N., Weir, N. M., Leiva, O., Ong, F. S., Bernstein, K. E., Schmaier, A. H., . . . Elased, K. M. (2013). Identification of prolyl carboxypeptidase as an alternative enzyme for processing

of renal angiotensin II using mass spectrometry. *Am J Physiol Cell Physiol, 304*(10), C945-953. doi:10.1152/ajpcell.00346.2012

Gu, S., Zhang, W., Chen, J., Ma, R., Xiao, X., Ma, X., . . . Chen, Y. (2014). EPC-derived microvesicles protect cardiomyocytes from Ang II-induced hypertrophy and apoptosis. *PLoS One, 9*(1), e85396.

Guo, L., Yin, A., Zhang, Q., Zhong, T., O'Rourke, S. T., & Sun, C. (2017). Angiotensin-(1–7) attenuates angiotensin II-induced cardiac hypertrophy via a Sirt3-dependent mechanism. *American Journal of Physiology-Heart and Circulatory Physiology, 312*(5), H980-H991.

Gupta, S., Maitra, R., Young, D., Gupta, A., & Sen, S. (2009). Silencing the myotrophin gene by RNA interference leads to the regression of cardiac hypertrophy. *American Journal of Physiology-Heart and Circulatory Physiology, 297*(2), H627-H636.

Gurung, S., Perocheau, D., Touramanidou, L., & Baruteau, J. (2021). The exosome journey: From biogenesis to uptake and intracellular signalling. *Cell Communication and Signaling, 19*(1), 1-19.

Gyurko, R., Wielbo, D., & Phillips, M. I. (1993). Antisense inhibition of AT1 receptor mRNA and angiotensinogen mRNA in the brain of spontaneously hypertensive rats reduces hypertension of neurogenic origin. *Regulatory peptides, 49*(2), 167-174.

Hagaman, J. R., Moyer, J. S., Bachman, E. S., Sibony, M., Magyar, P. L., Welch, J. E., . . . O'Brien, D. A. (1998). Angiotensin-Converting Enzyme and Male Fertility. *Proceedings of the National Academy of Sciences - PNAS, 95*(5), 2552-2557. doi:10.1073/pnas.95.5.2552

Hall, C., Gehmlich, K., Denning, C., & Pavlovic, D. (2021). Complex relationship between cardiac fibroblasts and cardiomyocytes in health and disease. *Journal of the American Heart Association, 10*(5), e019338.

Hall, J. M. (1992). Bradykinin receptors: Pharmacological properties and biological roles. *Pharmacology & therapeutics (Oxford), 56*(2), 131-190. doi:10.1016/0163-7258(92)90016-S

Hallet, B., & Sherratt, D. J. (1997). Transposition and site-specific recombination: adapting DNA cut-and-paste mechanisms to a variety of genetic rearrangements. *FEMS Microbiol Rev, 21*(2), 157-178. doi:10.1111/j.1574-6976.1997.tb00349.x

Hammoudi, N., Ishikawa, K., & Hajjar, R. J. (2015). Adeno-associated virus-mediated gene therapy in cardiovascular disease. *Current opinion in cardiology, 30*(3), 228-234.

Han, C., Yang, J., Sun, J., & Qin, G. (2021). Extracellular vesicles in cardiovascular disease: Biological functions and therapeutic implications. *Pharmacology & therapeutics*, 108025.

Hao, P., Liu, Y., Guo, H., Zhang, Z., Chen, Q., Hao, G., . . . Zhang, Y. (2020). Prolylcarboxypeptidase Mitigates Myocardial Ischemia/Reperfusion Injury by Stabilizing Mitophagy. *Front Cell Dev Biol, 8*, 584933. doi:10.3389/fcell.2020.584933

Harmer, D., Gilbert, M., Borman, R., & Clark, K. L. (2002). Quantitative mRNA expression profiling of ACE 2, a novel homologue of angiotensin converting enzyme. *FEBS letters, 532*(1-2), 107-110.

He, T.-C., Zhou, S., Da Costa, L. T., Yu, J., Kinzler, K. W., & Vogelstein, B. (1998). A simplified system for generating recombinant adenoviruses. *Proceedings of the National Academy of Sciences, 95*(5), 2509-2514.

Henne, W. M., Buchkovich, N. J., & Emr, S. D. (2011). The ESCRT pathway. *Developmental cell, 21*(1), 77-91.

Herin, L., Blanc, J., Basset, A., Laude, D., Laurent, S., & Elghozi, J. L. (2003). Different vascular responsiveness to angiotensin II in two normotensive rat strains. *Fundamental & clinical pharmacology, 17*(3), 315-321.

Hewitson, T. D., Ono, T., & Becker, G. J. (2008). Small Animal Models of Kidney Disease: A Review. In *Kidney Research* (Vol. 466, pp. 41-57). Totowa, NJ: Humana Press.

Hidalgo, P., & González, R. A. (2022). Journal: Encyclopedia of Infection and Immunity, 2022, p. 59-66. *Journal: Encyclopedia of Infection and Immunity*, 59-66.

Hinderer, S., & Schenke-Layland, K. (2019). Cardiac fibrosis–A short review of causes and therapeutic strategies. *Advanced drug delivery reviews, 146*, 77-82.

Hollands, C. (1986). The animals (scientific procedures) act 1986. *Lancet (London, England), 2*(8497), 32-33.

Hou, J., Kato, H., Cohen, R. A., Chobanian, A. V., & Brecher, P. (1995). ANGIOTENSIN-II-INDUCED CARDIAC FIBROSIS IN THE RAT IS INCREASED BY CHRONIC INHIBITION OF NITRIC-OXIDE SYNTHASE. *The Journal of clinical investigation, 96*(5), 2469-2477. doi:10.1172/JCI118305

Howard, C. M., & Baudino, T. A. (2014). Dynamic cell–cell and cell–ECM interactions in the heart. *Journal of molecular and cellular cardiology, 70*, 19-26.

Hu, Z., Shi, X.-Y., Okazaki, M., & Hoffman, B. B. (1995). Angiotensin II induces transcription and expression of alpha 1-adrenergic receptors in vascular smooth muscle cells. *American Journal of Physiology-Heart and Circulatory Physiology, 268*(3), H1006-H1014.

Huang, L., Sexton, D. J., Skogerson, K., Devlin, M., Smith, R., Sanyal, I., . . . Wu, Q.-l. (2003). Novel peptide inhibitors of angiotensin-converting enzyme 2. *Journal of Biological Chemistry, 278*(18), 15532-15540.

Huentelman, M. J., Grobe, J. L., Vazquez, J., Stewart, J. M., Mecca, A. P., Katovich, M. J., . . . Raizada, M. K. (2005). Protection from angiotensin II-induced cardiac hypertrophy and fibrosis by systemic lentiviral delivery of ACE2 in rats. *Experimental physiology, 90*(5), 783-790. doi:10.1113/expphysiol.2005.031096

Iaccarino, G., & Sorriento, D. (2018). Novel Insights in β-Adrenergic Receptor Signaling.

Ibrahim, N., Bosch, M. A., Smart, J. L., Qiu, J., Rubinstein, M., Rønnekleiv, O. K., . . . Kelly, M. J. (2003). Hypothalamic proopiomelanocortin neurons are glucose responsive and express KATP channels. *Endocrinology, 144*(4), 1331-1340.

Inuzuka, T., Fujioka, Y., Tsuda, M., Fujioka, M., Satoh, A. O., Horiuchi, K., . . . Ohba, Y. (2016). Attenuation of ligand-induced activation of angiotensin II type 1 receptor signaling by the type 2 receptor via protein kinase C. *Scientific reports, 6*(1), 21613.

Iriuchijima, J. (1973). Cardiac output and total peripheral resistance in spontaneously hypertensive rats. *Japanese Heart Journal, 14*(3), 267-272.

Iulita, M. F., Vallerand, D., Beauvillier, M., Haupert, N., A Ulysse, C., Gagné, A., . . . Tremblay, M.-È. (2018). Differential effect of angiotensin II and blood pressure on hippocampal inflammation in mice. *Journal of neuroinflammation, 15*(1), 1-14.

Iwata, M., Cowling, R. T., Gurantz, D., Moore, C., Zhang, S., Yuan, J. X.-J., & Greenberg, B. H. (2005). Angiotensin-(1–7) binds to specific receptors on cardiac fibroblasts to initiate antifibrotic and antitrophic effects. *American Journal of Physiology-Heart and Circulatory Physiology, 289*(6), H2356-H2363.

Iyer, S. N., Lu, D., Katovich, M. J., & Raizada, M. K. (1996). Chronic control of high blood pressure in the spontaneously hypertensive rat by delivery of angiotensin type 1 receptor antisense. *Proceedings of the National Academy of Sciences, 93*(18), 9960-9965.

Jackman, H. L., Massad, M. G., Sekosan, M., Tan, F., Brovkovych, V., Marcic, B. M., & Erdös, E. G. (2002). Angiotensin 1-9 and 1-7 release in human heart: role of cathepsin A. *Hypertension, 39*(5), 976-981.

Jacob-Dolan, C., & Barouch, D. H. (2022). COVID-19 vaccines: adenoviral vectors. *Annual review of medicine, 73*, 41-54.

Jankowski, V., Vanholder, R., van der Giet, M., Tölle, M., Karadogan, S., Gobom, J., . . . Anh Tran, T. N. (2007). Mass-spectrometric identification of a novel angiotensin peptide in human plasma. *Arteriosclerosis, thrombosis, and vascular biology, 27*(2), 297-302.

Jansen, F., Nickenig, G., & Werner, N. (2017). Extracellular vesicles in cardiovascular disease: potential applications in diagnosis, prognosis, and epidemiology. *Circulation research, 120*(10), 1649-1657.

Jeong, J. K., & Diano, S. (2013). Prolyl carboxypeptidase and its inhibitors in metabolism. *Trends in Endocrinology & Metabolism, 24*(2), 61-67.

Johnston, C. I. (2000). Angiotensin II type 1 receptor blockade: a novel therapeutic concept. *Blood pressure. Supplement, 1*, 9.

Johnstone, R. M., Adam, M., Hammond, J., Orr, L., & Turbide, C. (1987). Vesicle formation during reticulocyte maturation. Association of plasma membrane activities with released vesicles (exosomes). *Journal of Biological Chemistry, 262*(19), 9412-9420.

JT, S., Wam, B., Ac, B., & Sa, N. (2022). Adenoviral vectors for cardiovascular gene therapy applications: a clinical and industry perspective. *Journal of Molecular Medicine*, 1-27.

Kalluri, R., & LeBleu, V. S. (2020). The biology, function, and biomedical applications of exosomes. *Science, 367*(6478), eaau6977.

Kanzawa, N., Shintani, S., Ohta, K., Kitajima, S., Ehara, T., Kobayashi, H., . . . Tsuchiya, T. (2004). Achacin induces cell death in HeLa cells through two different mechanisms. *Archives of biochemistry and biophysics, 422*(1), 103-109.

Karamyan, V. T., & Speth, R. C. (2007). Enzymatic pathways of the brain renin–angiotensin system: unsolved problems and continuing challenges. *Regulatory peptides, 143*(1), 15.

Kaschina, E., Namsolleck, P., & Unger, T. (2017). AT2 receptors in cardiovascular and renal diseases. *Pharmacological research, 125*, 39-47.

Kaschina, E., Steckelings, U. M., & Unger, T. (2018). Hypertension and the renin-angiotensin-aldosterone system. In *Encyclopedia of Endocrine Diseases* (pp. 505-510): Elsevier Editora.

Katada, J., & Majima, M. (2002). AT2 receptor‐dependent vasodilation is mediated by activation of vascular kinin generation under flow conditions. *British journal of pharmacology, 136*(4), 484-491. doi:10.1038/sj.bjp.0704731

Keeler, A. M., & Flotte, T. R. (2019). Recombinant adeno-associated virus gene therapy in light of Luxturna (and Zolgensma and Glybera): where are we, and how did we get here? *Annual review of virology, 6*, 601-621.

Kehoe, K., Noels, H., Theelen, W., De Hert, E., Xu, S., Verrijken, A., . . . Lambeir, A.-M. (2018). Prolyl carboxypeptidase activity in the circulation and its correlation with body weight and adipose tissue in lean and obese subjects. *PLoS One, 13*(5), e0197603.

Keidar, S., Kaplan, M., & Gamliel-Lazarovich, A. (2007). ACE2 of the heart: from angiotensin I to angiotensin (1–7). *Cardiovascular research, 73*(3), 463-469.

Keller, C., Böttcher-Friebertshäuser, E., & Lohoff, M. (2022). TMPRSS2, a novel host-directed drug target against SARS-CoV-2. *Signal Transduction and Targeted Therapy, 7*(1), 1-3.

Kemp, C. D., & Conte, J. V. (2012). The pathophysiology of heart failure. *Cardiovascular Pathology, 21*(5), 365-371.

Kessler-Icekson, G., Barhum, Y., Schaper, J., Schaper, W., Kaganovsky, E., & Brand, T. (2002). ANP expression in the hypertensive heart. *Experimental & Clinical Cardiology, 7*(2-3), 80.

Khare, R., May, S. M., Vetrini, F., Weaver, E. A., Palmer, D., Rosewell, A., . . . Barry, M. A. (2011). Generation of a Kupffer cell-evading adenovirus for systemic and liver-directed gene transfer. *Molecular therapy, 19*(7), 1254-1262.

Kim, H. S., Krege, J. H., Kluckman, K. D., Hagaman, Hodgin, J. B., Best, C. F., . . . Smithies, O. (1995). Genetic Control of Blood Pressure and the Angiotensinogen Locus. *Proceedings of the National Academy of Sciences - PNAS, 92*(7), 2735-2739. doi:10.1073/pnas.92.7.2735

Kim, S., & Iwao, H. (2000). Molecular and cellular mechanisms of angiotensin II-mediated cardiovascular and renal diseases. *Pharmacological reviews, 52*(1), 11-34.

Kim, S., Ohta, K., Hamaguchi, A., Yukimura, T., Miura, K., & Iwao, H. (1995). Angiotensin II induces cardiac phenotypic modulation and remodeling in vivo in rats. *Hypertension, 25*(6), 1252-1259.

Kimes, B., & Brandt, B. (1976). Properties of a clonal muscle cell line from rat heart. *Experimental cell research, 98*(2), 367-381.

Klimas, J., Olvedy, M., Ochodnicka‐Mackovicova, K., Kruzliak, P., Cacanyiova, S., Kristek, F., . . . Ochodnicky, P. (2015). Perinatally administered losartan augments renal ACE 2 expression but not cardiac or renal Mas receptor in spontaneously hypertensive rats. *Journal of Cellular and Molecular Medicine, 19*(8), 1965-1974.

Kochanek, S., Clemens, P. R., Mitani, K., Chen, H.-H., Chan, S., & Caskey, C. T. (1996). A new adenoviral vector: Replacement of all viral coding sequences with 28 kb of DNA independently expressing both full-length dystrophin and beta-galactosidase. *Proceedings of the National Academy of Sciences, 93*(12), 5731-5736.

Konoshenko, M. Y., Lekchnov, E. A., Vlassov, A. V., & Laktionov, P. P. (2018). Isolation of extracellular vesicles: general methodologies and latest trends. *BioMed research international, 2018*.

Kotchen, T. A., Kotchen, J. M., Guthrie Jr, G. P., & Cottrill, C. M. (1979). Plasma renin activity, reactivity, concentration and substrate following hypertension during pregnancy. Effect of oral contraceptive agents. *Hypertension, 1*(4), 355-361.

Kowal, J., Arras, G., Colombo, M., Jouve, M., Morath, J. P., Primdal-Bengtson, B., . . . Thery, C. (2016). Proteomic comparison defines novel markers to characterize heterogeneous populations of extracellular vesicle subtypes. *Proceedings of the National Academy of Sciences - PNAS, 113*(8), E968-E977. doi:10.1073/pnas.1521230113

Kruse, T., Schneider, S., Reger, L. N., Kampmann, M., & Reif, O. W. (2022). A novel approach for enumeration of extracellular vesicles from crude and purified cell culture samples. *Engineering in Life Sciences, 22*(3-4), 334-343.

Kuang, S.-Q., Geng, L., Prakash, S. K., Cao, J.-M., Guo, S., Villamizar, C., . . . Milewicz, D. M. (2013). Aortic remodeling after transverse aortic constriction in mice is attenuated with AT1 receptor blockade. *Arteriosclerosis, thrombosis, and vascular biology, 33*(9), 2172-2179.

Kumamoto, K., Stewart, T. A., Johnson, A., & Erdös, E. (1981). Prolylcarboxypeptidase (angiotensinase C) in human lung and cultured cells. *The Journal of clinical investigation, 67*(1), 210-215.

Kurose, H. (2021). Cardiac fibrosis and fibroblasts. *Cells, 10*(7), 1716.

Kurtz, A. (2011). Renin release: sites, mechanisms, and control. *Annual review of physiology, 73*(1), 377-399. doi:10.1146/annurev-physiol-012110-142238

Kuznetsov, A. V., Javadov, S., Sickinger, S., Frotschnig, S., & Grimm, M. (2015). H9c2 and HL-1 cells demonstrate distinct features of energy metabolism, mitochondrial function and sensitivity to hypoxia-reoxygenation. *Biochimica et Biophysica Acta (BBA)-Molecular Cell Research, 1853*(2), 276-284.

Lai, R. C., Arslan, F., Lee, M. M., Sze, N. S. K., Choo, A., Chen, T. S., . . . El Oakley, R. M. (2010). Exosome secreted by MSC reduces myocardial ischemia/reperfusion injury. *Stem cell research, 4*(3), 214-222.

Lamichhane, T. N., Raiker, R. S., & Jay, S. M. (2015). Exogenous DNA loading into extracellular vesicles via electroporation is size-dependent and enables limited gene delivery. *Molecular pharmaceutics, 12*(10), 3650-3657.

Langenickel, T., Pagel, I., Höhnel, K., Dietz, R., & Willenbrock, R. (2000). Differential regulation of cardiac ANP and BNP mRNA in different stages of experimental heart failure. *American Journal of Physiology-Heart and Circulatory Physiology, 278*(5), H1500-H1506.

Langeveld, B., Van Gilst, W. H., Tio, R. A., Zijlstra, F., & Roks, A. J. (2005). Angiotensin-(1–7) attenuates neointimal formation after stent implantation in the rat. *Hypertension, 45*(1), 138-141.

Lappe, R., & Brody, M. (1984). Mechanisms of the central pressor action of angiotensin II in conscious rats. *American Journal of Physiology-Regulatory, Integrative and Comparative Physiology, 246*(1), R56-R62.

Laughlin, C., Cardellichio, C., & Coon, H. (1986). Latent infection of KB cells with adeno-associated virus type 2. *Journal of virology, 60*(2), 515-524.

Lee, C. S., Bishop, E. S., Zhang, R., Yu, X., Farina, E. M., Yan, S., . . . Wu, X. (2017). Adenovirus-mediated gene delivery: potential applications for gene and cell-based therapies in the new era of personalized medicine. *Genes & diseases, 4*(2), 43-63.

Leenaars, C. H., Kouwenaar, C., Stafleu, F. R., Bleich, A., Ritskes-Hoitinga, M., De Vries, R., & Meijboom, F. L. (2019). Animal to human translation: a systematic scoping review of reported concordance rates. *Journal of translational medicine, 17*(1), 1-22.

LeGrice, I. J., Pope, A. J., Sands, G. B., Whalley, G., Doughty, R. N., & Smaill, B. H. (2012). Progression of myocardial remodeling and mechanical dysfunction in the spontaneously hypertensive rat. *American Journal of Physiology-Heart and Circulatory Physiology, 303*(11), H1353-H1365.

Lemarié, C. A., & Schiffrin, E. L. (2010). The angiotensin II type 2 receptor in cardiovascular disease. *Journal of the renin-angiotensin-aldosterone system, 11*(1), 19-31.

Leotta, E., Patejunas, G., Murphy, G., Szokol, J., McGregor, L., Carbray, J., . . . Crystal, R. (2002). Gene therapy with adenovirus-mediated myocardial transfer of vascular endothelial

growth factor 121 improves cardiac performance in a pacing model of congestive heart failure. *The Journal of Thoracic and Cardiovascular Surgery, 123*(6), 1101-1113.
Li, B., Kim, D. S., Yadav, R. K., Kim, H. R., & Chae, H. J. (2015). Sulforaphane prevents doxorubicin-induced oxidative stress and cell death in rat H9c2 cells. *International journal of molecular medicine, 36*(1), 53-64.
Li, E. C., Heran, B. S., & Wright, J. M. (2014). Angiotensin converting enzyme (ACE) inhibitors versus angiotensin receptor blockers for primary hypertension. *Cochrane Database of Systematic Reviews*(8).
Li, H., Qi, Y., Li, C., Braseth, L. N., Gao, Y., Shabashvili, A. E., . . . Sumners, C. (2009). Angiotensin type 2 receptor–mediated apoptosis of human prostate cancer cellsAT2R-Induced Apoptosis of Prostate Cancer Cells. *Molecular cancer therapeutics, 8*(12), 3255-3265.
Li, J., Luo, J., Gu, D., Jie, F., Pei, N., Li, A., . . . Li, H. (2016). Adenovirus-Mediated Angiotensin II Type 2 Receptor Overexpression Inhibits Tumor Growth of Prostate Cancer In Vivo. *J Cancer, 7*(2), 184-191. doi:10.7150/jca.12841
Li, M., Liu, K., Michalicek, J., Angus, J. A., Hunt, J. E., Dell'Italia, L. J., . . . Husain, A. (2004). Involvement of chymase-mediated angiotensin II generation in blood pressure regulation. *The Journal of clinical investigation, 114*(1), 112-120. doi:10.1172/JCI200420805
Li, W., Li, Y., Chu, Y., Wu, W., Yu, Q., Zhu, X., & Wang, Q. (2019). PLCE1 promotes myocardial ischemia–reperfusion injury in H/R H9c2 cells and I/R rats by promoting inflammation. *Bioscience Reports, 39*(7).
Li, W., Moore, M. J., Vasilieva, N., Sui, J., Wong, S. K., Berne, M. A., . . . Greenough, T. C. (2003). Angiotensin-converting enzyme 2 is a functional receptor for the SARS coronavirus. *Nature, 426*(6965), 450-454.
Li, Y., Ren, S., Xia, J., Wei, Y., & Xi, Y. (2020). EIF4A3-induced circ-BNIP3 aggravated hypoxia-induced injury of H9c2 cells by targeting miR-27a-3p/BNIP3. *Molecular Therapy-Nucleic Acids, 19*, 533-545.
Li, Y., Wu, J., He, Q., Shou, Z., Zhang, P., Pen, W., . . . Chen, J. (2009). Angiotensin (1-7) prevent heart dysfunction and left ventricular remodeling caused by renal dysfunction in 5/6 nephrectomy mice. *Hypertension Research, 32*(5), 369-374. doi:10.1038/hr.2009.25
Li, Y. Y., Li, X.-h. X.-h., & Yuan, H. H. (2012). Angiotensin II type-2 receptor-specific effects on the cardiovascular system. *Cardiovascular diagnosis and therapy, 2*(1), 56-62. doi:10.3978/j.issn.2223-3652.2012.02.02
Liang, Y., Iqbal, Z., Wang, J., Xu, L., Xu, X., Ouyang, K., . . . Xia, J. (2022). Cell-derived extracellular vesicles for CRISPR/Cas9 delivery: engineering strategies for cargo packaging and loading. *Biomaterials Science, 10*(15), 4095-4106.
Libby, P. (2006). Inflammation and cardiovascular disease mechanisms. *The American journal of clinical nutrition, 83*(2), 456S-460S.
Libby, P., Ridker, P. M., & Maseri, A. (2002). Inflammation and atherosclerosis. *Circulation, 105*(9), 1135-1143.
Libby, P., & Theroux, P. (2005). Pathophysiology of coronary artery disease. *Circulation, 111*(25), 3481-3488.
Lin, H., Parmacek, M. S., Morle, G., Bolling, S., & Leiden, J. M. (1990). Expression of recombinant genes in myocardium in vivo after direct injection of DNA. *Circulation, 82*(6), 2217-2221.
Lin, L., Liu, X., Xu, J., Weng, L., Ren, J., Ge, J., & Zou, Y. (2016). Mas receptor mediates cardioprotection of angiotensin-(1-7) against Angiotensin II-induced cardiomyocyte autophagy and cardiac remodelling through inhibition of oxidative stress. *J Cell Mol Med, 20*(1), 48-57. doi:10.1111/jcmm.12687
Liu, D., Gao, L., Roy, S. K., Cornish, K. G., & Zucker, I. H. (2008). Role of oxidant stress on AT1 receptor expression in neurons of rabbits with heart failure and in cultured neurons. *Circ Res, 103*(2), 186-193. doi:10.1161/circresaha.108.179408
Liu, J., Hakucho, A., & Fujimiya, T. (2015). Angiotensinase C mRNA and protein downregulations are involved in ethanol-deteriorated left ventricular systolic dysfunction in spontaneously hypertensive rats. *BioMed research international, 2015*.

Liu, J., Jiang, M., Deng, S., Lu, J., Huang, H., Zhang, Y., . . . Wang, H. (2018). miR-93-5p-Containing Exosomes Treatment Attenuates Acute Myocardial Infarction-Induced Myocardial Damage. *Molecular therapy. Nucleic acids, 11*(C), 103-115. doi:10.1016/j.omtn.2018.01.010

Lo, J., Patel, V. B., Wang, Z., Levasseur, J., Kaufman, S., Penninger, J. M., & Oudit, G. Y. (2013). Angiotensin‐converting enzyme 2 antagonizes angiotensin II‐induced pressor response and NADPH oxidase activation in Wistar–Kyoto rats and spontaneously hypertensive rats. *Experimental physiology, 98*(1), 109-122. doi:10.1113/expphysiol.2012.067165

Loftus, I. (2014). 4 Mechanisms of Plaque Rupture. *Mechanisms of Vascular*, 43.

Lohmeier, T. E. (2012). Angiotensin II infusion model of hypertension: is there an important sympathetic component? *Hypertension, 59*(3), 539-541.

Longatti, A. (2015). The dual role of exosomes in hepatitis A and C virus transmission and viral immune activation. *Viruses, 7*(12), 6707-6715.

Loot, A. E., Roks, A. J., Henning, R. H., Tio, R. A., Suurmeijer, A. J., Boomsma, F., & van Gilst, W. H. (2002). Angiotensin-(1–7) attenuates the development of heart failure after myocardial infarction in rats. *Circulation, 105*(13), 1548-1550.

Lopez-Sendon, J., Swedberg, K., Torp-Pedersen, C., McMurray, J., Tamargo, J., Maggioni, A. P., . . . Sahlgrenska, A. (2004). Expert consensus document on angiotensin converting enzyme inhibitors in cardiovascular disease: The Task Force on ACE-inhibitors of the European Society of Cardiology. *European heart journal, 25*(16), 1454-1470.

Lu, H., Wu, C., Howatt, D. A., Balakrishnan, A., Moorleghen, J. J., Chen, X., . . . Daugherty, A. (2016). Angiotensinogen Exerts Effects Independent of Angiotensin II. *Arteriosclerosis, thrombosis, and vascular biology, 36*(2), 256-265. doi:10.1161/ATVBAHA.115.306740

Lu, L., Liu, M., Sun, R., Zheng, Y., & Zhang, P. (2015). Myocardial infarction: symptoms and treatments. *Cell biochemistry and biophysics, 72*(3), 865-867.

Luo, J., Deng, Z. L., Luo, X., Tang, N., Song, W. X., Chen, J., . . . He, T. C. (2007). A protocol for rapid generation of recombinant adenoviruses using the AdEasy system. *Nat Protoc, 2*(5), 1236-1247. doi:10.1038/nprot.2007.135

Lusky, M., Grave, L., Dieterle, A., Dreyer, D., Christ, M., Ziller, C., . . . Pavirani, A. (1999). Regulation of adenovirus-mediated transgene expression by the viral E4 gene products: requirement for E4 ORF3. *Journal of virology, 73*(10), 8308-8319.

Lyu, L., Wang, H., Li, B., Qin, Q., Qi, L., Nagarkatti, M., . . . Cui, T. (2015). A critical role of cardiac fibroblast-derived exosomes in activating renin angiotensin system in cardiomyocytes. *Journal of molecular and cellular cardiology, 89*(Pt B), 268-279. doi:10.1016/j.yjmcc.2015.10.022

Ma, H., Kong, J., Wang, Y. L., Li, J. L., Hei, N. H., Cao, X. R., . . . Dong, B. (2017). Angiotensin-converting enzyme 2 overexpression protects against doxorubicin-induced cardiomyopathy by multiple mechanisms in rats. *Oncotarget, 8*(15), 24548-24563. doi:10.18632/oncotarget.15595

Maier, C., Schadock, I., Haber, P. K., Wysocki, J., Ye, M., Kanwar, Y., . . . Adams, G. N. (2017). Prolylcarboxypeptidase deficiency is associated with increased blood pressure, glomerular lesions, and cardiac dysfunction independent of altered circulating and cardiac angiotensin II. *Journal of Molecular Medicine, 95*, 473-486.

Maier, C., Schadock, I., Haber, P. K., Wysocki, J., Ye, M., Kanwar, Y., . . . Batlle, D. (2017). Prolylcarboxypeptidase deficiency is associated with increased blood pressure, glomerular lesions, and cardiac dysfunction independent of altered circulating and cardiac angiotensin II. *Journal of molecular medicine (Berlin, Germany), 95*(5), 473-486. doi:10.1007/s00109-017-1513-9

Maioli, M., Asara, Y., Pintus, A., Ninniri, S., Bettuzzi, S., Scaltriti, M., . . . Ventura, C. (2007). Creating prodynorphin-expressing stem cells alerted for a high-throughput of cardiogenic commitment.

Mallela, J., Perkins, R., Yang, J., Pedigo, S., Rimoldi, J., & Shariat-Madar, Z. (2008). The functional importance of the N-terminal region of human prolylcarboxypeptidase. *Biochemical and biophysical research communications, 374*(4), 635-640.

Mallela, J., Yang, J., & Shariat-Madar, Z. (2009). Prolylcarboxypeptidase: A cardioprotective enzyme. *The international journal of biochemistry & cell biology, 41*(3), 477-481. doi:10.1016/j.biocel.2008.02.022

Malloci, M., Perdomo, L., Veerasamy, M., Andriantsitohaina, R., Simard, G., & Martínez, M. C. (2019). Extracellular Vesicles: Mechanisms in Human Health and Disease. *Antioxidants & redox signaling, 30*(6), 813-856. doi:10.1089/ars.2017.7265

Malpas, S. C., Groom, A. S., & Head, G. A. (1997). Baroreflex Control of Heart Rate and Cardiac Hypertrophy in Angiotensin II-Induced Hypertension in Rabbits. *Hypertension (Dallas, Tex. 1979), 29*(6), 1284-1290. doi:10.1161/01.HYP.29.6.1284

Marangoni, R. A., Santos, R. A., & Piccolo, C. (2014). Deficient prolylcarboxypeptidase gene and protein expression in left ventricles of spontaneously hypertensive rats (SHR). *Peptides (New York, N.Y. : 1980), 61*, 69-74. doi:10.1016/j.peptides.2014.08.016

Marques, F. Z., Romaine, S. P., Denniff, M., Eales, J., Dormer, J., Garrelds, I. M., . . . Kiszka, B. (2015). Signatures of miR-181a on the renal transcriptome and blood pressure. *Molecular Medicine, 21*(1), 739-748.

Marquez‐Aguirre, A., Sandoval‐Rodriguez, A., Gonzalez‐Cuevas, J., Bueno‐Topete, M., Navarro‐Partida, J., Arellano‐Olivera, I., . . . Armendariz‐Borunda, J. (2009). Adenoviral delivery of dominant‐negative transforming growth factor β type II receptor up‐regulates transcriptional repressor SKI‐like oncogene, decreases matrix metalloproteinase 2 in hepatic stellate cell and prevents liver fibrosis in rats. *The Journal of Gene Medicine: A cross‐disciplinary journal for research on the science of gene transfer and its clinical applications, 11*(3), 207-219.

Martini, L. (2004). *Encyclopedia of endocrine diseases*. Amsterdam;San Diego, Calif;Boston;: Elsevier.

Marwick, T. H., Gillebert, T. C., Aurigemma, G., Chirinos, J., Derumeaux, G., Galderisi, M., . . . Segers, P. (2015). Recommendations on the use of echocardiography in adult hypertension: a report from the European Association of Cardiovascular Imaging (EACVI) and the American Society of Echocardiography (ASE). *European Heart Journal-Cardiovascular Imaging, 16*(6), 577-605.

Masaki, H., Kurihara, T., Yamaki, A., Inomata, N., Nozawa, Y., Mori, Y., . . . Horiuchi, M. (1998). Cardiac-specific overexpression of angiotensin II AT2 receptor causes attenuated response to AT1 receptor-mediated pressor and chronotropic effects. *The Journal of clinical investigation, 101*(3), 527-535.

Masri, B., Morin, N., Cornu, M., Knibiehler, B., & Audigier, Y. (2004). Apelin (65‐77) activates p70 S6 kinase and is mitogenic for umbilical endothelial cells. *The FASEB journal, 18*(15), 1909-1911.

Masson, R., Nicklin, S. A., Craig, M. A., McBride, M., Gilday, K., Gregorevic, P., . . . Graham, D. (2009). Onset of experimental severe cardiac fibrosis is mediated by overexpression of Angiotensin-converting enzyme 2. *Hypertension, 53*(4), 694-700.

Masters, J. R. (2002). HeLa cells 50 years on: the good, the bad and the ugly. *Nature Reviews Cancer, 2*(4), 315-319.

Matsumoto, T., Wada, A., Tsutamoto, T., Ohnishi, M., Isono, T., & Kinoshita, M. (2003). Chymase inhibition prevents cardiac fibrosis and improves diastolic dysfunction in the progression of heart failure. *Circulation (New York, N.Y.), 107*(20), 2555-2558. doi:10.1161/01.CIR.0000074041.81728.79

Matyas, L., Schulte, K.-L., Dormandy, J., Norgren, L., Sowade, O., Grötzbach, G., . . . Wahlberg, E. (2005). Arteriogenic gene therapy in patients with unreconstructable critical limb ischemia: a randomized, placebo-controlled clinical trial of adenovirus 5-delivered fibroblast growth factor-4. *Human gene therapy, 16*(10), 1202-1211.

Maurice, J. P., Hata, J. A., Shah, A. S., White, D. C., McDonald, P. H., Dolber, P. C., . . . Koch, W. J. (1999). Enhancement of cardiac function after adenoviral-mediated in vivo intracoronary β 2-adrenergic receptor gene delivery. *The Journal of clinical investigation, 104*(1), 21-29.

McCollum, L. T., Gallagher, P. E., & Tallant, E. A. (2012). Angiotensin-(1–7) attenuates angiotensin II-induced cardiac remodeling associated with upregulation of dual-specificity phosphatase 1. *American Journal of Physiology-Heart and Circulatory Physiology*.
McConnell, M. J., & Imperiale, M. J. (2004). Biology of adenovirus and its use as a vector for gene therapy. *Human gene therapy, 15*(11), 1022-1033.
McFall, A., Nicklin, S. A., & Work, L. M. (2020). The counter regulatory axis of the renin angiotensin system in the brain and ischaemic stroke: Insight from preclinical stroke studies and therapeutic potential. *Cellular signalling, 76*, 109809.
McGee, S. (2021). *Evidence-based physical diagnosis e-book*: Elsevier Health Sciences.
McKINNEY, C. A., Fattah, C., Loughrey, C. M., Milligan, G., & Nicklin, S. A. (2014). Angiotensin-(1–7) and angiotensin-(1–9): function in cardiac and vascular remodelling. *Clinical science, 126*(12), 815-827.
McNamara, R. P., & Dittmer, D. P. (2020). Extracellular vesicles in virus infection and pathogenesis. *Current opinion in virology, 44*, 129-138.
Mehta, P. K., & Griendling, K. K. (2007). Angiotensin II cell signaling: physiological and pathological effects in the cardiovascular system. *American Journal of Physiology - Cell Physiology, 292*(1), 82-97. doi:10.1152/ajpcell.00287.2006
Meier, O., & Greber, U. F. (2004). Adenovirus endocytosis. *The Journal of Gene Medicine: A cross‐disciplinary journal for research on the science of gene transfer and its clinical applications, 6*(S1), S152-S163.
Melo, L. G., Agrawal, R., Zhang, L., Rezvani, M., Mangi, A. A., Ehsan, A., . . . Oyama, J. (2002). Gene therapy strategy for long-term myocardial protection using adeno-associated virus-mediated delivery of heme oxygenase gene. *Circulation, 105*(5), 602-607.
Mendonça, S. A., Lorincz, R., Boucher, P., & Curiel, D. T. (2021). Adenoviral vector vaccine platforms in the SARS-CoV-2 pandemic. *npj Vaccines, 6*(1), 97.
Meng, W., He, C., Hao, Y., Wang, L., Li, L., & Zhu, G. (2020). Prospects and challenges of extracellular vesicle-based drug delivery system: Considering cell source. *Drug delivery, 27*(1), 585-598.
Metcalfe, B. L., Huentelman, M. J., Parilak, L. D., Taylor, D. G., Katovich, M. J., Knot, H. J., . . . Raizada, M. K. (2004). Prevention of cardiac hypertrophy by angiotensin II type-2 receptor gene transfer. *Hypertension, 43*(6), 1233-1238.
Metzger, R., Bader, M., Ludwig, T., Berberich, C., Bunnemann, B., & Ganten, D. (1995). Expression of the mouse and rat mas proto‐oncogene in the brain and peripheral tissues. *FEBS letters, 357*(1), 27-32.
Metzner, C., & Zaruba, M. (2021). On the Relationship of Viral Particles and Extracellular Vesicles: Implications for Viral Vector Technology. *Viruses, 13*(7), 1238.
Mezzano, S. A., Ruiz-Ortega, M., & Egido, J. (2001). Angiotensin II and renal fibrosis. *Hypertension, 38*(3), 635-638.
Michel, M. C., Brodde, O.-E., & Insel, P. A. (1990). Peripheral adrenergic receptors in hypertension. *Hypertension, 16*(2), 107-120.
Milliken, A. S., Ciesla, J. H., Nadtochiy, S. M., & Brookes, P. S. (2023). Distinct effects of intracellular vs. extracellular acidic pH on the cardiac metabolome during ischemia and reperfusion. *Journal of molecular and cellular cardiology, 174*, 101-114.
Mitra, A. K., Gao, L., & Zucker, I. H. (2010). Angiotensin II-induced upregulation of AT(1) receptor expression: sequential activation of NF-kappaB and Elk-1 in neurons. *Am J Physiol Cell Physiol, 299*(3), C561-569. doi:10.1152/ajpcell.00127.2010
Mohammed, S. F., Hussain, S., Mirzoyev, S. A., Edwards, W. D., Maleszewski, J. J., & Redfield, M. M. (2015). Coronary microvascular rarefaction and myocardial fibrosis in heart failure with preserved ejection fraction. *Circulation, 131*(6), 550-559.
Molkentin, J. D., & Dorn, G. W. (2001). Cytoplasmic signaling pathways that regulate cardiac hypertrophy. *Annual review of physiology, 63*(1), 391-426. doi:10.1146/annurev.physiol.63.1.391
Momen-Heravi, F. (2017). Isolation of extracellular vesicles by ultracentrifugation. In *Extracellular Vesicles* (pp. 25-32): Springer.

Moravec, C. S., Schluchter, M. D., Paranandi, L., Czerska, B., Stewart, R. W., Rosenkranz, E., & Bond, M. (1990). Inotropic effects of angiotensin II on human cardiac muscle in vitro. *Circulation, 82*(6), 1973-1984.

Moreira Jr, E. D., Kitchin, N., Xu, X., Dychter, S. S., Lockhart, S., Gurtman, A., . . . Jennings, T. W. (2022). Safety and efficacy of a third dose of BNT162b2 Covid-19 vaccine. *New England Journal of Medicine, 386*(20), 1910-1921.

Morgan, H. L., Butler, E., Ritchie, S., Herse, F., Dechend, R., Beattie, E., . . . Graham, D. (2018). Modeling superimposed preeclampsia using Ang II (Angiotensin II) infusion in pregnant stroke-prone spontaneously hypertensive rats. *Hypertension, 72*(1), 208-218.

Moritani, T., Iwai, M., Kanno, H., Nakaoka, H., Iwanami, J., Higaki, T., . . . Horiuchi, M. (2013). ACE2 deficiency induced perivascular fibrosis and cardiac hypertrophy during postnatal development in mice. *Journal of the American Society of Hypertension, 7*(4), 259-266.

Mousavi, S. A., Malerød, L., Berg, T., & Kjeken, R. (2004). Clathrin-dependent endocytosis. *Biochemical Journal, 377*(Pt 1), 1.

Mueller, M. P., Tippins, D. J., & Stewart, A. J. (2017). *Animals and Science Education*: Springer.

Mukoyama, M., Nakajima, M., Horiuchi, M., Sasamura, H., Pratt, R. E., & Dzau, V. (1993). Expression cloning of type 2 angiotensin II receptor reveals a unique class of seven-transmembrane receptors. *Journal of Biological Chemistry, 268*(33), 24539-24542.

Mulcahy, L. A., Pink, R. C., & Carter, D. R. F. (2014). Routes and mechanisms of extracellular vesicle uptake. *Journal of Extracellular Vesicles, 3*(1), 24641.

Muñoz, E. L., Fuentes, F. B., Felmer, R. N., Yeste, M., & Arias, M. E. (2022). Extracellular vesicles in mammalian reproduction: a review. *Zygote*, 1-24.

MuÑOz, J. M., Braun-MenÉNdez, E., Fasciolo, J. C., & Leloir, L. F. (1939). Hypertensin: The Substance Causing Renal Hypertension. *Nature (London), 144*(3658), 980-980. doi:10.1038/144980a0

Muruve, D. A. (2004). The innate immune response to adenovirus vectors. *Human gene therapy, 15*(12), 1157-1166.

Nabel, E. G., Plautz, G., & Nabel, G. J. (1990). Site-specific gene expression in vivo by direct gene transfer into the arterial wall. *Science, 249*(4974), 1285-1288.

Nabika, T., Ohara, H., Kato, N., & Isomura, M. (2012). The stroke-prone spontaneously hypertensive rat: still a useful model for post-GWAS genetic studies? *Hypertension Research, 35*(5), 477-484.

Naim, C., Yerevanian, A., & Hajjar, R. J. (2013). Gene therapy for heart failure: where do we stand? *Current cardiology reports, 15*(2), 1-10.

Nakamura, M., & Sadoshima, J. (2018). Mechanisms of physiological and pathological cardiac hypertrophy. *Nature reviews cardiology, 15*(7), 387-407.

Naldini, L., Blömer, U., Gage, F. H., Trono, D., & Verma, I. M. (1996). Efficient transfer, integration, and sustained long-term expression of the transgene in adult rat brains injected with a lentiviral vector. *Proceedings of the National Academy of Sciences, 93*(21), 11382-11388.

Narang, P. Ferring Receives Approval from US FDA for Adstiladrin for High-Risk, BCG-Unresponsive Non-Muscle Invasive Bladder Cancer.

Naso, M. F., Tomkowicz, B., Perry, W. L., & Strohl, W. R. (2017). Adeno-associated virus (AAV) as a vector for gene therapy. *BioDrugs, 31*(4), 317-334.

Nayerossadat, N., Maedeh, T., & Ali, P. A. (2012). Viral and nonviral delivery systems for gene delivery. *Advanced biomedical research, 1*.

Neaverson, M. (1966). Metabolic acidosis in acute myocardial infarction. *British medical journal, 2*(5510), 383.

Neufeld, E. F., & Sweeley, C. C. (1972). Gene therapy for human genetic disease? *Science, 178*(4061), 648-648.

Ng, C. J., Bourquard, N., Hama, S. Y., Shih, D., Grijalva, V. R., Navab, M., . . . Reddy, S. T. (2007). Adenovirus-Mediated Expression of Human Paraoxonase 3 Protects Against the Progression of Atherosclerosis in Apolipoprotein E–Deficient Mice. *Arteriosclerosis, thrombosis, and vascular biology, 27*(6), 1368-1374.

Ng, C. J., Hama, S. Y., Bourquard, N., Navab, M., & Reddy, S. T. (2006). Adenovirus mediated expression of human paraoxonase 2 protects against the development of atherosclerosis in apolipoprotein E-deficient mice. *Molecular genetics and metabolism, 89*(4), 368-373.

Ng, K. K. F., & Vane, J. R. (1968). Fate of Angiotensin I in the Circulation. *Nature (London), 218*(5137), 144-150. doi:10.1038/218144a0

Nguyen, B. Y. (2020). *The Cardioprotective Role of Prolyl Carboxypeptidase (PRCP) in Cardiac Hypertrophic Remodelling*: The University of Manchester (United Kingdom).

Nguyen, B. Y., Zhou, F., Binder, P., Liu, W., Hille, S. S., Luo, X., . . . Ahmed, F. Z. (2023). Prolylcarboxypeptidase Alleviates Hypertensive Cardiac Remodeling by Regulating Myocardial Tissue Angiotensin II. *Journal of the American Heart Association*, e028298.

Ni, W., Yang, X., Yang, D., Bao, J., Li, R., Xiao, Y., . . . Yang, D. (2020). Role of angiotensin-converting enzyme 2 (ACE2) in COVID-19. *Critical Care, 24*(1), 1-10.

Nicklin, S. A., Buening, H., Dishart, K. L., De Alwis, M., Girod, A., Hacker, U., . . . Baker, A. H. (2001). Efficient and selective AAV2-mediated gene transfer directed to human vascular endothelial cells. *Molecular therapy, 4*(3), 174-181.

Nicklin, S. A., Wu, E., Nemerow, G. R., & Baker, A. H. (2005). The influence of adenovirus fiber structure and function on vector development for gene therapy. *Mol Ther, 12*(3), 384-393. doi:10.1016/j.ymthe.2005.05.008

Nisole, S., & Saïb, A. (2004). Early steps of retrovirus replicative cycle. *Retrovirology, 1*, 1-20.

Niwano, K., Arai, M., Koitabashi, N., Watanabe, A., Ikeda, Y., Miyoshi, H., & Kurabayashi, M. (2008). Lentiviral vector–mediated SERCA2 gene transfer protects against heart failure and left ventricular remodeling after myocardial infarction in rats. *Molecular therapy, 16*(6), 1026-1032.

Nolte-'t Hoen, E., Cremer, T., Gallo, R. C., & Margolis, L. B. (2016). Extracellular vesicles and viruses: Are they close relatives? *Proceedings of the National Academy of Sciences, 113*(33), 9155-9161.

Nuamnaichati, N., Parichatikanond, W., & Mangmool, S. (2022). Cardioprotective effects of glucagon-like peptide-1 (9-36) against oxidative injury in H9c2 cardiomyoblasts: Potential role of the PI3K/Akt/NOS pathway. *Journal of Cardiovascular Pharmacology, 79*(1), e50-e63.

Ocaranza, M. a. P., Godoy, I., Jalil, J. E., Varas, M., Collantes, P., Pinto, M., . . . Diaz-Araya, G. (2006). Enalapril attenuates downregulation of angiotensin-converting enzyme 2 in the late phase of ventricular dysfunction in myocardial infarcted rat. *Hypertension, 48*(4), 572-578.

Ocaranza, M. P., Lavandero, S., Jalil, J. E., Moya, J., Pinto, M., Novoa, U., . . . Varas, M. (2010). Angiotensin-(1–9) regulates cardiac hypertrophy in vivo and in vitro. *Journal of hypertension, 28*(5), 1054-1064.

Ocaranza, M. P., Michea, L., Chiong, M., Lagos, C. F., Lavandero, S., & Jalil, J. E. (2014). Recent insights and therapeutic perspectives of angiotensin-(1–9) in the cardiovascular system. *Clinical science, 127*(9), 549-557.

Odya, C. E., Marinkovic, D. V., Hammon, K. J., Stewart, T. A., & Erdös, E. (1978). Purification and properties of prolylcarboxypeptidase (angiotensinase C) from human kidney. *Journal of Biological Chemistry, 253*(17), 5927-5931.

Okada, T., Ramsey, W. J., Munir, J., Wildner, O., & Blaese, R. M. (1998). Efficient directional cloning of recombinant adenovirus vectors using DNA-protein complex. *Nucleic Acids Res, 26*(8), 1947-1950. doi:10.1093/nar/26.8.1947

Olliaro, P. (2021). What does 95% COVID-19 vaccine efficacy really mean? *The Lancet Infectious Diseases, 21*(6), 769.

Oudit, G. Y., Crackower, M. A., Backx, P. H., & Penninger, J. M. (2003). The role of ACE2 in cardiovascular physiology. *Trends in cardiovascular medicine, 13*(3), 93-101.

Oudit, G. Y., Zhong, J., Basu, R., Guo, D., Penninger, J. M., & Kassiri, Z. (2010). Angiotensin Converting Enzyme 2 Suppresses Pathological Hypertrophy, Myocardial Fibrosis and Diastolic Dysfunction. *Journal of cardiac failure, 16*(8), S16-S16. doi:10.1016/j.cardfail.2010.06.054

Pan, B.-T., & Johnstone, R. M. (1983). Fate of the transferrin receptor during maturation of sheep reticulocytes in vitro: selective externalization of the receptor. *Cell, 33*(3), 967-978.
Pang, J.-J., Xu, R.-K., Xu, X.-B., Cao, J.-M., Ni, C., Zhu, W.-L., . . . Chen, C. (2004). Hexarelin protects rat cardiomyocytes from angiotensin II-induced apoptosis in vitro. *American Journal of Physiology-Heart and Circulatory Physiology, 286*(3), H1063-H1069.
Park, B. M., Gao, S., Cha, S. A., Park, B. H., & Kim, S. H. (2013). Cardioprotective effects of angiotensin III against ischemic injury via the AT 2 receptor and KATP channels. *Physiological Reports, 1*(6), e00151.
Patel, V. B., Takawale, A., Ramprasath, T., Das, S. K., Basu, R., Grant, M. B., . . . Oudit, G. Y. (2015). Antagonism of angiotensin 1–7 prevents the therapeutic effects of recombinant human ACE2. *Journal of Molecular Medicine, 93*(9), 1003-1013.
Patel, V. B., Zhong, J. C., Grant, M. B., & Oudit, G. Y. (2016). Role of the ACE2/Angiotensin 1-7 Axis of the Renin-Angiotensin System in Heart Failure. *Circ Res, 118*(8), 1313-1326. doi:10.1161/circresaha.116.307708
Paul, M., Poyan Mehr, A., & Kreutz, R. (2006). Physiology of local renin-angiotensin systems. *Physiological reviews, 86*(3), 747-803.
Paul, O., & Chatterjee, S. (2021). Coronavirus disease (COVID-19) and the endothelium. In *Endothelial Signaling in Vascular Dysfunction and Disease* (pp. 205-211): Elsevier.
Pavel, J., Oroszova, Z., Hricova, L., & Lukacova, N. (2013). Effect of subpressor dose of angiotensin II on pain-related behavior in relation with neuronal injury and activation of satellite glial cells in the rat dorsal root ganglia. *Cellular and molecular neurobiology, 33*, 681-688.
Pawluczyk, I., Patel, S., & Harris, K. (2006). Pharmacological enhancement of the kallikrein-kinin system promotes anti-fibrotic responses in human mesangial cells. *Cellular Physiology and Biochemistry, 18*(6), 327-336.
Paz Ocaranza, M., Riquelme, J. A., García, L., Jalil, J. E., Chiong, M., Santos, R. A., & Lavandero, S. (2020). Counter-regulatory renin–angiotensin system in cardiovascular disease. *Nature reviews cardiology, 17*(2), 116-129.
Peach, M. J. (1977). RENIN-ANGIOTENSIN SYSTEM - BIOCHEMISTRY AND MECHANISMS OF ACTION. *Physiological reviews, 57*(2), 313-370. doi:10.1152/physrev.1977.57.2.313
Pedrioli, G., Piovesana, E., Vacchi, E., & Balbi, C. (2021). Extracellular Vesicles as Promising Carriers in Drug Delivery: Considerations from a Cell Biologist's Perspective. *Biology (Basel, Switzerland), 10*(5), 376. doi:10.3390/biology10050376
Peng, K., Tian, X., Qian, Y., Skibba, M., Zou, C., Liu, Z., . . . Liang, G. (2016). Novel EGFR inhibitors attenuate cardiac hypertrophy induced by angiotensin II. *Journal of Cellular and Molecular Medicine, 20*(3), 482-494.
Peng, Y., Zhao, M., Hu, Y., Guo, H., Zhang, Y., Huang, Y., . . . Wang, Z. (2022). Blockade of exosome generation by GW4869 inhibits the education of M2 macrophages in prostate cancer. *BMC immunology, 23*(1), 1-15.
Perlman, R. L. (2016). Mouse models of human diseaseAn evolutionary perspective. *Evolution, medicine, and public health, 2016*(1), 170-176.
Perlot, T., & Penninger, J. M. (2013). ACE2–From the renin–angiotensin system to gut microbiota and malnutrition. *Microbes and infection, 15*(13), 866-873.
Persson, P. B. (2003). Renin: origin, secretion and synthesis. *The Journal of physiology, 552*(3), 667-671. doi:10.1113/jphysiol.2003.049890
Peterson, M. C. (2005). Circulating transforming growth factor beta-1: a partial molecular explanation for associations between hypertension, diabetes, obesity, smoking and human disease involving fibrosis. *Medical science monitor: international medical journal of experimental and clinical research, 11*(7), RA229-232.
Pfeifer, M., Wolf, K., Blumberg, F. C., Elsner, D., Muders, F., Holmer, S. R., . . . Kurtz, A. (1997). ANP gene expression in rat hearts during hypoxia. *Pflügers Archiv, 434*, 63-69.
Phillips, M. I., & Kimura, B. (2005). Gene therapy for hypertension: antisense inhibition of the renin-angiotensin system. *Hypertension: Methods and Protocols*, 363-379.
Phillips, M. I., & Schmidt-Ott, K. M. (1999). The Discovery of Renin 100 Years Ago. *News in physiological sciences, 14*(6), 271-274. doi:10.1152/physiologyonline.1999.14.6.271

Piqueras, L., Kubes, P., Alvarez, A., O'Connor, E., Issekutz, A. C., Esplugues, J. V., & Sanz, M.-J. (2000). Angiotensin II induces leukocyte-endothelial cell interactions in vivo via AT1 and AT2 receptor-mediated P-selectin upregulation. *Circulation (New York, N.Y.), 102*(17), 2118-2123.

Pironti, G., Strachan, R. T., Abraham, D., Yu, S. M.-W., Chen, M., Chen, W., . . . Rockman, H. A. (2015). Circulating Exosomes Induced by Cardiac Pressure Overload Contain Functional Angiotensin II Type 1 Receptors. *Circulation (New York, N.Y.), 131*(24), 2120-2130. doi:10.1161/CIRCULATIONAHA.115.015687

Pollard, A. J., Launay, O., Lelievre, J.-D., Lacabaratz, C., Grande, S., Goldstein, N., . . . Wiedemann, A. (2021). Safety and immunogenicity of a two-dose heterologous Ad26. ZEBOV and MVA-BN-Filo Ebola vaccine regimen in adults in Europe (EBOVAC2): a randomised, observer-blind, participant-blind, placebo-controlled, phase 2 trial. *The Lancet Infectious Diseases, 21*(4), 493-506.

Poulter, N. (2010). ARBs in hypertension. *Br J Cardiol, 17*, s6-s9.

Pound, P., & Ritskes-Hoitinga, M. (2018). Is it possible to overcome issues of external validity in preclinical animal research? Why most animal models are bound to fail. *Journal of translational medicine, 16*(1), 1-8.

Povsic, T. J., Henry, T. D., Ohman, E. M., Pepine, C. J., Crystal, R. G., Rosengart, T. K., . . . Answini, G. A. (2021). Epicardial delivery of XC001 gene therapy for refractory angina coronary treatment (the EXACT trial): rationale, design, and clinical considerations. *American heart journal, 241*, 38-49.

Prathapan, A., & Raghu, K. (2018). Apoptosis in angiotensin II-stimulated hypertrophic cardiac cells-modulation by phenolics rich extract of Boerhavia diffusa L. *Biomedicine & Pharmacotherapy, 108*, 1097-1104.

Prathapan, A., Vineetha, V. P., & Raghu, K. G. (2014). Protective effect of Boerhaavia diffusa L. against mitochondrial dysfunction in angiotensin II induced hypertrophy in H9c2 cardiomyoblast cells. *PLoS One, 9*(4), e96220.

Qin, X. P., Zeng, S. Y., Tian, H. H., Deng, S. X., Ren, J. F., Zheng, Y. B., . . . Chen, S. Y. (2009). Involvement of prolylcarboxypeptidase in the effect of rutaecarpine on the regression of mesenteric artery hypertrophy in renovascular hypertensive rats. *Clinical and Experimental Pharmacology and Physiology, 36*(3), 319-324.

Rafieian-Kopaei, M., Setorki, M., Doudi, M., Baradaran, A., & Nasri, H. (2014). Atherosclerosis: process, indicators, risk factors and new hopes. *International journal of preventive medicine, 5*(8), 927.

Raimondi, F., & Warin-Fresse, K. (2016). Computed tomography imaging in children with congenital heart disease: indications and radiation dose optimization. *Archives of cardiovascular diseases, 109*(2), 150-157.

Raizada, M. K., & Sarkissian, S. D. (2006). Potential of gene therapy strategy for the treatment of hypertension. *Hypertension, 47*(1), 6-9.

Rajput, A., Varshney, A., Bajaj, R., & Pokharkar, V. (2022). Exosomes as new generation vehicles for drug delivery: Biomedical applications and future perspectives. *Molecules, 27*(21), 7289.

Ramaha, A., & Patston, P. A. (2002). Release and degradation of angiotensin I and angiotensin II from angiotensinogen by neutrophil serine proteinases. *Archives of biochemistry and biophysics, 397*(1), 77-83.

Rang, H. P., Ritter, J., Flower, R. J., & Henderson, G. (2020). *Rang & Dale's pharmacology* (Ninth ed.). Edinburgh?: Elsevier/Churchill Livingstone.

Rapacciuolo, A., Esposito, G., Caron, K., Mao, L., Thomas, S. A., & Rockman, H. A. (2001). Important role of endogenous norepinephrine and epinephrine in the development of in vivo pressure-overload cardiac hypertrophy. *Journal of the American College of Cardiology, 38*(3), 876-882.

Raposo, G., Nijman, H. W., Stoorvogel, W., Liejendekker, R., Harding, C. V., Melief, C., & Geuze, H. J. (1996). B lymphocytes secrete antigen-presenting vesicles. *The Journal of experimental medicine, 183*(3), 1161-1172.

Rapp, J. P. (2000). Genetic analysis of inherited hypertension in the rat. *Physiological reviews, 80*(1), 135-172.
Ravassa, S., López, B., Treibel, T. A., San José, G., Losada-Fuentenebro, B., Tapia, L., . . . González, A. (2023). Cardiac Fibrosis in heart failure: Focus on non-invasive diagnosis and emerging therapeutic strategies. *Molecular Aspects of Medicine, 93*, 101194.
Reckelhoff, J. F. (2001). Gender differences in the regulation of blood pressure. *Hypertension, 37*(5), 1199-1208.
Reckelhoff, J. F., Cardozo, L. L. Y., & Fortepiani, M. L. A. (2018). Models of hypertension in aging. In *Conn's Handbook of Models for Human Aging* (pp. 703-720): Elsevier.
Redfield, M. M. (2016). Heart failure with preserved ejection fraction. *New England Journal of Medicine, 375*(19), 1868-1877.
Ren, X.-S., Tong, Y., Qiu, Y., Ye, C., Wu, N., Xiong, X.-Q., . . . Zhu, G.-Q. (2020). MiR155-5p in adventitial fibroblasts-derived extracellular vesicles inhibits vascular smooth muscle cell proliferation via suppressing angiotensin-converting enzyme expression. *Journal of Extracellular Vesicles, 9*(1), 1698795-n/a. doi:10.1080/20013078.2019.1698795
Riet, L., Esch, J., Roks, A., van den Meiracker, T., & Danser, J. (2015). Hypertension Renin-Angiotensin-Aldosterone System Alterations. *Circulation research, 116*(6), 960-975. doi:10.1161/CIRCRESAHA.116.303587
Riordan, J. F. (2003). Angiotensin-I-converting enzyme and its relatives. *Genome biology, 4*(8), 1-5.
Robbins, I. M., Christman, B. W., Newman, J. H., Matlock, R., & Loyd, J. E. (1998). A survey of diagnostic practices and the use of epoprostenol in patients with primary pulmonary hypertension. *Chest, 114*(5), 1269-1275.
Robbins, P. D., & Ghivizzani, S. C. (1998). Viral vectors for gene therapy. *Pharmacology & therapeutics, 80*(1), 35-47.
Robinson, N. B., Krieger, K., Khan, F. M., Huffman, W., Chang, M., Naik, A., . . . Girardi, L. N. (2019). The current state of animal models in research: A review. *International Journal of Surgery, 72*, 9-13.
Rosenkranz, S. (2004). TGF-β1 and angiotensin networking in cardiac remodeling. *Cardiovascular research, 63*(3), 423-432.
Ross, R. (1993). The pathogenesis of atherosclerosis: a perspective for the 1990s. *Nature, 362*(6423), 801-809.
Ross, R. (1995). Cell biology of atherosclerosis. *Annual review of physiology, 57*(1), 791-804.
Rowe, W. P., Huebner, R. J., Gilmore, L. K., Parrott, R. H., & Ward, T. G. (1953). Isolation of a cytopathogenic agent from human adenoids undergoing spontaneous degeneration in tissue culture. *Proceedings of the Society for Experimental Biology and Medicine, 84*(3), 570-573.
Sachetelli, S., Liu, Q., Zhang, S.-L., Liu, F., Hsieh, T.-J., Brezniceanu, M.-L., . . . Sigmund, C. (2006). RAS blockade decreases blood pressure and proteinuria in transgenic mice overexpressing rat angiotensinogen gene in the kidney. *Kidney international, 69*(6), 1016-1023.
Sadoshima, J.-i., & Izumo, S. (1993). Molecular Characterization of Angiotensin II-Induced Hypertrophy of Cardiac Myocytes and Hyperplasia of Cardiac Fibroblasts Critical Role of the AT1 Receptor Subtype. *Circulation research, 73*(3), 413-423. doi:10.1161/01.RES.73.3.413
Sadoshima, J.-i., Xu, Y., Slayter, H. S., & Izumo, S. (1993). Autocrine release of angiotensin II mediates stretch-induced hypertrophy of cardiac myocytes in vitro. *Cell, 75*(5), 977-984. doi:10.1016/0092-8674(93)90541-W
Saeedi, R., Saran, V. V., Wu, S. S., Kume, E. S., Paulson, K., Chan, A. P., . . . Brownsey, R. W. (2009). AMP-activated protein kinase influences metabolic remodeling in H9c2 cells hypertrophied by arginine vasopressin. *American Journal of Physiology-Heart and Circulatory Physiology, 296*(6), H1822-H1832.
Sahoo, S., Kariya, T., & Ishikawa, K. (2021). Targeted delivery of therapeutic agents to the heart. *Nature reviews cardiology, 18*(6), 389-399.

Saleh, A. F., Lázaro-Ibáñez, E., Forsgard, M. A.-M., Shatnyeva, O., Osteikoetxea, X., Karlsson, F., . . . Harris, J. (2019). Extracellular vesicles induce minimal hepatotoxicity and immunogenicity. *Nanoscale, 11*(14), 6990-7001.

Saleh, M., & Ambrose, J. A. (2018). Understanding myocardial infarction. *F1000Research, 7*.

Sampaio, W. O., Souza dos Santos, R. A., Faria-Silva, R., da Mata Machado, L. T., Schiffrin, E. L., & Touyz, R. M. (2007). Angiotensin-(1-7) through receptor Mas mediates endothelial nitric oxide synthase activation via Akt-dependent pathways. *Hypertension, 49*(1), 185-192.

Sandmann, S., & Unger, T. (2002). Pathophysiological and clinical implications of AT(1)/AT(2) angiotensin II receptors in heart failure and coronary and renal failure. *Drugs (New York, N.Y.), 62*, 43-52. doi:10.2165/00003495-200262991-00005

Santin, Y., Sicard, P., Vigneron, F., Guilbeau-Frugier, C., Dutaur, M., Lairez, O., . . . Lezoualc'h, F. (2016). Oxidative stress by monoamine oxidase-A impairs transcription factor EB activation and autophagosome clearance, leading to cardiomyocyte necrosis and heart failure. *Antioxidants & redox signaling, 25*(1), 10-27.

Santos-Gallego, C. G., Picatoste, B., & Badimón, J. J. (2014). Pathophysiology of acute coronary syndrome. *Current atherosclerosis reports, 16*(4), 1-9.

Santos, R., Brosnihan, K. B., Jacobsen, D. W., DiCorleto, P. E., & Ferrario, C. M. (1992). Production of angiotensin-(1-7) by human vascular endothelium. *Hypertension, 19*(2_supplement), II56.

Santos, R. A., Campagnole-Santos, M. J., Baracho, N. C., Fontes, M. A., Silva, L. C., Neves, L. A., . . . Gropen Jr, C. (1994). Characterization of a new angiotensin antagonist selective for angiotensin-(1–7): evidence that the actions of angiotensin-(1–7) are mediated by specific angiotensin receptors. *Brain research bulletin, 35*(4), 293-298.

Santos, R. A., Castro, C. H., Gava, E., Pinheiro, S. V., Almeida, A. P., de Paula, R. D., . . . Irigoyen, M. C. (2006). Impairment of in vitro and in vivo heart function in angiotensin-(1-7) receptor MAS knockout mice. *Hypertension, 47*(5), 996-1002.

Santos, R. A., e Silva, A. C. S., Maric, C., Silva, D. M., Machado, R. P., de Buhr, I., . . . Bader, M. (2003). Angiotensin-(1–7) is an endogenous ligand for the G protein-coupled receptor Mas. *Proceedings of the National Academy of Sciences, 100*(14), 8258-8263.

Savina, A., Furlán, M., Vidal, M., & Colombo, M. I. (2003). Exosome release is regulated by a calcium-dependent mechanism in K562 cells. *Journal of Biological Chemistry, 278*(22), 20083-20090.

Schalekamp, M. A. D. H., & Danser, A. H. J. (2006). Angiotensin II production and distribution in the kidney: I. A kinetic model. *Kidney international, 69*(9), 1543-1552. doi:10.1038/sj.ki.5000303

Schiattarella, G. G., & Hill, J. A. (2015). Inhibition of hypertrophy is a good therapeutic strategy in ventricular pressure overload. *Circulation, 131*(16), 1435-1447.

Schiedner, G., Morral, N., Parks, R. J., Wu, Y., Koopmans, S. C., Langston, C., . . . Kochanek, S. (1998). Genomic DNA transfer with a high-capacity adenovirus vector results in improved in vivo gene expression and decreased toxicity. *Nature genetics, 18*(2), 180-183.

Schmidt, B., Drexler, H., & Schieffer, B. (2004). Therapeutic Effects of Angiotensin (AT1) Receptor Antagonists: Potential Contribution of Mechanisms Other Than AT1 Receptor Blockade. In (Vol. 4, pp. 361-368). New Zealand: Adis International.

Schultz, J. E. J., Witt, S. A., Glascock, B. J., Nieman, M. L., Reiser, P. J., Nix, S. L., . . . Doetschman, T. (2002). TGF-β1 mediates the hypertrophic cardiomyocyte growth induced by angiotensin II. *The Journal of clinical investigation, 109*(6), 787-796.

Schulz, J. B., Cookson, M. R., & Hausmann, L. (2016). The impact of fraudulent and irreproducible data to the translational research crisis–solutions and implementation. *Journal of Neurochemistry, 139*, 253-270.

Schwarzer, M. (2016). Models to investigate cardiac metabolism. In *The Scientist's Guide to Cardiac Metabolism* (pp. 103-122): Elsevier.

Schweda, F., & Kurtz, A. (2011). Regulation of renin release by local and systemic factors. *Reviews of physiology, biochemistry and pharmacology, 161*, 1.

Segura, A. M., Frazier, O., & Buja, L. M. (2014). Fibrosis and heart failure. *Heart failure reviews, 19*(2), 173-185.

Serdar, C. C., Cihan, M., Yücel, D., & Serdar, M. A. (2021). Sample size, power and effect size revisited: simplified and practical approaches in pre-clinical, clinical and laboratory studies. *Biochemia medica, 31*(1), 27-53.

Serfozo, P., Wysocki, J., Gulua, G., Schulze, A., Ye, M., Liu, P., . . . García-Horsman, J. A. (2020). Prolyl Oligopeptidase-Dependent Angiotensin II Conversion to Angiotensin-(1-7) in the circulation. *Hypertension (Dallas, Tex.: 1979), 75*(1), 173.

Serfozo, P., Wysocki, J., Gulua, G., Schulze, A., Ye, M., Liu, P., . . . Batlle, D. (2020). Ang II (Angiotensin II) Conversion to Angiotensin-(1-7) in the Circulation Is POP (Prolyloligopeptidase)-Dependent and ACE2 (Angiotensin-Converting Enzyme 2)-Independent. *Hypertension, 75*(1), 173-182. doi:10.1161/hypertensionaha.119.14071

Serneri, G. G. N., Boddi, M., Cecioni, I., Vanni, S., Coppo, M., Papa, M. L., . . . Toscano, T. (2001). Cardiac angiotensin II formation in the clinical course of heart failure and its relationship with left ventricular function. *Circulation research, 88*(9), 961-968.

Shanks, N., Greek, R., & Greek, J. (2009). Are animal models predictive for humans? *Philosophy, ethics, and humanities in medicine, 4*(1), 1-20.

Shanmugam, S., & Sandberg, K. (1996). ONTOGENY OF ANGIOTENSIN II RECEPTORS. *Cell biology international, 20*(3), 169-176. doi:10.1006/cbir.1996.0021

Shariat-Madar, Z., Mahdi, F., & Schmaier, A. H. (2002). Identification and Characterization of Prolylcarboxypeptidase as an Endothelial Cell Prekallikrein Activator. *The Journal of biological chemistry, 277*(20), 17962-17969. doi:10.1074/jbc.M106101200

Shariat-Madar, Z., Rahimy, E., Mahdi, F., & Schmaier, A. H. (2005). Overexpression of prolylcarboxypeptidase enhances plasma prekallikrein activation on Chinese hamster ovary cells. *American Journal of Physiology - Heart and Circulatory Physiology, 289*(6), 2697-2703. doi:10.1152/ajpheart.00715.2005

Sharma, N. M., Haibara, A. S., Katsurada, K., Nandi, S. S., Liu, X., Zheng, H., & Patel, K. P. (2021). Central Ang II (Angiotensin II)-mediated sympathoexcitation: Role for HIF-1α (hypoxia-inducible factor-1α) facilitated glutamatergic tone in the paraventricular nucleus of the hypothalamus. *Hypertension, 77*(1), 147-157.

Shayakhmetov, D. M., & Lieber, A. (2000). Dependence of adenovirus infectivity on length of the fiber shaft domain. *Journal of virology, 74*(22), 10274-10286.

Shenoy, V., Qi, Y., Katovich, M. J., & Raizada, M. K. (2011). ACE2, a promising therapeutic target for pulmonary hypertension. *Current opinion in pharmacology, 11*(2), 150-155.

Shimizu, I., & Minamino, T. (2016). Physiological and pathological cardiac hypertrophy. *Journal of molecular and cellular cardiology, 97*, 245-262.

Shimizu, I., Minamino, T., Toko, H., Okada, S., Ikeda, H., Yasuda, N., . . . Nojima, A. (2010). Excessive cardiac insulin signaling exacerbates systolic dysfunction induced by pressure overload in rodents. *The Journal of clinical investigation, 120*(5), 1506-1514.

Shirley, J. L., de Jong, Y. P., Terhorst, C., & Herzog, R. W. (2020). Immune responses to viral gene therapy vectors. *Molecular therapy, 28*(3), 709-722.

Simmonds, S. J., Cuijpers, I., Heymans, S., & Jones, E. A. (2020). Cellular and molecular differences between HFpEF and HFrEF: a step ahead in an improved pathological understanding. *Cells, 9*(1), 242.

Simon, G., Abraham, G., & Cserep, G. (1995). Pressor and subpressor angiotensin II administration two experimental models of hypertension. *American journal of hypertension, 8*(6), 645-650.

Sims, B., Gu, L., Krendelchtchikov, A., & Matthews, Q. L. (2014). Neural stem cell-derived exosomes mediate viral entry. *International journal of nanomedicine, 9*, 4893-4897. doi:10.2147/IJN.S70999

Skeggs Jr, L. T., Kahn, J. R., & Shumway, N. P. (1956). The preparation and function of the hypertensin-converting enzyme. *The Journal of experimental medicine, 103*(3), 295.

Skidgel, R. A., & Erdös, E. G. (1998). Cellular carboxypeptidases. *Immunological reviews, 161*(1), 129-141.

Skinner, S., Lumbers, E. R., & Symonds, E. (1969). Alteration by oral contraceptives of normal menstrual changes in plasma renin activity, concentration and substrate. *Clinical science, 36*(1), 67-76.

Skotland, T., Ekroos, K., Kauhanen, D., Simolin, H., Seierstad, T., Berge, V., . . . Llorente, A. (2017). Molecular lipid species in urinary exosomes as potential prostate cancer biomarkers. *European Journal of Cancer, 70*, 122-132.

Skotland, T., Sagini, K., Sandvig, K., & Llorente, A. (2020). An emerging focus on lipids in extracellular vesicles. *Advanced drug delivery reviews, 159*, 308-321.

SM Wold, W., & Toth, K. (2013). Adenovirus vectors for gene therapy, vaccination and cancer gene therapy. *Current gene therapy, 13*(6), 421-433.

Smith, J. S., Tian, J., Lozier, J. N., & Byrnes, A. P. (2004). Severe Pulmonary Pathology after Intravenous Administration of Vectors in Cirrhotic Rats. *Molecular therapy, 9*(6), 932-941. doi:10.1016/j.ymthe.2004.03.010

Snyder, R. A., & Wintroub, B. U. (1986). Inhibition of angiotensin-converting enzyme by des-Leu10-angiotensin I: a potential mechanism of endogenous angiotensin-converting enzyme regulation. *Biochimica et Biophysica Acta (BBA)-Protein Structure and Molecular Enzymology, 871*(1), 1-5.

Soden, M., Klett, C., Hasmann, T., & Hackenthal, E. (1994). Angiotensinogen: an acute-phase protein? *Hypertension, 23*(1_supplement), I126.

Song, Y., Zhang, C., Zhang, J., Jiao, Z., Dong, N., Wang, G., . . . Wang, L. (2019). Localized injection of miRNA-21-enriched extracellular vesicles effectively restores cardiac function after myocardial infarction. *Theranostics, 9*(8), 2346.

Sonoda, H., Yokota-Ikeda, N., Oshikawa, S., Kanno, Y., Yoshinaga, K., Uchida, K., . . . Ueda, A. (2009). Decreased abundance of urinary exosomal aquaporin-1 in renal ischemia-reperfusion injury. *American Journal of Physiology-Renal Physiology, 297*(4), F1006-F1016.

Sparks, M. A., Rianto, F., Diaz, E., Revoori, R., Hoang, T., Bouknight, L., & Stegbauer, J. (2021). Direct Actions of AT1 Receptors in Cardiomyocytes Do Not Contribute to Cardiac Hypertrophy. *Hypertension (Dallas, Tex. 1979), 77*(2), 393-404. doi:10.1161/HYPERTENSIONAHA.119.14079

Stadler, T., Veltmar, A., Qadri, F., & Unger, T. (1992). Angiotensin II evokes noradrenaline release from the paraventricular nucleus in conscious rats. *Brain research, 569*(1), 117-122.

Staessen, J. A., Wang, J., Bianchi, G., & Birkenhäger, W. H. (2003). Essential hypertension. *The Lancet, 361*(9369), 1629-1641.

Stone, D., David, A., Bolognani, F., Lowenstein, P., & Castro, M. (2000). Viral vectors for gene delivery and gene therapy within the endocrine system. *The Journal of endocrinology, 164*(2), 103-118.

Sugawara, H., Moniwa, N., Kuno, A., Ohwada, W., Osanami, A., Shibata, S., . . . Miura, T. (2021). Activation of the angiotensin II receptor promotes autophagy in renal proximal tubular cells and affords protection from ischemia/reperfusion injury. *Journal of pharmacological sciences, 145*(2), 187-197. doi:10.1016/j.jphs.2020.12.001

Sukumaran, V., Veeraveedu, P. T., Gurusamy, N., Lakshmanan, A. P., Yamaguchi, K. i., Ma, M., . . . Kodama, M. (2012). Olmesartan attenuates the development of heart failure after experimental autoimmune myocarditis in rats through the modulation of ANG 1–7 mas receptor. *Molecular and cellular endocrinology, 351*(2), 208-219.

Sun, L., Jia, H., Ma, L., Yu, M., Yang, Y., Liu, Y., . . . Zou, Z. (2018). Metabolic profiling of hypoxia/reoxygenation injury in H9c2 cells reveals the accumulation of phytosphingosine and the vital role of Dan-Shen in Xin-Ke-Shu. *Phytomedicine, 49*, 83-94.

Sun, X.-H., Wang, X., Zhang, Y., & Hui, J. (2019). Exosomes of bone-marrow stromal cells inhibit cardiomyocyte apoptosis under ischemic and hypoxic conditions via miR-486-5p targeting the PTEN/PI3K/AKT signaling pathway. *Thrombosis research, 177*, 23-32.

Suzuki, K., Yamada, H., Fujii, R., Munetsuna, E., Yamazaki, M., Ando, Y., . . . Hamajima, N. (2022). Circulating microRNA-27a and -133a are negatively associated with incident hypertension: a five-year longitudinal population-based study. *Biomarkers, 27*(5), 496-502. doi:10.1080/1354750X.2022.2070281

Szabó, C., Pacher, P., Zsengellér, Z., Vaslin, A., Komjáti, K., Benkö, R., . . . Kollai, M. (2004). Angiotensin II-mediated endothelial dysfunction: role of poly (ADP-ribose) polymerase activation. *Molecular Medicine, 10*, 28-35.

Sze, S. K., de Kleijn, D. P., Lai, R. C., Tan, E. K. W., Zhao, H., Yeo, K. S., . . . Mitchell, W. (2007). Elucidating the secretion proteome of human embryonic stem cell-derived mesenchymal stem cells. *Molecular & Cellular Proteomics, 6*(10), 1680-1689.

Takata, Y., & Kato, H. (1995). Adrenoceptors in SHR: alterations in binding characteristics and intracellular signal transduction pathways. *Life sciences, 58*(2), 91-106.

Takeda, K., Nakata, T., Takesako, T., Itoh, H., Hirata, M., Kawasaki, S., . . . Nakagawa, M. (1991). Sympathetic inhibition and attenuation of spontaneous hypertension by PVN lesions in rats. *Brain research, 543*(2), 296-300.

Takemoto, M., Egashira, K., Tomita, H., Usui, M., Okamoto, H., Kitabatake, A., . . . Takeshita, A. (1997). Chronic angiotensin-converting enzyme inhibition and angiotensin II type 1 receptor blockade: effects on cardiovascular remodeling in rats induced by the long-term blockade of nitric oxide synthesis. *Hypertension, 30*(6), 1621-1627.

Tan, F., Morris, P., Skidgel, R., & Erdös, E. (1993). Sequencing and cloning of human prolylcarboxypeptidase (angiotensinase C). Similarity to both serine carboxypeptidase and prolylendopeptidase families. *Journal of Biological Chemistry, 268*(22), 16631-16638.

Tan, L.-B., Jalil, J. E., Pick, R., Janicki, J. S., & Weber, K. T. (1991). Cardiac Myocyte Necrosis Induced by Angiotensin II. *Circulation research, 69*(5), 1185-1195. doi:10.1161/01.RES.69.5.1185

Tanimoto, K., Sugiyama, F., Goto, Y., Ishida, J., Takimoto, E., Yagami, K., . . . Murakami, K. (1994). Angiotensinogen-deficient mice with hypotension. *The Journal of biological chemistry, 269*(50), 31334-31337. doi:10.1016/S0021-9258(18)31697-1

Tatemoto, K., Takayama, K., Zou, M.-X., Kumaki, I., Zhang, W., Kumano, K., & Fujimiya, M. (2001). The novel peptide apelin lowers blood pressure via a nitric oxide-dependent mechanism. *Regulatory peptides, 99*(2-3), 87-92.

Tham, Y. K., Bernardo, B. C., Ooi, J. Y., Weeks, K. L., & McMullen, J. R. (2015). Pathophysiology of cardiac hypertrophy and heart failure: signaling pathways and novel therapeutic targets. *Archives of toxicology, 89*(9), 1401-1438.

Théry, C., Amigorena, S., Raposo, G., & Clayton, A. (2006). Isolation and characterization of exosomes from cell culture supernatants and biological fluids. *Current protocols in cell biology, 30*(1), 3.22. 21-23.22. 29.

Théry, C., Witwer, K. W., Aikawa, E., Alcaraz, M. J., Anderson, J. D., Andriantsitohaina, R., . . . Atkin‐Smith, G. K. (2018). Minimal information for studies of extracellular vesicles 2018 (MISEV2018): a position statement of the International Society for Extracellular Vesicles and update of the MISEV2014 guidelines. *Journal of Extracellular Vesicles, 7*(1), 1535750.

Thomas, W. G., Brandenburger, Y., Autelitano, D. J., Pham, T., Qian, H., & Hannan, R. D. (2002). Adenoviral-directed expression of the type 1A angiotensin receptor promotes cardiomyocyte hypertrophy via transactivation of the epidermal growth factor receptor. *Circ Res, 90*(2), 135-142. doi:10.1161/hh0202.104109

Thygesen, K., Alpert, J. S., White, H. D., & Infarction, J. E. A. A. W. T. F. f. t. R. o. M. (2007). Universal definition of myocardial infarction. *Journal of the American College of Cardiology, 50*(22), 2173-2195.

Tigerstedt, R., & Bergman, P. (1898). Niere und Kreislauf 1. *Skandinavisches Archiv für Physiologie, 8*(1), 223-271.

Tikellis, C., & Thomas, M. C. (2012). Angiotensin-Converting Enzyme 2 (ACE2) Is a Key Modulator of the Renin Angiotensin System in Health and Disease. *International journal of peptides, 2012*, 256294-256298. doi:10.1155/2012/256294

Tilemann, L., Ishikawa, K., Weber, T., & Hajjar, R. J. (2012). Gene therapy for heart failure. *Circulation research, 110*(5), 777-793.

Timmermans, P. B., Chiu, A. T., & Thoolen, M. J. (1987). Calcium handling in vasoconstriction to stimulation of alpha1-and alpha2-adrenoceptors. *Canadian journal of physiology and pharmacology, 65*(8), 1649-1657.

Tipnis, S. R., Hooper, N. M., Hyde, R., Karran, E., Christie, G., & Turner, A. J. (2000). A human homolog of angiotensin-converting enzyme: cloning and functional expression as a captopril-insensitive carboxypeptidase. *Journal of Biological Chemistry, 275*(43), 33238-33243.

TOLLEFSON, A. E., RYERSE, J. S., SCARIA, A., HERMISTON, T. W., & WOLD, W. S. (1996). The E3-11.6-kDa Adenovirus Death Protein (ADP) Is Required for Efficient Cell Death: Characterization of Cells Infected withadpMutants. *Virology, 220*(1), 152-162.

Tong, Y., Ye, C., Ren, X.-S., Qiu, Y., Zang, Y.-H., Xiong, X.-Q., . . . Zhu, G.-Q. (2018). Exosome-Mediated Transfer of ACE (Angiotensin-Converting Enzyme) From Adventitial Fibroblasts of Spontaneously Hypertensive Rats Promotes Vascular Smooth Muscle Cell Migration. *Hypertension (Dallas, Tex. 1979), 72*(4), 881-888. doi:10.1161/HYPERTENSIONAHA.118.11375

Torretti, J. (1982). Sympathetic control of renin release. *Annual review of pharmacology and toxicology, 22*(1), 167-192. doi:10.1146/annurev.pa.22.040182.001123

Trask, A. J., Groban, L., Westwood, B. M., Varagic, J., Ganten, D., Gallagher, P. E., . . . Ferrario, C. M. (2010). Inhibition of Angiotensin-Converting Enzyme 2 Exacerbates Cardiac Hypertrophy and Fibrosis in Ren-2 Hypertensive Rats. *American journal of hypertension, 23*(6), 687-693. doi:10.1038/ajh.2010.51

Tsutsumi, Y., Matsubara, H., Masaki, H., Kurihara, H., Murasawa, S., Takai, S., . . . Nakagawa, K. (1999). Angiotensin II type 2 receptor overexpression activates the vascular kinin system and causes vasodilation. *The Journal of clinical investigation, 104*(7), 925-935.

Uddin, M. N., & Roni, M. A. (2021). Challenges of storage and stability of mRNA-based COVID-19 vaccines. *Vaccines, 9*(9), 1033.

UK, N. A.-A., Atherton, J. J., Bauersachs, J., UK, A. J. C., Carerj, S., Ceconi, C., . . . Ezekowitz, J. (2016). 2016 ESC Guidelines for the diagnosis and treatment of acute and chronic heart failure. *Eur. Heart J., 37*, 2129-2200.

Umbaugh, D. S., & Jaeschke, H. (2021). Extracellular vesicles: Roles and applications in drug-induced liver injury. *Advances in clinical chemistry, 102*, 63-125.

Valadi, H., Ekström, K., Bossios, A., Sjöstrand, M., Lee, J. J., & Lötvall, J. O. (2007). Exosome-mediated transfer of mRNAs and microRNAs is a novel mechanism of genetic exchange between cells. *Nature cell biology, 9*(6), 654-659.

Valensi, P., Lorgis, L., & Cottin, Y. (2011). Prevalence, incidence, predictive factors and prognosis of silent myocardial infarction: a review of the literature. *Archives of cardiovascular diseases, 104*(3), 178-188.

Van Berlo, J. H., Maillet, M., & Molkentin, J. D. (2013). Signaling effectors underlying pathologic growth and remodeling of the heart. *The Journal of clinical investigation, 123*(1), 37-45.

Van Diepen, S., Katz, J. N., Albert, N. M., Henry, T. D., Jacobs, A. K., Kapur, N. K., . . . Sweitzer, N. K. (2017). Contemporary management of cardiogenic shock: a scientific statement from the American Heart Association. *Circulation, 136*(16), e232-e268.

Van Kesteren, C., Van Heugten, H., Lamers, J., Saxena, P. R., Schalekamp, M., & Danser, A. (1997). Angiotensin II-mediated growth and antigrowth effects in cultured neonatal rat cardiac myocytes and fibroblasts. *Journal of molecular and cellular cardiology, 29*(8), 2147-2157.

Van Zwieten, P., Kam, K., Pijl, A., Hendriks, M., Beenen, O., & Pfaffendorf, M. (1996). Hypertensive diabetic rats in pharmacological studies. *Pharmacological Research, 33*(2), 95-105.

Varnavski, A. N., Calcedo, R., Bove, M., Gao, G., & Wilson, J. M. (2005). Evaluation of toxicity from high-dose systemic administration of recombinant adenovirus vector in vector-naïve and pre-immunized mice. *Gene therapy, 12*(5), 427-436. doi:10.1038/sj.gt.3302347

Vázquez, E., Coronel, I., Bautista, R., Romo, E., Villalón, C. M., Avila-Casado, M. C., . . . Escalante, B. (2005). Angiotensin II-dependent induction of AT(2) receptor expression after renal ablation. *Am J Physiol Renal Physiol, 288*(1), F207-213. doi:10.1152/ajprenal.00216.2004

Vecchio, I., Tornali, C., Bragazzi, N. L., & Martini, M. (2018). The Discovery of Insulin: An Important Milestone in the History of Medicine. *Frontiers in endocrinology (Lausanne), 9*, 613-613. doi:10.3389/fendo.2018.00613

Vilas-Boas, W. W., Ribeiro-Oliveira Jr, A., Pereira, R. M., da Cunha Ribeiro, R., Almeida, J., Nadu, A. P., . . . dos Santos, R. A. S. (2009). Relationship between angiotensin-(1-7) and angiotensin II correlates with hemodynamic changes in human liver cirrhosis. *World journal of gastroenterology: WJG, 15*(20), 2512.

Villarroya-Beltri, C., Baixauli, F., Gutiérrez-Vázquez, C., Sánchez-Madrid, F., & Mittelbrunn, M. (2014). *Sorting it out: regulation of exosome loading.* Paper presented at the Seminars in cancer biology.

Villela, D. C., Passos-Silva, D. G., & Santos, R. A. (2014). Alamandine: a new member of the angiotensin family. *Current opinion in nephrology and hypertension, 23*(2), 130-134.

Vogel, R., Coumans, F. A., Maltesen, R. G., Böing, A. N., Bonnington, K. E., Broekman, M. L., . . . Hajji, N. (2016). A standardized method to determine the concentration of extracellular vesicles using tunable resistive pulse sensing. *Journal of Extracellular Vesicles, 5*(1), 31242.

Waller, A. (1909). THE ELECTRO-CARDIOGRAM OF MAN AND OF THE DOG AS SHOWN BY EINTHOVEN'S STRING GALVANOMETER. *The Lancet, 173*(4473), 1448-1450.

Wallingford, N., Perroud, B., Gao, Q., Coppola, A., Gyengesi, E., Liu, Z.-W., . . . Shariat-Madar, Z. (2009). Prolylcarboxypeptidase regulates food intake by inactivating α-MSH in rodents. *The Journal of clinical investigation, 119*(8), 2291-2303.

Wallingford, N., Perroud, B., Gao, Q., Coppola, A., Gyengesi, E., Liu, Z.-W., . . . Diano, S. (2009). Prolylcarboxypeptidase regulates food intake by inactivating alpha-MSH in rodents. *The Journal of clinical investigation, 119*(8), 2291-2303. doi:10.1172/JCI37209

Walther, W., & Stein, U. (2000). Viral vectors for gene transfer. *Drugs, 60*(2), 249-271.

Wang, G.-K., Zhu, J.-Q., Zhang, J.-T., Li, Q., Li, Y., He, J., . . . Jing, Q. (2010). Circulating microRNA: a novel potential biomarker for early diagnosis of acute myocardial infarction in humans. *European heart journal, 31*(6), 659-666.

Wang, H., Reaves, P. Y., Gardon, M. L., Keene, K., Goldberg, D. S., Gelband, C. H., . . . Raizada, M. K. (2000). Angiotensin I–converting enzyme antisense gene therapy causes permanent antihypertensive effects in the SHR. *Hypertension, 35*(1), 202-208.

Wang, J. (2014). Identification and characterization of human plasma prekallikrein-prolylcarboxypeptidase interaction sites.

Wang, J., Chen, S., & Bihl, J. (2020). Exosome-Mediated Transfer of ACE2 (Angiotensin-Converting Enzyme 2) from Endothelial Progenitor Cells Promotes Survival and Function of Endothelial Cell. *Oxidative medicine and cellular longevity, 2020*, 4213541-4213511. doi:10.1155/2020/4213541

Wang, J., Gareri, C., & Rockman, H. A. (2018). G-Protein–Coupled Receptors in Heart Disease. *Circulation research, 123*(6), 716-735. doi:10.1161/CIRCRESAHA.118.311403

Wang, J., Guo, X., & Dhalla, N. S. (2004). Modification of myosin protein and gene expression in failing hearts due to myocardial infarction by enalapril or losartan. *Biochimica et Biophysica Acta (BBA)-Molecular Basis of Disease, 1690*(2), 177-184.

Wang, J., He, W., Guo, L., Zhang, Y., Li, H., Han, S., & Shen, D. (2017). The ACE2-Ang (1-7)-Mas receptor axis attenuates cardiac remodeling and fibrosis in post-myocardial infarction. *Molecular Medicine Reports, 16*(2), 1973-1981.

Wang, J., Matafonov, A., Madkhali, H., Mahdi, F., Watson, D., Schmaier, A. H., . . . Shariat-Madar, Z. (2014). Prolylcarboxypeptidase Independently Activates Plasma Prekallikrein (Fletcher Factor). *Current molecular medicine, 14*(9), 1173-1185. doi:10.2174/1566524014666141015153519

Wang, J., & Yang, X. (2012). The function of miRNA in cardiac hypertrophy. *Cellular and molecular life sciences, 69*(21), 3561-3570.

Wang, K., Gan, T.-Y., Li, N., Liu, C.-Y., Zhou, L.-Y., Gao, J.-N., . . . Zhang, Y.-H. (2017). Circular RNA mediates cardiomyocyte death via miRNA-dependent upregulation of MTP18 expression. *Cell Death & Differentiation, 24*(6), 1111-1120.

Wang, L., He, J., Ma, H., Cai, Y., Liao, X., Zeng, W., . . . Wang, L. (2005). Chronic administration of angiotensin-(1-7) attenuates pressure-overload left ventricular hypertrophy and fibrosis in rats. *第一军医大学学报 (J First Mil Med Univ), 25*, 482.

Wang, L., Liu, J., Xu, B., Liu, Y.-L., & Liu, Z. (2018). Reduced exosome miR-425 and miR-744 in the plasma represents the progression of fibrosis and heart failure. *The Kaohsiung journal of medical sciences, 34*(11), 626-633.

Wang, M., Luo, W., Yu, T., Liang, S., Sun, J., Zhang, Y., . . . Li, G. (2022). Corynoline protects ang II-induced hypertensive heart failure by increasing PPARα and Inhibiting NF-κB pathway. *Biomedicine & Pharmacotherapy, 150*, 113075.

Wang, X., Xia, J., Yang, L., Dai, J., & He, L. (2023). Recent progress in exosome research: isolation, characterization and clinical applications. *Cancer Gene Therapy*, 1-15.

Watkins, S. J., Borthwick, G. M., & Arthur, H. M. (2011). The H9C2 cell line and primary neonatal cardiomyocyte cells show similar hypertrophic responses in vitro. *In Vitro Cellular & Developmental Biology-Animal, 47*(2), 125-131.

Weaver, E. A. (2019). Dose effects of recombinant adenovirus immunization in rodents. *Vaccines, 7*(4), 144.

Wei, H., Ahn, S., Shenoy, S. K., Karnik, S. S., Hunyady, L., Luttrell, L. M., & Lefkowitz, R. J. (2003). Independent β-arrestin 2 and G protein-mediated pathways for angiotensin II activation of extracellular signal-regulated kinases 1 and 2. *Proceedings of the National Academy of Sciences, 100*(19), 10782-10787.

Weitzman, M. D. (2005). Functions of the adenovirus E4 proteins and their impact on viral vectors. *Frontiers in Bioscience-Landmark, 10*(2), 1106-1117.

Welch, W. J. (2008). Angiotensin II–Dependent Superoxide: Effects on Hypertension and Vascular Dysfunction. *Hypertension, 52*(1), 51-56.

Whittaker, P., Kloner, R., Boughner, D., & Pickering, J. (1994). Quantitative assessment of myocardial collagen with picrosirius red staining and circularly polarized light. *Basic research in cardiology, 89*, 397-410.

Wiesel, P., Mazzolai, L., Nussberger, J. r., & Pedrazzini, T. (1997). Two-kidney, one clip and one-kidney, one clip hypertension in mice. *Hypertension, 29*(4), 1025-1030.

Williams, B. (2001). Angiotensin II and the pathophysiology of cardiovascular remodeling. *The American journal of cardiology, 87*(8), 10-17.

Wilson, A. J., Wang, V. Y., Sands, G. B., Young, A. A., Nash, M. P., & LeGrice, I. J. (2017). Increased cardiac work provides a link between systemic hypertension and heart failure. *Physiological Reports, 5*(1), e13104.

Wirth, T., Parker, N., & Ylä-Herttuala, S. (2013). History of gene therapy. *Gene, 525*(2), 162-169.

Wolfram, J. A., & Donahue, J. K. (2013). Gene Therapy to Treat Cardiovascular Disease. *Journal of the American Heart Association, 2*(4), e000119-n/a. doi:10.1161/JAHA.113.000119

Wollert, K. C., & Drexler, H. (1999). The renin–angiotensin system and experimental heart failure. *Cardiovascular research, 43*(4), 838-849.

Wright, P., & Thomas, M. (2018). Pathophysiology and management of heart failure. *Hypertension, 52*, 59.59.

Wu, B., Liu, J., Zhao, R., Li, Y., Peer, J., Braun, A. L., . . . Huang, Y. (2018). Glutaminase 1 regulates the release of extracellular vesicles during neuroinflammation through key metabolic intermediate alpha-ketoglutarate. *Journal of neuroinflammation, 15*(1), 1-14.

Wu, C., Xu, Q., Wang, H., Tu, B., Zeng, J., Zhao, P., . . . Huang, Y. (2022). Neutralization of SARS-CoV-2 pseudovirus using ACE2-engineered extracellular vesicles. *Acta pharmaceutica Sinica. B, 12*(3), 1523-1533. doi:10.1016/j.apsb.2021.09.004

Wu, C., Xu, Y., Lu, H., Howatt, D. A., Balakrishnan, A., Moorleghen, J. J., . . . Daugherty, A. (2015). Cys18-Cys137 Disulfide Bond in Mouse Angiotensinogen Does Not Affect AngII-Dependent Functions In Vivo. *Hypertension (Dallas, Tex. 1979), 65*(4), 800-805. doi:10.1161/HYPERTENSIONAHA.115.05166

Wu, Y., Yang, H., Yang, B., Yang, K., & Xiao, C. (2013). Association of polymorphisms in prolylcarboxypeptidase and chymase genes with essential hypertension in the Chinese Han population. *Journal of the Renin-Angiotensin-Aldosterone System, 14*(3), 263-270.

Wu, Z., Asokan, A., & Samulski, R. J. (2006). Adeno-associated virus serotypes: vector toolkit for human gene therapy. *Molecular therapy, 14*(3), 316-327.

Xia, Y., & Karmazyn, M. (2004). Obligatory Role for Endogenous Endothelin in Mediating the Hypertrophic Effects of Phenylephrine and Angiotensin II in Neonatal Rat Ventricular Myocytes: Evidence for Two Distinct Mechanisms for Endothelin Regulation. *The Journal of pharmacology and experimental therapeutics, 310*(1), 43-51. doi:10.1124/jpet.104.065185

Xiao, J., Pan, Y., Li, X., Yang, X., Feng, Y., Tan, H., . . . Yu, X. (2016). Cardiac progenitor cell-derived exosomes prevent cardiomyocytes apoptosis through exosomal miR-21 by targeting PDCD4. *Cell death & disease, 7*(6), e2277-e2277.

Xu, S., Lind, L., Zhao, L., Lindahl, B., & Venge, P. (2012). Plasma prolylcarboxypeptidase (angiotensinase C) is increased in obesity and diabetes mellitus and related to cardiovascular dysfunction. *Clinical chemistry, 58*(7), 1110-1115.

Yan, L., Zhang, J. D., Wang, B., Lv, Y. J., Jiang, H., Liu, G. L., . . . Guo, X. F. (2013). Quercetin inhibits left ventricular hypertrophy in spontaneously hypertensive rats and inhibits angiotensin II-induced H9C2 cells hypertrophy by enhancing PPAR-γ expression and suppressing AP-1 activity. *PLoS One, 8*(9), e72548.

Yang, H. Y. T., ErdÖS, E. G., & Chiang, T. S. (1968). New Enzymatic Route for the Inactivation of Angiotensin. *Nature (London), 218*(5148), 1224-1226. doi:10.1038/2181224a0

Yang, N. (1991). In vivo and in vitro gene transfer to mammalian somatic cells by particle bombardment. *Proc Natl Acad Sci USA, 88*, 2726-2730.

Yang, Y., Nunes, F. A., Berencsi, K., Furth, E. E., Gönczöl, E., & Wilson, J. M. (1994). Cellular immunity to viral antigens limits E1-deleted adenoviruses for gene therapy. *Proceedings of the National Academy of Sciences, 91*(10), 4407-4411.

Yasuno, S., Kuwahara, K., Kinoshita, H., Yamada, C., Nakagawa, Y., Usami, S., . . . Nakao, K. (2013). Angiotensin II type 1a receptor signalling directly contributes to the increased arrhythmogenicity in cardiac hypertrophy: Angiotensin type 1 receptor and arrhythmogenicity. *British journal of pharmacology, 170*(7), 1384-1395. doi:10.1111/bph.12328

Ye, M., Wysocki, J., Gonzalez-Pacheco, F. R., Salem, M., Evora, K., Garcia-Halpin, L., . . . Batlle, D. (2012). Murine recombinant angiotensin-converting enzyme 2: effect on angiotensin II-dependent hypertension and distinctive angiotensin-converting enzyme 2 inhibitor characteristics on rodent and human angiotensin-converting enzyme 2. *Hypertension, 60*(3), 730-740. doi:10.1161/hypertensionaha.112.198622

Yiannikouris, F., Wang, Y., Shoemaker, R., Larian, N., Thompson, J., English, V. L., . . . Cassis, L. A. (2015). Deficiency of Angiotensinogen in Hepatocytes Markedly Decreases Blood Pressure in Lean and Obese Male Mice. *Hypertension (Dallas, Tex. 1979), 66*(4), 836-842. doi:10.1161/HYPERTENSIONAHA.115.06040

Yoshida, M., Watanabe, Y., Yamanishi, K., Yamashita, A., Yamamoto, H., Okuzaki, D., . . . Okamura, H. (2014). Analysis of genes causing hypertension and stroke in spontaneously hypertensive rats: gene expression profiles in the brain. *International journal of molecular medicine, 33*(4), 887-896.

Zaborowski, M. P., Balaj, L., Breakefield, X. O., & Lai, C. P. (2015). Extracellular vesicles: composition, biological relevance, and methods of study. *Bioscience, 65*(8), 783-797.

Zeng, J., Zhang, Y., Mo, J., Su, Z., & Huang, R. (1998). Two-kidney, two clip renovascular hypertensive rats can be used as stroke-prone rats. *Stroke, 29*(8), 1708-1714.

Zevolis, E., Philippou, A., Moustogiannis, A., Chatzigeorgiou, A., & Koutsilieris, M. (2022). The Effects of Mechanical Loading Variations on the Hypertrophic, Anti-Apoptotic, and Anti-Inflammatory Responses of Differentiated Cardiomyocyte-like H9C2 Cells. *Cells, 11*(3), 473.

Zhai, P., Yamamoto, M., Galeotti, J., Liu, J., Masurekar, M., Thaisz, J., . . . Sadoshima, J. (2005). Cardiac-specific overexpression of AT1 receptor mutant lacking G alpha q/G alpha i coupling causes hypertrophy and bradycardia in transgenic mice. *The Journal of clinical investigation, 115*(11), 3045-3056. doi:10.1172/JCI25330

Zhang-James, Y., Middleton, F. A., & Faraone, S. V. (2013). Genetic architecture of Wistar-Kyoto rat and spontaneously hypertensive rat substrains from different sources. *Physiological genomics, 45*(13), 528-538.

Zhang, Y., & Bergelson, J. M. (2005). Adenovirus receptors. *Journal of virology, 79*(19), 12125-12131. doi:10.1128/jvi.79.19.12125-12131.2005

Zhang, Y., Bi, J., Huang, J., Tang, Y., Du, S., & Li, P. (2020). Exosome: a review of its classification, isolation techniques, storage, diagnostic and targeted therapy applications. *International journal of nanomedicine*, 6917-6934.

Zhang, Y., Hong, X.-m., Xing, H.-x., Li, J.-p., Huo, Y., & Xu, X.-p. (2009). E112D polymorphism in the prolylcarboxypeptidase gene is associated with blood pressure response to benazepril in Chinese hypertensive patients. *Chinese medical journal, 122*(20), 2461-2465.

Zhang, Y., Liu, Y., Liu, H., & Tang, W. H. (2019). Exosomes: biogenesis, biologic function and clinical potential. *Cell & bioscience, 9*(1), 1-18.

Zhao, S., Shetty, J., Hou, L., Delcher, A., Zhu, B., Osoegawa, K., . . . Fraser, C. M. (2004). Human, mouse, and rat genome large-scale rearrangements: stability versus speciation. *Genome research, 14*(10A), 1851-1860. doi:10.1101/gr.2663304

Zhao, Y. X., Yin, H. Q., Yu, Q. T., Qiao, Y., Dai, H. Y., Zhang, M. X., . . . Dong, B. (2010). ACE2 Overexpression Ameliorates Left Ventricular Remodeling and Dysfunction in a Rat Model of Myocardial Infarction. *Human gene therapy, 21*(11), 1545-1554. doi:10.1089/hum.2009.160

Zhong, G., Chen, F., Cheng, Y., Tang, C., & Du, J. (2003). The role of hydrogen sulfide generation in the pathogenesis of hypertension in rats induced by inhibition of nitric oxide synthase. *Journal of hypertension, 21*(10), 1879-1885.

Zhong, J., Basu, R., Guo, D., Chow, F. L., Byrns, S., Schuster, M., . . . Kassiri, Z. (2010). Angiotensin-converting enzyme 2 suppresses pathological hypertrophy, myocardial fibrosis, and cardiac dysfunction. *Circulation, 122*(7), 717-728.

Zhong, Z., Froh, M., Wheeler, M., Smutney, O., Lehmann, T., & Thurman, R. (2002). Viral gene delivery of superoxide dismutase attenuates experimental cholestasis-induced liver fibrosis in the rat. *Gene therapy, 9*(3), 183-191.

Zhou, H., O'Neal, W., Morral, N., & Beaudet, A. L. (1996). Development of a complementing cell line and a system for construction of adenovirus vectors with E1 and E2a deleted. *Journal of virology, 70*(10), 7030-7038.

Zhou, H., Pisitkun, T., Aponte, A., Yuen, P. S., Hoffert, J. D., Yasuda, H., . . . Knepper, M. A. (2006). Exosomal Fetuin-A identified by proteomics: a novel urinary biomarker for detecting acute kidney injury. *Kidney international, 70*(10), 1847-1857.

Zhou, H., Yuan, Y., Liu, Y., Deng, W., Zong, J., Bian, Z. Y., . . . Tang, Q. Z. (2014). Icariin attenuates angiotensin II-induced hypertrophy and apoptosis in H9c2 cardiomyocytes by inhibiting reactive oxygen species-dependent JNK and p38 pathways. *Experimental and therapeutic medicine, 7*(5), 1116-1122.

Zhou, M.-S., Schulman, I. H., & Raij, L. (2004). *Nitric oxide, angiotensin II, and hypertension.* Paper presented at the Seminars in nephrology.

Zhu, L., Carretero, O. A., Liao, T.-D., Harding, P., Li, H., Sumners, C., & Yang, X.-P. (2010a). Role of Prolylcarboxypeptidase in Angiotensin II Type 2 Receptor–Mediated Bradykinin Release in Mouse Coronary Artery Endothelial Cells. *Hypertension, 56*(3), 384-390.

Zhu, L., Carretero, O. A., Liao, T.-D., Harding, P., Li, H., Sumners, C., & Yang, X.-P. (2010b). Role of Prolylcarboxypeptidase in Angiotensin II Type 2 Receptor–Mediated Bradykinin Release in Mouse Coronary Artery Endothelial Cells. *Hypertension (Dallas, Tex. 1979), 56*(3), 384-390. doi:10.1161/HYPERTENSIONAHA.110.155051

Zhu, X., Badawi, M., Pomeroy, S., Sutaria, D. S., Xie, Z., Baek, A., . . . Perle, K. L. (2017). Comprehensive toxicity and immunogenicity studies reveal minimal effects in mice following sustained dosing of extracellular vesicles derived from HEK293T cells. *Journal of extracellular vesicles, 6*(1), 1324730.

Zhu, Y.-C., Zhu, Y.-Z., Gohlke, P., Stauss, H. M., & Unger, T. (1997). Effects of angiotensin-converting enzyme inhibition and angiotensin II AT1 receptor antagonism on cardiac

parameters in left ventricular hypertrophy. *The American journal of cardiology, 80*(3), 110A-117A.

Zhu, Y. C., Zhu, Y. Z., Lu, N., Wang, M. J., Wang, Y. X., & Yao, T. (2003). Role of angiotensin AT1 and AT2 receptors in cardiac hypertrophy and cardiac remodelling. *Clinical and Experimental Pharmacology and Physiology, 30*(12), 911-918.

Zhu, Z., Zhang, S. H., Wagner, C., Kurtz, A., Maeda, N., Coffman, T., & Arendshorst, W. J. (1998). Angiotensin AT1B Receptor Mediates Calcium Signaling in Vascular Smooth Muscle Cells of AT1A Receptor-Deficient Mice. *Hypertension (Dallas, Tex. 1979), 31*(5), 1171-1177.

Zhuo, J. L., Imig, J. D., Hammond, T. G., Orengo, S., Benes, E., & Navar, L. G. (2002). Ang II accumulation in rat renal endosomes during Ang II-induced hypertension: role of AT1 receptor. *Hypertension, 39*(1), 116-121.

Zmysłowski, A., & Szterk, A. (2017). Current knowledge on the mechanism of atherosclerosis and pro-atherosclerotic properties of oxysterols. *Lipids in health and disease, 16*(1), 1-19.

Zou, X., Wang, J., Chen, C., Tan, X., Huang, Y., Jose, P. A., . . . Zeng, C. (2020). Secreted Monocyte miR-27a, via Mesenteric Arterial Mas Receptor-eNOS Pathway, Causes Hypertension. *American journal of hypertension, 33*(1), 31-42. doi:10.1093/ajh/hpz112

Zsebo, K., Yaroshinsky, A., Rudy, J. J., Wagner, K., Greenberg, B., Jessup, M., & Hajjar, R. J. (2014). Long-term effects of AAV1/SERCA2a gene transfer in patients with severe heart failure: analysis of recurrent cardiovascular events and mortality. *Circulation research, 114*(1), 101-108.